UNIWERSYTET MEDYCZNY
IM. PIASTÓW ŚLĄSKICH WE WROCŁAWIU

Katarzyna Bednarska

Potencjał wybranych środków wazoprotekcyjnych i substancji roślinnych do hamowania nieenzymatycznej glikacji oraz pułapkowania reaktywnych związków α-dikarbonylowych

The potential of selected vasoprotective agents and plant substances to inhibit non-enzymatic glycation and trap reactive α-dicarbonyl compounds

Rozprawa doktorska

w dziedzinie nauk medycznych i nauk o zdrowiu
w dyscyplinie nauki farmaceutyczne

Promotor:
Prof. dr hab. n. farm. Izabela Fecka
Katedra i Zakład Farmakognozji i Leku Roślinnego
UMW

Wrocław 2023

Dziękuję promotorowi mojej rozprawy doktorskiej,

dr. hab. n. farm. Izabeli Feckiej, prof. UMW

Za możliwość rozwoju naukowego, życzliwość i zaufanie.

Dziękuję moim bliskim,

za wsparcie i wiarę we mnie.

Pracę dedykuję Mojej Rodzinie i Przyjaciołom.

Spis Treści

Wykaz prac naukowych wchodzących w skład cyklu:

P1. **Bednarska K.**, Fecka I. Potential of Vasoprotectives to Inhibit Non-Enzymatic Protein Glycation, and Reactive Carbonyl and Oxygen Species Uptake.
Int. J. Mol. Sci. 2021, 22(18), 10026; https://doi.org/10.3390/ijms221810026

IF$_{2021}$: 6,2
Pkt. MNiSW/KBN: 140,00

P2. **Bednarska K.**, Fecka I., Scheijen J.L.J.M., Sanne A., Vangrieken P., Schalkwijk C.G. *A Citrus and Pomegranate Complex Reduces Methylglyoxal in Healthy Elderly Subjects: Secondary Analysis of a Double-Blind Randomized Cross-Over Clinical Trial.*
Int. J. Mol. Sci. 2023, *24*(17), 13168; https://doi.org/10.3390/ijms241713168

IF$_{2022}$: 5,6
Pkt. MNiSW/KBN: 140,00

P3. **Bednarska K.**, Kuś P.,Fecka I. *Investigation of the Phytochemical Composition, Antioxidant Activity, and Methylglyoxal Trapping Effect of Galega officinalis L. Herb In Vitro.*
Molecules 2020, *25*(24), 5810; https://doi.org/10.3390/molecules25245810

IF$_{2020}$: 4,4
Pkt. MNiSW/KBN: 140,00

P4. **Bednarska K**., Fecka I. *Aspalathin and Other Rooibos Flavonoids Trapped α-Dicarbonyls and Inhibited Formation of Advanced Glycation End Products In Vitro.*
Int. J. Mol. Sci. 2022, *23*(23), 14738; https://doi.org/10.3390/ijms232314738

IF$_{2022}$: 5,6
Pkt. MNiSW/KBN: 140,00

Łączna punktacja prac stanowiących rozprawę doktorską według wykazu czasopism naukowych MEiN, zgodny z rokiem ukazania się prac, wynosi **560** punktów. Sumaryczny *Impact Factor* (IF) wymienionych prac zgodny z rokiem ich ukazania to **21,8**.

Badania opisane w **publikacjach P1, P3 i P4** realizowano w ramach:

- projektu badawczego z programu „Młodzi Naukowcy" zatytułowanego: „Ocena zdolności wiązania reaktywnych dikarbonyli i właściwości antyglikooksydacyjnych wybranych związków naturalnych i syntetycznych o potencjale wazoprotekcyjnym", finansowanego ze środków Uniwersytetu Medycznego im. Piastów Śląskich we Wrocławiu, nr projektu: STM.D110.20.131, lata 2020 – 2021 (**publikacje P1 i P3**);
- projektu konkursowego zatytułowanego: „Hamowanie powstawania końcowych produktów zaawansowanej glikacji albumin i hemoglobiny oraz zdolność do wychwytu

metyloglioksalu przez aspalatynę i ekstrakty z *Aspalathus linearis*", finansowanego ze środków Uniwersytetu Medycznego im. Piastów Śląskich we Wrocławiu, nr projektu: SUBK.D110.22.045, lata 2021 – 2022 (**publikacja P4**).

Publikacja P2 powstała w ramach współpracy z naukowcami z Katedry Medycyny Wewnętrznej Uniwersytetu w Maastricht w Holandii oraz firmą BioActor specjalizującą się w tworzeniu suplementów diety opartych na surowcach roślinnych (Maastricht, Holandia).

Z tematyką rozprawy doktorskiej związane są także niżej wymienione 3 publikacje mojego współautorstwa, które nie zostały włączone do cyklu:

Bernacka, K.; **Bednarska, K.**; Starzec, A.; Mazurek, S.; Fecka, I. *Antioxidant and Antiglycation Effects of Cistus × incanus Water Infusion, Its Phenolic Components, and Respective Metabolites. Molecules* 2022, 27, 2432; https://doi.org/10.3390/molecules27082432.

IF$_{2022}$: 4.4
Pkt. MNiSW/KBN: 140,00

Fecka, I.; **Bednarska, K.**; Włodarczyk, M. *Fragaria × ananassa cv. Senga Sengana Leaf: An Agricultural Waste with Antiglycation Potential and High Content of Ellagitannins, Flavonols, and 2-Pyrone-4,6-dicarboxylic Acid. Molecules* 2022, 27, 5293; https://doi.org/10.3390/molecules27165293.

IF$_{2022}$: 4.4
Pkt. MNiSW/KBN: 140,00

Fecka, I.; **Bednarska, K.**; Kowalczyk, A. *In Vitro Antiglycation and Methylglyoxal Trapping Effect of Peppermint Leaf (Mentha × piperita L.) and Its Polyphenols*. *Molecules* 2023, 28, 2865; https://doi.org/10.3390/molecules28062865.

IF$_{2022}$: 4.4
Pkt. MNiSW/KBN: 140,00

Pełen wykaz dorobku naukowego, potwierdzony przez Bibliotekę Uniwersytetu Medycznego we Wrocławiu, stanowi załącznik nr 5.

STRESZCZENIE

Związki α-dikarbonylowe (α-DC) są głównymi prekursorami procesu nieenzymatycznej glikacji prowadzącego do powstawania AGE (końcowych produktów zaawansowanej glikacji). Metylglioksal (MGO) uważany jest za najbardziej reaktywny związek karbonylowy w największym stopniu odpowiedzialny za indukcję procesu glikacji. Zwiększone stężenia MGO i AGE w ustroju generalnie związane są z chorobami kardiometabolicznymi. Uważa się, że zarówno MGO jak i AGE są kluczowymi czynnikami rozwoju powikłań naczyniowych, stanowiących główną przyczynę śmiertelności wśród osób chorych na cukrzycę. Wykazano, że obniżenie poziomu MGO w surowicy obniża ryzyko wystąpienia incydentów sercowo-naczyniowych u osób z cukrzycą. Badania *in vitro* i *in vivo* dowodzą, że polifenole wykazują zdolność do wiązania α-DC i hamowania procesu glikacji na drodze różnych mechanizmów. W niniejszej rozprawie doktorskiej postawiono hipotezę, że środki wazoprotekcyjne, ich analogi strukturalne i wybrane flawonoidowe substancje roślinne posiadają zdolność hamowania nieenzymatycznej glikacji i/lub neutralizowania reaktywnych α-DC. Na podstawie tej hipotezy głównym celem badawczym było zidentyfikowanie nowych substancji o wysokim potencjale antyglikacyjnym i/lub pułapkującym α-DC. Cel zakładał również weryfikację zdolności do obniżania systemowego stężenia α-DC w modelu *in vivo* dla wyslekcjonowanej w testach *in vitro* hesperydyny. W badaniach zastosowano metody chromatograficzne, spektrometryczne, spektrofotometryczne i spektrofluorymetryczne. Wyniki potwierdziły hipotezę, że wybrane związki wazoprotekcyjne, ich analogii i flawonoidowe substancje roślinne posiadają zdolność do hamowania procesu nieenzymatycznej glikacji, a niektóre także silne właściwości wiążące α-DC. Związkami najsilniej hamującymi proces glikacji w modelu *in vitro* z jednoczesnym efektem pułapkującym MGO były hesperetyna, hesperydyna, kwercetyna, izowiteksyna, witeksyna i floretyna (przewyższały aminoguanidynę i metforminę). W badaniu *in vivo* u pacjentów otrzymujących przez okres 4 tygodni suplement diety, którego głównym składnikiem była hesperydyna w dawce dobowej 450 mg, zaobserowowano istotne statystycznie obniżenie stężenia MGO w osoczu w porównaniu z placebo. W oparciu o przeprowadzone badania fitochemiczne, a następnie testy *in vitro,* stwierdzono, że ziele rutwicy (*Galega officinalis*) i rooibos (*Aspalathus linearis*), stosowane jako hipoglikemizujące i wspomagające układ krążenia, są bogatym źródłem związków pułapkujących α-DC (guanidynowych, flawonoidowych i innych polifenoli) oraz wykazujących silny efekt antyoksydacyjny i antyglikacyjny.

ABSTRACT

α-Dicarbonyl compounds (α-DC) are the main precursors of the non-enzymatic glycation process leading to the formation of AGEs (advanced glycation end products). Methylglyoxal (MGO) is considered the most reactive carbonyl compound largely responsible for inducing the glycation process. Elevated levels of MGO and AGEs in the body are generally associated with cardiometabolic diseases. Both MGO and AGEs are believed to be key factors in the development of vascular complications, which are the main cause of mortality among diabetic patients. It has been shown that reducing serum MGO levels decreases the risk of cardiovascular incidents in diabetic individuals. *In vitro* and *in vivo* studies demonstrate that polyphenols can bind α-DC and inhibit the glycation process through various mechanisms. In this doctoral thesis, it was hypothesized that vasoprotective agents, their structural analogs, and selected flavonoid plant substances can inhibit non-enzymatic glycation and/or neutralize reactive α-DC. Based on this hypothesis, the main research objective was to identify new substances with high antiglycation potential and/or α-DC trapping capability. The aim also included verifying the ability to reduce systemic α-DC concentration in an *in vivo* model for hesperidin selected in *in vitro* tests. Chromatographic, spectrometric, spectrophotometric, and spectrofluorometric methods were used in the studies. The results confirmed the hypothesis that selected vasoprotective compounds, their analogs, and flavonoid plant substances have the ability to inhibit the non-enzymatic glycation process, and some also have strong α-DC binding properties. The compounds that most strongly inhibited the glycation process in an *in vitro* model, while simultaneously showing an MGO trapping effect, were hesperetin, hesperidin, quercetin, isovitexin, vitexin, and phloretin (higher than aminoguanidine and metformin). In an *in vivo* study of patients receiving a supplement for 4 weeks, with hesperidin being the main ingredient at a daily dose of 450 mg, a statistically significant reduction in plasma MGO concentration was observed compared to placebo. Based on the conducted phytochemical studies and subsequent *in vitro* tests, it was found that goat's rue (*Galega officinalis*) and rooibos (*Aspalathus linearis*) used as hypoglycemic and circulatory support agents are rich sources of α-DC trapping compounds (guanidine, flavonoids, and other polyphenols) and exhibit strong antioxidant and antiglycation effects.

1. Wprowadzenie

Cukrzyca jest przewlekłą chorobą metaboliczną, charakteryzującą się produkcją niewystarczającej ilości hormonu anabolicznego insuliny, lub też niewystarczająco skutecznym jego wykorzystywaniem. Jej głównym objawem jest hiperglikemia - permanentnie podwyższony poziom glukozy we krwi. Cukrzyca jest obecnie jednym z największych wyzwań stojących przed ochroną zdrowia na świecie, zarówno w krajach rozwiniętych, jak i rozwijających się, z częstością występowania wynoszącą prawie 10% dorosłej populacji [1]. W 2021 r. na cukrzycę chorowało 537 milionów ludzi na całym świecie, a oczekuje się, że liczba ta wzrośnie do około 642 milionów do roku 2045 [2]. Niezależnie od postaci i typu choroby wszyscy pacjenci z cukrzycą narażeni są na ryzyko powikłań sercowo-naczyniowych, stanowiących obecnie główną przyczynę śmiertelności wśród osób chorych na cukrzycę. Naczyniowe powikłania cukrzycy klasyfikowane są jako uszkodzenie małych naczyń (mikroangiopatia) lub dużych naczyń (makroangiopatia) organizmu. Dysfunkcja mikronaczyniowa w cukrzycy rozwija się stopniowo w obrębie drobnych naczyń siatkówki, nerek i nerwów, powodując odpowiednio retinopatię cukrzycową, nefropatię i neuropatię. Z kolei dysfunkcja makronaczyniowa polega głównie na postępującej miażdżycy oraz zwężaniu naczyń krwionośnych i dotyczy tętnic wieńcowych, szyjnych i obwodowych, zwiększając tym samym ryzyko zawału mięśnia sercowego i udaru mózgu. Szacuje się, że wskaźnik zachorowalności na powikłania mikronaczyniowe wśród osób z cukrzycą jest co najmniej 4-20 razy wyższy niż w populacji osób bez cukrzycy, podczas gdy wskaźnik powikłań makronaczyniowych jest średnio 2-4 razy wyższy niż u osób bez cukrzycy [3]. Cukrzyca, choć zwykle mówi się o niej w kontekście wyżej wymienionych klasycznych powikłań naczyniowych, przyczynia się również do powstawania przewlekłych i ostrych zmian neuropoznawczych, które upośledzają funkcjonowanie układu nerwowego [4]. Charakterystyczne dla przebiegu cukrzycy długotrwale podwyższone stężenie glukozy i jego bezpośrednie następstwa biochemiczne mają kluczowe znaczenie dla rozwoju powikłań cukrzycowych [5]. Obecnie istnieją liczne dowody oparte o badania eksperymentalne i kliniczne, wskazujące, że zwiększone wytwarzanie metyloglioksalu (MGO) w komórkach w warunkach hiperglikemii odgrywa kluczową rolę w rozwoju i progresji powikłań naczyniowych cukrzycy [6–10]. MGO jest związkiem organicznym zaliczanym do grupy α-dikarbonyli (ang. *α-dicarbonyl compounds,* α-DC). α-DC stanowią podgrupę związków określanych zbiorczo jako reaktywne związki karbonylowe (ang. *Reactive Carbonyl Species,* RCS), do których zaliczny jest także gliokasl (GO) i 2-deoksyglukozon (3-DG).

Spośród nich MGO jest najbardziej reaktywnym dikarbonylem, dobrze znanym z indukcji procesu nieenzymatycznej glikacji makromolekuł (białek, peptydów, lipoprotein, kwasów nukleinowych) i ostatecznie prowadzącym do powstawania końcowych produktów zaawansowanej glikacji (AGE) [11]. Z uwagi na swoją wysoką rekatywność to na nim skupia się większość dotychczasowych badań związanych z procesam glikacji oraz rozwojem chorób cywilizacyjnych. Ponieważ MGO powstaje głównie jako produkt uboczny glikolizy, wysokie stężenie glukozy w organizmie przekłada się na zwiększone poziomy MGO u osób chorych na cukrzycę [12]. Liczne badania sugerują, że MGO jest nierozerwalnie związany nie tylko z hiperglikemią w cukrzycy, ale także z angiopatią i innymi czynnikami ryzyka powikłań naczyniowych w cukrzycy, takimi jak nadciśnienie tętnicze, dyslipidemia czy otyłość, a u osób z tymi schorzeniami stężenie metyloglioksalu jest istotnie statystycznie podwyższone [13–17].

Detoksykacja MGO w organizmie człowieka zachodzi głównie za pośrednictwem systemu znanego jako system glioksalazy. System ten składa się z dwóch enzymów: glioksalazy I (Glo1) i glioksalazy II (Glo2), zapewniających utrzymanie wewnątrzkomórkowych poziomów MGO i innych związków α-dikarbonylowych na bezpiecznym poziomie w prawidłowych warunkach fizjologicznych. Jednakże gdy system glioksalazy jest przeciążony lub nie funkcjonuje prawidłowo (np. z powodu stale podwyższonego poziomu glukozy lub niedoboru Glo1/Glo2), może to prowadzić do akumulacji metyloglioksalu w komórkach i tkankach [18,19]. Wysoka reaktywność metyloglioksalu jako ketoaldehydu związana jest z reakcją addycji nukleofilowej z udziałem wolnych grup aminowych i guanidynowych makromolekuł, której cząsteczka ta podlega niezwykle łatwo. W pierwszym etapie reakcji grupa aminowa lub guanidynowa działa jako nukleofil i atakuje atom węgla w grupie karbonylowej (aldehydowej lub ketonowej) metyloglioksalu, który wykazuje charakter elektrofilowy (aldehydy na ogół ulegają dużo łatwiej addycji nukleofilowej niż ketony). Rezultatem tej reakcji jest utworzenie wiązania σ między atomem azotu w grupie aminowej/guanidynowej a atomem węgla jednej z grup karbonylowych metyloglioksalu. W międzyczasie para elektronów z wiązania π między atomem węgla a tlenem w cząsteczce MGO przesuwa się na atom tlenu, tworząc na nim cząstkowy ładunek ujemny. W środowisku wodnym produktem przejściowym ataku nukleofilowego jest karbinoloamina [20]. Drugim etapem jest eliminacja cząsteczki wody, która zachodzi w obecności kwasu lub zasady. W wyniku tych dwóch etapów powstają drugorzędowe iminy (aldimina lub ketimina z ugrupowaniem azometynowym >C=N–R, zasady Schiffa), podlegające rearanżacji, w wyniku

której powstają stabilne produkty znane jako Amadori [21]. Te z kolei mogą następnie ulec dalszym modyfikacjom, w wyniku których powstają końcowe produkty zaawansowanej glikacji. MGO jest jednym z najważniejszych prekursorów AGE *in vivo*, a AGE pochodzące z MGO są wynikiem modyfikacji aminokwasów, głównie argininy i lizyny [22]. W nieodwracalnej reakcji z grupą guanidynową argininy, MGO prowadzi głównie do powstania trzech cyklicznych hydroimidazolonów: MG-H1 (Nδ-(5-hydro-5-metylo-4-imidazolon-2-yl)ornityna), MG-H2 (kwas 2-amino-5-(2-amino-5-hydro-5-metylo-4-imidazolon-1-yl)pentanowy) i MG-H3 (kwas 2-amino-5-(2-amino-4-hydro-4-metylo-5-imidazolon-1-yl)pentanowy) [23]. Izoforma MG-H1, która jest głównym AGE pochodzącym z reakcji z MGO, stanowiącym ponad 90% wszystkich adduktów metyloglioksalu, została dodatnio skorelowana z występowaniem uszkodzenia śródbłonka naczyniowego [24]. Inny AGE powstający analogicznie podczas reakcji MGO z lizyną Nε-(1-karboksyetylo)lizyna, znany jako CEL, okazał się pozytywnie korelować z insulinoopornością u pacjentów z cukrzycą [25]. Ponadto, MGO może również krzyżowo wiązać reszty argininy i lizyny, tworząc addukt MODIC – 2-ammonio-6-((2-[(4-ammonio-5-okso-5-oksopentylo)amino]-4-metylo-4,5-dihydro-1H-imidazolo-5-ylideno)amino)heksanian [26]. Dysfunkcje pojawiające się w obrębie układu krążenia w związku z modyfikacją strukturalną aminokwsów przez MGO są naturalną konsekwencją zmian strukturalnych w białkach pełniących w organizmie kluczowe funkcje [27]. Udowodniony wpływ α-DC i AGE na powstawanie uszkodzeń śródbłonka spowodował wzrost zainteresowania potencjalnym zastosowaniem związków wychwytujących α-DC i posiadających właściwości antyglikacyjne i/lub antyoksydacyjne jako czynników ochronnych w zapobieganiu powikłaniom naczyniowym cukrzycy. Uznaje się, że zmniejszenie systemowego stężenia α-dikarbonyli może przyczynić się do opóźnienia powstawania szkodliwych produktów glikacji (AGE), co ma kluczowe znaczenie dla pacjentów, którzy z powodu cukrzycy i innych chorób kardiometabolicznych doświadczają podwyższonego stężenia reaktywnych karbonyli (stres karbonylowy) [28]. Ponadto dowiedziono, że zmniejszenie stężenia metyloglioksalu we krwi może zmniejszać ryzyko wystąpienia incydentów sercowo-naczyniowych u pacjentów z cukrzycą [29].

Do tej pory zaproponowano co najmniej kilkanaście związków, które mogą być potencjalnie użyteczne jako terapia przeciw α-dikarbonylom. Wśród nich znajdują się związki o charakterze eksperymentalnym, takie jak aminoguanidyna [30] i alagebrium [31]; zarejestrowane leki, takie jak metformina [32], tiazolidynodiony [33], inhibitory konwertazy angiotensyny [34], blokery

receptora angiotensyny [35,36], statyny [37] oraz składniki suplementów diety, takie jak L-karnozyna [38], pirydoksamina [39] i kwercetyna [40]. Zarówno aminoguanidyna, jak i alagebrium zostały wykluczone z dalszych faz badań klinicznych ze względu na występowanie działań niepożądanych budzących obawy o bezpieczeństwo ich stosowania [41]. W przypadku zarejestrowanych leków, z wyjątkiem metforminy, brak jednoznacznych dowodów skuteczności w zakresie schorzeń związanych z α-DC w badaniach klinicznych na ludziach [42].

Powszechnie wiadomo, że niektóre antyoksydanty roślinne, takie jak polifenole czy flawonoidy, mają korzystny wpływ na ogólne zdrowie kardiometaboliczne, a dodatkowo mogą modulować ryzyko rozwoju chorób sercowo-naczyniowych i metabolicznych, w tym cukrzycy i jej powikłań [43,44]. Zdolność do związania reaktywnych dikarbonyli, prawdopodobnie będąca częścią składową tego ogólnego korzystnego efektu, została udowodniona w kilku badaniach *in vitro* miedzy innymi dla kwercetyny [40], kemferolu [45], katechiny [46] i naryngeniny [47]. Badania *in vitro* wykazały również, że mechanizm wychwytywania występuje w warunkach fizjologicznych - tworzenie adduktów metyloglioksalu z mirycetyną [48] oraz genisteiną [49] u myszy, a także metyloglioksalu z metforminą u ludzi [32]. Jednak brak takich badań w odniesieniu do związków z grupy leków wazoprotekcyjnych, w tym bioflawonoidów i leków syntetycznych. Do tej pory nie przebadano również substancji roślinnych tradycyjnie stosowanych w łagodzeniu objawów cukrzycy czy jako środki wspomagające układ krążenia, których profil działania i budowa chemiczna głównych składników wskazują, że mogą być skuteczne w zmniejszaniu stężeń α-DC i AGE.

2. Cel podjętych badań

W niniejszej rozprawie doktorskiej postawiono hipotezę, że środki wazoprotekcyjne, stosowane w terapii przewlekłej niewydolności żylnej, a także ich analogi strukturalne posiadają zdolność hamowania nieenzymatycznej glikacji i/lub neutralizowania reaktywnych α-dikarbonyli. Na podstawie tej hipotezy głównym celem badawczym było zidentyfikowanie nowych substancji o wysokim potencjale antyglikacyjnym i/lub pułapkującym α-DC (głównie metyloglioksal) w porównaniu do uznanych związków o takiej aktywności (aminoguanidyny, metforminy, kwercetyny). Badaniom poddano naturalne i syntetyczne środki flebotropowe, a także wybrane flawonoidy oraz substancje roślinne flawonoidowe lub zawierające inne składniki (polifenolowe, pochodne guanidyny) o właściwościach antyoksydacyjnych, hipoglikemizujących i wykazujących

efekt ochronnych przed powikłaniami cukrzycy, szczególnie ze strony układu sercowo-naczyniowego. Ponieważ właściwości przeciwutleniające i przeciwrodnikowe tych substancji mogą warunkować hamowanie utleniania cukrów prostych, takich jak glukoza i fruktoza, oraz glikowanych makromolekuł, a przez to osłabiać proces glikacji, sieciowania białek i zmniejszać wytwarzanie szkodliwych dla komórki końcowych produktów zaawansowanej glikacji, dodatkowo zweryfikowano i porównano ich potencjał antyoksydacyjny. Dalszym celem badania było wyjaśnienie, przynajmniej częściowe, mechanizmów leżących u podstawy efektu antyglikacyjnego (anty-AGE) oraz wskazanie elementów struktury chemicznej tych związków istotnych dla zdolności wiązania MGO i innych α-DC pochodzących głównie z metabolizmu węglowodanów. Badania podstawowe przeprowadzono w modelach *in vitro*. Aktywność jednego ze związków o najwyższej aktywności zweryfikowano w badaniu klinicznym z udziałem zdrowych ochotników.

Cele cząstkowe publikacji stanowiących podstawę rozprawy obejmowały:

- W **publikacji P1** celem było wyselekcjonowanie związku lub związków o najwyższym potencjale hamującym proces nieenzymatycznej glikacji w modelu *in vitro* z albuminą wołową i MGO lub GO, a następnie zweryfikowanie ich zdolności wiązania metyloglioksalu i glioksalu w mieszaninach modelowych odzwierciedlających warunki fizjologiczne (UHPLC-ESI-MS). Badaniom poddano będące w użyciu substancje czynne klasyfikowane w systemie ATC (*ang. The Anatomical Therapeutic Chemical Classification System*) w kategorii C05 "Leki ochraniające ścianę naczyń" oraz ich strukturalne analogi (aglikony i inne). Zbadano również ich aktywność przeciwutleniającą i przeciwrodnikową *per se*, będącą prawdopodobnie składową efektu wazoprotekcyjnego i antyglikacyjnego oraz przebieg reakcji wiązania α-dikarbonyli w czasie z wykorzystaniem derywatyzacji MGO i GO (**Rycina 1.**).

- Celem **publikacji P2** była weryfikacja czy hesperydyna, wytypowana w publikacji **P1** jako jeden ze związków wykazujących najsilniejszą aktywność przeciwglikacyjną i pułapkującą α-DC, ma zdolność do obniżania osoczowego stężenia α-dikarbonyli w warunkach *in vivo*. Badanie stanowiło wtórną analizę podwójnie zaślepionego, randomizowanego badania klinicznego typu naprzemiennego u zdrowych osób w podeszłym wieku, w którym uczestnicy otrzymywali kompleks ekstraktu z naowocni pomarańczy słodkiej i koncentratu soku z owoców

granatowca z hesperydyną jako głównym składnikiem (badany produkt to suplement diety o oznaczonej zawartości hesperydyny i punikalaginy). W tym celu próbki osocza pacjentów poddane zostały procesowi derywatyzacji, a następnie stężenia MGO, GO i 3-DG zostały zmierzone z wykorzystaniem metody UPLC-MS/MS; do oceny statystycznej wyników zastosowano model mieszany.

- W **publikacjach P3** i **P4** celem było potwierdzenie założenia, iż substancje roślinne o właściwościach antyoksydacyjnych i hipoglikemizujących posiadające w składzie chemicznym glikozydy flawonoidowe, inne polifenole lub pochodne guanidyny mogą hamować glikację, m.in. przez wychwytywanie α-dikarbonyli. Badaniom poddano ziele rutwicy (*Galegae herba)* stosowane dawniej w leczeniu objawów cukrzycy oraz jej składniki aktywne, jak galegina (izopentenyloguanidyna), która była pierwowzorem w syntezie metforminy i innych hipoglikemizujących biguanidów. W ostatniej pracy z cyklu oceniono właściwości przeciwglikacyjne i pułapkujące aspalatyny, *C*-glikozydu dihydrochalkonu oraz *C*-glikozydów flawonów występującego w rooibos - herbacie z czerwonokrzewu (*Aspalathus linearis* (Burm.f.) R.Dahlgren). Podjęto też próbę wskazania najbardziej istotnych elementów budowy chemicznej flawonoidów warunkujących zdolność wychwytywania MGO i GO. Surowce te wyselekcjonowano na podstawie ich znanych właściwości leczniczych/prozdrowotnych i korzystnego wpływu w hiperglikemii oraz w zaburzeniach ze strony układu sercowo-naczyniowego. W obu publikacjach przeprowadzono szczegółową analizę jakościową i ilościową składu chemicznego przygotowanych przetworów (naparów, wyciągów wodno-alkoholowych). W oparciu o uzyskany profil fitochemiczny dla każdego z surowców wybrano związki reprezentacyjne o różnej strukturze, z grup takich jak flawonoidy, kwasy hydroksycynamonowe i pochodne guanidyny, z przeznaczeniem zbadania ich zdolność do wychwytu α-DC oraz zweryfikowania i porównania właściwości antyglikacyjnych i/lub antyoksydacyjnych. W odniesieniu do rooibos ocenie poddano surowiec fermentowany (czerwony rooibos) i niefermentowany (zielony rooibos), oba dostępne komercyjnie.

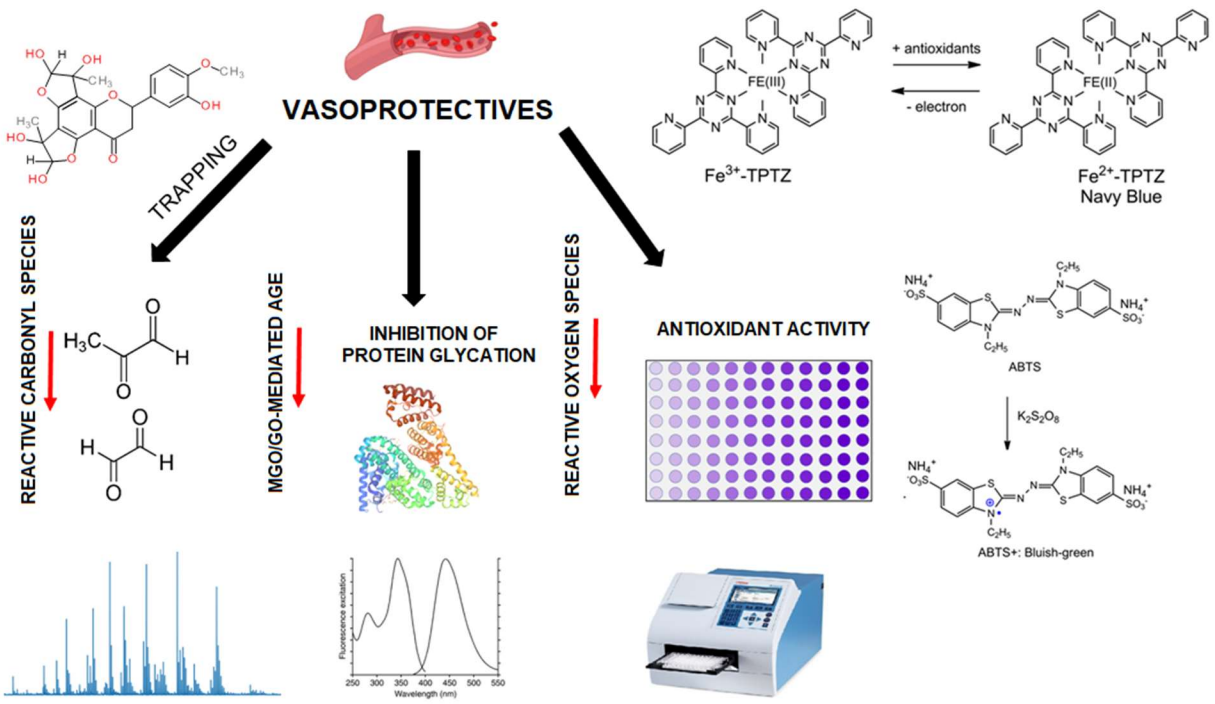

Rycina 1. Abstrakt graficzny do **publikacji P1.**

3. Materiały i metody

Metody zastosowane w badaniach zostały szczegółowo opisane w artykułach wchodzących w skład cyklu 4 publikacji, będącego podstawą niniejszej rozprawy doktorskiej. Poniżej znajduje się ogólny opis zastosowanych metod i modeli badawczych.

3.1. Materiał badawczy

W **publikacji P1, P3, P4** materiał badawczy stanowiły wzorce substancji wazoprotekcyjnych, w tym bioflawonoidów (diosmina, hepserydyna, trokserutyna) i ich analogów (diosmetyna, hesperetyna, rutyna) oraz dobesylanu wapnia, a także aspalatyny, witeksyny, izowiteksny, eriodykcjolu, kwercetyny, floretyny, floroglucynolu, kwasu chlorogenowego, siarczanu galeginy, aminoguanidyny i chlorowodorku metforminy pochodzące od certyfikowanych dostawców (Sigma-Aldrich Sp. z o.o., Poznań, Poland; Extrasynthese, Genay Cedex, France; SelectLab, Münster, Niemcy; PPF Hasco-Lek S.A.). Aminoguanidynę (związek referencyjny), metforminę, kwercetynę i floretynę zastosowano w charakterze aktywnych substancji odniesienia.

Substancje roślinne tj. ziele rutwicy (*Galegae herba*, *Galega officinalis* L.) nabyto w Zakładach Konfekcjonowania Ziół FLOS (Mokrsko, Polska) posiadających certyfikaty GMP i ISO 9002 (serie nr 1099, 1108, 1010; oznaczone odpowiednio jako Gof1, Gof2 i Gof3). Rooibos fermentowany (czerwony rooibos, RR) i niefermentowany (zielony rooibos, GR) stanowiący wysuszone, rozdrobnione liście i wierzchołkowe części pędów *Aspalathus linearis* (Burm. f.) R. Dahlgren pochodziły z Republiki Południowej Afryki i zakupiono je u polskiego producenta herbat OXALIS POLSKA Sp. z o.o. (Radzionków, Polska). Z substancji roślinnych przygotowano przetwory – napary i wyciągi wodno-alkoholowe.

W **publikacji P2** materiał badawczy stanowiły próbki osocza pozyskane z krwi obwodowej pobranej na czczo. Osocze pozyskane zostało na potrzeby badania klinicznego zarejestrowanego na clinicaltrials.gov pod numerem NCT03781999, prowadzonego przez firmę BioActor BV (Maastricht, Holandia) oraz Uniwersytet w Maastricht.

3.2. Przygotowanie naparów i wyciągów roślinnych do badań in vitro

Około 0,2 g wysuszonego i drobno sproszkowanego ziela *Galega officinalis* L. ekstrahowano 10 mL wrzącej wody przez 15 minut (napar), a także 10 mL metanolu lub mieszaniny wody i metanolu (1:1, 3:7; v/v) w łaźni ultradźwiękowej (Bandelein Sonorex Digital 10P; Bandelin, Berlin, Niemcy) w temperaturze 40 °C przez 15 min. Parametr DER określający stosunek ilości substancji roślinnej do ilości otrzymanego wyciągu roślinnego wynosił 1:50 (**publikacja P3**). Około 0,25 g wysuszonych, rozdrobnionych liści i wierzchołkowych części pędów *Aspalathus linearis* (Burm. f.) R. Dahlgren (fermentowanych i niefermentowanych) ekstrahowano 25 mL wrzącej wody (napary) lub mieszaniny wody i etanolu (1:1, v/v) przez 15 minut (w łaźni ultradźwiękowej w temperaturze 40 °C). DER otrzymanych przetworów roślinnego wynosił 1:100 (**publikacja P4**). Napary i wyciągi sączono przez filtr Durapore 0,22 i 0,45 μm (Millipore; Burlington, MA, USA) do fiolek oraz analizowano przy użyciu metod chromatografii cieczowej opisanych poniżej (**publikacja P3, P4**).

3.3 Zastosowane modele *in vitro*

Badania przeprowadzono w modelach *in vitro* reakcji wiązania α-dikarbonyli przez wybrane związki lub przetwory substancji roślinnych oraz reakcji hamowania powstawania zaawansowanych końcowych produktów glikacji białek na przykładzie surowiczej albuminy wołowej (BSA) jako białka celowanego (**publikacje P1, P3, P4**).

3.3.1. Model procesu glikacji

Badanie aktywności antyglikacyjnej przeprowadzono z wykorzystaniem BSA inkubowanej z badanym związkiem lub przetworem roślinny oraz MGO lub GO w roztworze soli fizjologicznej buforowanej fosforanami (PBS, pH 7,4) z 0,02% (m/v) azydkiem sodu, który zapobiegał wzrostowi mikroorganizmów w próbce. Następnie tak przygotowane mieszaniny pozostawiono w symulowanych warunkach fizjologicznych bez dostępu światła słonecznego w temperaturze 37 °C i wytrząsano z prędkością 50 obrotów na minutę przez 7 dni w zamkniętych fiolkach zabezpieczonych parafilmem. Mieszaninę poreakcyjną analizowano wykorzystując metodę spektrofluorymetryczną (**P1, P4**)

3.3.2. Model reakcji wiązania α-dikarbonyli

Badanie zdolności wiązania dikarbonyli przeprowadzono tworząc model reakcyjny, w którym inkubowano badany związek lub napar/wyciąg roślinny z MGO lub GO przez 1 godzinę w roztworze soli fizjologicznej buforowanej fosforanami (PBS, pH 7,4) w temperaturze 37 °C i wytrząsano z prędkością 40 obrotów na minutę. Reakcję kończono dodając niewielką ilość kwasu octowego lodowatego i umieszczając zebrane próbki w łaźni wodnej z lodem. Następnie próbki filtrowano wykorzystując hydrofilowe filtry strzykawkowe Millex (Durapore 0,22 μm). Roztwory podstawowe α-dikarbonyli były przygotowywane bezpośrednio przed rozpoczęciem każdej serii eksperymentów, a pH buforowanego roztworu soli fizjologicznej było monitorowane przed każdym badaniem. Przefiltorwaną mieszaninę poreakcyjną analizowano przy użyciu metod UHPLC-ESI-MS (**publikacja P1, P3, P4).**

3.4. Ocena aktywności antyglikacyjnej (metoda spektrofluorymetryczna)

W **publikacji P1** pomiar intensywności fluorescencji całkowitej końcowych produktów zaawansowanej glikacji (AGE) przeprowadzono przy użyciu spektrofotometru fluorescencyjnego Cary Eclipse 500 (Agilent, Santa Clara, CA, USA) przy długości fali 350 nm dla wzbudzenia i 450 nm dla emisji. Dane opracowano za pomocą oprogramowania Cary Eclipse Control Software (Agilent, Santa Clara, CA, USA). W **publikacji P4** intensywność fluorescencji AGEs analizowano za pomocą czytnika Synergy HTX Multi-Mode Microplate Reader (BioTek Instruments Inc., Winooski, VT, USA) przy 360 nm dla wzbudzenia i 460 nm dla emisji. Przetwarzanie i opracowanie danych przeprowadzono przy użyciu oprogramowania Gen5 (BioTek Instruments

Inc., Winooski, VT, USA). Związek referencyjny o znanych silnych właściwościach antyglikacyjnych stanowiła każdorazowo aminoguanidyna.

3.5. Derywatyzacja α-dikarbonyli i ocena przebiegu w czasie reakcji wiązania metyloglioksalu i glioksalu

Wybrane związki inkubowano z MGO lub GO w roztworze soli fizjologicznej buforowanej fosforanami (PBS, pH 7,4) w temperaturze 37 °C z prędkością 40 obrotów na minutę w celu symulacji warunków fizjologicznych przez 1, 2, 4, 8 i 24 godziny. Mieszaninę reakcyjną pobierano w każdym punkcie czasowym i natychmiast umieszczono w łaźni wodnej z lodem, dodając niewielką ilosć kwasu octowego lodowatego w celu zatrzymania reakcji wiązania dikarbonyli. Derywatyzację pozostałego MGO i GO przeprowadzono przez dodanie 1,2-fenylenodiaminy (o-PDA) i wytrząsano worteksem przez 5 s. Następnie mieszaniny pozostawiano w temperaturze otoczenia w ciemności przez 30 minut. Analizę UHPLC-DAD wykorzystano do pomiaru stężenia metylochinoksaliny i chinoksaliny powstałych odpowiednio w reakcji metyloglioksalu i glioksalu z o-PDA (**publikacja P1**). Do oceny przebiegu w czasie reakcji wiązania metyloglioksalu i glioksalu w **publikacji P1** wykorzystano ten sam sytem i eluenty co w **publikacji P3**, a pola powierzchni pików metylochinoksaliny i chinoksaliny monitorowano przy długościach fali odpowiednio 316 i 314 nm. Profil gradientu i warunki analizy przedstawiono szczegółowo w odnośnej pracy.

3.6. Ocena aktywności przeciwutleniającej i przeciwrodnikowej (metody spektrofotometryczne)

Pomiar aktywności przeciwutleniającej *per se* indywidualnych związków oraz przetworów roślinnych przeprowadzono z wykorzystaniem trzech testów: ABTS, FRAP i DPPH. Wszystkie pomiary wykonano za pomocą spektrofotometru Multiskan GO (Thermo Fisher Scientific, USA).

3.6.1. Test FRAP

Roztwór podstawowy odczynnika FRAP otrzymano przez zmieszanie 2,4,6-(tripirydylo)-*s*-triazyny (TPTZ) w kwasie solnym z heksahydratem chlorku żelaza (III) i buforem octanowym (pH 3,6) w stosunku 1:1:10 (v/v/v). Świeżo przygotowany odczynnik FRAP dodano do roztworów badanych substancji o różnych stężeniach i dokładnie wymieszano w 96-dołkowej mikropłytce. Absorbancję niebieskiego kompleksu tripirydylotriazyny żelazawej (Fe^{2+}/TPTZ) odczytano po 4

minutach inkubacji (z dala od światła) przy długości fali 593 nm. Wyniki wyrażono w μM Fe^{2+}. Wszystkie pomiary wykonano w trzech powtórzeniach w zakresie stężeń 5-1000 μM analizowanych związków (**publikacja P1**).

3.6.2. Test DPPH

Roztwór podstawowy odczynnika DPPH przygotowano przez rozpuszczenie 2,2-difenylo-1-pikrylohydrazylu w metanolu. Probówki z odczynnikiem DPPH chroniono przed światłem, przykrywając je folią aluminiową do momentu użycia. W 96-dołkowej mikropłytce roztwory badanych substancji w różnych stężeniach mieszano z metanolowym roztworem DPPH. Płytkę inkubowano przez 30 minut w ciemności w temperaturze otoczenia, a absorbancję rejestrowano przy długości fali 517 nm. Kwas galusowy został użyty jako kontrola pozytywna. Wszystkie pomiary wykonano w trzech powtórzeniach. Procentową aktywność zmiatania wolnych rodników DPPH obliczono w następujący sposób: inhibicja rodnika DPPH [%] = $(A_0 - A_1)/A_0 \times 100\%$, gdzie A_0 to średnia absorbancja kontroli, a A_1 to średnia absorbancja ekstraktu/standardu z DPPH. Wartości IC_{50} obliczono z pomocą analizy regresji liniowej (**publikacja P3**)

3.6.3. Test ABTS

Roztwór podstawowy kationorodnika $ABTS^+$ przygotowano przez zmieszanie równych ilości wodnych roztworów kwasu 2,2-difenylo-1-pikrylohydrazylowego, 2,2-azino-bis-(3-etylobenzotiazolino-6-sulfonowego) oraz nadsiarczanu potasu ($K_2S_2O_8$, 2,45 mM) i inkubowanie mieszaniny w ciemności w temperaturze 25 °C przez 12 h. Roztwór podstawowy rozcieńczono następnie metanolem do osiągnięcia absorbancji przy 734 nm. W 96-dołkowej mikropłytce zmieszano odczynnik $ABTS^+$ z badanymi substancjami o różnych stężeniach. Płytkę inkubowano przez 15 minut w ciemności w temperaturze otoczenia, a następnie zmierzono absorbancję przy 517 nm. Wszystkie pomiary wykonano w trzech powtórzeniach, stosując zakres stężeń 5-1000 μM badanych związków. Krzywą standardową przygotowano przy użyciu różnych stężeń troloksu w zakresie 100-1000 μM. Aktywność zmiatania rodnika ABTS obliczono w następujący sposób: inhibicja rodnika ABTS [%] = $(A_0 - A_1)/A_0 \times 100$, gdzie A_0 to średnia absorbancja kontroli, a A_1 to średnia absorbancja próbki z ABTS. Wartości IC_{50} obliczono z pomocą analizy regresji liniowej i wykorzystano do wyrażenia zdolności antyoksydacyjnej (**publikacja P1, P3**).

3.7. Projekt i populacja badania klinicznego

Badanie kliniczne, którego wtórna analiza jest podstawą **publikacji P2** zostało zatwierdzone przez lokalną Komisję Etyki Medycznej Centrum Medycznego Uniwersytetu w Maastricht+ i przeprowadzone zgodnie z Deklaracją Helsińską z 1975 r. ze zmianami z 2013 r. oraz holenderskimi przepisami dotyczącymi badań medycznych z udziałem ludzi z 1998 r. Eksperyment kliniczny przeprowadzono od czerwca 2018 r. do stycznia 2019 r. Wszyscy uczestnicy wyrazili pisemną, świadomą zgodę przed zebraniem danych. Badanie zostało zarejestrowane na stronie clinicaltrials.gov jako NCT03781999. Do wzięcia udziału w projekcie zostały zrekrutowane 42 starsze, zdrowe, niepalące osoby w wieku 60-75 lat (wg WHO wiek podeszły). Badanie to zostało zaprojektowane jako randomizowane, kontrolowane placebo, podwójnie zaślepione badanie krzyżowe (**Rycina 2.**). Pacjenci byli losowo przydzielani do jednej z sekwencji po zapisaniu się do badania. Randomizację przeprowadzono z wykorzystaniem dedykowanego oprogramowania. Uczestnicy otrzymywali komercyjnie dostępny suplement diety (Citrus & Pomegranate Complex; Actiful®, BioActor BV, Maastricht, Holandia) zawierający 500 mg ekstraktu z naowocni pomarańczy słodkiej (*Citrus* × *sinensis* (L.) Osbeck) i 200 mg koncentratu soku z owoców granatowca (*Punica granatum* L). Badany produkt (CPC) był standaryzowany chromatograficznie (LC) przez producenta. Dzienna dawka zawierała 450 mg hesperydyny i 60 mg punikalaginy. Jako placebo zastosowano maltodekstrynę (Gonmisol, Barcelona, Hiszpania). Zarówno produkt badany jak i placebo miały formę kapsułki, z których każda zawierała 350 mg odpowiedniej substancji. CPC i placebo były identyczne pod względem wyglądu i smaku. Pacjenci byli proszeni o przyjmowanie 2 kapsułek żelatynowych przed śniadaniem, popijając 200 mL wody przez 4 tygodnie. Uczestnicy przyjmowali produkt badany lub placebo przez 4 tygodnie w losowej kolejności, oddzielone 4-tygodniowym okresem wypłukania. Próbki krwi pobierano od pacjentów na początku i końcu każdeo okresu przyjmowania CPC i placebo (4 próbki). Otrzymane w ten sposób materiał biologiczny analizowano w wykorzystaniem UPLC-MS/MS w celu oznaczenia osoczowego stężenia metylogliokSalu, glioksalu i 3-deoksyglukozonu.

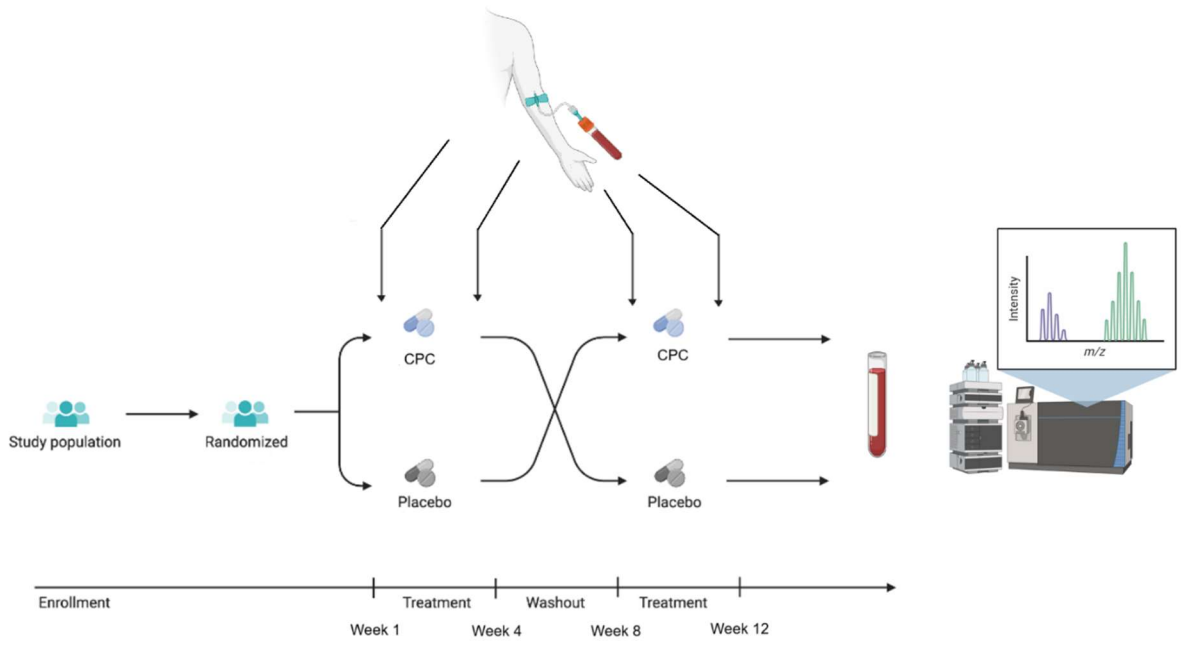

Rycina 2. Schemat metodologii zastosowanej w badaniu klinicznym - **publikacja P2**.

3.8 Metody chromatograficzne

3.8.1. UHPLC-ESI-MS

Analizę zdolności wiązania MGO i GO oraz badanie jakościowe (i ilościowe w odniesieniu do pochodnych guanidyny) składu naparów i wyciągów roślinnych wykonano metodami chromatografii cieczowej sprzężonej ze spektrometrem mas (MS) i/lub detektorem z matrycą fotodiodową (DAD) oraz przy użyciu kolumny oktadecylowej Kinetex C18 (150 × 2.1 mm, 2.6 µm; Phenomenex, Torrance, CA, USA). Eksperymenty przeprowadzono z wykorzystaniem systemu Thermo Scientific DionexUltiMate 3000 (Thermo Fisher Scientific, Waltham, MA, USA) wyposażonego w pompę czterokanałową (LPG-3400D, Thermo Fisher Scientific, Waltham, MA, USA), detektor z matrycą fotodiodową (DAD-3000) i autosampler UltiMate 3000RS (WPS-3000) sprzężony z Compact ESI-QqTOF-MS (Bruker Daltonics, Brema, Niemcy). Analizy prowadzono w trybie jonów ujemnych (ESI^-) i dodatnich (ESI^+). Fazami ruchomymi użytymi do stworzenia gradientu fazy ruchomej były: 0,1% (v/v) kwas mrówkowy w wodzie i 0,1% (v/v) kwas mrówkowy w acetonitrylu, odpowiednio jako eluenty A i B. Do kalibracji wewnętrznej użyto klastrów mrówczanu sodu w stężeniach 10 mM. Pozostałe paramtery takie jak prędkość

przepływu, program gradientu, zakres długości fal dla pomiarów (UV/Vis, nm), objętość nastrzyku, ciśnienie azotu, temperatura źródła jonów, napięcie kapilary oraz energia zderzeń różniły się w zależności od potrzeb i opisane zostały szczegółowo w **publikacjach P1, P3 i P4.** Otrzymane chromatogramy UHPLC, wraz z bazowymi i fragmentacyjnymi widmami jonów pseudomolekularnych i fragmentacyjnych, analizowano przy użyciu oprogramowania Compass Data Analysis (Bruker Daltonics, Brema, Niemcy).

3.8.2. UPLC-MS/MS

Do oznaczania stężeń α-dikarbonyli w badaniu klinicznym (**publikacja P2**) zastosowano system Waters Acquity I w połączeniu ze spektrometrem mas Xevo TQ-XS (Waters, Milford, MA, USA) wyposażonym w kolumnę oktadecylową C18 Acquity UPLC HSS T3 (50 × 2,1 mm, 1,8 μm; Waters Corporation, Milford, MA, USA). Jako eluenty wykorzystano 5% (v/v) roztwór kwasu mrówkowego w wodzie (eluent A) i acetonitrylu (eluent B) przy prędkości przepływu 800 μL/min. Objętość nastrzyku wynosiła 10 μL, a temperatura kolumny 30 °C. Pomiar stężenia MGO, GO i 3-DG przeprowadzono obliczając stosunek powierzchni każdego nieznakowanego obszaru piku do odpowiadającego mu obszaru piku wzorca wewnętrznego. Jonizacja metodą elektrorozpylania została przeprowadzona w trybie jonów dodatnich (ESI^+) przy napięciu kapilarnym 0,5 kV, temperaturze źródła 150 °C i temperaturze desolwatacji 600°C. Do analizy danych wykorzystano oprogramowanie Masslynx (V4.1, SCN 644, Waters, Milford, MA, USA).

3.8.3. HPLC-DAD

Oznaczenie zawartości flawonoidów, fenolokwasów i sumy polifenoli w przetworach z *G. officinalis* w **publikacji P3** wykonano z wykorzystaniem kolumny oktadecylowej Kinetex C18 (150 × 2.1 mm, 2.6 μm; Phenomenex, Torrance, CA, USA) w systemie Thermo Scientific DionexUltiMate 3000 (Thermo Fisher Scientific; Waltham, MA, USA) wyposażonym w pompę (LPG-3400D; Thermo Fisher Scientific, Waltham, MA, USA), detektor fotodiodowy (DAD-3000) i autosampler UltiMate 3000RS (WPS-3000). Fazy ruchome użyte do utworzenia gradientu stanowiły: 0,1% (v/v) kwas mrówkowy w wodzie i 0,1% (v/v) kwas mrówkowy w acetonitrylu. Pomiary UV/Vis prowadzono w zakresie długości fal 200-600 nm, co 2 nm, a chromatogramy rejestrowano przy 220, 254, 280, 320 i 360 nm (flawonole analizowano przy 360 nm, flawanonole przy 280 nm, a fenolokwasy pochodne kwasu hydroksycynamonowego przy 320 nm). Uzyskane dane analizowano za pomocą oprogramowania Chromeleon Chromatography Data System

(Thermo Fisher Scientific, Waltham, MA, USA). Program gradientu i pozostałe parametry analizy HPLC-DAD opisano szczegółowo w **publikacji P3.**

Zawartość flawonoidów z grupy dihydrochalkonów, flawonów i flawonoli w przetworach *A. linearis* w **publikacji P4** oznaczono w systemie Smartline (Knauer Wissenschaftliche Geräte GmbH, Berlin, Niemcy) z pompą (Managare 5000), dynamiczną komorą mieszania (V7119-1), detektorem DAD 2800, ręcznym 6-portowym zaworem wtryskowym (A1366) i termostatem kolumny (Jetstream Plus). Do rozdziału wykorzystano kolumnę Hypersil GOLD C18 (250 × 4.6 mm, 5 µm; Thermo Fisher Scientific, Waltham, MA, USA) z prekolumną C18 (10 × 4.6 mm, 5 µm; Thermo Fisher Scientific, Waltham, MA, USA). Dane zostały przetworzone przy użyciu programu EuroChrom for Windows Basic Edition V3.05 (V7568-5). Zastosowano następujące eluenty: 1,5% (v/v) kwas mrówkowy w wodzie i 1,5% (v/v) kwas mrówkowy w acetonitrylu. Pomiary UV/Vis wykonano w zakresie długości fal 200-600 nm co 2 nm. Dihydrochalkony i flawanony analizowano przy 280 nm, natomiast flawony i flawonole przy 360 nm. Zawartości związków określono metodą wzorca zewnętrznego na podstawie powierzchni odpowiadających im pików.

3.9. Analiza statystyczna

Wartości średnie, maksymalne, minimalne, mediany i odchylenia standardowe dla wszystkich danych obliczano w programie Excel (Microsoft Corporation, Redmond, WA, USA) (**publikacja P1, P3, P4**). W celu określenia istotność różnic dla wyników otrzymanych w badaniach spektrofluorymetrycznych zweryfikowano hipotezy o normalności rozkładu danych za pomocą testu Shapiro-Wilka. Następnie przeprowadzono jednoczynnikową analizę wariancji ANOVA oraz test *post-hoc* porównań wielokrotnych Tuckeya przy użyciu oprogramowania GraphPad Prism 9 (GraphPad Software, San Diego, CA, USA). Wartości *p* równe lub mniejsze niż 0,05 uznano za istotne (**publikacja P1, P4**).

W badaniu klinicznym zmiany między wartościami stężenia α-dikarbonyli na początku i na końcu każdego 4-tygodniowego okresu podwójnie ślepej próby uznano za efekt leczenia CPC. Do oceny efektów leczenia w tym badaniu zastosowano liniowy model mieszany z symetrią złożoną jako strukturą kowariancyjną. Uczestnik został zdefiniowany jako efekt losowy, podczas gdy leczenie i okres zostały potraktowane jako efekty stałe. Badanie interakcji między leczeniem a okresem wykazało brak efektu przeniesienia poprzedniego leczenia i dlatego nie zostało

uwzględnione w ostatecznym modelu. Efekty leczenia wyrażono jako średnie najmniejszych kwadratów z 95% CI, a istotność statystyczną ustalono przy 2-stronnej wartości *p* równej 0,05. Do analiz wykorzystano oprogramowanie SPSS Statistics 23 (IBM Corporation, Armonk, NY, USA). Do wizualizacji danych wykorzystano oprogramowanie GraphPad Prism 5 (GraphPad Software, San Diego, CA, USA) (**publikacja P2**).

4. Najważniejsze wyniki i podsumowanie przeprowadzonych badań

Zakres prac naukowo-badawczych cyklu publikacji przedstawionych jako rozprawa doktorska skupiał się na ocenie zdolności wiązania α-dikarbonyli (metyloglioksalu i glioksalu) przez grupę substancji o właściwościach wazoprotekcyjnych i charakteryzujących się aktywnością w układzie sercowo-naczyniowym (ochraniających ścianę naczyń lub szerzej cytoprotekcyjnch), głównie w kontekście profilaktyki powikłań cukrzycy (angiopatii cukrzycowych). W badaniach wykorzystano naturalne i syntetyczne związki, ich analogi strukturalne i przetwory z substancji roślinnych o powyższym profilu działania. Pochodzące zasadniczo z przemian węglowodanów reaktywne α-DC odpowiedzialne są w organizmach żywych za szereg szkodliwych reakcji występujących równolegle i wzajemnie się aktywujących, w tym nasilają stres karbonylowy, stres oksydacyjny, nieenzymatyczną glikację, generują powstawanie wiązań krzyżowych białek, AGE i modyfikacji licznych makromolekuł (insuliny, hemoglobiny, albumin osocza, lipoprotein, kolagenu, krystaliny i innych) [50]. Prowadzi to ostatecznie do stanu zapalnego i zaburzeń funkcjonowania komórek, tkanek i narządów oraz skutkuje progresją chorób kardiometabolicznych, m.in. cukrzycy i jej powikłań [5]. Ponieważ procesy te są ze sobą powiązane, w przeprowadzonych badaniach oceniono także efekt antyoksydacyjny i antyglikacyjny wybranych substancji.

Leki wazorptotekcyjne (wenoaktywne, flebotropowe) to szeroka i bardzo różnorodna pod względem budowy chemicznej grupa leków, mających na celu ochronę układu naczyniowego i poprawę jego funkcjonowania. Do tej kategorii leków, oznaczonej kodem C05 w systemie ATC (ang. *the Anatomical Therapeutic Chemical Classification System*), zaliczamy między innymi bioflawonoidy (C05CA) i dobesylan wapnia (C05BX) [51]. Pomimo że leki z tej grupy wykorzystywane są z powodzeniem w lecznictwie już od kilku dekad to do tej pory niewiele uwagi poświęcono mechanizmom molekularnym leżącym u podstaw ich potencjalnego działania ochronnego przed reaktywnymi karbonylami. Dlatego w **publikacji P1** zbadano, czy substancje

stosowane jako środki wazoprotekcyjne (diosmina, trokserutyna, rutyna i dobesylan wapnia) oraz ich analogi strukturalne (hesperydyna i aglikony bioflawonoidów), mają potencjał wychwytywania metyloglioksalu i glioksalu, zdolność do hamowania indukowanej przez α-dikrarbonyle nieenzymatycznej glikacji makromolekuł (w modelu z albuminą wołową). Porównano także ich aktywność przeciwglikacyjną i przeciwutleniającą *in vitro,* w odniesieniu do uznanych inhibitorów aminoguanidyny, metforminy i kwercetyny. Badanie wykazało, że w warunkach eksperymentu kwercetyna, rutyna, diosmetyna, hesperetyna, hesperydyna i metformina wykazywały aktywność w kierunku bezpośredniego wychwytywania metyloglioksalu, podczas gdy glioksal był pułapkowany jedynie przez rutynę, diosmetynę, hesperetynę i hesperydynę. Trokserutyna, diosmina i dobesylan wapnia nie pułapkowały reaktywnych dikarbonyli, prawdopodobnie z powodu różnic w budowie chemicznej. Metformina natomiast w warunkach eksperymentu nie tworzyła adduktu z glioksalem. Podsumowanie wyników pułapkowania metyloglioksalu i glioksalu dla wszystkich związków zbadanych w **publikacjach P1, P3, P4** znajduje się w **Tabeli 1** i **2**. Poza wskazaniem, czy dany związek może tworzyć addukty z MGO i GO, na podstawie mas jonów psudomoleklularnych i fragmentacji, zaproponowano również ich potencjalne struktury chemiczne (**Rycina 3** przedstawia propozycję struktur adduktów na przykładzie aspalatyny i notofaginy z MGO i GO). Analizę prowadzono z wykorzystaniem trybu EIC (ang. *Extracted Ion Chromatogram*). Pozwoliło to uzyskać precyzyjne dane na temat intensywności określonego jonu (lub zakresu jonów) w funkcji czasu podczas analizy LC-MS. W trybie EIC każdorazowo poszukiwano jonów pseudomolekularnych zwiększonych o 72 Da lub 144 Da odpowiednio dla adduktów mono-MGO i di-MGO oraz o 58 Da lub 116 Da dla adduktów mono-GO i di-GO.

Po raz pierwszy wykazano bezpośrednią aktywność wychwytywania MGO i GO dla hesperetyny, hesperydyny i diosmetyny. Badanie potwierdziło również następujące zależności między strukturą a aktywnością flawonoidów: (1) podstawienie grupy hydroksylowej w pozycji C-7 pierścienia benzenowego A powoduje zmniejszenie zdolności wychwytywania metyloglioksalu i glioksalu (kwercetyna i rutyna vs. trokserutyna, diosmetyna vs. diosmina, hesperetyna vs. hesperydyna); (2) wiązanie podwójne w pierścieniu heterocyklicznym C również zmniejsza wychwytywanie α-dikarbonyli (hesperetyna i hesperydyna vs. diosmetyna i diosmina). Wbrew wcześniejszym doniesieniom [52] uzyskane wyniki ujawniły również, że budowa pierścienia fenylowego B jest istotna dla aktywności pułapkującej flawonoidów. Podstawienie

grupy -OH w pozycji C-4' pierścienia B stabilizuje cząsteczkę, zapobiegając tworzeniu się struktur semichinonu i chinonometydu oraz dalszemu rozszczepianiu heterocyklicznego pierścienia C. W ten sposób pierwotna struktura flawonoidu jest prawdopodobnie bardziej stabilna, a aktywność pułapkująca podtrzymana.

Tabela 1. Addukty metyloglioksalu i badanych substancji powstałe po 1 h inkubacji w buforowanym roztworze soli fizjologicznej o pH 7,4 w temperaturze 37 °C.

Substancja	**Źródło**	**Pik**	**Rt [min]**	**$[M-H]^-$ lub $[M+H]^+$ mono-MGO addukt (*m*/*z*)**	**Pik**	**Rt [min]**	**$[M-H]^-$ lub $[M+H]^+$ di-MGO addukt (*m*/*z*)**
Flawonole							
Rutyna[P1]	S	a- c	8.69; 8.84; 8.85	681.1698	a-c	7.90; 8.26; 8.44	753.1885
Trokserutyna[P1]	S	-	-	n.d.	-	-	n.d.
Kwercetyna[P1]		a-b	10.93; 11.06	373.0567	a	10.01	445.0779
Flawony							
8-C-glukozyd apigeniny (witeksyna)[P4]	S	a-b	20.55; 20.86	503.1205	-	-	n.d.
6-C-glukozyd apigeniny (izowiteksyna)[P4]	S	a-b	20.82; 21.50	503.1191	-	-	n.d.
Diosmina[P1]	S	-	-	n.d.	-	-	n.d.
Diosmetyna[P1]	S	a-b	12.19, 12.36	371.0758	a	11.24	443.0970
Flawanony							
Hesperidydyna[P1]	S	a-f	8.97; 9.19; 9.82; 9.95; 10.88; 10.98;	681.1972	-	-	n.d.
Hesperetyna[P1]	S	a-b	12.04; 12.93	373.0913	a	10.80	445.1103
Eriodykcjol[P4]	S	a-d	21.50; 21.57; 22.46; 24.67	359.0772	-	-	n.d.
Chalkony							
Aspalatyna[P4]	S	a-b	19.85; 21.45	523.1475	-	-	n.d.
	GR	a-d	19.85; 21.45; 25.65; 26.93	523.1475	-	-	n.d.
Notofagina[P4]	GR	a-c	21.95; 23.43; 28.05	507.1519	-	-	n.d.
Floretyna[P4]	S	a	28.82	345.0993	a-b	27.05; 27.46	417.1197

Pochodne guanidyny							
Metformina[P1]	S	a	1.48	184.1158[g]	a-b	1.57; 1.64	256.1297
		b	1.20	202.1229			
Galegina[P3]	S	a-c	1.41; 2.28; 2.61	200.1367	-	-	n.d.
	Inf	a	2.61	200.1386	-	-	n.d.
Hydroksygalegina[P3]	Inf	a	0.98	216.1334	-	-	n.d.
Związki syntetyczne							
Dobesylan wapnia[P1]	S	-	-	n.d.	-	-	n.d.
Floroglucynol[P4]	S	a-b	4.28; 17.32	197.0549	a-c	8.43; 14.28; 16.71	269.0813
					a-b*	14.56; 15.01	341.1067

P1, publikacja P1; P2, publikacja P2; P3, publikacja P3; P4, publikacja P4; S, standard; GR, wyciąg wodno-etanolowy z zielonego rooibos; Inf, napar; litery a-f reprezentują zidentyfikowane izomery tego samego związku; g, forma imidazolonu utworzona przez eliminację jednej cząsteczki wody z mono-MGO-metforminy; n.d., nie wykryto adduktu; *, tri-MGO-floroglucynol

Tabela 2. Addukty glioksalu i badanych substancji powstałe po 1 h inkubacji w buforowanym roztworze soli fizjologicznej o pH 7,4 w temperaturze 37 °C.

Substancja	**Źródło**	**Pik**	**Rt [min]**	**$[M-H]^-$ lub $[M+H]^+$ mono-GO addukt (*m*/*z*)**	**Pik**	**Rt [min]**	**$[M-H]^-$ or $[M+H]^+$ di-GO addukt (*m*/*z*)**
Flawonole							
Rutyna[P1]	S	a-b	8.09; 8.41;	667.1445	-	-	n.d.
Trokserutyna[P1]	S	-	-	n.d.	-	-	n.d.
Kwercetyna[P1]	S	-	-	n.d.	-	-	n.d.
Flawony							
8-C-glukozyd apigeniny (witeksyna)[P4]	S	a-b	19.03; 19.19	489.1033	-	-	n.d.
6-C-glukozyd apigeniny (izowiteksyna)[P4]	S	-	-	n.d.	-	-	n.d.
Diosmina[P1]	S	-	-	n.d.	-	-	n.d.
Diosmetyna[P1]	S	a-b	11.64, 12.1	357.0605	-	-	n.d.
Flawanony							
Hesperidydyna[P1]	S	a-b	11.05; 11.37	677.1861	-	-	n.d.
Hesperetyna[P1]	S	a-c	11.28; 12.37; 13.78	359.0771	a	12.99	417.0808
Eriodykcjol[P4]	S	a-b	21.56; 22.13	345.0813	-	-	n.d.
Chalkony							

Aspalatyna[P4]	S	a-c	18.68; 19.81; 24.86	509.1311	-	-	n.d.
	GR	a-c	18.68; 19.81; 24.86	509.1314	-	-	n.d.
Notofagina[P4]	GR	-	-	n.d.	-	-	n.d.
Floretyna[P4]	S	a	26.88	331.0833	-	-	n.d.
Pochodne guanidyny							
Metformina[P1]	S	a	1.48	184.1158[g]	a-b	1.57; 1.64	256.1297
Galegina[P3]	S	a-c	1.41; 2.28; 2.61	200.1367	-	-	n.d.
	Inf	a	2.61	200.1386	-	-	n.d.
Hydroksygalegina[P3]	Inf	a	0.98	216.1334	-	-	n.d.
Związki syntetyczne							
Dobesylan wapnia[P1]	S	-	-	n.d.	-	-	n.d.
Floroglucynol	S	a	13.79	183.0366	a	8.15	241.0482

P1, publikacja P1; P2, publikacja P2; P3, publikacja P3; P4, publikacja P4; S, standard; GR, wyciąg wodno-etanolowy z zielonego rooibos; Inf, napar; litery a-c reprezentują zidentyfikowane izomery tego samego związku; n.d., nie wykryto adduktu

Dla związków wykazujących zdolność do bezpośredniego wychwytywania metyloglioksalu (rutyna, kwercetyna, diosmetyna, hesperydyna, hesperetyna, metformina) i glioksalu (rutyna, diosmetyna, hesperydyna, hesperetyna) przeprowadzono badanie przebiegu w czasie reakcji pułapkowania. Aby określić ilość MGO/GO pozostałą po inkubacji w każdym punkcie czasowym, próbki derywatyzowano za pomocą 1,2-fenylenodiaminy (o-PDA). Badanie wykazało, że aktywność pułapkowania metyloglioksalu różniła się między badanymi związkami, podczas gdy glioksal był wychwytywany przez wszystkie badane związki z podobną skutecznością. W ciągu 24 godzin hesperetyna, kwercetyna, rutyna i diosmetyna zdołały wychwycić od 68 do 85 % MGO i zostały uznane za najbardziej skuteczne spośród badanych związków. Nieco niższe wartości odnotowano dla hesperydyny ~ 40%. Wśród najsilniej działających związków widoczne były różnice w kinetyce reakcji wychwytywania MGO. Hesperetyna i kwercetyna wiązały 50% metyloglioksalu w ciągu zaledwie dwóch godzin. Natomiast diosmetyna i rutyna były w stanie wychwycić mniej niż 15% MGO w tym samym czasie i oba związki potrzebowały ponad 8 godzin, aby wyeliminować 50% metyloglioksalu. Dla metforminy stosowanej jako lek pierwszego rzutu w cukrzycy typu 2, zdolność do wychwytywania

metylogliooksalu wykazano wcześniej w badaniach *in vitro* i *in vivo* [32,53]. Jednak wyniki naszego eksperymentu sugerują, że jej aktywność w wychwytywaniu MGO w porównaniu z substancjami flawonoidowymi była stosunkowo niska (ok. 17%). Po 24 godzinach inkubacji hesperetyna i rutyna okazały się najbardziej skuteczne w wychwytywaniu glioksalu, wygaszając odpowiednio 81% i 75% GO. Tylko nieznacznie mniej skuteczna była hesperydyna i diosmetyna z (ok. 67%). Wyniki sugerują, że glioksal wydaje się być szybciej wychwytywany w porównaniu do metylogliooksalu. Zarówno hesperetyna, jak i rutyna były w stanie wyeliminować z roztworu prawie 50% glioksalu w ciągu zaledwie jednej godziny, a hesperydyna i diosmetyna w czasie 2 godzin.

Wszystkie związki niezależnie od aktywności pułapkującej przebadano również pod kątem zdolności do hamowania procesu nieenzymatycznej glikacji białek. W modelu z metylogliooksalem jako czynnikiem indukującym proces glikacji i albuminą wołową jako białkiem celowanym, najsilniejszymi inhibitorami tworzenia AGE okazały się hesperetyna, hesperydyna, dobesylan wapnia i kwercetyna z aktywnością hamującą odpowiednio 57%, 52%, 50% i 47%. Aktywność aminoguanidyny, użytej jako inhibitor referencyjny, była niższa niż w przypadku powyżej wymienionych substancji i porównywalna z aktywnością metforminy, diosminy i trokserutyny na poziomie ~ 40%. Aminoguanidyna była bardziej aktywna jedynie od rutyny (33%) i diosmetyny (31%). Nieco inne wyniki uzyskano w modelu z glioksalem jako czynnikiem glikującym, gdzie diosmetyna (40%) i hesperydyna (31%) były najsilniejszymi inhibitorami glikacji, a ich aktywność przewyższała aktywność aminoguanidyny (31%). Hesperetyna, kwercetyna, rutyna, a następnie dobesylan wapnia i diosmina wykazywały podobną, nieco słabszą aktywność w przedziale 20-27%, natomiast najsłabszą zdolność hamowania glikacji indukowanej GO wykazywały trokserutyna (8%) i metformina (6%). Testy aktywności przeciwutleniającej potwierdziły, że związkami o wysokim potencjale przeciwutleniającym - redukującym i przeciwrodnikowym są kwercetyna, rutyna, hesperetyna i dobesylan wapnia, a ich aktywność jest zależna od stężenia. Potwierdzono również, że aktywność antyoksydacyjna aglikonów flawonoidowych jest generalnie wyższa niż odpowiednich glikozydów. Interesującym przykładem związku wykazującego silne właściwości antyglikacyjne przy jednoczesnym braku potencjału do pułpakowania α-DC był dobesylan wapnia. Prawdopodobnie główną składową efektu antyglikacyjnego tego związku są silne właściwości antyoksydacyjne jak wykazano w badaniu własnym. Warto zaznaczyć, że z uwagi na wysoką biodostępność, stężenie dobesylanu wapnia w osoczu uzyskiwane po zażyciu

dawki terapeutycznej 500 mg (niewydolność żylna: od 500 do 1000 mg na dobę; retinopatia cukrzycowa: od 1000 do 1500 mg na dobę) przewyższa stężenia, jakie mogą osiągać bioflawonoidy mające w badaniach własnych podobną aktywność antyglikacyjną (np. hesperetyna czy hesperydyna) nawet 5 razy [54, 55, 56]. A zatem mimo podobnych wyników w testach *in vitro,* można założyć, że efekt w ludzkim organizmie będzie silniejszy dla związku osiagającego wyższe stężenia w ustroju. Tym samym biodostępność jest niewątpliwie czynnikiem jaki należy brać pod uwagę przy projektowaniu dalszych badań.

Wyniki **publikacji P1** wskazują jednoznacznie, że substancje wazoprotekcyjne i ich analogi strukturalne mogą skutecznie wychwytywać MGO i GO (bioflawonoidy) oraz ograniczać proces glikacji indukowany α-dikarbonylami, dodatkowo wykazaując aktywność antyoksydacyjną, co może korzystnie wpływać na śródbłonek naczyń krwionośnych.

W kolejnej publikacji (**publikacja P2**) dokonano weryfikacji zdolności hesperydyny do obniżania osoczowego stężenia metyloglioksalu *in vivo.* W próbie klinicznej z udziałem zdrowych ochotników wykorzystano kombinację ekstraktu z naowocni pomarańczy słodkiej (*Citrus* × *sinensis* (L.) Osbeck) i koncentratu soku z owocu granatowca (*Punica granatum* L.) (produkt CPC), w którym hesperydyna była głównym składnikiem. Zarówno dla glikozydu – hesperydyny, jak i jej aglikonu – hesperetyny, będącej głównym metabolitem jelitowym hesperydyny w organizmie ludzkim, wcześniejsze badania *in vitro* opisane w **publikacji P1** wykazały zdolność do wiązania MGO i GO. Hesperydyna, mimo że nie jest klasyfikowana w systemie ATC jako substancja wazoprotekcyjna stanowi składnik preparatów złożonych stosowanych w przewlekłej niewydolności żylnej i zaburzeniach mikrokrążenia, objawiających się obrzękami i bólem. Eksperyment kliniczny (wtórna analiza podwójnie zaślepionego, randomizowanego, krzyżowego badania klinicznego u zdrowych osób w podeszłym wieku) udowodnił, że stosowanie CPC przez okres 4 tygodni spowodowało spadek steżenia wszystkich trzech α-dikarbonyli, dla aktórych wykoano oznaczenia, tj.: MGO, GO i 3-DG. Statystycznie istotny spadek stężenia w osoczu w porównaniu z placebo zaobserwowano dla MGO, wykazując redukcję o -18,7 nM/L (9,8% od wartości wyjściowej). Z kolei obniżenie stężeń GO i 3-DG wywołane CPC nie było istotne statystycznie i wynosił odpowiednio -7,8 nM/L (spadek o 6,6% w stosunku do wartości wyjściowych) i -16,6 nM/L (spadek o 2,9% w stosunku do wartości wyjściowych). Wcześniejsze badania obserwacyjne wykazały, że stężenia metyloglioksalu są istotnie związane z

występowaniem zdarzeń sercowo-naczyniowych w cukrzycy. Różnica w stężeniach MGO w osoczu między diabetykami, którzy doświadczyli zdarzeń sercowo-naczyniowych, a tymi, którzy ich nie doświadczyli, wynosi od 5% do 13% [29]. Oznacza to, że zmniejszenie stężenia MGO w osoczu o 9,8%, jak stwierdzono w niniejszym badaniu z CPC, może mieć znaczenie kliniczne (**publikacja P2**). Badanie przeprowadzone w ramach **publikacj P2** stanowiły wtórną analizę materiału biologicznego pozyskanego na potrzeby badania klinicznego zatytuowanego „*The Effect of a Combination of Orange and Pomegranate Actives on Physical Fitness in Elderly People*". Szczegóły dotyczące badania i produktu badanego znajdują się w sekcji Metody 3.7.

W **publikacji P3** i **P4** zweryfikowano tezę, iż substancje roślinne posiadające w składzie chemicznym pochodne guanidyny, glikozydy flawonoidowe oraz inne polifenole o aktywności antyoksydacyjnej mogą hamować glikację, m.in. przez wychwytywanie α-dikarbonyli. Surowce roślinne do badań wybrano na podstawie ich znanych właściwości leczniczych lub prozdrowotnych oraz korzystnego wpływu na hiperglikemię i zaburzenia ze strony układu krążenia.

W **publikacji P3** przedmiot badań stanowiło ziele rutwicy (*Galegae herba*) stosowane dawniej w leczeniu objawów cukrzycy takich jak polidypsja i poliuria [57]. Współczesna literatura naukowa dostarcza informacji potwierdzających, że rutwica lekarska zawiera składniki, które mogą wpływać na metabolizm glukozy, obniżając jej stężenie we krwi, np. galegina, stanowiąca pierwowzór dla powszechnie stosowanej dziś metforminy [58]. Ponadto w badaniach na zwierzętach z wykorzystaniem gryzoni zaobserwowano korelację między przyjmowaniem ekstraktów z ziela rutwicy a utratą masy ciała i zwiększaniem wydzielania insuliny przez komórki β trzustki [59,60]. Z powodu braku współczesnych badań dotyczących profilu bezpieczeństwa, ziele rutwicy jest w Polsce i Unii Europejskiej rzadziej stosowane, choć nadal bywa wykorzystywane leczniczo w krajach mniej uprzemysłowionych. Niewiele też wiadomo o jego składnikach innych niż alkaloidy i częściowo o flawonoidach. Dlatego w pierwszym etapie badań przeprowadzono profilowanie składu chemicznego ziela rutwicy (trzy serie Gof1, Gof2 i Gof3) przy użyciu metod chromatograficznych (UHPLC-ESI-MS, HPLC-DAD). Dla każdej grupy związków zidentyfikowanych w surowcu wybrano związek reprezentatywny do dalszych badań aktywności *in vitro* – galeginę z grupy pochodnych guanidynowych, rutynę jako przedstawiciela oligoglikozydów flawonoli, kwas chlorogenowy z grupy estrów kwasu hydroksycynamonowego.

Wyselekcjonowane związki oraz przetwory z surowca postanowiono przetestować następnie pod kątem zdolności wychwytywania MGO i aktywności przeciwutleniającej, aby ocenić, czy mają one właściwości potencjalnie przydatne w ochronie naczyń krwionośnych. Analiza UHPLC-ESI-MS wyciągów wodnych i wodno-metanolowych ziela rutwicy pozwoliła na wykrycie 39 związków. Wśród pochodnych guanidynowych zidentyfikowano galeginę i hydroksygaleginę, natomiast w grupie trójpierścioniowych alkaloidów chinazolinowych zidentyfikowano wazycynę, hydroksywazycynę, *O*-heksozyd wazycyny i wazycynon. Wśród pochodnych kwasu hydroksycynamonowego w surowcu dominowały estry kwasów kawowego, ferulowego i *p*-kumarowego z kwasem heksarowym (aldarowym). Analiza związków w grupie flawonoidów potwierdziła obecność piętnastu związków. Większość wykrytych flawonoidów stanowiły *O*-glikozydy flawonoli - kemferolu, kwercetyny, izoramnetyny. Zidentyfikowanych zostało siedem glikozydów kemferolu, sześć glikozydów kwercetyny i tylko jedna pochodną izoramnetyny. Ponadto zaobserwowano jeden flawanonol (glikozyd taksyfoliny). Glukoza, galaktoza i ramnoza były połączone z aglikonami jako mono-, di- lub triglikozydy. Wszystkie zidentyfikowane związki wraz z nazwami chemicznymi i profilami fragmentacji MS/MS znajdują się w odnośnej publikacji. W testach *in vitro* zaobserwowano, że poza rutyną i kwercetyną również galegina posiada zdolność do wychwytywania MGO podobnie jak metformina (wykorzystana jako substancja odniesienia). Nie stwierdzono natomiast aktywności pułapkującej dla kwasu chlorogenowego. Wśród związków obecnych w naparze z ziela *G. officinalis* aktywność wychwytującą MGO wykazywały rutyna, galegina i hydroksygalegina. Ustalono, że przyczyną, dla której addukty z metyloglioksalem wykryto jedynie dla powyższych związków wynika prawdopodobnie z tego, że to one stanowiły główne składowe naparu i były w nim obecne w najwyższym stężeniu mogąc najefektywniej wiązać się z MGO. Dla powstałych adduktów przestawiono propozycje wzorów strukturalnych w oparciu o wyniki analizy UHPLC-ESI-MS. Przy uwzględnieniu wartości IC_{50} wyrażonych w stężeniu mikromolowym, aktywność przeciwrodnikowa dla zbadanych indywidualnych związków układa się w następującej kolejności w teście DPPH: kwas galusowy > kwercetyna > rutyna > kwas chlorogenowy >>> siarczan galeginy. W teście ABTS szereg był następujący: kwercetyna > troloks > rutyna > kwas chlorogenowy >>> siarczan galeginy. Chociaż metformina nie wykazała działania antyoksydacyjnego *per se* związanego z przenoszeniem elektronu (testy DPPH, ABTS), niektóre badania donoszą o jej właściwościach chelatujących, które mogą hamować katalizowane przez jony metali przejściowych reakcje utlenianiai. Wartości % inhibicji obliczone zarówno dla

naparów, jak i ekstraktów wodno-metanolowych (w stężeniu 18 μg/mL w DPPH i 2 μg/mL w ABTS) wykazały wyższą aktywność hamującą niż rutyna i kwas chlorogenowy, ale niższą niż kwercetyna. Może to sugerować, że aktywność przeciwutleniająca przetworów *G. officinalis* opiera się nie tylko na związkach polifenolowych. Analiza fitochemiczna ekstraktów z ziela rutwicy wykazała również obecność trójpierścieniowych alkaloidów chinazolinowych, które według ostatnich badań posiadają silną aktywność przeciwrodnikową i mogą przyczyniać się do potencjału antyoksydacyjnego *Galegae herba*. Można również założyć synergizm pomiędzy zidentyfikowanymi składnikami badanych przetworów. Na podstawie uzyskanych wyników został wysunięty wniosek, że polifenole i pochodne guanidyny zawarte w przetworach z ziela *G. officinalis* wykazują potencjał antyoksydacyjny i wychwytujący MGO, co w przyszłości może zostać wykorzystane w profilaktyce schorzeń, w których metylglioksal odgrywa kluczową rolę. Niemniej jednak szczególnie z uwagi na raportowaną wcześniej toksyczność [61] konieczne są dalsze badania w modelach *in vivo*.

W **publikacji P4** analizie poddano części nadziemne czerwonokrzewu - *Aspalathus linearis* (Burm.f.) R.Dahlgren. Roślina ta jest uprawiana dla herbaty znanej jako rooibos, występującej komercyjnie w dwóch odmianach, niefermentowanej (zielony rooibos, GR) i fermentowanej (czerwony rooibos, RR) [62]. Dotychczasowe dane literaturowe sugerują, że może mieć ona pozytywny wpływ na układ krążenia. Liczne badania eksperymentalne dowodzą, że surowiec ten działa ochronnie na naczynia krwionośne dzięki właściwościom antyoksydacyjnym i przeciwzapalnym [63,64]. Ponadto polifenole zawarte w przetworach z czerwonokrzewu uwrażliwiają hepatocyty na insulinę i przez to mogą opóźniać rozwój insulinooporności [65]. Znane są również właściwości hipoglikemiczne *A. linearis*, dlatego może być on szczególnie polecany pacjentom w stanie przedcukrzycowymi i z cukrzycą jako środek wspomagający [66]. Pomimo tak obszernych badań nad korzystnymi właściwościami kardiometabolicznymi *A. linearis*, do tej pory nie oceniono, czy mechanizm działania jego głównych składników obejmuje również wychwytywanie metylogliokslu i glioksalu oraz aktywność antyglikacyjną. W związku z powyższym, w ostatniej publikacji cyklu (**publikacja P4**) ocenie poddano aspalatynę, dihydrochalkon o strukturze *C*-glikozydu występujący w herbacie rooibos oraz pozostałe składniki tego surowca wytypowane na podstawie profilu fitochemicznego – witeksynę i izowiteksynę jako przedstawicieli *C*-glikozydów flawonów, eriodykcjol z flawanonów i floretynę jako aglikon notofaginy. Oceniono także napary i wyciągi wodno-etanolowego z surowca fermentowanego i

niefermentowanego o składzie bardziej zbliżonym do materiału wyjściowego. Potencjał antyglikacyjny i zdolność pułapkowania MGO i GO badanych substancji porównano z analogicznymi właściwościami metforminy i floroglucynolu - trifenolu będącego podstawą układu pierścienia A flawonoidów. Ponadto zbadano właściwości antyglikacyjne wyciągów wodno-etanolowych z rooibos. Badanie składu chemicznego wykazało, że przetwory z RR i GR charakteryzowały się obecnością *C*-glikozydów dihydrochalkonów - aspalatyny i notofaginy, podczas gdy acetyloaspalatynę zaobserwowano jedynie w RR. Oba surowce zawierały również po dwie pary diastereoizomerów *C*-glikozydów eriodykcjolu: (*S*)-6-*C*-, (*R*)-6-*C*-, (*S*)-8-*C*- i (*R*)-6-*C*-glukozyd eriodykcjolu. Najliczniejszą grupą flawonoidów występującą w fermentowanym rooibos były flawony. W analizowanych ekstraktach *A. linearis* zidentyfikowano izomery pozycyjne *C*-glikozydów apigeniny i luteoliny: witeksynę/izowiteksynę oraz orientynę/izoorientynę, a także di-*C*-glikozydy, m.in. karlinozyd. Aglikony flawonów, takie jak luteolina i chrysoeriol, oraz flawanony, głównie eriodykcjol, zostały zidentyfikowane w niesfermentowanym materiale roślinnym, podczas gdy *O*-glikozydy flawonoli, jak biokwercetyna (3-*O*-robinobiozyd kwercytyny), rutyna, hiperozyd i izokwercytryna zostały wykryte w większych ilościach w sfermentowanym rooibos. Główną różnicę w składzie obu rodzajów rooibos stanowi zawartość aspalatyny, która jest znacznie wyższa w niesfermentowanym materiale roślinnym. W sfermentowanym surowcu ulega ona procesom utleniania i jest przekształcana w *C*-glukozydy eriodykcjolu. Ocena ilościowa zawartości flawonoidów pozwoliła ustalić, że wyciąg wodno-etanolowy z GR zawierał aż 65,5 mg/100 mL (1443,1 μM/L) flawonoidów, podczas gdy tak samo przygotowany ekstrakt z RR zawierał ich jedynie 13,6 mg/100 mL (320,2 μM/L). Tak więc rooibos zielony był ok. 4,5 razy bogatszy we flawonoidy i 15,6 razy bogatszy w dihydrochalkony niż czerwony. Zdolność do wychwytywania metyloglioksalu i glioksalu została zbadana dla poszczególnych flawonoidów zidentyfikowanych w przetworach z rooibos (aspalatyny, witeksyny, izowiteksyny i eriodiktyolu) wobec substancji odniesienia o znanej aktywności pułapkującej i podobnej budowie chemicznej (floretyna, floroglucynol) oraz w odniesieniu do aminoguanidyny i metforminy. Następnie te same testy przeprowadzono z wykorzystaniem ekstraktów GR i RR. Wyniki tego badania pozwoliły stwierdzić, że w warunkach eksperymentu wszystkie badane związki (aspalatyna, witeksyna, izowiteksyna, eriodykcjol, floretyna, floroglucynol) wykazywały aktywność w kierunku bezpośredniego wychwytywania metyloglioksalu, podczas gdy tylko aspalatyna, witeksyna i eriodykcjol wykazywały zdolność do

wychwytywania glioksalu. Podobnie floretyna i floroglucynol stosowane jako substancje odniesienia wychwytywały oba α-dikarbonyle. W przypadku wyciągu wodno-etanolowego RR nie zaobserwowano adduktów ani z MGO, ani z GO, co prawdopodobnie wynika z niskiego stężenia flawonoidów w ekstrakcie w porównaniu do GR - jak wykazano w pierwszym etapie pracy. W wyciągu z GR tylko dihydrochalkony były źródłem adduktów z MGO (aspalatyna i nothofagina) i GO (aspalatyna). Dla wszystkich związków wykazujących aktywność w kierunku bezpośredniego pułapkowania α-DC w oparciu o wyniki uzyskane w analizie UHPLC-ESI-MS zaproponowano struktury adduktów uwzględniając możliwe warianty podstawienia cząsteczki dikarbonylu oraz formę hemiactalową i hemiketalową powstałej cząsteczki. Struktury adduktów na przykładzie aspalatyny i notofaginy przedstawiono na **Rycinie 3**.

W oparciu o wyniki uzyskane w **publikacji P4** można potwierdzić, że to układ floroglucynolu pierścienia benzenowego A flawonoidów determinuje reakcję pułapkowania α-dikarbonyli. Ułożenie grup -OH w pierścieniu benzenowym w pozycji *meta* względem siebie stwarza warunki do addycji nukleofilowej MGO i GO. Pierścień A z wolnymi dwoma lub trzema grupami hydroksylowymi i niepodstawionymi protonami przy bezpośrednio sąsiadujących atomach węgla (układ floroglucynolu) jest kluczowym elementem aktywności pułapkującej flawonoidów. Zaburzenie tej struktury poprzez związanie lub brak jednej z wolnych grup hydroksylowych (np. w C-7 w pierścieniu A) lub wprowadzenie podstawników przy sąsiadujących z nimi pozycjach (jak w C-8 i C-6 *C*-glikozydów) wpływa na obniżenie lub zniesienie zdolności do wychwytywania α-DC (zablokowanie pozycji przyłączenia α-DC). Jednak potrzebne są dalsze badania, by wyjaśnić szczegółowo wagę tych modyfikacji w budowie flawonoidów.

Badanie aktywności antyglikacyjnej rooibos przeprowadzono w dwóch modelach *in vitro* – podobnie jak we wcześniejszych publikacjach. W modelu wykorzystującym metyloglioksal wszystkie badane związki wykazywały dość wysoką aktywność hamującą powstawanie AGE. Największą aktywność antyglikacyjną zaobserwowano dla *C*-glukozydów apigeniny, tj. izowiteksyny (84%) i witeksyny (82%), a wartości te przewyższały aktywność aminoguanidyny (75%) użytej jako odnośnik. Podobnie floretyna będąca aglikonem notofaginy, posiadała silną aktywność anty-AGE na poziomie aminoguanidyny (79%). Główny składnik zielonego rooibos aspalatyna hamowała powstawanie AGE na poziomie 61%, ale wynik ten był nadal wyższy niż aktywność metforminy (52%). Floroglucynol, którego struktura stanowi rdzeń dihydrochalkonów

rooibos (pierścień A flawonoidów), charakteryzował się aktywnością antyglikacyjną podobną do aspalatyny (60%). Floroglucynol jest substancją czynną leków przeciwskurczowych w niektórych krajach głównie poza Europą, a jego zdolność do wychwytywania reaktywnych form karbonylowych wykazano wcześniej. Eriodykcjol był najmniej skuteczny w hamowaniu AGE indukowanych przez MGO (43%). W modelu glikacji indukowanej glioksalem izowiteksyna (6-*C*-glukozyd apigeniny) okazała się również najsilniejszym czynnikiem antyglikacyjnym (82%), a jej potencjał hamujący tworzenie AGE był ponad dwukrotnie wyższy niż aminoguanidyny (36%) i trzykrotnie wyższy niż metforminy (25%) - różnice te były istotne statystycznie. Aktywność floretyny i witeksyny była podobna i wynosiła ok. 30%. Aspalatyna hamowała glikację wywołaną GO jedynie na poziomie 13%. Aktywność floroglucynolu była natomiast marginalna (<3%), a w przypadku eriodykcjolu nie zaobserwowano hamującego wpływu na tworzenie AGE wywołane glioksalem. W modelu z GO, podobnie jak w poprzednim modelu, jedynie wyciąg wodno-etanolowy z GR wykazywał aktywność przejawiającą się działaniem hamującym glikację białek. Efekt hamujący ekstraktu z niefermentowanego rooibos był na poziomie 16 % (zbliżonym do aktywności głównego składnika aspalatyny).

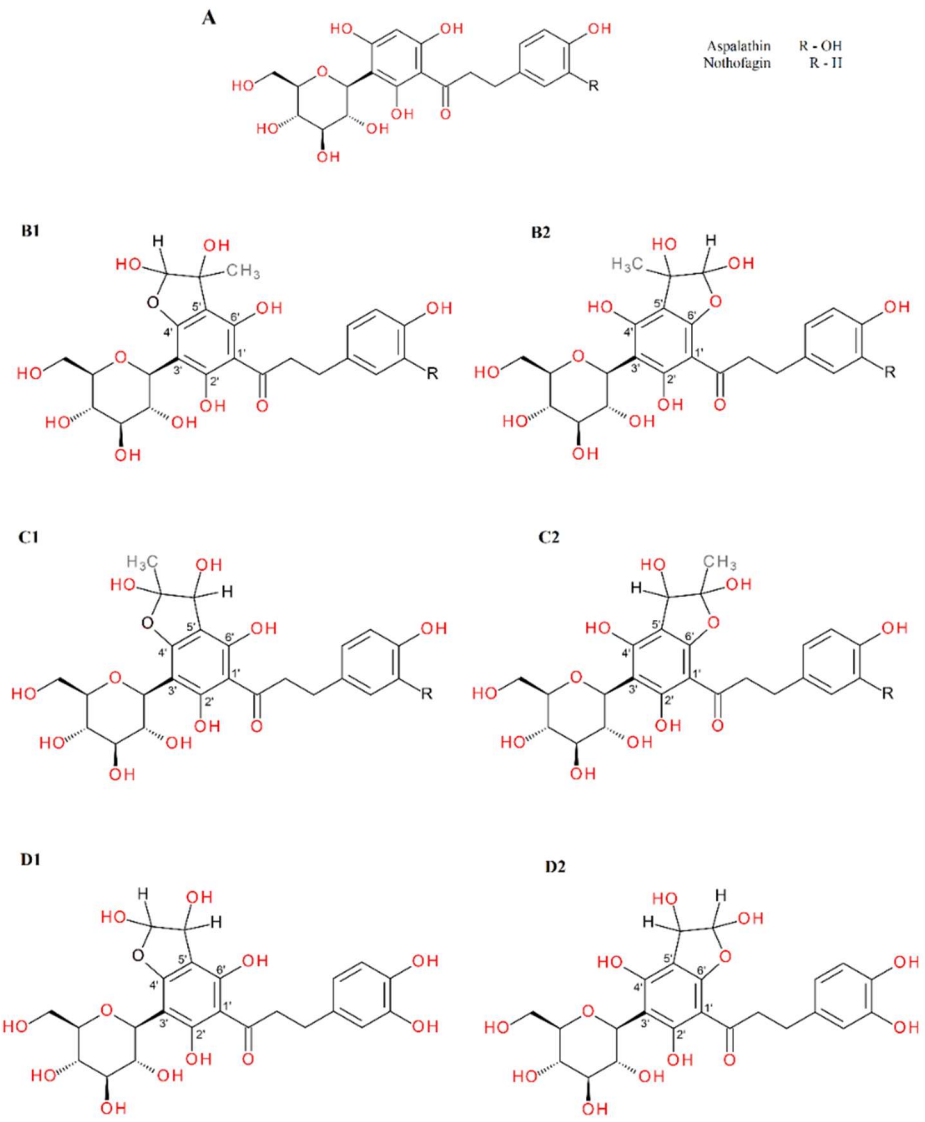

Rycina 3. Propozycje struktur chemicznych adduktów powstałych w reakcji aspalatyny/notofaginy z metyloglioksalem/glioksalem po 1 h inkubacji w roztworze soli fizjologicznej buforowanym fosforanami (pH 7.4) w temperaturze 37 °C; (A), aspalatyna/notofagina; (B1, B2), formy hemiacetalowe mono-MGO-aspalatyny/notofaginy; (C1, C2), formy hemiketalowe mono-MGO-aspalatyny/notofaginy; (D1, D2), izomery mono-GO-aspalatyny. Możliwe są również inne izomery.

Hamowanie nieenzymatycznej glikacji związane jest prawdopodobnie z kilkoma różnymi mechanizmami. Przeprowadzone dotychczas badania wskazują, że elementami składowymi aktywności przeciwglikacyjnej są: aktywność przeciwutleniająca, przeciwrodnikowa, zdolność do chelatowania metali przejściowych oraz zdolność związków do wychwytywania α-DC. Często działania te występują jednocześnie, zwłaszcza w grupie naturalnych związków flawonoidowych.

Przykładem flawonoidu działającego poprzez wszystkie te mechanizmy jest kwercetyna – antyoksydant dobrze znany w kontekście hamowania procesu glikacji, który charakteryzuje się bardzo silnym działaniem przeciwrodnikowym, właściwościami chelatującymi oraz zdolnością do wychwytywania MGO i GO [67]. Odmiennie dla pochodnej guanidyny - galeginy - potwierdzono jedynie aktywność pułapkującą i tworzenie adduktów, podobnie jak dla aminoguanidyny i metforminy. Biorąc pod uwagę powyższe, należy uwzględnić różnice w mechanizmach warunkowane budową chemiczną substancji pułapkującej α-DC, gdyż ostatecznie nawet związki nie posiadające zdolności wychwytywania MGO i GO wykazywały silne lub umiarkowane działanie antyglikacyjne (dobesylan wapnia, diosmina, trokserutyna). Przykładem z **publikacji P4** może być także izowiteksyna, która okazała się najskuteczniejsza jako inhibitor glikacji indukowanej przez GO, a jednocześnie nie posiada zdolności jego wychwytywania. Jak wiadomo izowiteksyna charakteryzuje się zarówno zdolnością chelatowania metali przejściowych, jak i silnymi właściwościami przeciwutleniającymi, co razem wzięte może skutkować silnym efektem przeciwglikacyjnym [68,69]. Ponadto warto zwrócić uwagę na fakt, że końcowe produkty zaawansowanej glikacji pochodzące z reakcji z MGO i GO mogą różnić się właściwościami – niektóre badania donoszą, że addukty białek z glioksalem wykazują znacznie słabsze właściwości fluorescencji, przez co uzyskane wyniki mogą być niższe niż w rzeczywistości [70]. Różnice w liczbie adduktów powstałych w reakcji z MGO i GO można prawdopodobnie przypisać temu, że w roztworach wodnych głównymi formami GO są uwodniony monomer, dimer i trimer [71]. W konsekwencji reakcje badanych związków z glioksalem uległy znacznemu spowolnieniu w wyniku transformacji wymienionych form glioksalu do wolnego GO. Istnieje zatem możliwość, że zarówno izowiteksyna, jak i notofagina, które w eksperymencie opisanym w **publikacji P4** nie wykazały zdolności do wychwytywania GO, mogą go wiązać w innych warunkach. Jednakże związki z grupy flawonów (witeksyna) i dihydrochalkonów (aspalatyna i floretyna) wykazały potencjał przyłączania cząsteczek glioksalu w zastosowanych warunkach doświadczenia; można zatem założyć, że w przypadku izowiteksyny i notofaginy proces ten zachodzi nieco trudniej, być może ze względu na molekularne warunki przestrzenne. Aby wyjaśnić te rozbieżności, potrzebne są dalsze badania.

Podsumowując, w wyniku przeprowadzonych badań udało się potwierdzić postawioną hipotezę, że środki wazoprotekcyjne, stosowane w terapii przewlekłej niewydolności żylnej (dobesylan wapnia dodatkowo w retinopatii cukrzycowej [54]), a także ich analogi strukturalne

posiadają zdolność hamowania nieenzymatycznej glikacji i/lub neutralizowania reaktywnych α-dikarbonyli. Przedstawione wyniki sugerują, że niektóre z badanych substancji i przetworów roślinnych mogą być potencjalnie użyteczne jako terapia wspomagająca w prewencji schorzeń związanych z wysokimi stężeniami α-dikarbonyli w organizmie, m.in. w zapobieganiu angiopatiom cukrzycowym. Ponadto ustalono, że zdolność pułapkowania jest tylko jedną ze składowych efektu antyglikacyjnego i nie jest wymagana, by skutecznie chronić białka i analogicznie inne makromolekuły przed szkodliwym działaniem α-dikarbonyli bądź cukrów redukujących (glukoza, fruktoza). Potwierdzono, że na efekt antyglikacyjny istotnie wpływa też aktywność antyoksydacyjną, właściwości redukujące, przeciwrodnikowe i prawdobodobnie zdolność do chelatowania jonów metali przejściowych. Właściwości te mogą zapewniać ochronę przed modyfikacjami strukturalnymi na poziomie cząsteczki będącej obiektem glikacji (białko, peptyd, lipoproteina, kwas nukleinowy) lub zapobiegają utlenianiu glukozy, fruktozy i wczesnych produktów glikacji oraz nadmiernemu tworzeniu się reaktywnych α-dikarbonyli. Na potencjalną użyteczność kliniczną substancji o charakterze antyglikacyjnym i anty-AGE wpływ mają również wspomniane wczesniej parametry, takie jak dobra rozpuszczalność i dostępność biologiczna.

Zdolność wiązania α-DC oraz hamowania procesów nieenzymatycznej glikacji obserwuje się dla wielu zróżnicowanych pod względem budowy chemicznej związków naturalnych i sytentycznych. Jednak wyselekcjonowanie związków charakteryzujących się wysoką aktywnością i odpowiednimi parametrami fizykochemicznymi i farmakokinetycznymi, dającymi możliwość zastosowania ich w terapii może być złożonym procesem, a selekcja powinna być oparta na wcześniejszym rozpatrzeniu kilku różnych mechanizmów działania oraz budowy chemicznej.

5. Wnioski

1. Oprócz znanych zastosowań terapeutycznych, leki wazoprotekcyjne i ich strukturalne analogi, szczególnie hesperetyna, hesperydyna i dobesylan wapnia, z uwagi na właściwości antyglikacyjne i/lub pułapkujące α-dikarbonyle, obok kwercetyny mogą być rozważane jako potencjalni kandydaci do zastosowań w prewencji powikłań naczyniowych u pacjentów z cukrzycą lub w stanie przedcukrzycowym, a także w innych powikłaniach cukrzycy wynikających z akumulacji MGO i AGE. Konieczne są jednak dalsze badania w tym zakresie. Obecnie jedynie dobesylan wapnia wskazany jest w retinopatii cukrzycowej.
2. Na przykładzie (bio)flawonoidów, pochodnych guanidyny i dobesylanu wapnia potwierdzono, że składowymi efektu antyglikacyjnego jest zdolność substancji do pułapkowania α-dikarbonyli oraz aktywność przeciwutleniająca. Pozostaje do ustalenia, która ze składowych jest bardziej istotna dla efektu ogólnego.
3. Flawonoidy można uznać ogólnie za substancje pułapkujące α-dikarbonyle, a elementem struktury warunkującym ich aktywność jest układ floroglucynolu, dlatego też podstawienie lub brak grupy hydroksylowej w pozycji C-7 i/lub C-5 pierścienia A oraz obecność podstawnika przy sąsiadujących z nimi atomach węgla (w C-8 i/lub C-6) powoduje osłabienie lub zniesienie zdolności wychwytywania α-dikarbonyli. Pozostałe elementy struktury flawonoidów mają mniejsze znaczenie, aczkolwiek są istotne dla stabilności cząsteczki, efektu antyoksydacyjnego i antyglikacyjnego.
4. Substancje roślinne posiadające w składzie chemicznym flawonoidy, a także inne polifenole lub pochodne guanidyny (Galega officinalis L., Alspalatus linearis (Burm.f.) R.Dahlgren), mogą hamować nieenzymatyczną glikację, m.in. przez wychwytywanie α-dikarbonyli i właściwości przeciwutleniające. Przetwory z ziela rutwicy i czerwonokrzewu oraz ich indywidualne związki (np. galegina, aspalatyna, izowiteksyna, witeksyna) mogą stanowić obiecujący materiał do dalszych badań w modelach in vivo jako potencjalne środki w profilaktyce schorzeń związanych z nadmiernym wytwarzaniem α-dikarbonyli i AGE.

5. Zastosowanie produktu będącego kombinacją wyciągu z naowocni pomarańczy słodkiej (Citrus × sinensis (L.) Osbeck) i koncentratu z soku owocu granatowca (Punica granatum L.) w postaci suplementu diety o oznaczonej zawartości hesperydyny, jako głównego składnika w dawce 450 mg, przez 4 tygodnie obniża istotnie statystycznie stężenie metyloglioksalu w osoczu zdrowych osób w podeszłym wieku o 9.8%. Efekt ten może mieć znaczenie kliniczne w zmniejszeniu ryzyka wystąpienia zdarzeń sercowo-naczyniowych u osób z cukrzycą i stanowić wstęp do dalszych badań w grupie pacjentów z hiperglikemią, jako wsparcie farmakoterapii zasadniczej lub w profilaktyce powikłań naczyniowych. W celu ustalenia dokładnych efektów farmakologicznych oraz optymalizacji dawkowania konieczne są dalsze badania
6. Obniżanie stężenia reaktywnych α-dikarbonyli u pacjentów będących w grupie ryzyka chorób związanych z ich wysokimi stężeniami jako potencjalnej terapii wspomagającej lub w profilaktyce może stanowić obiecujący kierunek terapeutyczny. Pomimo, że efekt biochemiczny w badaniach in vivo substancji pułapkujących α-DC nie przekracza zwykle kilkunastu procent (np. kwercetyna, hesperydyna w próbach klinicznych) to wielololetnie obserwacje sugerują, że już tak niewielka redukcja stężenia najbardziej reaktywnego metyloglioksalu może być klinicznie istotna.

6. Piśmiennictwo

1. Mariadoss, A.V.A.; Sivakumar, A.S.; Lee, C.H.; Kim, S.J. Diabetes Mellitus and Diabetic Foot Ulcer: Etiology, Biochemical and Molecular Based Treatment Strategies via Gene and Nanotherapy. Biomedicine and Pharmacotherapy 2022, 151.
2. Bereda, G. Brief Overview of Diabete Mellitus. Diabetes Management 2021, 21-27.
3. Yuchen, C.; Hejia, Z.; Fanke, M.; Qixin, D.; Liyang, C.; Xi, G.; Yanxia, C.; Xiongyi, Y.; Zhuohang, X.; Guoguo, Y.; et al. Exploring the Shared Molecular Mechanism of Microvascular and Macrovascular Complications in Diabetes: Seeking the Hub of Circulatory System Injury. Front Endocrinol (Lausanne) 2023, 14, 1032015.
4. Stanciu, G.D.; Bild, V.; Ababei, D.C.; Rusu, R.N.; Cobzaru, A.; Paduraru, L.; Bulea, D. Link between Diabetes and Alzheimer's Disease Due to the Shared Amyloid Aggregation and Deposition Involving Both Neurodegenerative Changes and Neurovascular Damages. J Clin Med 2020, 9, 1–25.
5. Paul, S.; Ali, A.; Katare, R. Molecular Complexities Underlying the Vascular Complications of Diabetes Mellitus – A Comprehensive Review. J Diabetes Complications 2020, 34, 107613.
6. Miyata, T.; Van Ypersele De Strihou, C.; Ueda, Y.; Ichimori, K.; Inagi, R.; Onogi, H.; Ishikawa, N.; Nangaku, M.; Kurokawa, K. Angiotensin II Receptor Antagonists and Angiotensin-Converting Enzyme Inhibitors Lower in Vitro the Formation of Advanced Glycation End Products: Biochemical Mechanisms. Journal of the American Society of Nephrology 2002, 13, 2478–2487.
7. Akagawa, M.; Mori, A.; Sakamoto, K.; Nakahara, T. Methylglyoxal Impairs β 2-Adrenoceptor-Mediated Vasodilatory Mechanisms in Rat Retinal Arterioles 2018, 41, 272-276.
8. Berlanga, J.; Cibrian, D.; Guillénguill´guillén, I.; Freyre, F.; Alba, J.S.; Lopez-Saura, P.; Merino, N.; Aldama, A.; Quintela, A.M.; Triana, M.E. Methylglyoxal Administration Induces Diabetes-like Microvascular Changes and Perturbs the Healing Process of Cutaneous Wounds. Clin Sci (Lond) 2005, 109, 83-95.
9. Qi, W.; Keenan, H.A.; Li, Q.; Ishikado, A.; Kannt, A.; Sadowski, T.; Yorek, M.A.; Wu, I.H.; Lockhart, S.; Coppey, L.J.Pyruvate Kinase M2 Activation May Protect against the Progression of Diabetic Glomerular Pathology and Mitochondrial Dysfunction. Nat Med 2017, 23, 753–762.

10. Sena, C.M.; Matafome, P.; Crisóstomo, J.; Rodrigues, L.; Fernandes, R.; Pereira, P.; Seiça, R.M. Methylglyoxal Promotes Oxidative Stress and Endothelial Dysfunction. Pharmacol Res 2012, 65, 497-506.

11. Zheng, J.; Ou, J.; Ou, S. Alpha-Dicarbonyl Compounds. In Chemical Hazards in Thermally-Processed Foods; Springer Singapore 2019, 19–46.

12. Schalkwijk, C.G.; Stehouwer, C.D.A. Methylglyoxal, a Highly Reactive Dicarbonyl Compound, in Diabetes, Its Vascular Complications, and Other Age-Related Diseases. Physiol Rev 2020, 100, 407–461.

13. Ogawa, S.; Nakayama, K.; Nakayama, M.; Mori, T.; Matsushima, M.; Okamura, M.; Senda, M.; Nako, K.; Miyata, T.; Ito, S. Methylglyoxal Is a Predictor in Type 2 Diabetic Patients of Intima-Media Thickening and Elevation of Blood Pressure. Hypertension 2010, 56, 471–476.

14. Wang, X.; Desai, K.; Chang, T.; Wu, L. Vascular Methylglyoxal Metabolism and the Development of Hypertension. Journal of Hypertension 2005, 23(8), 1565-1573.

15. Masania, J.; Malczewska-Malec, M.; Razny, U.; Goralska, J.; Zdzienicka, A.; Kiec-Wilk, B.; Gruca, A.; Stancel-Mozwillo, J.; Dembinska-Kiec, A.; Rabbani, N. Dicarbonyl Stress in Clinical Obesity. Glycoconj J 2016, 33, 581–589.

16. Maessen, D.E.; Hanssen, N.M.; Lips, M.A.; Scheijen, J.L.; Willems van Dijk, K.; Pijl, H.; Stehouwer, C.D.; Schalkwijk, C.G. Energy Restriction and Roux-En-Y Gastric Bypass Reduce Postprandial α-Dicarbonyl Stress in Obese Women with Type 2 Diabetes. Diabetologia 2016, 59, 2013–2017.

17. Ravid, M.; Brosh, D.; Ravid-Safran, D.; Levy, Z.; Rachmani, R. Main Risk Factors for Nephropathy in Type 2 Diabetes Mellitus Are Plasma Cholesterol Levels, Mean Blood Pressure, and Hyperglycemia. Arch Intern Med 1998, 11, 998-1004.

18. Hanssen, N.M.J.; Stehouwer, C.D.A.; Schalkwijk, C.G. Methylglyoxal Stress, the Glyoxalase System, and Diabetic Chronic Kidney Disease. Curr Opin Nephrol Hypertens 2019, 28, 26–33.

19. Aragonès, G.; Rowan, S.; Francisco, S.G.; Whitcomb, E.A.; Yang, W.; Perini-Villanueva, G.; Schalkwijk, C.G.; Taylor, A.; Bejarano, E. The Glyoxalase System in Age-Related Diseases: Nutritional Intervention as Anti-Ageing Strategy. Cells 2021, 10, 1852.

20. Coukos, J.S.; Moellering, R.E. Methylglyoxal Forms Diverse Mercaptomethylimidazole Crosslinks with Thiol and Guanidine Pairs in Endogenous Metabolites and Proteins. ACS Chem Biol 2021, 16, 2453–2461.

21. Sergi, D.; Boulestin, H.; Campbell, F.M.; Williams, L.M. The Role of Dietary Advanced Glycation End Products in Metabolic Dysfunction. Mol Nutr Food Res 2021, 65, 1900934.

22. Lai, S.W.T.; Lopez Gonzalez, E.D.J.; Zoukari, T.; Ki, P.; Shuck, S.C. Methylglyoxal and Its Adducts: Induction, Repair, and Association with Disease. Chem Res Toxicol 2022, 35, 1720–1746.

23. Galligan, J.J.; Wepy, J.A.; Streeter, M.D.; Kingsley, P.J.; Mitchener, M.M.; Wauchope, O.R.; Beavers, W.N.; Rose, K.L.; Wang, T.; Spiegel, D.A. Methylglyoxal-Derived Posttranslational Arginine Modifications Are Abundant Histone Marks. Proc Natl Acad Sci USA 2018, 115, 9228–9233.

24. Beisswenger, P.J.; Howell, S.K.; Russell, G.B.; Miller, M.E.; Rich, S.S.; Mauer, M. Early Progression of Diabetic Nephropathy Correlates with Methylglyoxal-Derived Advanced Glycation End Products. Diabetes Care 2013, 36, 3234–3239.

25. Ahmed, K.A.; Muniandy, S.; Ismail, I.S. Role of N ε-(Carboxymethyl)Lysine in the Development of Ischemic Heart Disease in Type 2 Diabetes Mellitus. J Clin Biochem Nutr 2007, 41. 97-105.

26. Smuda, M.; Henning, C.; Raghavan, C.T.; Johar, K.; Vasavada, A.R.; Nagaraj, R.H.; Glomb, M.A. Comprehensive Analysis of Maillard Protein Modifications in Human Lenses: Effect of Age and Cataract. Biochemistry 2015, 54, 2500–2507.

27. Tamae, D.; Lim, P.; Wuenschell, G.E.; Termini, J. Mutagenesis and Repair Induced by the DNA Advanced Glycation End Product N 2-1-(Carboxyethyl)-2′-Deoxyguanosine in Human Cells. Biochemistry 2011, 50, 2321–2329.

28. Borg, D.J.; Forbes, J.M. Targeting Advanced Glycation with Pharmaceutical Agents: Where Are We Now? Glycoconj J 2016, 33, 653–670.

29. Hanssen, N.M.J.; Scheijen, J.L.J.M.; Jorsal, A.; Parving, H.H.; Tarnow, L.; Rossing, P.; Stehouwer, C.D.A.; Schalkwijk, C.G. Higher Plasma Methylglyoxal Levels Are Associated with Incident Cardiovascular Disease in Individuals with Type 1 Diabetes: A 12-Year Follow-up Study. Diabetes 2017, 66, 2278–2283.

30. Bolton, W.K.; Cattran, D.C.; Williams, M.E.; Adler, S.G.; Appel, G.B.; Cartwright, K.; Foiles, P.G.; Freedman, B.I.; Raskin, P.; Ratner, R.E. Randomized Trial of an Inhibitor of Formation of Advanced Glycation End Products in Diabetic Nephropathy. Am J Nephrol 2004, 24, 32–40.

31. Bakris, G.L.; Bank, A.J.; Kass, D.A.; Neutel, J.M.; Preston, R.A.; Oparil, S. Advanced Glycation End-Product Cross-Link Breakers: A Novel Approach to Cardiovascular Pathologies Related to the Aging Process. Am J Hypertens 2004, 17, 23–30.

32. Kinsky, O.R.; Hargraves, T.L.; Anumol, T.; Jacobsen, N.E.; Dai, J.; Snyder, S.A.; Monks, T.J.; Lau, S.S. Metformin Scavenges Methylglyoxal to Form a Novel Imidazolinone Metabolite in Humans. Chem Res Toxicol 2016, 29, 227–234.

33. Quinn, C.E.; Hamilton, P.K.; Lockhart, C.J.; McVeigh, G.E. Thiazolidinediones: Effects on Insulin Resistance and the Cardiovascular System. Br J Pharmacol 2008, 153, 636–645.

34. Šebeková, K.; Gazdíková, K.; Syrová, D.; Blažíček, P.; Schinzel, R.; Heidland, A.; Spustová, V.; Dzúrik, R. Effects of Ramipril in Nondiabetic Nephropathy: Improved Parameters of Oxidatives Stress and Potential Modulation of Advanced Glycation End Products. J Hum Hypertens 2003, 17, 265–270.

35. Miyata, T.; Van Ypersele De Strihou, C.; Ueda, Y.; Ichimori, K.; Inagi, R.; Onogi, H.; Ishikawa, N.; Nangaku, M.; Kurokawa, K. Angiotensin II Receptor Antagonists and Angiotensin-Converting Enzyme Inhibitors Lower in Vitro the Formation of Advanced Glycation End Products: Biochemical Mechanisms. Journal of the American Society of Nephrology 2002, 13, 2478–2487.

36. Miller, A.G.; Tan, G.; Binger, K.J.; Pickering, R.J.; Thomas, M.C.; Nagaraj, R.H.; Cooper, M.E.; Wilkinson-Berka, J.L. Candesartan Attenuates Diabetic Retinal Vascular Pathology by Restoring Glyoxalase-I Function. Diabetes 2010, 59, 3208–3215.

37. Rezaie-Majd, A.; Maca, T.; Bucek, R.A.; Valent, P.; Müller, M.R.; Husslein, P.; Kashanipour, A.; Minar, E.; Baghestanian, M. Simvastatin Reduces Expression of Cytokines Interleukin-6, Interleukin-8, and Monocyte Chemoattractant Protein-1 in Circulating Monocytes from Hypercholesterolemic Patients. Arterioscler Thromb Vasc Biol 2002, 22, 1194–1199.

38. Freund, M.A.; Chen, B.; Decker, E.A. The Inhibition of Advanced Glycation End Products by Carnosine and Other Natural Dipeptides to Reduce Diabetic and Age-Related Complications. Compr Rev Food Sci Food Saf 2018, 17, 1367–1378.

39. Ramis, R.; Ortega-Castro, J.; Caballero, C.; Casasnovas, R.; Cerrillo, A.; Vilanova, B.; Adrover, M.; Frau, J. How Does Pyridoxamine Inhibit the Formation of Advanced Glycation End Products? The Role of Its Primary Antioxidant Activity. Antioxidants 2019, 8(9), 344.

40. Li, X.; Zheng, T.; Sang, S.; Lv, L. Quercetin Inhibits Advanced Glycation End Product Formation by Trapping Methylglyoxal and Glyoxal. J Agric Food Chem 2014, 62, 12152–12158.

41. Engelen, L.; Stehouwer, C.D.A.; Schalkwijk, C.G. Current Therapeutic Interventions in the Glycation Pathway: Evidence from Clinical Studies. Diabetes Obes Metab 2013, 15, 677–689.

42. Piazza, M.; Hanssen, N.M.J.; Persson, F.; Scheijen, J.L.; van de Waarenburg, M.P.H.; van Greevenbroek, M.M.J.; Rossing, P.; Hovind, P.; Stehouwer, C.D.A.; Parving, H.H.; et al. Irbesartan Treatment Does Not Influence Plasma Levels of the Dicarbonyls Methylglyoxal, Glyoxal and 3-Deoxyglucosone in Participants with Type 2 Diabetes and Microalbuminuria: An IRMA2 Sub-Study. Diabetic Medicine 2021, 38, 14405.

43. Bumrungpert, A.; Pavadhgul, P.; Chongsuwat, R.; Komindr, S. Nutraceutical Improves Glycemic Control, Insulin Sensitivity, and Oxidative Stress in Hyperglycemic Subjects: A Randomized, Double-Blind, Placebo-Controlled Clinical Trial. Nat Prod Commun 2020, 15, 1-11.

44. Carrizzo, A.; Izzo, C.; Forte, M.; Sommella, E.; Di Pietro, P.; Venturini, E.; Ciccarelli, M.; Galasso, G.; Rubattu, S.; Campiglia, P. A Novel Promising Frontier for Human Health: The Beneficial Effects of Nutraceuticals in Cardiovascular Diseases. Int J Mol Sci 2020, 21, 1–40.

45. Zhu, H.; Poojary, M.M.; Andersen, M.L.; Lund, M.N. The Effect of Molecular Structure of Polyphenols on the Kinetics of the Trapping Reactions with Methylglyoxal. Food Chem 2020, 319, 126500.

46. Han, L.; Lin, Q.; Liu, G.; Han, D.; Niu, L.; Su, D. Catechin Inhibits Glycated Phosphatidylethanolamine Formation by Trapping Dicarbonyl Compounds and Forming Quinone. Food Funct 2019, 10, 2491–2503.

47. Zhu, H.; Poojary, M.M.; Andersen, M.L.; Lund, M.N. Effect of PH on the Reaction between Naringenin and Methylglyoxal: A Kinetic Study. Food Chem 2019, 298, 125086.

48. Zhang, S.; Xiao, L.; Lv, L.; Sang, S. Trapping Methylglyoxal by Myricetin and Its Metabolites in Mice. J Agric Food Chem 2020, 68, 9408–9414.

49. Wang, P.; Chen, H.; Sang, S. Trapping Methylglyoxal by Genistein and Its Metabolites in Mice. Chem Res Toxicol 2016, 29, 406–414.

50. Negre-Salvayre, A.; Salvayre, R.; Augé, N.; Pamplona, R.; Portero-Otín, M. Hyperglycemia and Glycation in Diabetic Complications. Antioxid Redox Signal 2009, 11, 3071-3109.

51. Yun, S. Venoactive Drugs, Summary of the Clinical Trials and Guidelines. Annals of Phlebology 2021, 19, 21–26.

52. Shao, X.; Chen, H.; Zhu, Y.; Sedighi, R.; Ho, C.T.; Sang, S. Essential Structural Requirements and Additive Effects for Flavonoids to Scavenge Methylglyoxal. J Agric Food Chem 2014, 62, 3202–3210.

53. Bednarska, K.; Fecka, I. Potential of Vasoprotectives to Inhibit Non-Enzymatic Protein Glycation, and Reactive Carbonyl and Oxygen Species Uptake. Int J Mol Sci 2021, 22, 10026.

54. Zhang, X., Liu, W., Wu, S., Jin, J., Li, W., & Wang, N. Calcium dobesilate for diabetic retinopathy: a systematic review and meta-analysis. Science China Life Sciences 2005, 58, 101-107.

55. Guo, X.; Hou, L.; Yin, Y.; Wu, J.; Zhao, F.; Xia, L.; Cheng, X.; Liu, Q.; Liu, L.; Xu, E. Negative Interferences by Calcium Dobesilate in the Detection of Five Serum Analytes Involving Trinder Reaction-Based Assays. PLoS One 2018, 13, 0192440.

56. Kanaze, F.I.; Bounartzi, M.I.; Georgarakis, M.; Niopas, I. Pharmacokinetics of the Citrus Flavanone Aglycones Hesperetin and Naringenin after Single Oral Administration in Human Subjects. Eur J Clin Nutr 2007, 61, 472–477.

57. Witters, L.A. The Blooming of the French Lilac. Journal of Clinical Investigation 2001, 108, 1105–1107.

58. Bednarska, K.; Kuś, P.; Fecka, I. Investigation of the Phytochemical Composition, Antioxidant Activity, and Methylglyoxal Trapping Effect of Galega Officinalis L. Herb in Vitro. Molecules 2020, 25, 5810.

59. Palit, P.; Furman, B.L.; Gray, A.I. Novel Weight-Reducing Activity of Galega Officinalis in Mice. Journal of Pharmacy and Pharmacology 2010, 51, 1313–1319.

60. Hachkova, H.; Nagalievska, M.; Soliljak, Z.; Kanyuka, O.; Kucharska, A.Z.; Sokół-łętowska, A.; Belonovskaya, E.; Buko, V.; Sybirna, N. Medicinal Plants Galega Officinalis l. And Yacon Leaves as Potential Sources of Antidiabetic Drugs. Antioxidants 2021, 10, 1362.

61. Rasekh, H.R.; Nazari, P.; Kamli-Nejad, M.; Hosseinzadeh, L. Acute and Subchronic Oral Toxicity of Galega Officinalis in Rats. J Ethnopharmacol 2008, 116, 21–26.

62. Joubert, E.; de Beer, D. Rooibos (Aspalathus Linearis) beyond the Farm Gate: From Herbal Tea to Potential Phytopharmaceutical. South African Journal of Botany 2011, 77, 869–886.

63. Dludla, P. V.; Muller, C.J.F.; Joubert, E.; Louw, J.; Essop, M.F.; Gabuza, K.B.; Ghoor, S.; Huisamen, B.; Johnson, R. Aspalathin Protects the Heart against Hyperglycemia-Induced Oxidative Damage by up-Regulating Nrf2 Expression. Molecules 2017, 22, 129.

64. Suchal, K.; Malik, S.; Khan, S.I.; Malhotra, R.K.; Goyal, S.N.; Bhatia, J.; Kumari, S.; Ojha, S.; Arya, D.S. Protective Effect of Mangiferin on Myocardial Ischemia-Reperfusion Injury in Streptozotocin-Induced Diabetic Rats: Role of AGE-RAGE/MAPK Pathways. Sci Rep 2017, 7, 42027.

65. Mazibuko-Mbeje, S.E.; Dludla, P. V.; Roux, C.; Johnson, R.; Ghoor, S.; Joubert, E.; Louw, J.; Opoku, A.R.; Muller, C.J.F. Aspalathin-Enriched Green Rooibos Extract Reduces Hepatic Insulin Resistance by Modulating PI3K/AKT and AMPK Pathways. Int J Mol Sci 2019, 20, 633.

66. Son, M.J.; Minakawa, M.; Miura, Y.; Yagasaki, K. Aspalathin Improves Hyperglycemia and Glucose Intolerance in Obese Diabetic Ob/Ob Mice. Eur J Nutr 2013, 52, 1607–1619.

67. Bhuiyan, M.N.I.; Mitsuhashi, S.; Sigetomi, K.; Ubukata, M. Quercetin Inhibits Advanced Glycation End Product Formation via Chelating Metal Ions, Trapping Methylglyoxal, and Trapping Reactive Oxygen Species. Biosci Biotechnol Biochem 2017, 81, 882–890.

68. Peng, X.; Zheng, Z.; Cheng, K.W.; Shan, F.; Ren, G.X.; Chen, F.; Wang, M. Inhibitory Effect of Mung Bean Extract and Its Constituents Vitexin and Isovitexin on the Formation of Advanced Glycation Endproducts. Food Chem 2008, 106, 475–481.

69. Cheng, D.; Wang, R.; Wang, C.; Hou, L. Mung Bean (Phaseolus Radiatus L.) Polyphenol Extract Attenuates Aluminum-Induced Cardiotoxicity through an ROS-Triggered Ca2+/JNK/NF-KB Signaling Pathway in Rats. Food Funct 2017, 8, 851–859.

70. Nevin, C.; McNeil, L.; Ahmed, N.; Murgatroyd, C.; Brison, D.; Carroll, M. Investigating the Glycating Effects of Glucose, Glyoxal and Methylglyoxal on Human Sperm. Sci Rep 2018, 8, 9002.

71. Shao, X.; Bai, N.; He, K.; Ho, C.T.; Yang, C.S.; Sang, S. Apple polyphenols, phloretin and phloridzin: New trapping agents of reactive dicarbonyl species. Chem. Res. Toxicol. 2008, 21, 2042–2050.

OSIĄGNIĘCIA

Tytuł zawodowy:

- magister farmacji (2018 r., nr dyplomu: 8286)

Praca zawodowa:

- 2023 – obecnie | Clinical Research Associate II | Syneos Health
- 2022 – 2022 | Clinical Research Associate I | Syneos Health
- 2020 – 2022 | Jr Specialist at the Center of Population Diagnostic | Łukasiewicz Research Network – PORT Polish Center for Technology Development
- 2017 – 2018 | Clinical Study Coordinator/Sub-investigator | Medical Clinic "Persona"

Edukacja:

- 2019 – 2023 | Szkoła Doktorska na Wydziale Lekarskim Kształcenia Podyplomowego Uniwersytetu Medycznego we Wrocławiu.
- 2013 – 2018 | Studia na kierunku Farmacja na Wydziale Farmaceutycznym Uniwersytetu Medycznego we Wrocławiu im. Piastów Śląskich, zakończone uzyskaniem tytułu magistra farmacji.

Kursy, szkolenia:

- 2023: Kurs "Oncology Monitoring Program for oncology research (Immuno-oncology; CAR T-cell Therapy; RECIST and IRECIST; Medical Imaging in Oncology; CTCAE for Oncology Clinical Trials)", Syneos Health
- 2022: Kurs "Design and Interpretation of Clinical Trials", Uniwersytet Johnsa Hopkinsa.
- 2022: Szkolenie "Internationally qualified Clinical Research Associate Programme", Syneos Health
- 2022: Szkolenie: "Pediatric Drug Development: Therapeutic Orphan to Foster Child", Syneos Health
- 2021: Kurs prowadzenia i zarządzania zespołem badawczym, Uniwersyt Medyczny im Piastów Śląskich we Wrocławiu.
- 2021: Kurs „Systematic Sample Preparation Method Development for LC-MS/MS Assays: Blood Assays", Biotage.
- 2021: Kurs „Systematic Sample Preparation Method Development for LC-MS/MS Assays: Urine Assays", Biotage.
- 2021: Kurs skutecznego planowania i zarządzania projektami naukowymi oraz pozyskiwania środków na badania naukowe, Uniwersyt Medyczny im Piastów Śląskich we Wrocławiu.

Staże zagraniczne:

- Staż naukowy w Katedrze Medycyny Wewnętrznej Uniwersytetu w Maastricht (Holandia). Podczas stażu realizowłam badania, których wyniki przedstawiono w **publikacji P2** i rozwijałam swoje umiejętności z zakresu niekomercyjnych badań klinicznych.

Nagrody:

- Stypendium Rektora dla najlepszych studentów w roku akademickim 2018/2019.
- Stypendium Projakościowe Szkoły Doktorskiej za osiągnięcia w pracy naukowej w roku akademickim 2021/2022.
- I miejsce w kategorii prezentacji posterowych eksperymentalnych za pracę pt. „Badanie zdolności rutyny i trokserutyny do pułapkowania metyloglioksalu" na V Ogólnopolskiej Konferencji Naukowej „Współczesne zastosowanie metod analitycznych w farmacji i medycynie", która odbyła się 27.11.2020 we Wrocławiu.
- I miejsce w kategirii prezentacji posterowych eksperymentalnych za pracę „Antyglikacyjne właścwości mięty pieprzowej i jej głównych składników" na VI Ogólnooplskiej konferencji Naukowej „Współczesne zastosowanie metod analitycznych w farmacji i medycynie", która odbyła się 03.12.2021 we Wrocławiu.

Projekty naukowe:

- Realizacja zadań naukowych - funkcja **młody naukowiec,** w ramach projektu badawczego: „ Ocena zdolności wiązania reaktywnych dikarbonyli i właściwości antyglikooksydacyjnych wybranych związków naturalnych i syntetycznych o potencjale wazo protekcyjnym." finansowanego ze środków Uniersytetu Medycznego im. Piastów Śląskich we Wrocławiu; nr projektu: STM.D110.20.131; 2020 – 2021; kierownik: prof. dr hab. n. farm. Izabela Fecka.
- Realizacja zadań naukowych - funkcja **kierownik projektu,** w ramach projektu konkursowego: „Hamowanie powstawania końcowych produktów zaawansowanej glikacji albumin i hemoglobiny oraz zdolność do wychwytu metyloglioksalu przez aspalatynę i ekstrakty z Aspalathus Linearis." finansowanego ze środków Uniersytetu Medycznego im. Piastów Śląskich we Wrocławiu; nr projektu: SUBK.D110.22.045; 2021 – 2022.
- Realizacja zadań naukowych - funkcja **uczestnika projektu,** w projekcie „Ocena składu chemiczneg i potencjału biologicznego wybranych substancji pochodzenia roślinnego o właściwościach lecniczych i prozdrowotnych" finansowanego ze środków Uniersytetu Medycznego im. Piastów Śląskich we Wrocławiu; nr projektu: SUB.D110.21.101; 2021.
- Realizacja zadań naukowych - funkcja **uczestnika projektu,** w projekcie „Poszukiwanie substancji o wysokim potencjale antyoksydacyjnym, antyglikooksydacyjnym i

antylipooksydacyjnym do zastosowań terapeutycznych" finansowanego ze środków Uniersytetu Medycznego im. Piastów Śląskich we Wrocławiu; nr projektu: SUBZ.D110.22.019; 2022.

- Realizacja zadań naukowych - funkcja **uczestnika projektu,** w projekcie „Research on chronic complications of diabetes" finansowanego ze środków Uniersytetu Medycznego im. Piastów Śląskich we Wrocławiu, nr projektu: SUBZ.C310.22.075; 2022-2023.

Zajęcia dydaktyczne ze studentami:

- Farmakognozja, ćwiczenia laboratoryjne – Farmacja, III rok (2019-2023).

Koła naukowe w okresie studiów farmaceutycznych i doktoranckich

- Studenckie Koło Naukowe przy Zakładzie Chemii Leków (2016-2018).
- Studenckie Koło Naukowe przy Katedrze i Zakładzie Farmakognozji i Leku Roślinnego (2016-2018).
- Studenckie Koło Naukowe przy Zakładzie Toksykologii (2016-2018).

Popularyzacja nauki:

- Dolnośląski Festiwal Nauki 2021 - uczestnictwo w przygotowaniu zajęć laboratoryjnych i prezentacji.

Publikacje naukowe wchodzące w skład cyklu stanowiącego rozprawę doktorską

P1. Potential of Vasoprotectives to Inhibit Non-Enzymatic Protein Glycation, and Reactive Carbonyl and Oxygen Species Uptake

International Journal of
Molecular Sciences

MDPI

Article

Potential of Vasoprotectives to Inhibit Non-Enzymatic Protein Glycation, and Reactive Carbonyl and Oxygen Species Uptake

Katarzyna Bednarska * and Izabela Fecka

Department of Pharmacognosy and Herbal Medicines, Faculty of Pharmacy, Wroclaw Medical University, ul. Borowska 211, 50-556 Wroclaw, Poland; izabela.fecka@umed.wroc.pl
* Correspondence: katarzyna.bednarska@student.umed.wroc.pl

Abstract: Reactive carbonyl species (RCS) such as methylglyoxal (MGO) or glyoxal (GO) are the main precursors of the formation of advanced glycation end products (AGEs). AGEs are a major factor in the development of vascular complications in diabetes. Vasoprotectives (VPs) exhibit a wide range of activities beneficial to cardiovascular health. The present study aimed to investigate selected VPs and their structural analogs for their ability to trap MGO/GO, inhibit AGE formation, and evaluate their antioxidant potential. Ultra-high-performance liquid chromatography coupled with an electrospray ionization mass spectrometer (UHPLC-ESI-MS) and diode-array detector (UHPLC-DAD) was used to investigate direct trapping capacity and kinetics of quenching MGO/GO, respectively. Fluorimetric and colorimetric measurements were used to evaluate antiglycation and antioxidant action. All tested substances showed antiglycative effects, but hesperetin was the most effective in RCS scavenging. We demonstrated that rutin, diosmetin, hesperidin, and hesperetin could trap both MGO and GO by forming adducts, whose structures we proposed. MGO-derived AGE formation was inhibited the most by hesperetin, and GO-derived AGEs by diosmetin. High reducing and antiradical activity was confirmed for quercetin, rutin, hesperetin, and calcium dobesilate. Therefore, in addition to other therapeutic applications, some VPs could be potential candidates as antiglycative agents to prevent AGE-related complications of diabetes.

Keywords: methylglyoxal trapping; reactive carbonyl species; vasoprotective; antiglycation activity; advanced glycation end products; antioxidant activity; diabetes complications

Citation: Bednarska, K.; Fecka, I. Potential of Vasoprotectives to Inhibit Non-Enzymatic Protein Glycation, and Reactive Carbonyl and Oxygen Species Uptake. *Int. J. Mol. Sci.* **2021**, *22*, 10026. https://doi.org/10.3390/ijms221810026

Academic Editor: Ok-Nam Bae

Received: 11 August 2021
Accepted: 14 September 2021
Published: 16 September 2021

1. Introduction

In patients with long-term uncontrolled hyperglycemia in diabetes, pathological structural-functional changes in the vascular endothelium are observed [1]. These are mainly associated with increased non-enzymatic glycation of proteins and consequently with excessive formation and deposition of advanced glycation end products (AGEs) in the extracellular space and within cells of the blood vessel wall [2]. Vascular complications are the main cause of morbidity and mortality in type 2 diabetes mellitus (T2DM) [3]. Currently, there are no effective pharmacological strategies known to prevent vascular endothelial damage in diabetic patients [4]. AGE formation in vivo is mostly attributed to the reaction of carbonyl groups of 1,2-dicarbonyl compounds (reactive carbonyl species, RCS) such as methylglyoxal (MGO) or glyoxal (GO) with the free amino groups of proteins and other biomacromolecules, resulting in the formation of covalently cross-linked aggregates [5]. Chemically, the mechanism of this reaction is based on nucleophilic addition to the carbonyl group, and the resulting products are intermediates that further undergo transformation by various other chemical reactions to the advanced glycation end products [6]. In diabetic patients, the concentration of RCS is elevated by up to 6-fold; it enhances the non-enzymatic process of protein glycation and subsequent formation of AGEs [7]. RCS-mediated AGEs affect the stability of blood vessel walls by reducing their integrity and consequently increasing permeability [8]. They induce local inflammation through

the activation of protein kinase C and nuclear factor NF-kB, which leads to increased synthesis and secretion of proinflammatory cytokines and stimulation of macrophages and neutrophils [9]. They also contribute to excessive secretion of prothrombotic factors and decreased sensitivity to vasodilatory agents [10]. However, 1,2-dicarbonyl compounds, particularly methylglyoxal, adversely affect the vascular wall not only indirectly through induction of AGE formation, but also directly [11]. MGO promotes oxidative stress by inducing the formation of hydrogen peroxide (H_2O_2), superoxide anion radical (O^{2-}), and peroxynitrite anion ($ONOO^-$), impairing the antioxidant defense system and reducing the intracellular level of glutathione [12]. Methylglyoxal is also able to induce apoptosis by increasing the Bax/Bcl-2 ratio, activation of caspase-9 and caspase-3, and promoting the mitochondrial apoptosis pathway [13]. The proven participation of RCS and AGEs in the development of endothelial damage has prompted research on the potential use of RCS-trapping, antiglycative, and antioxidant compounds as protective agents in diabetic complications [14]. Among several mechanisms that may potentially reduce the levels of RCS and AGEs in the system, one is direct trapping of 1,2-dicarbonyls, resulting in the formation of specific adducts [15]. This activity has already been proven in several in vitro studies for quercetin [16], catechin [17], epicatechin [18], genistein [19], luteolin, kaempferol, and naringenin [20]. The in vitro studies also revealed that the trapping mechanism occurs under physiological conditions—the formation of adducts of methylglyoxal and myricetin in mice as well as methylglyoxal and metformin in humans has been demonstrated [21,22].

According to the Anatomical Therapeutic Chemical Classification System (ATC code), drugs in the vasoprotective category (C05) can be divided into several groups including antivaricose therapy agents (C05B) such as calcium dobesilate (C05BX01) and capillary stabilizers (C05C), which include bioflavonoids (C05CA) such as rutin (C05CA 01), diosmin (C05CA 03), and troxerutin (C05CA 04). They are most often used in conditions such as hemorrhoids, varicose veins, and poor circulation (venous stasis) [23]. However, many scientific studies over the years have demonstrated the protective, multidirectional effects of flavonoids on the cardiovascular system [24,25]. It has been shown that flavonoids can benefit vascular health through antioxidant activity, inhibiting the reactions leading to the production of reactive oxygen species (ROS) [26]. Moreover, flavonoids show spasmolytic activity by inhibiting cyclic adenosine monophosphate (cAMP), which results in vascular smooth muscle relaxation [27]. The inhibition of proteolytic enzymes exhibited by bioflavonoids leads to the strengthening of connective tissue in the blood vessel wall, increasing its sealing and flexibility [28,29]. Nevertheless, the chemical structure of selected compounds from the C05 category may also suggest their potential trapping activity toward reactive carbonyl compounds.

Despite the therapeutic use of vasoprotective (phlebotropic) medicines over the past few decades, little attention has been paid to the molecular mechanisms underlying their potential protective effects in vascular endothelial damage induced by RCS. Therefore, the aim of this study was to verify whether selected substances used as vasoprotective agents (bioflavonoids C05CA and calcium dobesilate used in the treatment of varicose veins C05BX) and their structural analogs (hesperidin and aglycones, except quercetin not used in therapy) have methylglyoxal and glyoxal trapping potential, capacity to inhibit RCS-induced non-enzymatic protein glycation, and exhibit antioxidant activity. Furthermore, for compounds demonstrating the ability to trap RCS, the reaction of methylglyoxal and glyoxal scavenging was studied over time. The antiglycation and antioxidant effects of phlebotropic substances were compared to analogous properties of metformin, the primary oral antidiabetic drug. The findings may shed new light on the potential prospective use of VPs in preventing vascular endothelial damage caused by reactive carbonyl compounds and non-enzymatic glycation.

2. Results and Discussion

2.1. Antiglycation Assay in RCS-BSA Model In Vitro

Several studies over the years have documented that the process of non-enzymatic protein glycation contributes to the onset and progression of many chronic diseases including diabetes [30]. A great effort has been dedicated to identifying clinically relevant agents able to inhibit AGE formation to delay or prevent the consequences of the glycation process [31]. Aminoguanidine (AG), which is effective at inhibiting glycation, has been tested in clinical trials to alleviate diabetes-related complications. These trials showed that AG provided some beneficial effect on diabetic complications, but severe side effects ruled it out as a drug candidate [32]. Therefore, the search for compounds that can effectively inhibit glycation is still ongoing.

Under in vivo conditions, reactive dicarbonyl compounds are the main inducers of the formation of advanced glycation end products; hence, we decided to investigate compounds with vasoprotective potential and their structural analogs (troxerutin, rutin, quercetin, hesperidin, hesperetin, calcium dobesilate) for RCS-mediated AGE inhibitory activity. Inhibition of their formation was measured using an in vitro biological model where bovine serum albumin (BSA) served as the protein target and methylglyoxal (MGO-BSA-model) or glyoxal (GO-BSA-model) as the glycating agent. The chemical structures of the tested compounds are shown in Figure 1. Aminoguanidine proved to be one of the compounds with the strongest antiglycation activity and was used as a known reference inhibitor of the glycation process. For comparison, metformin used as an antidiabetic agent, whose glycation-inhibiting effect has also been shown in several studies [33,34], was also examined.

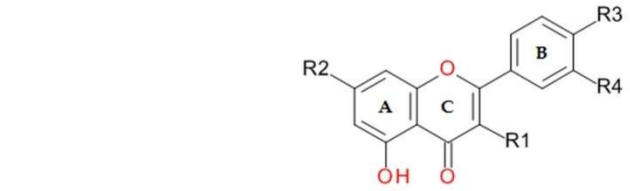

Compound	R_1	R_2	R_3	R_4
Rutin	-O-rutinose	-OH	-OH	-OH
Troxerutin	-O-rutinose	-O-C_2H_2OH	O-C_2H_2OH	O-C_2H_2OH
Quercetin	-OH	-OH	-OH	-OH
Diosmin	-H	-O-rutinose	-O-CH_3	-OH
Diosmetin	-H	-OH	-O-CH_3	-OH

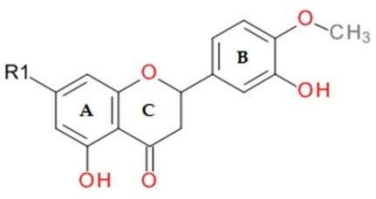

Compound	R_1
Hesperidin	-O-rutinose
Hesperetin	-OH

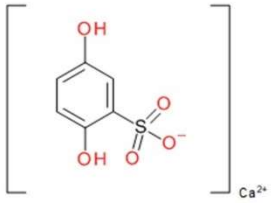

Calcium dobesylate

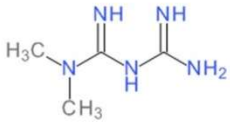

Metformin

Figure 1. Chemical structures of rutin, quercetin, troxerutin, diosmin, diosmetin, hesperidin, hesperetin, calcium dobesilate, and metformin.

This study found beneficial effects of all tested VPs and their structural analogs (aglycones) on the inhibition of AGE formation as observed in MGO-BSA and GO-BSA models. Nevertheless, their activity varied. Results expressed as percentage of inhibition of RCS-mediated AGEs are shown in Figure 2.

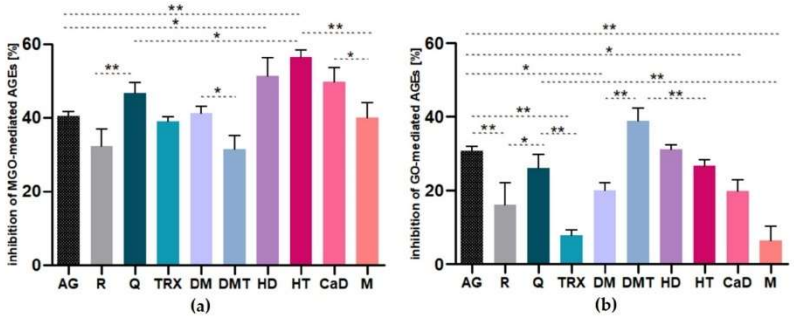

Figure 2. Anti-glycation activity after seven days of incubation of bovine serum albumin with glycative agents (5 mM) and tested compound (1 mM) expressed as % inhibition of: (**a**) MGO-mediated-AGE formation, (**b**) GO-mediated-AGE formation. The results are representative of three experiments performed in triplicate ± SD. Data were analyzed by one-way analysis of variance ANOVA ($p < 0.0001$) followed by Tukey's multiple comparison test; only significant differences are displayed: * $p < 0.05$, ** $p < 0.01$. Abbreviations: AG, aminoguanidine; R, rutin; Q, quercetin; TRX, troxerutin; DM, diosmin; DMT, diosmetin; HD, hesperidin; HT, hesperetin; CaD, calcium dobesilate; M, metformin.

In the MGO-BSA-model, hesperetin (56.50 ± 1.93%), hesperidin (51.52 ± 0.51%), calcium dobesilate (49.67 ± 4.08%), and quercetin (46.62 ± 1.75%) were found to be the most potent inhibitors of AGE formation. The activity of aminoguanidine used as the reference inhibitor was lower (40.46 ± 1.17%) than for the above-mentioned substances and comparable to the activity of diosmin (41.19 ± 3.78%), metformin (40.00 ± 2.86%), and troxerutin (39.05 ± 1.08%). Activity of the reference inhibitor used was higher only than the activity of rutin (33.46 ± 1.66%) and diosmetin (31.30 ± 5.07%). The results were slightly different for the GO-BSA-model, where diosmetin (38.82 ± 1.08%) and hesperidin (31.13 ± 3.58%) were the most potent inhibitors of glycation, their activity exceeding the activity of aminoguanidine (30.62 ± 1.28%). Hesperetin (26.74 ± 1.93%), quercetin (26.21± 2.00%), rutin (21.33 ± 0.85%), and next calcium dobesilate (19.94 ± 3.89%) and diosmin (19.96 ± 3.51%) showed similar, slightly less potent activity, while the poorest glycation inhibitory capacity was exhibited by troxerutin (7.85 ± 1.41%) and metformin (6.39 ± 1.63%).

In our study, hesperetin and hesperidin showed the most potent antiglycation activity in the model with MGO and a moderately strong effect in the model with GO. A study by Li et al. [35] reported the relatively strong activity of hesperetin (inhibition rate 56.7%) in a BSA model with glucose as the glycating agent and was more potent than its 7-*O*-rutinoside derivative, hesperidin (46.8%). This indicates that the free hydroxyl group at C-7 in ring A contributes to the antiglycative effect. Our observations are in agreement with reports of Matsuda et al. [36] where blocking of the 7-hydroxyl group reduced the antiglycation action. We observed a similar relationship for quercetin and troxerutin (3′,4′,7-tris[*O*-(2-hydroxyethyl)]rutin). In both biological models, the quercetin aglycone exhibited greater AGE inhibitory activity compared with troxerutin. Rutin (quercetin-3-*O*-rutinoside) also inhibited the process of protein glycation to a lesser extent than quercetin. Matsuda et al. [36] suggested that methylation of the hydroxyl group at the C-4′ position of the B ring of flavonoids increases the antiglycative effect. Indeed, in the model with MGO as the glycating agent, hesperetin had the highest activity, and in the GO-BSA-

model it was diosmetin; both compounds have a methoxyl group at the C-4′ position. The obtained results also showed that 7-*O*-rutinoside/aglycone pairs like diosmin/diosmetin and hesperidin/hesperetin showed different relationships in both tests. Flavones (with a double bond at C-2/C-3 of the C ring) were characterized by higher aglycone activity in the GO-BSA assay, and flavanones (without a double bond at C-2/C-3 of the C ring) by higher aglycone activity in the MGO-BSA assay. However, this observation requires further explanation. Among quercetin derivatives, the aglycone showed a higher effect than glycosides in both models.

Calcium dobesilate (CaD) is particularly noteworthy among the non-flavonoid compounds we studied. CaD is an angioprotective agent proposed to treat diabetic retinopathy (DR) by protecting against retinal vascular damage [37]. It can slow progression of DR during long-term oral treatment and prevent intravascular and extravascular retinal hemorrhages, reduce the frequency of exudate formation, and enhance visual acuity by reducing microvascular permeability [38]. Our study suggests that CaD also possesses potent activity to inhibit MGO- and GO-induced AGE formation.

In the antiglycation assays, we used aminoguanidine as a reference with well-known glycation inhibitory activity. We also decided to test metformin, a first-line drug for the management of diabetes type 2 because both compounds have a guanidine-derived structure. We found that the glycation inhibitory activity of both compounds in the methylglyoxal model was very similar at about 40%. However, in the model with glyoxal as the glycation agent, we observed that aminoguanidine exceeded the inhibitory activity of metformin by more than 6-fold. In a study by Mehta et al. [39], aminoguanidine and metformin were used as RCS scavengers to investigate the prevention of glyoxal toxicity in isolated rat hepatocytes. The authors observed that at comparable concentrations, metformin failed to prevent glyoxal-induced protein carbonylation, whereas aminoguanidine reduced the carbonylation of proteins. These observations may support, at least partially, our findings on the poor effects of metformin on inhibiting non-enzymatic glycation induced by glyoxal.

The process of non-enzymatic protein glycation is tightly linked to the enhanced production of free radicals and non-enzymatic glucose oxidation [37]. The formation of advanced glycation end products is a major source of reactive oxygen species, and the oxidative microenvironment triggered by the accumulation of AGEs can also promote their enhanced production [38]. Therefore, compounds inhibiting the formation of AGEs may act not only through direct quenching of RCS, but also through antioxidant or metal ion chelating activity [39,40]. The results of our experiment indicate that, indeed, in vitro antiglycative action is not only associated with RCS trapping activity. Compounds such as calcium dobesilate, diosmin, and troxerutin lacking the ability to trap methylglyoxal and glyoxal nevertheless exhibited antiglycation activity through other mechanisms. A more in-depth investigation of the relationship between structure and activity, with both quantitative and mechanistic aspects, is necessary to explain and fully understand the experimental observations.

2.2. Non-Enzymatic Antioxidant Activity

It is well known that oxidative stress can lead to cell and tissue damage, contributing to vascular endothelial dysfunction. Oxidative stress is also known to play a primary role in methylglyoxal-induced endothelial damage, and it is closely linked to the process of protein glycation [40]. Since restriction of the production of free radicals in the glycation process can decrease the formation of AGEs [41], we decided to investigate VPs and their structural analogs for antioxidant-reducing and antiradical activity.

ABTS (2,2′-azino-bis(3-ethylbenz-thiazoline-6-sulfonic acid assay) and FRAP (ferric reducing antioxidant power assay) are frequently used methods to assess the antioxidant capacity of a biological material, pure compound, or mixture of substances. Both are spectrophotometric techniques based on a single electron transfer mechanism (SET) [42,43]. FRAP allows one to directly determine the reducing ability of the sample [44]. The use of the ABTS assay enables measurement of the total antioxidant activity of the samples [45].

Vasoprotective substances and their structural analogs were tested for antioxidant activity using FRAP and ABTS assays. Metformin was examined to determine whether generally the first-line medication prescribed for type 2 diabetes has a reducing or antiradical activity. Trolox was used to plot the calibration curve in the ABTS test, and iron(II) sulfate solution was used in the FRAP test. Table 1 summarizes the antioxidant activity values expressed as percent inhibition and concentration required for a 50% reduction in radical activity (IC_{50}, μM) in the ABTS assay and as an Fe^{2+} iron ion equivalent (Fe(II), μM) in the FRAP assay. In order to clearly show the differences in the activity of the studied compounds in scavenging free radicals and reducing Fe^{3+} ions, we chose the results obtained for concentrations of 4.6 μM and 9.1 μM, respectively.

Table 1. Antioxidant activity of selected vasoprotectives and their structural analogs compared to metformin.

Sample	FRAP	ABTS	
	Fe(II) [a] [μM]	IC50 [μM]	Inhibition [%]
Rutin	30.14 ± 0.20	2.41 ± 0.05	69.17 ± 0.24 [b]
Quercetin	133.29 ± 0.30	3.81 ± 0.04	66.40 ± 1.12 [b]
Troxerutin	1.68 ± 0.43	24.12 ± 2.42	17.63 ± 0.93 [b]
Diosmin	5.77 ± 0.20	11.10 ± 1.44	30.41 ± 1.86 [b]
Diosmetin	25.62 ± 0.41	7.05 ± 0.05	39.92 ± 0.26 [b]
Hesperidin	53.08 ± 0.51	5.21 ± 0.07	48.94 ± 0.57 [b]
Hesperetin	99.27 ± 0.92	5.67 ± 0.13	49.80 ± 0.73 [b]
Calcium dobesilate	54.98 ± 0.65	5.13 ± 0.19	51.35 ± 0.88 [b]
Metformin	n.a.	n.a.	n.a.
Trolox	n.t.	11.29 ± 0.91	29.04 ± 0.81 [c]

Values are mean triplicate ($n = 3$); [a] calculated for samples at final concentration ~4.9 μM; [b] calculated for samples at final concentration ~9.1 μM; [c] calculated for samples at final concentration ~7.9 μM; n.a., no activity; n.t., not tested; FRAP assay antioxidant activity values were expressed as Fe^{2+} iron ion equivalent; ABTS assay antioxidant activity values were expressed as percent inhibition and concentration required for a 50% reduction of radical activity.

The current in vitro assays demonstrated the concentration-dependent antioxidant activity of the tested compounds, as shown in Figure 3. The higher the concentration of the sample used, the analogously greater the antiradical activity. In the FRAP assay, the most potent reducing ability was found for quercetin (133.3 μM Fe^{2+}) and hesperetin (99.3 μM Fe^{2+}), followed by calcium dobesilate (55.0 μM Fe^{2+}), hesperidin (53.1 Fe^{2+}), rutin (30.1 μM Fe^{2+}), and diosmetin (25.6 μM Fe^{2+}). In contrast, the lowest activity was recorded for diosmin (5.8 μM Fe^{2+}) and troxerutin (1.7 μM Fe^{2+}), while metformin showed no reducing action.

The ABTS assay showed the greatest antioxidant potential expressed as % inhibition for rutin (69.2%) and quercetin (66.4%), followed by similar inhibitory activity for calcium dobesilate (51.4%), hesperetin (49.8%), and hesperidin (48.9%). Slightly lower inhibition percentage values were observed for diosmetin (37.5%), diosmin (27.6%), and Trolox (29.0%) used as a positive control. The lowest inhibition activity was noted for troxerutin (10.8%), while metformin showed no scavenging activity in this assay. The IC_{50} values for the different tested compounds showed a similar trend as the percent inhibition values. The lowest IC_{50}, and consequently the highest antioxidant activity, was demonstrated by rutin (2.4 μM), followed by quercetin (3.8 μM), calcium dobesilate (5.1 μM), hesperidin (5.2 μM), hesperetin (5.7 μM), and diosmetin (7.1 μM). Slightly higher IC_{50} values and thus lower antioxidant activity were shown by diosmin (11.1 μM) and Trolox (11.3 μM), and the lowest by troxerutin (24.1 μM).

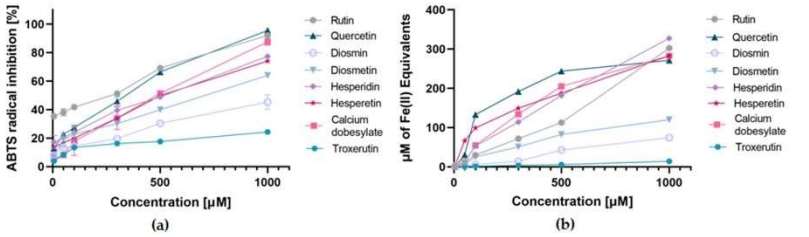

Figure 3. Concentration-dependent antioxidant activity of investigated vasoprotectives in (**a**) ABTS assay expressed as percent of radical inhibition; (**b**) FRAP assay expressed as Fe^{2+} iron ion equivalent (Fe(II) μM); all measurements were performed in triplicate in the concentration range of 5–1000 μM of tested compounds; results are presented as means ± SD (n = 3).

The FRAP assay indicated that the reducing activity of aglycones was higher than that of rutinosides—the effect of quercetin/diosmetin/hesperetin was more potent than troxerutin and rutin/diosmin/hesperidin. This pattern has been previously reported, for example, for kaempferol glycosides exhibiting about 30–40% lower antioxidant activity than the kaempferol aglycone [46]. Our study also indicated that glycosylation or ethylation of hydroxyl groups, exemplified by quercetin derivatives, significantly decreased the reducing potential of the compound (quercetin >>> rutin > troxerutin). Blocking the flavonoid phenolic group at C-4′ also diminished the reducing properties (quercetin > hesperetin > diosmetin). In contrast, saturation of the double bond at C-2/C-3 (flavanones vs. flavones) increased activity (hesperidin >>> diosmin, hesperetin >>> diosmetin). These relationships showed that the reducing ability depends mainly on the number of free hydroxyl groups in the molecule and the degree of oxidation of the three-carbon linker in the C-ring. A similar clear structure–activity relationship was not demonstrated using the ABTS test. In both antioxidant assays and the MGO-BSA antiglycation test, hesperidin and calcium dobesilate showed comparable effects.

Interestingly, metformin showed no antioxidant activity in either the FRAP assay or the ABTS assay, however, there are reports that it has the ability to inhibit intracellular formation of ROS [47]. A study by Logie et al. [48] showed that metformin can chelate metal ions, which may be directly responsible for its antioxidant effect. A similar conclusion emerges for troxerutin, which showed very low activity in both antioxidant assays, but some publications have reported its antiradical activity in vivo [49]. This effect can also be explained by chelating activity, confirmed in several studies [50].

It should be noted that high in vitro activity does not necessarily reflect in vivo activity [51]. An important limitation is the bioavailability of vasoprotective flavonoids. Rutinosides are known to have low bioavailability due to their poor solubility and lipophilicity [52]. Although quercetin and hesperetin have shown high reducing and antiradical activity, it should be taken into account that their bioavailability is around 20%; only this amount of orally administered dose reaches the bloodstream [53]. Quercetin taken at 500 mg reaches a plasma concentration of about 1.4 μM [54], and hesperetin (500 mg) about 2.7 μM [55], so they were lower than the IC_{50} concentrations for which the activities were specified in our study. In comparison, calcium dobesilate, whose radical inhibitory capacity was comparable to that of hesperetin (at ~5 μM), reached a plasma concentration of about 19 μM after 500 mg administration [56].

2.3. Direct Methylglyoxal/Glyoxal Trapping Capacity

RCS trapping is one of the mechanisms that potentially reduce plasma concentration of methylglyoxal and glyoxal [57]. Therefore, selected VPs and their structural analogs have been examined for their ability to trap reactive carbonyl species. After 1 h incubation of each test compound (rutin, troxerutin, diosmin, diosmetin, hesperidin, hesperetin, calcium dobesilate) with methylglyoxal or glyoxal under simulated physiological conditions, the

reaction mixture was further analyzed by UHPLC-MS to detect potentially formed adducts of the test compound with MGO/GO. In the study, quercetin and metformin were used as reference compounds with recognized activity for direct trapping of 1,2-dicarbonyls. The extract ion chromatogram (EIC) mode was used to search for pseudomolecular ions increased by 72 Da/144 Da for mono-MGO/di-MGO adducts or by 58 Da/116 Da for mono-GO/di-GO adducts. All compounds except metformin, for which the positive ion mode was used, were analyzed in negative electrospray ionization mode.

The study revealed that under the experiment conditions quercetin, rutin, diosmetin, hesperetin, hesperidin, and metformin showed activity toward direct trapping of methylglyoxal, whereas glyoxal was directly trapped only by rutin, diosmetin, hesperetin, and hesperidin. The products of the reaction between MGO and GO with tested compounds and the fragmentation pattern of each product are listed in Tables 2 and 3, respectively. Troxerutin and calcium dobesilate did not trap RCS, probably due to chemical structure differences.

Table 2. Adducts of methylglyoxal and investigated compounds formed after 1 h of incubation in pH 7.4 of phosphate buffer solution at 37 °C.

Compound	Peak	Rt [min]	$[M-H]^-$ or $[M+H]^+$ Mono-MGO Adduct (*m*/*z*)	MS/MS (*m*/*z*)	Peak	Rt [min]	$[M-H]^-$ or $[M+H]^+$ Di-MGO Adduct (*m*/*z*)	MS/MS (*m*/*z*)
Rutin [1]	a	8.69	681.1698	663, 609, 301	a	7.90	753.1885	681, 644, 609, 301
	b	8.84	681.1701	663, 609, 301	b	8.26	753.1890	681, 644, 609, 301
	c	8.85	681.1684	663, 609, 301	c	8.44	753.1840	681, 644, 609, 301
Quercetin [2]	a	10.93	373.0567	n.d.	a	10.01	445.0779	n.d.
	b	11.06	373.0562					
Troxerutin	-	-	n.d.	n.d.	-	-	n.d.	n.d.
Diosmin	-	-	n.d.	n.d.	-	-	n.d.	n.d.
Diosmetin [3]	a	12.19	371.0758	353, 338, 299	a	11.24	443.0970	425, 410, 299
	b	12.36	371.0766	353, 338, 299				
Hesperidin [4]	a	8.97	681.1972	609, 373, 301	-	-	n.d.	n.d.
	b	9.19	681.1981	609, 373, 301				
	c	9.82	681.1966	609, 373, 301				
	d	9.95	681.1979	609, 373, 301				
	e	10.88	681.1965	609, 373, 301				
	f	10.98	681.1960	609, 373, 301				
Hesperetin [5]	a	12.04	373.0913	355, 340, 301	a	10.80	445.1103	427, 409
	b	12.93	373.0899	355, 340, 301				
Calcium dobesilate	-	-	n.d.	n.d.	-	-	n.d.	n.d.
Metformin [6]	a	1.48	184.1158	n.d.	a	1.57	256.1297	n.d.
	b	1.20	202.1229		b	1.64	256.1300	

Pseudomolecular ion (*m*/*z*): [1] 609; [2] 301; [3] 299; [4] 609; [5] 301; [6] 130; Rt, retention time; n.d., not detected; letters of the alphabet (a–f) represent different isomers of the same compound.

In the reaction of rutin with methylglyoxal, after one hour of incubation, the appearance of three major peaks with pseudomolecular ion masses at m/z 681 and retention times of 8.69, 8.84, 8.85 min, respectively, were observed (Table 2). They corresponded to the molecular weight of mono-MGO-rutin adduct (M*r* 682 Da). All of them produced fragment ions at m/z 663, indicating elimination (neutral lost) of a water molecule [M–18–H]$^-$ and at 609, which suggests loss of one MGO molecule [M–72–H]$^-$. Three other peaks a–c with m/z 753 (Rt 7.90, 8.26, 8.44 min) were also present, and were identified as di-MGO-rutin adducts as they gave fragments at m/z 681, representing the mass of the di-MGO adduct minus one methylglyoxal moiety [M–72–H]$^-$, and 609, indicating the loss of two methylglyoxal molecules [M–144–H]$^-$. With glyoxal, rutin formed only mono-GO adducts. Two peaks appeared on the chromatogram with pseudomolecular ions of 667 characterized by retention times of 8.09 and 8.41 min, and since their masses were greater

than that of rutin by the mass of a single glyoxal molecule, they were further characterized as mono-GO-rutin adducts (Table 3). The ability of rutin to trap methylglyoxal has been previously reported in several studies [58,59]. Mass spectra of the adducts formed by rutin and MGO/GO and proposed chemical structures are shown in Figure 4.

Table 3. Adducts of glyoxal and investigated compounds formed after 1 h of incubation in pH 7.4 phosphate buffer solution at 37 °C.

Compound	Peak	Rt [min]	$[M-H]^-$ or $[M+H]^+$ Mono-GO Adduct (*m*/*z*)	MS/MS (*m*/*z*)	Peak	Rt [min]	$[M-H]^-$ or $[M+H]^+$ Di-GO Adduct (*m*/*z*)	MS/MS (*m*/*z*)
Rutin [1]	a b	8.09 8.41	667.1445 667.1448	n.d. n.d.	-	-	n.d.	n.d.
Quercetin [2]	-	-	n.d.	n.d.	-	-	n.d.	n.d.
Troxerutin	-	-	n.d.	n.d.	-	-	n.d.	n.d.
Diosmin	-	-	n.d.	n.d.	-	-	n.d.	n.d.
Diosmetin [3]	a b	11.64 12.1	357.0605 357.0602	324, 313, 299, 284 324, 313, 299, 284	-	-	n.d.	n.d.
Hesperidin [4]	a b	11.05 11.37	677.1861 677.1844	609, 301 609, 301	-	-	n.d.	n.d.
Hesperetin [5]	a b c	11.28 12.37 13.78	359.0771 359.0762 359.0768	341, 326, 301 341, 326, 301 341, 326, 301	a	12.99	417.0808	399, 301
Calcium dobesilate	-	-	n.d.	n.d.	-	-	n.d.	n.d.
Metformin	-	-	n.d.	n.d.	-	-	n.d.	n.d.

Pseudomolecular ion (*m*/*z*): [1] 609; [2] 301; [3] 299; [4] 609; [5] 301; Rt, retention time; n.d., not detected; letters of the alphabet (a–c) represent different isomers of the same compound.

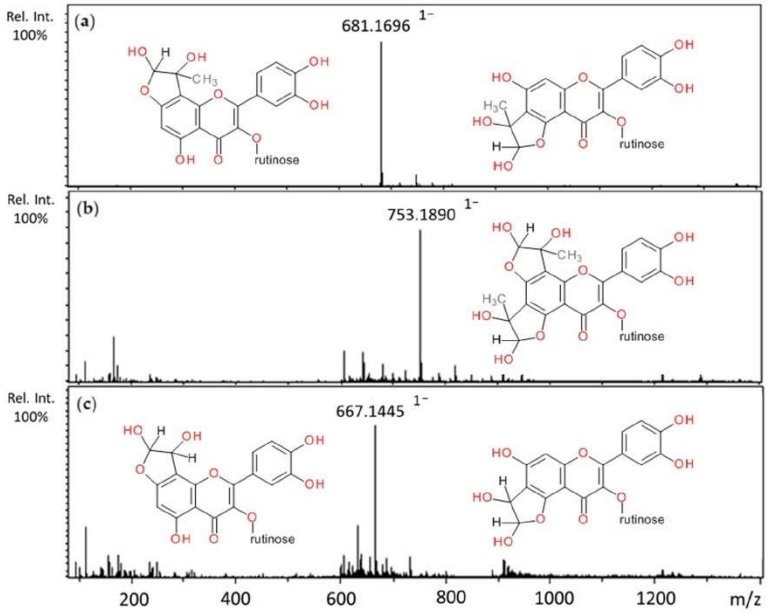

Figure 4. Mass spectra of methylglyoxal and glyoxal adducts with rutin after 1 h incubation in pH 7.4 phosphate buffer solution at 37 °C and their proposed chemical structure: (**a**) mono-MGO-rutin; (**b**) di-MGO-rutin; (**c**) mono-GO-rutin; other isomeric forms are also possible.

Incubation of diosmetin with MGO resulted in three chromatographic peaks at 11.24, 12.09, and 12.36 min with m/z values of 443 and 371 (a and b, Table 2). The first was described as di-MGO-diosmetin because the pseudomolecular ion mass corresponding to diosmetin increased by two methylglyoxal molecules (144 Da) and MS/MS analysis confirmed this—a fragment ion with m/z 299 corresponding to diosmetin was noted. The other two peaks with m/z at 371 were 72 Da greater than the pseudomolecular ion of diosmetin; therefore, they were proposed as mono-MGO-diosmetin adducts. The fragmentation pattern indicated that di-MGO-diosmetin and mono-MGO-diosmetin lost a water molecule to form daughter ions at m/z 425 and 353 $[M–18–H]^-$, followed by a methyl group (15 Da) in the B ring resulting in ions at m/z 410 and 338 $[M–18–15–H]^-$, respectively. The reaction of diosmetin and glyoxal led to the formation of two main peaks in the UHPLC chromatogram with pseudomolecular ions at m/z 357 (Rt 11.64 and 12.10 min), both heavier by 58 Da than the pseudomolecular ion of diosmetin (m/z 299), and therefore were assigned as mono-GO-diosmetin adducts (Table 3). The fragment ions observed in the MS/MS analysis similarly showed that both mono-MGO-diosmetin and mono-GO-diosmetin first lost the water and then the methyl group $[M–18–15–H]^-$. Mass spectra of the adducts formed by diosmetin and MGO/GO and the proposed chemical structures are shown in Figure 5.

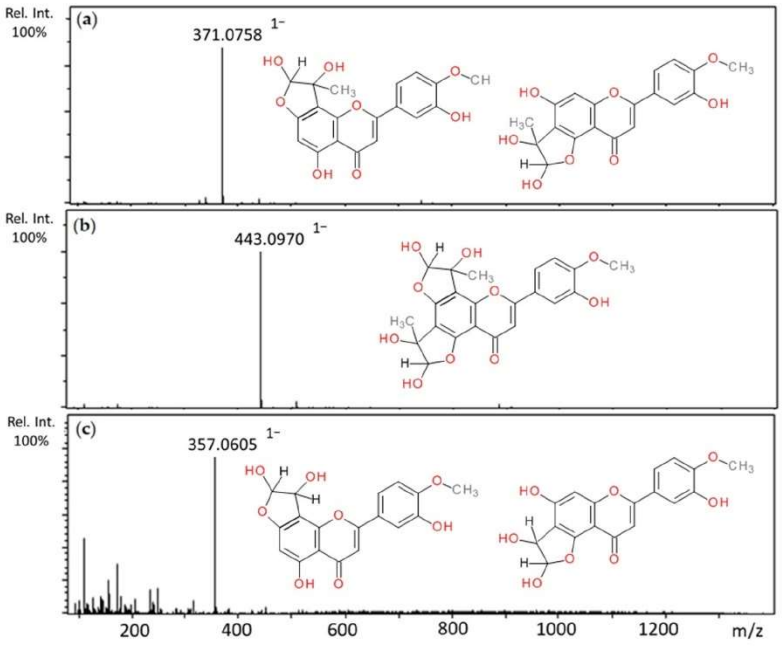

Figure 5. Mass spectra of methylglyoxal and glyoxal adducts with diosmetin after 1 h incubation in pH 7.4 phosphate buffer solution at 37 °C and their proposed chemical structure: (**a**) mono-MGO-diosmetin; (**b**) di-MGO-diosmetin; (**c**) mono-GO-diosmetin; other isomeric forms are also possible.

Hesperidin and methylglyoxal after 1 h of incubation produced six chromatographic peaks with the pseudomolecular ions at m/z 681, and retention times 8.97, 9.19, 9.82, 9.95, 10.88, and 10.98 min (Table 2). The fragmentation pattern was the same for each ion; three principal daughter ions were produced with masses at m/z 609, 373, and 301. The molecular weight of the resulting ions (682 Da) was greater than the molecular weight of hesperidin by 72 Da, and were therefore identified as mono-MGO-hesperidin adducts. The presence of

fragment ions at m/z 609 (the hesperidin pseudomolecular ion) further confirmed this. The fragmentations with m/z 373 and 301 suggest the loss of the rutinose moiety by mono-MGO-hesperidin $[M–308–H]^-$ and methylglyoxal $[M–308–72–H]^-$, respectively. After incubation of hesperidin with glyoxal, two major peaks appeared on the chromatogram at 11.05 and 11.37 min with m/z at 677 (Table 3). Both were recognized as mono-GO-hesperidin adducts as their pseudomolecular ion values were greater than the ion for hesperidin (m/z 609) by 58 Da. This was later supported by MS/MS data where a daughter ion was observed with the m/z value of 609 $[M–58–H]^-$. A 301 ion was also observed, suggesting, as described above, the loss of rutinose by the hesperidin molecule $[609–308–H]^-$. Mass spectra of the adducts formed by hesperidin and MGO/GO and proposed chemical structures are shown in Figure 6.

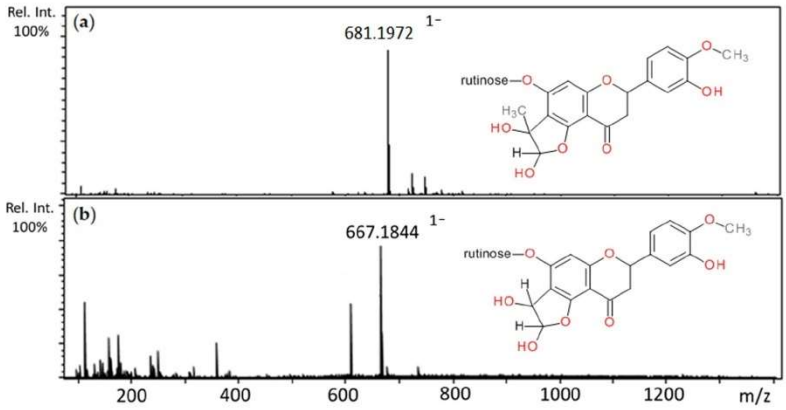

Figure 6. Mass spectra of methylglyoxal and glyoxal adducts with hesperidin after 1 h incubation in pH 7.4 phosphate buffer solution at 37 °C and their proposed chemical structure: (**a**) mono-MGO-hesperidin; (**b**) mono-GO-hesperidin; other isomeric forms are also possible.

After one-hour incubation of hesperetin and methylglyoxal, three major peaks were detected with pseudomolecular ion masses and retention times, respectively: 373 (12.04 and 12.93 min) and 445 (10.80 min). Peaks with an anion at 371, greater than the ion of hesperetin (m/z 301) by 72 Da, corresponding to the coupling of one molecule of methylglyoxal, were identified as mono-MGO-hesperetin adducts (Table 2). The loss of one water molecule resulted in the most abundant fragment ion of m/z 355 $[M–18–H]^-$. The peak at m/z 445 was labeled as di-MGO-hesperetin as its molecular weight equaled the mass of the hesperetin plus two MGO molecules (M*r* 446 Da). Similarly, loss of one molecule of water by the di-MGO-hesperetin adduct led to the formation of the most abundant daughter ion with m/z 427 $[M–18–H]^-$. The elimination of the second water molecule resulted in the ion at m/z 409. Four major peaks with molecular ions at 359 (a–c) and 417 with retention times of 11.28, 12.37, 13.78, 12.99 were observed after 1 h incubation of hesperetin and glyoxal (Table 3). Peaks with m/z at 359 having pseudomolecular ions heavier than the hesperetin ion (m/z 301) by 58 Da were considered as mono-GO-hesperetin adducts, as confirmed by MS/MS data. A peak with m/z 417 greater than the ion for hesperetin by 116 Da (mass corresponding to two glyoxal molecules) was analogously identified as a di-GO-hesperetin adduct. Its fragment ion at 409, reduced by 18 Da (after water loss), was noted on the MS/MS spectrum. Previous studies have demonstrated the ability of hesperetin to form similar adducts with acrolein [60]. Mass spectra of the adducts formed by hesperetin and MGO/GO and the proposed chemical structures are shown in Figure 7.

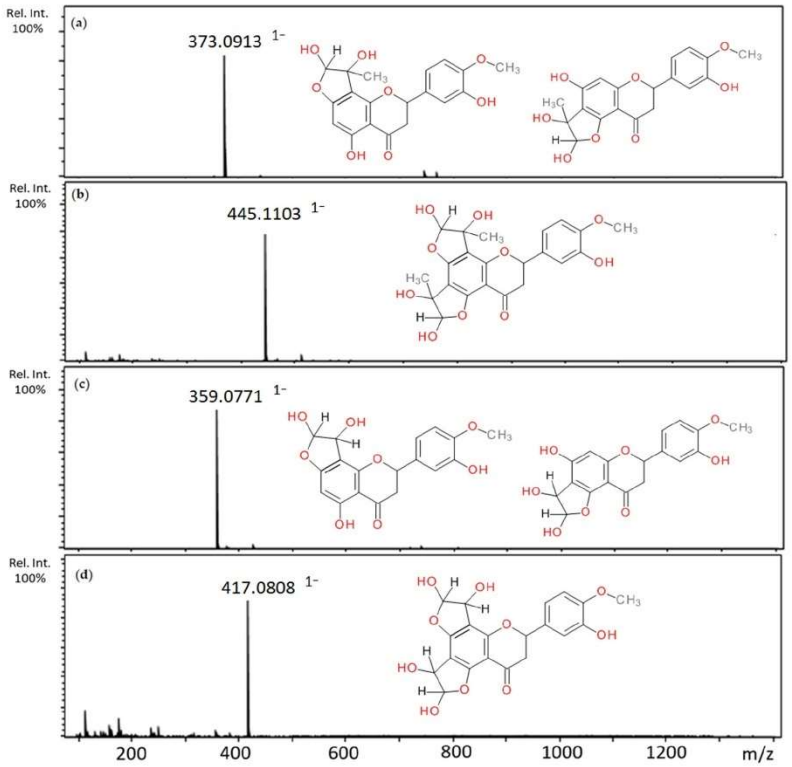

Figure 7. Mass spectra of methylglyoxal and glyoxal adducts with hesperetin after 1 h incubation in pH 7.4 phosphate buffer solution at 37 °C and their proposed chemical structure: (**a**) mono-MGO-hesperetin; (**b**) di-MGO-hesperetin; (**c**) mono-GO-hesperetin; (**d**) di-GO-hesperetin; other isomeric forms are also possible.

Quercetin incubated with methylglyoxal resulted in two peaks characterized as mono-MGO-quercetin and one as di-MGO-quercetin; their pseudomolecular ions were at m/z 373 (a–b) for the mono-adducts (quercetin precursor ion m/z 301 increased by 72 Da) and 445 (quercetin precursor ion m/z 301 increased by 144 Da) for the di-adduct (Table 2). Li et al. [16] reported that quercetin has the potential to trap glyoxal; however, this activity was not observed under the conditions of our study. Mass spectra of the adducts formed by quercetin and MGO and the proposed chemical structures are shown in Figure 8.

Incubation of metformin and methylglyoxal led to four chromatographic peaks with pseudomolecular ions $[M+H]^+$ with 202 at Rt 1.20 min, 184 at 1.46 min, 256 at 1.57 min, and 1.67 min (Table 2). The first ion was described as mono-MGO-metformin due to the ion mass corresponding to metformin increased by one methylglyoxal molecule (72 Da). Based on the literature reports on structural studies of metformin and methylglyoxal adducts [22], the second peak at m/z 184 was identified as (E)-1,1-dimethyl-2-(5-methyl-4-oxo-4,5-dihydro-1H-imidazol-2-yl)guanidine (metformin-MG imidazolinone) and was formed by eliminating one water molecule from mono-MGO-metformin (Mr, 129 + 72 – 18 = 183 Da). The other two peaks with the ions at m/z about 256 were attributed to metformin conjugated with two methylglyoxal molecules as their mass, corresponding to the pseudomolecular ion of metformin-MG imidazolinone (m/z 184), increased by another 72 Da (184 + 72 = 256 Da). The peak with the ion at 184 was dominant compared to the peak with the ion at 202, which

may suggest that the monoadduct of metformin with methylglyoxal is more stable after the elimination of one water molecule. However, after 1 h of incubation, both chemical structures of the metformin mono-adduct formed by the reaction were observed. Metformin and glyoxal did not form adducts under conditions of the experiment. Mass spectra of the adducts formed by metformin and MGO and the proposed chemical structures are shown in Figure 9.

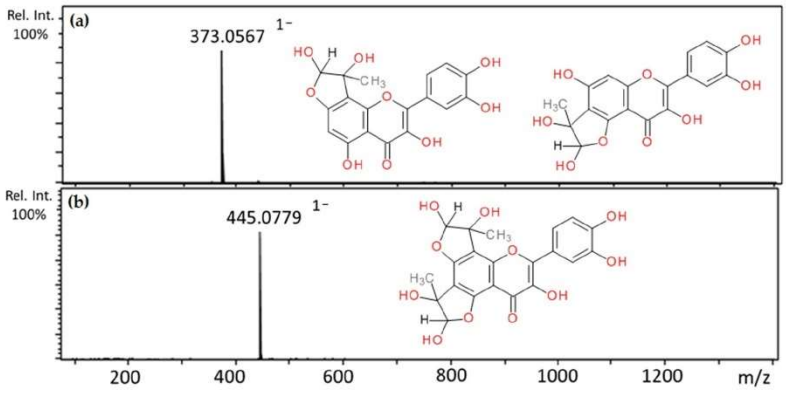

Figure 8. Mass spectra of methylglyoxal adducts with quercetin after 1 h incubation in pH 7.4 phosphate buffer solution at 37 °C and their proposed chemical structure: (**a**) mono-MGO-quercetin; (**b**) di-MGO-quercetin; other isomeric forms are also possible.

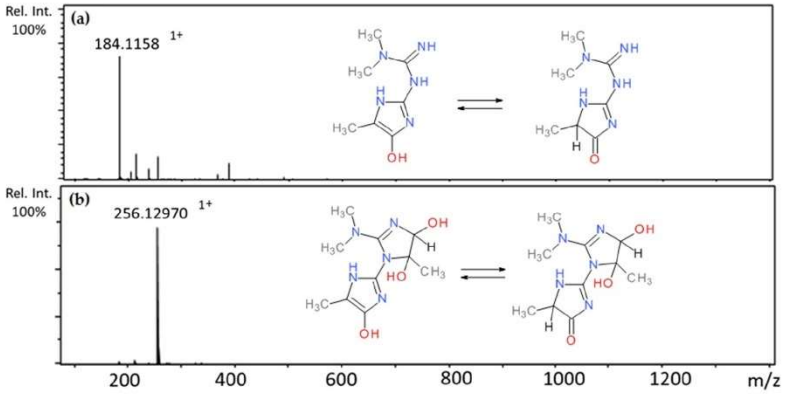

Figure 9. Mass spectra of methylglyoxal adducts with metformin after 1 h incubation in pH 7.4 phosphate buffer solution at 37 °C and their proposed chemical structure (isomers): (**a**) mono-MGO-metformin; (**b**) di-MGO-metformin; other isomeric forms are also possible.

2.4. Time Course Study of RCS Scavenging Reaction

For compounds demonstrating the ability to directly trap methylglyoxal (rutin, quercetin, diosmetin, hesperidin, hesperetin, metformin) and glyoxal (rutin, diosmetin, hesperidin, hesperetin), a time course study of the trapping reaction was performed. To determine the amount of MGO/GO remaining after incubation at each time point, samples were derivatized with PDA. This method of measuring RCS concentration in various samples is often used in both in vitro and in vivo studies [61].

Activity over time expressed as a percentage of remaining MGO/GO after reacting with the tested compounds for 1, 2, 4, 8, and 24 h is shown in Figure 10. Data points represent the mean % of remaining MGO/GO with the standard deviation from two independent experiments.

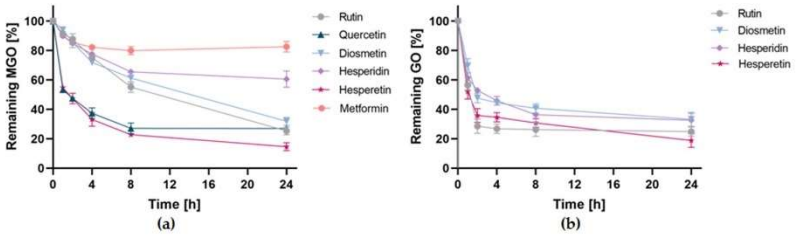

Figure 10. RCS trapping efficiency of tested compounds in pH 7.4 phosphate buffer solution at 37 °C for 1, 2, 4, 8, and 24 h expressed as % of remaining MGO/GO; (**a**) reaction with methylglyoxal; (**b**) reaction with glyoxal. All data are presented as means ± SD (n = 2).

The study showed that methylglyoxal scavenging activity varied among the tested compounds, while glyoxal was scavenged by all tested compounds with quite similar efficacy. Within 24 h, hesperetin, rutin, quercetin, and diosmetin succeeded in trapping 85.41 ± 2.71%, 74.67 ± 2.69%, 73.01 ± 1.89%, and 68.17 ± 2.71% of MGO, respectively, and were found to be the most effective of the tested compounds. At the same time, hesperidin (39.48 ± 5.47%) and metformin (17.42 ± 3.57%) showed the lowest efficiency. Among the most potent compounds, differences in the kinetics of the MGO trapping reaction were evident. Hesperetin and quercetin trapped 50% of methylglyoxal in as little as two hours. In contrast, diosmetin and rutin were only able to trap less than 15% of the MGO at the same time, and both compounds took more than 8 h to quench 50% of the methylglyoxal. Metformin is used in diabetes, for which the ability to trap methylglyoxal was demonstrated in vitro and in vivo. However, the results of our study suggest that its activity in trapping MGO compared to flavonoid substances was relatively low.

After 24 h of incubation, hesperetin and rutin were found to be the most effective in trapping glyoxal by quenching 81.17 ± 4.66% and 75.12 ± 3.11% of GO, respectively. Only slightly less effective was hesperidin with 67.44 ± 4.64% and diosmetin with 66.76 ± 4.76%. Glyoxal seems to be trapped more rapidly in comparison to methylglyoxal. Both hesperetin and rutin were able to quench nearly 50% of glyoxal in just one hour, and diosmetin and hesperidin within 2 h.

The results indicated that among the tested compounds, hesperetin was the most efficient in trapping both methylglyoxal and glyoxal. The weak activity of hesperidin (hesperetin-7-*O*-rutinoside) compared to hesperetin is probably due to the substitution of the hydroxyl group at C-7, resulting in changes in charge distribution in the molecule and therefore decrease general trapping activity [62]. Despite a very similar structure, the quenching ability of MGO and GO was higher for hesperetin than for diosmetin, which is probably attributed to the presence of a double bond at C-2 and C-3 in the heterocyclic ring C of diosmetin. Its presence has been reported to decrease the trapping activity of RCS [63], which is in agreement with our results. The B ring is not thought to play a prominent role in trapping activity. The same study reported that the number of hydroxyl groups in the B ring does not significantly affect the trapping effect [63]. However, the findings of our study suggested that the presence of a substituted hydroxyl group in the B ring at C-4′ stabilizes the molecule, prevents quinone formation, and further C-ring cleavage, thereby preserving the original structure and the consequent trapping activity. This structural feature has also been shown to favorably affect antiglycation potential, possibly via enhancing the RCS trapping activity.

Although our results suggest that selected vasoprotective flavonoids have the ability to trap both methylglyoxal and glyoxal, previous studies have indicated that methylglyoxal is preferred in the trapping reaction. An in vitro study by Li et al. [16] in a model simulating physiological conditions showed that quercetin reduced methylglyoxal concentrations more than twice as efficiently as glyoxal when both compounds were present in solution at the same initial concentration. An in vivo study in humans, on the other hand, showed that although quercetin significantly reduced MGO plasma concentrations in patients (~10%), it had no statistically significant effect on glyoxal concentrations [64]. It should also be noted that according to some studies, compounds sharing the same trapping mechanism can act synergistically; the study of Shao et al. [62] showed that a mixture of quercetin and phloretin traps methylglyoxal more effectively than each compound alone.

The efficiency of RCS trapping in plasma by the investigated substances under in vivo conditions may vary greatly due to the metabolism. Most substances during phase II reactions are conjugated with, for example, glucuronic acid, sulfuric acid, or amino acids [65]. The form to which the drug is metabolized is individual for a given substance and may depend on many factors including the composition of the gut microbiota if absorption occurs in the large intestine (for rutinosides, e.g., hesperidin, diosmin, rutin, troxerutin) [66]. During the phase II reaction, any hydroxyl group of flavonoids can be substituted including those responsible for the trapping activity in ring A (C-5 and C-7), which is likely to reduce the activity of these compounds in plasma [67]. A series of studies related to metabolism is required to assess the exact trapping activity of individual compounds in humans. However, in vitro studies provide the background for clinical trials and are crucial for the selection of potentially useful molecules.

In summary, quercetin, rutin, diosmetin, hesperetin, hesperidin, and metformin were shown to be able to directly trap methylglyoxal, and rutin, diosmetin, hesperetin and hesperidin were shown to trap glyoxal. Hesperetin was found to be the most effective among VPs tested in trapping both methylglyoxal and glyoxal. After 24 h, it scavenged the highest percentage of both RCS.

Additionally, to the best of our knowledge, this is the first time direct RCS trapping activity has been confirmed for hesperetin, hesperidin, and diosmetin. Our study also confirmed the following structure and flavonoid activity relationships: (a) substitution of the hydroxyl group at the C-7 position results in a decrease in the trapping of methylglyoxal and glyoxal, as well as reducing activity; and (b) the double bond in the ring C decreases the MGO/GO trapping and reducing ability. Furthermore, we put forward our hypothesis that the B ring is essential in the trapping activity of flavonoids, which is contrary to earlier reports. Zhu et al. [63] previously claimed that it does not play a significant role in this activity. The findings of our study suggest that the substitution of a phenol group at the C-4′ position of the phenyl ring B stabilizes the molecule, preventing the formation of semiquinone and quinine methide structures, and further cleavage of the heterocyclic C ring. Thus, the original flavonoid structure is preserved and the trapping activity is maintained.

All of the investigated compounds inhibited the formation of RCS-induced AGEs, most likely through several different mechanisms. We observed that the capacity to directly trap RCS was not the only determinant of a potent antiglycative effect, since the ability to inhibit the non-enzymatic process of protein glycation is also greatly influenced by reducing and antiradical (antioxidant) activity. Calcium dobesilate as a potent antioxidant without RCS trapping action showed high antiglycation potential in the MGO-BSA model. In addition, it is characterized by high bioavailability compared to other tested phlebotropic compounds. Among the investigated chemicals with RCS trapping potential, hesperetin was the most potent antiglycative agent in the MGO-BSA model, and in the GO-BSA model, it was shown to be diosmetin.

The antioxidant activity assays showed that the compounds with high reducing and antiradical potential were quercetin, rutin, hesperetin, and calcium dobesilate, and their

activities were concentration dependent. It was also confirmed that the activity of flavonoid aglycones was higher than that of glycosides.

3. Methods

3.1. Chemicals and Standards

Methylglyoxal (40% in water), glyoxal (40% in water), 2,2-diphenyl-1-picrylhy-drazyl, 2,2-azino-bis-(3-ethylbenzothiazoline-6-sulfonic acid), methanol (HPLC grade), acetonitrile (HPLC gradient grade and LC-MS grade), water (LC-MS grade), diosmin, diosmetin, hesperidin, hesperetin, Trolox, metformin hydrochloride, bovine serum albumin, DMSO, 98–100% formic acid, 2-methylquinoxaline, quinoxaline, o-phenylenediamine, 2, 4, 6-tripyridyl-*s*-triazine, iron(III) chloride hexahydrate, and iron(II) sulfate heptahydrate were purchased from Merck-Sigma-Aldrich (Sigma-Aldrich Sp. z o.o., Poznań, Poland); NaCl, KCl, Na_2HPO_4, and KH_2PO_4 (reagent grade) were obtained from Chempur (Piekary Śląskie, Poland); quercetin and rutin were from Extrasynthese (Genay Cedex, France); calcium dobesilate was purchased from PPF Hasco-Lek S. A. (Wroclaw, Poland). Water used in the study was glass-distilled and deionized. The stock solutions of standards (3 mM) were prepared by dissolving the appropriate amount of a reference compound in 5 mL of methanol or DMSO. Working standard solutions for the derivatization experiment in the range of 5–210 µM were made by mixing with 50% aq. (aqueous) methanol (*v*/*v*), filtered through hydrophilic Millex Syringe Filters (Durapore 0.22 µm; Millipore, Burlington, MA, USA) and stored at −20 °C.

3.2. Antiglycation Assay in BSA-RCS In Vitro Model

The formation of advanced glycation end products was measured following a slightly modified method proposed by Liu et al. [68]. In brief, 90 µM bovine serum albumin was incubated with methylglyoxal and glyoxal at 5 mM in sodium phosphate buffer at 100 mM and pH 7.4, with 0.02% sodium azide (to prevent microbial growth). The compounds investigated for inhibition of non-enzymatic glycation were added at a final concentration of 1 mM. Then, the reaction solution was incubated at 37 °C, shaken at 40 revolutions per minute for seven days in closed vials away from light. Measurement of the fluorescent intensity of total AGEs after incubation was carried out using a Cary Eclipse 500 spectrophotometer (Agilent, Santa Clara, CA, USA) at a wavelength of 350 nm for excitation and 450 nm for emission. Data acquisition was obtained with the Cary Eclipse Control Software (Agilent, Santa Clara, CA, USA). The measurements from three experiments were all performed in triplicate, and the percent inhibition of AGE formation was calculated using the following equation:

$$\text{Inhibition of RCS-mediated AGES [\%]} = \{1 - [(FI_1)/(FI_0)]\} \times 100$$

where FI_0 is mean fluorescence intensity of the blank sample and FI_1 is the mean fluorescence intensity of the sample.

3.3. Antioxidant Activity

3.3.1. ABTS Assay

The ABTS radical scavenging activity was determined according to the slightly modified method described by Chen and Kang [69]. The $ABTS^{\bullet+}$ stock solution was prepared by mixing equal quantities of aqueous solutions of 2,2-diphenyl-1-picrylhydrazyl,2,2-azino-bis-(3-ethylbenzothiazoline-6-sulfonic acid (ABTS, 7.0 mM) and potassium persulfate ($K_2S_2O_8$, 2.45 mM) and incubating the mixture in the dark at 25 °C for 12 h. The stock solution of ABTS and $K_2S_2O_8$ was then diluted with methanol to reach absorbance at 734 nm. In a 96-well microplate, 200 µL of $ABTS^{\bullet+}$ reagent was mixed with 20 µL of each tested sample at different concentrations. The plate was incubated for 15 min in the dark at ambient temperature and the absorbance was taken at 517 nm using a Multiskan GO microplate spectrophotometer (Thermo Fisher Scientific; Waltham, MA, USA). All measurements were performed in triplicate using the concentration range of 5–1000 µM of the tested

compounds. The standard curve was prepared using different concentrations of Trolox in the range of 100–1000 μM. The ABTS radical scavenging activity was calculated as follows:

$$\text{ABTS radical inhibition [\%]} = (A_0 - A_1)/A_0 \times 100$$

where A_0 is the mean absorbance of the control and A_1 is the mean absorbance of the sample with ABTS. The IC_{50} values were calculated using linear regression analysis and used to express the antioxidant capacity.

3.3.2. FRAP Assay

The ferric reducing antioxidant power assay (FRAP) was performed according to the method proposed by Benzie and Strain [70] with slight modification. The stock solution of FRAP reagent was obtained by mixing 10 mM 2,4,6-tripyridyl-*s*-triazine (TPTZ) in 40 mM hydrochloric acid with 20 mM iron(III) chloride hexahydrate and 300 mM acetate buffer (pH 3.6) at 1:1:10 (*v*/*v*/*v*). The freshly prepared FRAP reagent (200 μL) was added to solutions of tested compounds at different concentrations (20 μL) and thoroughly mixed in a 96-well microplate. The absorbance of a blue ferrous tripyridyltriazine complex (Fe^{2+}/TPTZ) was read after 4 min of incubation in the dark at 593 nm using a Multiskan GO microplate spectrophotometer (Thermo Fisher Scientific; Waltham, MA, USA). Results were expressed in Fe^{2+} μM. All measurements were performed in triplicate in the concentration range 5–1000 μM of the analyzed compounds.

3.4. Direct Methylglyoxal and Glyoxal Trapping Capacity

Methylglyoxal and glyoxal direct trapping capacity was investigated according to the slightly modified Sang et al. [71] method. Briefly, 0.6 mM methylglyoxal (MGO) or glyoxal (GO) was incubated for 1 h with 0.2 mM of rutin, troxerutin, diosmin, diosmetin, hesperidin, hesperetin, calcium dobesilate, metformin hydrochloride, and quercetin in 100 mM phosphate buffer saline (PBS; pH 7.4) at 37 °C to equal physiological conditions and shaken at 40 revolutions per minute. The incubation reaction was terminated by adding 2.5 μL of acetic acid (≥99%) and placing the collected samples in an ice water bath. The samples were further filtered through hydrophilic Millex Syringe Filters (Durapore 0.22 μm; Millipore, Burlington, MA, USA) and analyzed using UHPLC-ESI-MS to investigate their ability to form adducts with methylglyoxal and glyoxal. The trapping agent solutions were freshly prepared before each series of experiments was begun, and the pH of the sodium phosphate buffer was determined immediately before use.

3.5. Time Course Study of MGO and GO Scavenging Reaction

The time course of the MGO and GO scavenging reaction was investigated for the compounds' indicated activity in methylglyoxal and glyoxal direct quenching assay in UHPLC-ESI-QqTOF-MS analysis. The study was carried out according to the method of Shao et al. [62] with slight modification. The direct trapping study found using an excess of MGO and GO allows compounds to form both mono- and di-adducts with α-oxoaldehydes. Therefore, methylglyoxal or glyoxal at a final concentration of 0.6 mM and each selected compound at 0.2 mM were incubated in 100 mM phosphate buffer saline (PBS; pH 7.4) at 37 °C with a speed of 40 revolutions per minute to simulate physiological conditions for 1, 2, 4, 8, and 24 h. Afterward, 500 μL of reaction mixtures were collected at each time point and placed in an ice water bath, then 2.5 μL of acetic acid (≥99%) was added to stop the reaction. The derivatization of the remaining MGO and GO in an aliquot amount of each sample was carried out by adding 1,2-phenylenediamine (PDA) at 100 mM and shaken by vortex for 5 s. The mixtures were kept at ambient temperature for 30 min for derivatization of the remaining methylglyoxal or glyoxal to complete. The UHPLC analysis was used to measure the amount of methylquinoxaline and quinoxaline formed through the reaction of methylglyoxal and glyoxal with PDA, respectively. The stock solutions of MGO, GO, and PDA were prepared immediately before the beginning of the study. The pH of the phosphate buffer was also determined shortly before the experiment.

3.6. UHPLC-ESI-QqTOF-MS Analysis

The study of the formation of methylglyoxal and glyoxal adducts was performed using the same UHPLC system configured as above (Section 4), interfaced with Compact ESI-QqTOF-MS (Bruker Daltonics; Bremen, Germany). Mobile phases consisted of A (0.1% formic acid in water) and B (0.1% acetic acid in 100% acetonitrile). The following gradient mobile phase program at a flow rate of 0.3 mL/min was used: 0–12 min, 97–65% A in B; 12–14 min, 65% A in B; 14–17 min, 65–20% A in B; 17–19 min 20% A in B. Then, the system returned to the initial setting and washed with 97% A in B until the system was stabilized before the next analysis. Both positive and negative ion modes were used for data acquisition. As a nebulizing and drying gas, nitrogen was used at temperature 210 °C, 2.0 bar pressure, and flow 0.8 L/min. For internal calibration sodium formate clusters (10 mM) were used. The injection volume was 1 mL. Additional operating conditions of the mass spectrometer were as follows: capillary voltage was set at 5 kV (ESI^+, ESI^-), collisional energy was 8.0 eV, and for the MS/MS mode, it was 35 and 40 eV. The data acquisition and processing were carried out with Compass Data Analysis software (Bruker Daltonics; Bremen, Germany.

3.7. UHPLC-DAD Analysis

Derivatized methylglyoxal and glyoxal were analyzed by the Thermo Scientific Dionex UltiMate 3000 UHPLC system (Thermo Fisher Scientific; Waltham, MA, USA) incorporated with a quaternary pump (LPG-3400D), UltiMate 3000 RS autosampler (WPS-3000), and fast separation photodiode array detector (DAD-3000). Derivatives were separated on a Kinetex C18 column (150 × 2.1 mm × 2.6 µm) (Phenomenex; Torrance, CA, USA) and a temperature-controlled column compartment (TCC–3000) was used to maintain its temperature at 40 °C. The binary mobile phase system consisted of 0.1% (*v*/*v*) formic acid in water (solvent C) and 0.1% (*v*/*v*) formic acid in acetonitrile (solvent D). The column eluted with a binary gradient system at a flow rate of 400 µL/min: 100% C from 0 to 4 min, 100–77% C in D from 4 to 25 min, and held at 77% C in D for 0.5 min, 77–100% C in D from 25.5 to 30 min, and then 100% C from 30 to 32 min. The injection volume was 10 µL. The peak areas of methylquinoxaline and quinoxaline were monitored at wavelengths of 316 and 314 nm, respectively. Data acquisition was carried out with the Chromeleon Chromatography Data System (Thermo Fisher Scientific; Waltham, MA, USA).

3.8. Linearity and Calibration of UHPLC-DAD Method

The applied UHPLC-DAD method was validated by the determination of linearity, LOD, and LOQ. Calibration equations for quantified metylquinoxaline and quinoxaline were assessed at seven concentration levels, and triplicate injections were performed for each concentration. The values of LOD were established at a signal-to-noise ratio (S/N) of 0.3 and LOQ was calculated at S/N of 1. Results of the method validation for standards are shown in Table 4.

Table 4. Validation parameters of the UHPLC-DAD method.

Compound	Method	λ [nm]	Linear Equation	R^2	Range [µM]	LOD [µM]	LOQ [µM]
Methyloquinoxaline	UHPLC-DAD	316	y = 2739.8843x + 5.0076	0.9995	5–210	0.29	0.96
Quinoxaline	UHPLC-DAD	314	y = 325.4515x + 1.7417	0.9998	5–210	0.19	0.64

λ, wavelength; y = ax + b; y, peak area; R^2, coefficient of determination; LOD, limit of detection; LOQ, limit of quantitation; $n = 3 \times 7$.

3.9. Statistical Analysis

Data were analyzed using the Shapiro–Wilk test to assess normality of distribution, followed by one-way analysis of variance (ANOVA) with Tukey's multiple comparison test using the GraphPad Prism 9 software. p values equal or less than 0.05 were considered significant.

4. Conclusions

To conclude, in addition to other therapeutic applications, some vasoprotective medicines and their structural analogs such as hesperetin, diosmetin, quercetin, and calcium dobesilate could be considered as potential antiglycative agents against glycation-related complications of diabetes. While the current study has clearly indicated that tested VPs and their structural analogs can effectively trap MGO and GO or reduce RCS-mediated glycation, a key limitation that must be considered is that the results presented here are only from in vitro models. The relevance of these results to humans must be experimentally proven using in vivo models. Although RCS trapping and reducing are simple, direct chemical reactions, which may suggest that the in vitro results have a high probability of being confirmed in vivo, the bioavailability of individual substances should also be taken into account.

Author Contributions: Conceptualization, I.F.; Methodology, I.F. and K.B.; Validation, K.B.; Formal analysis, K.B.; Investigation, K.B.; Data curation, K.B. and I.F.; Writing—original draft preparation, K.B.; Writing—review and editing, I.F.; Visualization, K.B. and I.F.; Supervision, I.F.; Project administration, I.F. and K.B.; Funding acquisition, I.F. and K.B. All authors have read and agreed to the published version of the manuscript.

Funding: This research was financially supported by the Wroclaw Medical University (grant number SUB.D110.21.101 and STM.D110.20.131).

Institutional Review Board Statement: Not applicable.

Informed Consent Statement: Not applicable.

Data Availability Statement: Data supporting reported results are available from the corresponding author.

Conflicts of Interest: The authors declare no conflict of interest.

References

1. Avogaro, A.; Albiero, M.; Menegazzo, L.; De Kreutzenberg, S.; Fadini, G.P. Endothelial dysfunction in diabetes: The role of reparatory mechanisms. *Diabetes Care* **2011**, *34*, 285–290. [CrossRef]
2. Janda, K.; Krzanowski, M.; Gajda, M.; Dumnicka, P.; Jasek, E.; Fedak, D.; Pietrzycka, A.; Kuźniewski, M.; Litwin, J.A.; Sułowicz, W. Vascular effects of advanced glycation end-products: Content of immunohistochemically detected AGEs in radial artery samples as a predictor for arterial calcification and cardiovascular risk in asymptomatic patients with chronic kidney disease. *Dis. Markers* **2015**, *2015*, 153978. [CrossRef] [PubMed]
3. Grundy, S.M.; Benjamin, I.J.; Burke, G.L.; Chait, A.; Eckel, R.H.; Howard, B.V.; Mitch, W.; Smith, S.C.; Sowers, J.R. Diabetes and cardiovascular disease: A statement for healthcare professionals from the american heart association. *Circulation* **1999**, *100*, 1134–1146. [CrossRef] [PubMed]
4. Lunder, M.; Janić, M.; Šabovič, M. Prevention of Vascular Complications in Diabetes Mellitus Patients: Focus on the Arterial Wall. *Curr. Vasc. Pharmacol.* **2019**, *11*, 6–15. [CrossRef] [PubMed]
5. Chaudhuri, J.; Bains, Y.; Guha, S.; Kahn, A.; Hall, D.; Bose, N.; Gugliucci, A.; Kapahi, P. The Role of Advanced Glycation End Products in Aging and Metabolic Diseases: Bridging Association and Causality. *Cell Metab.* **2018**, *28*, 337–352. [CrossRef]
6. Salahuddin, P.; Rabbani, G.; Khan, R.H. The role of advanced glycation end products in various types of neurodegenerative disease: A therapeutic approach. *Cell. Mol. Biol. Lett.* **2014**, *19*, 407–437. [CrossRef] [PubMed]
7. Odani, H.; Shinzato, T.; Matsumoto, Y.; Usami, J.; Maeda, K. Increase in three α,β-dicarbonyl compound levels in human uremic plasma: Specific in vivo determination of intermediates in advanced Maillard reaction. *Biochem. Biophys. Res. Commun.* **1999**, *256*, 89–93. [CrossRef]
8. Murakami, M.; Simons, M. Regulation of vascular integrity. *J. Mol. Med.* **2009**, *87*, 571–582. [CrossRef]
9. Liakopoulos, V.; Roumeliotis, S.; Gorny, X.; Eleftheriadis, T.; Mertens, P.R. Oxidative stress in patients undergoing peritoneal dialysis: A current review of the literature. *Oxid. Med. Cell. Longev.* **2017**, *2017*, 3494867. [CrossRef]
10. Semchyshyn, H.M. Reactive carbonyl species in vivo: Generation and dual biological effects. *Sci. World J.* **2014**, *2014*, 27–31. [CrossRef]
11. Mukohda, M.; Yamawaki, H.; Nomura, H.; Okada, M.; Hara, Y. Methylglyoxal inhibits smooth muscle contraction in isolated blood vessels. *J. Pharmacol. Sci.* **2009**, *310*, 305–310. [CrossRef]
12. Miyata, T.; Sugiyama, S.; Saito, A.; Kurokawa, K. Reactive carbonyl compounds related uremic toxicity. *Kidney Int. Suppl.* **2001**, *59*, 25–31. [CrossRef]

13. Rodrigues, T.; Matafome, P.; Santos-Silva, D.; Sena, C.; Seiça, R. Reduction of methylglyoxal-induced glycation by pyridoxamine improves adipose tissue microvascular lesions. *J. Diabetes Res.* **2013**, *2013*, 690650. [CrossRef]
14. Iacobini, C.; Vitale, M.; Pesce, C.; Pugliese, G.; Menini, S. Diabetic complications and oxidative stress: A 20-year voyage back in time and back to the future. *Antioxidants* **2021**, *10*, 727. [CrossRef] [PubMed]
15. Borg, D.J.; Forbes, J.M. Targeting advanced glycation with pharmaceutical agents: Where are we now? *Glycoconj. J.* **2016**, *33*, 653–670. [CrossRef]
16. Li, X.; Zheng, T.; Sang, S.; Lv, L. Quercetin inhibits advanced glycation end product formation by trapping methylglyoxal and glyoxal. *J. Agric. Food Chem.* **2014**, *62*, 12152–12158. [CrossRef] [PubMed]
17. Han, L.; Lin, Q.; Liu, G.; Han, D.; Niu, L.; Su, D. Catechin inhibits glycated phosphatidylethanolamine formation by trapping dicarbonyl compounds and forming quinone. *Food Funct.* **2019**, *10*, 2491–2503. [CrossRef]
18. Shin, E.R.; Jung, W.; Kim, M.K.; Chong, Y. Identification of (−)-epigallocatechin (EGC) as a methylglyoxal (MGO)-trapping agent and thereby as an inhibitor of advanced glycation end product (AGE) formation. *Appl. Biol. Chem.* **2018**, *61*, 587–591. [CrossRef]
19. Wang, P.; Chen, H.; Sang, S. Trapping Methylglyoxal by Genistein and Its Metabolites in Mice. *Chem. Res. Toxicol.* **2016**, *29*, 406–414. [CrossRef]
20. Shao, X. Scavenging Effects of Dietary Flavonoids on Reactive Dicaronyl Species and Their Possible Implications on the Inhibition of the Formation of Advanced Glycation-End Products. Ph.D. Thesis, The State University of New Jersey, New Brunswick, NJ, USA, 2010. [CrossRef]
21. Zhang, S.; Xiao, L.; Lv, L.; Sang, S. Trapping methylglyoxal by myricetin and its metabolites in mice. *J. Agric. Food Chem.* **2020**, *68*, 9408–9414. [CrossRef] [PubMed]
22. Kinsky, O.R.; Hargraves, T.L.; Anumol, T.; Jacobsen, N.E.; Dai, J.; Snyder, S.A.; Monks, T.J.; Lau, S.S. Metformin Scavenges Methylglyoxal to Form a Novel Imidazolinone Metabolite in Humans. *Chem. Res. Toxicol.* **2016**, *29*, 227–234. [CrossRef]
23. Gohel, M.; Davies, A. Pharmacological Agents in the Treatment of Venous Disease: An Update of the Available Evidence. *Curr. Vasc. Pharmacol.* **2009**, *7*, 303–308. [CrossRef]
24. Rees, A.; Dodd, G.F.; Spencer, J.P.E. The effects of flavonoids on cardiovascular health: A review of human intervention trials and implications for cerebrovascular function. *Nutrients* **2018**, *10*, 1852. [CrossRef] [PubMed]
25. Cium, L.; Milaciu, M.V.; Runcan, O.; Vesa, C.; Negrean, V.; Pern, M.; Donca, V.I. The Effects of Flavonoids in Cardiovascular Diseases. *Molecules* **2020**, *25*, 4320. [CrossRef]
26. Ullah, A.; Munir, S.; Badshah, S.L.; Khan, N.; Ghani, L.; Poulson, B.G.; Emwas, A.; Jaremko, M. Important Flavonoids and Their Role as a Therapeutic Agent. *Molecules* **2020**, *25*, 5243. [CrossRef] [PubMed]
27. Lemmens-Gruber, R.; Marchart, E.; Rawnduzi, P.; Engel, N.; Benedek, B.; Kopp, B. Investigation of the spasmolytic activity of the flavonoid fraction of Achillea millefolium s.l. on isolated guinea-pig ilea. *Arzneim.-Forsch./Drug Res.* **2006**, *56*, 582–586. [CrossRef]
28. Kim, M.H. Flavonoids inhibit VEGF/bFGF-induced angiogenesis in vitro by inhibiting the matrix-degrading proteases. *J. Cell. Biochem.* **2003**, *89*, 529–538. [CrossRef]
29. Jakimiuk, K.; Gesek, J.; Atanasov, A.G.; Tomczyk, M. Flavonoids as inhibitors of human neutrophil elastase. *J. Enzyme Inhib. Med. Chem.* **2021**, *36*, 1016–1028. [CrossRef]
30. Maessen, D.E.M.; Stehouwer, C.D.A.; Schalkwijk, C.G. The role of methylglyoxal and the glyoxalase system in diabetes and other age-related diseases. *Clin. Sci.* **2015**, *128*, 839–861. [CrossRef]
31. Nenna, A.; Nappi, F.; Avtaar Singh, S.; Sutherland, F.; Di Domenico, F.; Chello, M.; Spadaccio, C. Pharmacologic approaches against Advanced Glycation End Products (AGEs) in diabetic cardiovascular disease. *Res. Cardiovasc. Med.* **2015**, *4*, e26949. [CrossRef]
32. Bolton, W.K.; Cattran, D.C.; Williams, M.E.; Adler, S.G.; Appel, G.B.; Cartwright, K.; Foiles, P.G.; Freedman, B.I.; Raskin, P.; Ratner, R.E.; et al. Randomized Trial of an Inhibitor of Formation of Advanced Glycation End Products in Diabetic Nephropathy. *Am. J. Nephrol.* **2004**, *24*, 32–40. [CrossRef]
33. Kiho, T.; Kato, M.; Usui, S.; Hirano, K. Effect of buformin and metformin on formation of advanced glycation end products by methylglyoxal. *Clin. Chim. Acta* **2005**, *358*, 139–145. [CrossRef]
34. Beisswenger, P.J.; Ruggiero-Lopez, D. Metformin inhibition of glycation processes. *Diabetes Metab.* **2003**, *29*, 6S95–6S103. [CrossRef]
35. Li, D.; Mitsuhashi, S.; Ubukata, M. Protective effects of hesperidin derivatives and their stereoisomers against advanced glycation end-products formation. *Pharm. Biol.* **2012**, *50*, 1531–1535. [CrossRef] [PubMed]
36. Matsuda, H.; Wang, T.; Managi, H.; Yoshikawa, M. Structural requirements of flavonoids for inhibition of protein glycation and radical scavenging activities. *Bioorg. Med. Chem.* **2003**, *11*, 5317–5323. [CrossRef] [PubMed]
37. Liu, J.; Li, S.; Sun, D. Calcium Dobesilate and Micro-vascular diseases. *Life Sci.* **2019**, *221*, 348–353. [CrossRef]
38. Vojnicovic, B. Doxium (Calcium dobesilate) reducesblood hyperviscosity and lowers elevated intraocular pressure in patients with diabetic rethinopathy and glaucoma. *Ophthalmic Res.* **1991**, *23*, 12–20. [CrossRef]
39. Mehta, R.; Wong, L.; O'Brien, P.J. Cytoprotective mechanisms of carbonyl scavenging drugs in isolated rat hepatocytes. *Chem. Biol. Interact.* **2009**, *178*, 317–323. [CrossRef] [PubMed]
40. Sena, C.M.; Matafome, P.; Crisóstomo, J.; Rodrigues, L.; Fernandes, R.; Pereira, P.; Seiça, R.M. Methylglyoxal promotes oxidative stress and endothelial dysfunction. *Pharmacol. Res.* **2012**, *65*, 497–506. [CrossRef]

41. Reddy, V.P.; Beyaz, A. Inhibitors of the Maillard reaction and AGE breakers as therapeutics for multiple diseases. *Drug Discov. Today* **2006**, *11*, 646–654. [CrossRef]
42. Tiveron, A.P.; Melo, P.S.; Bergamaschi, K.B.; Vieira, T.M.F.S.; Regitano-D'Arce, M.A.B.; Alencar, S.M. Antioxidant activity of Brazilian vegetables and its relation with phenolic composition. *Int. J. Mol. Sci.* **2012**, *13*, 8943–8957. [CrossRef]
43. Giuffrè, A.M. Bergamot (*Citrus bergamia*, Risso): The effects of cultivar and harvest date on functional properties of juice and cloudy juice. *Antioxidants* **2019**, *8*, 221. [CrossRef] [PubMed]
44. Payne, A.C.; Mazzer, A.; Clarkson, G.J.J.; Taylor, G. Antioxidant assays—Consistent findings from FRAP and ORAC reveal a negative impact of organic cultivation on antioxidant potential in spinach but not watercress or rocket leaves. *Food Sci. Nutr.* **2013**, *1*, 439–444. [CrossRef]
45. Ilyasov, I.R.; Beloborodov, V.L.; Selivanova, I.A.; Terekhov, R.P. ABTS/PP decolorization assay of antioxidant capacity reaction pathways. *Int. J. Mol. Sci.* **2020**, *21*, 1131. [CrossRef]
46. Plumb, G.W.; Price, K.R.; Williamson, G. Antioxidant properties of flavonol glycosides from tea. *Redox Rep.* **1999**, *4*, 13–16. [CrossRef] [PubMed]
47. Ouslimani, N.; Peynet, J.; Bonnefont-Rousselot, D.; Thérond, P.; Legrand, A.; Beaudeux, J.L. Metformin decreases intracellular production of reactive oxygen species in aortic endothelial cells. *Metabolism* **2005**, *54*, 829–834. [CrossRef] [PubMed]
48. Logie, L.; Harthill, J.; Patel, K.; Bacon, S.; Hamilton, D.L.; Macrae, K.; McDougall, G.; Wang, H.H.; Xue, L.; Jiang, H.; et al. Cellular responses to the metal-binding properties of metformin. *Diabetes* **2012**, *61*, 1423–1433. [CrossRef] [PubMed]
49. Hosseinimehr, S.J.; Ghasemi, F.; Flahatgar, F.; Rahmanian, N.; Ghasemi, A.; Asgarian-Omran, H. Atorvastatin sensitizes breast and lung cancer cells to ionizing radiation. *Iran. J. Pharm. Res.* **2020**, *19*, 80–88. [CrossRef]
50. Dadpisheh, S.; Ahmadvand, H.; Jafaripour, L.; Nouryazdan, N.; Babaeenezhad, E.; Shati, H.; Bagheri, S. Effect of troxerutin on oxidative stress induced by sciatic nerve ischemia-reperfusion injury in rats. *J. Kerman Univ. Med. Sci.* **2020**, *27*, 338–347.
51. Badarinath, A.V.; Rao, K.M.; Madhu, C.; Chetty, S.; Ramkanth, S.; Rajan, T.V.S.; Gnanaprakash, K. A Review on in-vitro antioxidant methods: Comparisions, correlations and considerations. *Int. J. PharmTech Res.* **2010**, *2*, 1276–1285.
52. Zhang, X.Y.; Liu, W.; Wu, S.S.; Jin, J.L.; Li, W.H.; Wang, N.L. Calcium dobesilate for diabetic retinopathy: A systematic review and meta-analysis. *Sci. China Life Sci.* **2015**, *58*, 101–107. [CrossRef]
53. Hollman, P.C.H.; Van Trijp, J.M.P.; Buysman, M.N.C.P.; Martijn, M.S.; Mengelers, M.J.B.; De Vries, J.H.M.; Katan, M.B. Relative bioavailability of the antioxidant flavonoid quercetin from various foods in man. *FEBS Lett.* **1997**, *418*, 152–156. [CrossRef]
54. Jin, F.; Nieman, D.C.; Shanely, R.A.; Knab, A.M.; Austin, M.D.; Sha, W. The variable plasma quercetin response to 12-week quercetin supplementation in humans. *Eur. J. Clin. Nutr.* **2010**, *64*, 692–697. [CrossRef] [PubMed]
55. Kanaze, F.I.; Bounartzi, M.I.; Georgarakis, M.; Niopas, I. Pharmacokinetics of the citrus flavanone aglycones hesperetin and naringenin after single oral administration in human subjects. *Eur. J. Clin. Nutr.* **2007**, *61*, 472–477. [CrossRef]
56. Guo, X.; Hou, L.; Yin, Y.; Wu, J.; Zhao, F.; Xia, L.; Cheng, X.; Liu, Q.; Liu, L.; Xu, E.; et al. Negative interferences by calcium dobesilate in the detection of five serum analytes involving Trinder reaction-based assays. *PLoS ONE* **2018**, *13*, e0192440. [CrossRef] [PubMed]
57. Lo, C.Y.; Hsiao, W.T.; Chen, X.Y. Efficiency of trapping methylglyoxal by phenols and phenolic acids. *J. Food Sci.* **2011**, *76*, 90–96. [CrossRef]
58. Yoon, S.R.; Shim, S.M. Inhibitory effect of polyphenols in Houttuynia cordata on advanced glycation end-products (AGEs) by trapping methylglyoxal. *LWT-Food Sci. Technol.* **2015**, *61*, 158–163. [CrossRef]
59. Bednarska, K.; Kuś, P.; Fecka, I. Investigation of the phytochemical composition, antioxidant activity, and methylglyoxal trapping effect of *Galega officinalis* L. Herb in vitro. *Molecules* **2020**, *25*, 5810. [CrossRef] [PubMed]
60. Wang, W.; Qi, Y.; Rocca, J.R.; Sarnoski, P.J.; Jia, A.; Gu, L. Scavenging of Toxic Acrolein by Resveratrol and Hesperetin and Identification of Adducts. *J. Agric. Food Chem.* **2015**, *63*, 9488–9495. [CrossRef]
61. Nemet, I.; Varga-Defterdarović, L.; Turk, Z. Preparation and quantification of methylglyoxal in human plasma using reverse-phase high-performance liquid chromatography. *Clin. Biochem.* **2004**, *37*, 875–881. [CrossRef]
62. Shao, X.; Chen, H.; Zhu, Y.; Sedighi, R.; Ho, C.T.; Sang, S. Essential structural requirements and additive effects for flavonoids to scavenge methylglyoxal. *J. Agric. Food Chem.* **2014**, *62*, 3202–3210. [CrossRef] [PubMed]
63. Zhu, H.; Poojary, M.M.; Andersen, M.L.; Lund, M.N. The effect of molecular structure of polyphenols on the kinetics of the trapping reactions with methylglyoxal. *Food Chem.* **2020**, *319*, 126500. [CrossRef]
64. Van Den Eynde, M.D.G.; Geleijnse, J.M.; Scheijen, J.L.J.M.; Hanssen, N.M.J.; Dower, J.I.; Afman, L.A.; Stehouwer, C.D.A.; Hollman, P.C.H.; Schalkwijk, C.G. Quercetin, but not epicatechin, decreases plasma concentrations of methylglyoxal in adults in a randomized, double-blind, placebo-controlled, crossover trial with pure flavonoids. *J. Nutr.* **2018**, *148*, 1911–1916. [CrossRef] [PubMed]
65. Walle, T. Absorption and metabolism of flavonoids. *Free Radic. Biol. Med.* **2004**, *36*, 829–837. [CrossRef]
66. Murota, K.; Nakamura, Y.; Uehara, M. Flavonoid metabolism: The interaction of metabolites and gut microbiota. *Biosci. Biotechnol. Biochem.* **2018**, *82*, 600–610. [CrossRef] [PubMed]
67. Boersma, M.G.; Van der Woude, H.; Bogaards, J.; Boeren, S.; Vervoort, J.; Cnubben, N.H.P.; Van Iersel, M.L.P.S.; Van Bladeren, P.J.; Rietjens, I.M.C.M. Regioselectivity of phase II metabolism of luteolin and quercetin by UDP-glucuronosyl transferases. *Chem. Res. Toxicol.* **2002**, *15*, 662–670. [CrossRef]

68. Liu, W.; Ma, H.; Frost, L.; Yuan, T.; Dain, J.A.; Seeram, N.P. Pomegranate phenolics inhibit formation of advanced glycation endproducts by scavenging reactive carbonyl species. *Food Funct.* **2014**, *5*, 2996–3004. [CrossRef]
69. Chen, L.; Kang, Y.H. Antioxidant and enzyme inhibitory activities of plebeian herba (*Salvia plebeia* R. Br.) under different cultivation conditions. *J. Agric. Food Chem.* **2014**, *62*, 2190–2197. [CrossRef]
70. Blois, M.S. Antioxidant determinations by the use of a stable free radical. *Nature* **1958**, *181*, 1199–1200. [CrossRef]
71. Sang, S.; Shao, X.; Bai, N.; Lo, C.Y.; Yang, C.S.; Ho, C.T. Tea polyphenol (−)-epigallocatechin-3-gallate: A new trapping agent of reactive dicarbonyl species. *Chem. Res. Toxicol.* **2007**, *20*, 1862–1870. [CrossRef]

P2. A citrus and pomegranate complex reduces methylglyoxal in healthy elderly subjects: secondary analysis of a double-blind randomized cross-over clinical trial

International Journal of
Molecular Sciences

MDPI

Communication

A Citrus and Pomegranate Complex Reduces Methylglyoxal in Healthy Elderly Subjects: Secondary Analysis of a Double-Blind Randomized Cross-Over Clinical Trial

Katarzyna Bednarska [1,*], Izabela Fecka [1,2,*], Jean L. J. M. Scheijen [3,4], Sanne Ahles [5,6], Philippe Vangrieken [3,4] and Casper G. Schalkwijk [3,4]

[1] Department of Pharmacognosy, Faculty of Pharmacy, Wroclaw Medical University, Borowska 211, 50-556 Wroclaw, Poland
[2] The Committee on Therapeutics and Pharmaceutical Sciences, The Polish Academy of Sciences, Pl. Defilad 1, 00-901 Warsaw, Poland
[3] Department of Internal Medicine, Maastricht University Medical Center+, 6229 ER Maastricht, The Netherlands; j.scheijen@maastrichtuniversity.nl (J.L.J.M.S.); p.vangrieken@maastrichtuniversity.nl (P.V.); c.schalkwijk@maastrichtuniversity.nl (C.G.S.)
[4] CARIM School for Cardiovascular Diseases, Faculty of Health, Medicine and Life Sciences, Maastricht University, 6229 ER Maastricht, The Netherlands
[5] Department of Nutrition and Movement Sciences, School of Nutrition and Translational Research in Metabolism (NUTRIM), Maastricht University, 6229 ER Maastricht, The Netherlands; s.ahles@maastrichtuniversity.nl
[6] BioActor BV, 6229 GS Maastricht, The Netherlands
* Correspondence: katarzyna.bednarska@student.umw.edu.pl (K.B.); izabela.fecka@umw.edu.pl (I.F.)

Abstract: Reactive α-dicarbonyls (α-DCs), such as methylglyoxal (MGO), glyoxal (GO), and 3-deoxyglucosone (3-DG), are potent precursors in the formation of advanced glycation end products (AGEs). In particular, MGO and MGO-derived AGEs are thought to be involved in the development of vascular complications in diabetes. Experimental studies showed that citrus and pomegranate polyphenols can scavenge α-DCs. Therefore, the aim of this study was to evaluate the effect of a citrus and pomegranate complex (CPC) on the α-DCs plasma levels in a double-blind, placebo-controlled cross-over trial, where thirty-six elderly subjects were enrolled. They received either 500 mg of *Citrus sinensis* peel extract and 200 mg of *Punica granatum* concentrate in CPC capsules or placebo capsules for 4 weeks, with a 4-week washout period in between. For the determination of α-DCs concentrations, liquid chromatography tandem mass spectrometry was used. Following four weeks of CPC supplementation, plasma levels of MGO decreased by 9.8% (−18.7 nmol/L; 95% CI: −36.7, −0.7 nmol/L; $p = 0.042$). Our findings suggest that CPC supplementation may represent a promising strategy for mitigating the conditions associated with MGO involvement. This study was registered on clinicaltrials.gov as NCT03781999.

Keywords: hesperidin; punicalagin; α-dicarbonyls; methylglyoxal; glyoxal; 3-deoxyglucosone; *Punica* × *granatum*; *Citrus* × *sinensis*

check for updates

Citation: Bednarska, K.; Fecka, I.; Scheijen, J.L.J.M.; Ahles, S.; Vangrieken, P.; Schalkwijk, C.G. A Citrus and Pomegranate Complex Reduces Methylglyoxal in Healthy Elderly Subjects: Secondary Analysis of a Double-Blind Randomized Cross-Over Clinical Trial. *Int. J. Mol. Sci.* **2023**, *24*, 13168. https://doi.org/10.3390/ijms241713168

Academic Editors: Dejan Stojković, Marija Ivanov and Ana Ćirić

Received: 29 July 2023
Revised: 18 August 2023
Accepted: 23 August 2023
Published: 24 August 2023

1. Introduction

Despite substantial advances in diabetes treatment, vascular complications remain a significant clinical concern and are the primary cause of mortality among diabetes patients [1]. Several different biochemical pathways are involved in diabetes-induced endothelial damage and vascular complications, but an elevated level of systemic α-dicarbonyl compounds (α-DCs) is considered one of the key factors in the development of vascular complications [2]. The α-DCs are a subclass within the large group of compounds collectively referred to as reactive carbonyl species (RCS). These compounds feature two carbonyl groups (>C=O) on the same molecule, typically at consecutive carbon atoms, leading to

the 'alpha' or 'α' designation. Within these compounds, the C-1 and C-2 carbons bond directly to oxygen, forming a keto-aldehyde or dialdehyde structure with two neighboring carbonyl groups. The most investigated α-dicarbonyl compounds include methylglyoxal (MGO, CH3-C(=O)-CH(=O)), glyoxal (GO, O=CH-CH(=O)), and 3-deoxyglucosone (3-DG, OHCH2-(CHOH)2-CH2-C(=O)-CH(=O)) [3]. The state of increased α-DCs is termed carbonyl stress. Among them, MGO is the most reactive and plays a significant role as a precursor in the non-enzymatic glycation process, ultimately resulting in advanced glycation end-product (AGE) formation [4]. The process of non-enzymatic glycation involves the excessive nucleophilic addition of the carbonyl groups of reducing sugars or α-DCs to the amino and guanidino groups of various biomacromolecules, such as peptides, proteins, lipoproteins, and nucleic acids. MGO is produced predominantly through the non-enzymatic degradation of triose phosphates, glyceraldehyde-3-phosphate, and dihydroxyacetone phosphate, as a metabolic side product of glucose metabolism during glycolysis [5]. Additionally, it can be formed through the non-enzymatic oxidation of glucose and fructose and early glycation products (Amadori products) [3]. Thus, excessive consumption of simple sugars may contribute to increased MGO and other α-DCs concentrations in tissues and plasma. A presumably similar mechanism of MGO formation occurs in individuals with poorly controlled glycemia, in whom glucose concentrations increase significantly over a long period [6].

A natural consequence of the modification of biomacromolecules by MGO is the loss of their original spatial structure. This results in a loss of physiological function, leading to various cellular disorders [7,8]. The major MGO-derived AGE, N^{δ}-(5-hydro-5-methyl-4-imidazolone-2-yl)ornithine (MG-H1), produced in the reaction of MGO with arginine, has been positively correlated with the occurrence of vascular endothelial damage [9,10]. Another AGE, formed analogously during the reaction of MGO with lysine N^{ε}-(1-carboxyethyl)lysine, known as CEL, was found to correlate positively with insulin resistance in diabetic patients [11]. Moreover, AGEs accumulate in the extracellular space in tissues and organs. Their role in the development of cardiometabolic and neurodegenerative diseases has been demonstrated in numerous studies [12–15]. The glyoxalase system, comprising glyoxalase I (Glo1) and glyoxalase II (Glo2), primarily detoxifies MGO in the human body, maintaining relatively low intracellular MGO levels under normal physiological conditions [16,17]. However, when the glyoxalase system is overwhelmed or not functioning, factors, such as permanently elevated glucose levels or deficiencies in Glo1/Glo2, can lead to the accumulation of MGO in cells and tissues [18].

Excessive MGO formation can further increase the production of reactive oxygen species and nitrogen species and consequently induce oxidative stress, which further contributes to the development and progression of vascular complications in diabetes [19]. MGO-derived AGEs, through the RAGE receptor and nuclear factor NF-κB, trigger an increase in the secretion of pro-inflammatory cytokines, interleukins 6 and 8, and tumor necrosis factor and contribute to the enhanced production of superoxide anion, peroxynitrite, and hydrogen peroxide [20,21]. Oxidative stress and inflammation are suspected to play key roles in MGO-induced vascular endothelial damage [22].

Preventing diabetes vascular complications necessitates a multidirectional therapeutic approach, as simply targeting risk factors, like glycemic control and a healthy lifestyle, may not be sufficient. Diabetes is a complex metabolic disorder, and the pathogenesis of its vascular complications involves multiple interlinked biochemical, molecular, and physiological processes and, therefore, requires multidirectional therapy. Lowering systemic levels of MGO, GO, and 3-DG may delay the formation of AGEs, particularly crucial in patients experiencing pathophysiological increases in α-DCs (dicarbonyl stress) due to diabetes.

To date, several agents have been studied and proposed to be useful as an anti-MGO therapy. Among them are experimental compounds, such as aminoguanidine [23] and alagebrium [24]; registered drugs, such as metformin [25], thiazolidinediones [26], angiotensin-converting enzyme inhibitors [27], angiotensin receptor blockers [28,29], and

statins [30]; and supplements, such as L-carnosine [31], pyridoxamine [32], or thiamine (vitamin B1) [33]. However, both aminoguanidine and alagebrium were excluded from further phases of clinical trials due to side effects resulting in safety concerns. For registered drugs and supplements, excluding metformin [25], the absence of clear evidence of efficacy in human clinical trials has led to the discontinuation of attempts to employ them in pharmacotherapy [34].

Plant-derived dietary supplements and nutraceuticals are becoming increasingly popular all over the world as a result of growing customer awareness regarding their potential health benefits [35]. It is well established that some plant polyphenols like flavonoids have beneficial effects on general cardiometabolic health and may modulate the risk of the development of cardiovascular and metabolic diseases, including diabetes and its vascular complications [36,37]. The literature provides studies on the phytochemical composition of *Citrus sinensis* and *Punica granatum* and confirms that both plants are abundant in bioactive polyphenolic components, mainly flavonoids in the case of sweet orange and ellagitannins in the case of pomegranate fruit [38,39].

Several experimental in vitro studies have proved that citrus and pomegranate polyphenols can scavenge reactive α-dicarbonyls and prevent the formation of AGEs [40–45]. Hesperidin, the primary flavonoid glycoside in sweet orange extract, forms adducts with MGO and GO, potentially reducing their concentrations in the system. Hesperidin aglycone, hesperetin, also has MGO and GO trapping ability and is a known inducer of Glo1 [40,46]. Pomegranate fruit extract's principal polyphenolic compounds, punicalagin and ellagic acid, exhibit potent antioxidant activity. Some in vitro experimental studies report that ellagic acid and urolithin A, a gut microbiota metabolite of ellagitannins and ellagic acid, inhibit non-enzymatic glycation by scavenging MGO [43].

Despite experimental evidence, controlled human studies on the effects of orange and pomegranate actives on α-DCs levels are lacking. Therefore, this post hoc analysis of a double-blind, randomized, cross-over clinical trial in apparently healthy elderly participants examines the impact of a combination of citrus extract and pomegranate concentrate (CPC) on α-DCs levels. The results may shed light on potential therapeutic approaches to inhibit hyperglycemia-induced vascular endothelial damage.

2. Results and Discussion

A total of 42 healthy participants were initially screened for eligibility in the study, out of which 37 volunteers were enrolled, and 36 completed both the placebo and treatment phases, with no dropouts during the follow-up period. The final study population comprised 27 females and 9 males. The average age ± SD of the study population at the start of the study was 66 ± 4 y, and the average BMI was 25.3 ± 0.3 kg/m^2. The basic baseline characteristics of the study subjects and α-dicarbonyl concentrations at the beginning of the study are summarized in Table 1.

Table 1. Baseline characteristics of 36 healthy subjects randomly allocated at the start of the study.

Characteristic	Minumum	Maximum	Means	SD
Age, y	60	75	66	4
Men:women	-	-	9:27	-
BMI, kg/m^2	19.7	29.2	25.3	2.1
Plasma α-dicarbonyls, nmol/L				
MGO	145	301	190.1	32.2
GO	53	285	117.7	37.2
3-DG	436	786	569.2	74.6

n = 36; BMI, body mass index; MGO, methylglyoxal; GO, glyoxal; 3-DG, 3-deoxyglucosone; SD, standard deviation.

The study population, despite being elderly, was deemed apparently healthy. The baseline mean MGO concentration for the participants was 190.1 nmol/L. This falls within the

accepted physiological range of 60–250 nmol/L, as measured using liquid chromatography–tandem mass spectrometry [47,48]. The baseline GO concentration in the study was 117.7 nmol/L, which is notably lower compared to concentrations observed in healthy non-diabetic populations, typically ranging from 330 to 1150 nmol/L [49,50]. Meanwhile, the average baseline concentration of 3-DG was 569.2 nmol/L, aligning with the reported range of 160–1046 nmol/L for healthy individuals [49].

The 4-week treatment with CPC resulted in a significant decrease in plasma MGO concentrations compared with the placebo treatment, showing a reduction of 18.7 nmol/L (9.8% reduction from baseline). However, the decrease in GO and 3-DG concentrations with CPC treatment was not statistically significant, with reductions of 7.8 nmol/L (6.6% reduction from baseline) and 16.6 nmol/L (2.9% reduction from baseline), respectively. The total treatment effect is summarized in Table 2.

Table 2. The total effects of 4-week sweet orange peel extract and pomegranate concentrate combination supplementation on plasma levels of α-dicarbonyls.

Plasma α-Dicarbonyls	Treatment Effect, nmol/L	95% Confidence Interval for Difference		*p*
		Lower Bound	Upper Bound	
MGO	−18.7	−36.7	−0.7	0.042
GO	−7.8	−29.5	13.8	0.473
3-DG	−16.6	−43.9	10.7	0.229

Values are least-square means from a linear mixed model for repeated measures with compound symmetry as the covariant structure, $n = 36$; Treatment effect = (treatment − placebo); p, the mean difference was significant at <0.05; Measurements of α-dicarbonyls in fasting plasma samples from the start and end of every intervention period were performed as described in the Section 3.

Figure 1 illustrates the changes in MGO, GO, and 3-DG levels over the course of the study in subjects randomly assigned to one of two groups in which the intervention sequences were reversed (T-P sequence or P-T sequence). Following CPC treatment, a reduction in MGO concentration was observed (Figure 1A), regardless of the sequence of administration, with MGO levels decreasing from 195.84 nmol/L to 190.97 nmol/L for the T-P sequence and from 187.01 nmol/L to 174.89 nmol/L for the P-T sequence. In subjects who received CPC as the first intervention, a slight increase in GO concentration from 123.26 nmol/L to 127.05 nmol/L was noted. Conversely, for the group receiving CPC as the second intervention, the GO levels decreased from 120.36 nmol/L to 110.26 nmol/L (Figure 1B). Subjects receiving CPC in the T-P sequence had their plasma 3-DG levels slightly increased from 559.44 nmol/L to 561.85 nmol/L, while CPC taken in the second sequence lowered 3-DG levels from 592.96 nmol/L to 567.63 nmol/L (Figure 1C). No significant interaction between treatment and period and no carryover and sequence effect were observed.

The placebo used in this study, maltodextrin, is a low-active polysaccharide derived from the partial hydrolysis of starch [51]. It seemed unlikely that maltodextrin could affect α-DCs levels, particularly since it is commonly used as a food additive, an ingredient in tablet masses, and in human intervention studies as an oral placebo [52]. However, maltodextrin has a high glycemic index, even higher than table sugar, and its consumption causes a sharp postprandial rise in blood glucose levels, potentially resulting in excessive MGO production [6,53]. It is worth noting that, since the study was not designed to measure α-dicarbonyls concentrations, the choice of placebo was based on the primary outcomes of the original study [54].

Previous experimental in vitro studies have found that citrus and pomegranate polyphenols can trap reactive α-dicarbonyls [40,42,44,45]. Under controlled experimental conditions that simulate the physiological environment in terms of pH and temperature, some compounds, such as flavonoids and biguanides, directly react with MGO to form stable adducts, effectively removing the highly reactive MGO from the solution. The adducts resulting from the interaction of MGO with various natural and synthetic compounds have

been identified in both in vivo and in vitro experiments, including animal models [55,56] and human subjects [25]. Moreover, it seems that MGO adducts formed by natural compounds like quercetin retain the beneficial physiological effects of the original polyphenol molecule, such as its antioxidant activity [57].

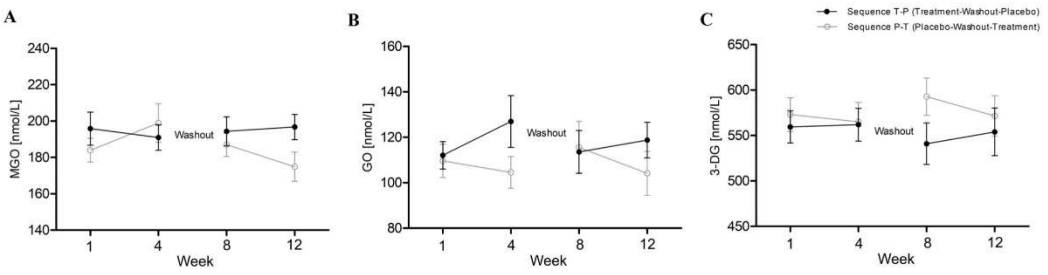

Figure 1. Changes in α-dicarbonyls concentrations during the study expressed in nmol/L unit. The T-P sequence represents a group of participants who first received the CPC treatment and then, after a washout period, were given a placebo. The P-T sequence refers to those participants who initially received the placebo and then, following a washout period, were administered the CPC. Data are presented as actual mean ± SEM (standard error of measurement). Fasting plasma sampling from the start and end of each intervention period was performed as described in the Section 3; time points on the axis x are marked as consecutive weeks of the study (weeks 1 and 8 are the start of each intervention period and weeks 4 and 12 are the end of the intervention period). (**A**) MGO levels; (**B**) GO levels; (**C**) 3-DG levels.

Zhang et al.'s study [55,56] demonstrated that the oral administration of myricetin and taxifolin resulted in the formation of MGO adducts, which were later detected in the urine and feces of mice. When administered to mice via oral gavage, myricetin trapped MGO in the gastrointestinal tract and circulatory system, forming both mono- and di-MGO adducts. Additionally, the phase II metabolites of myricetin, including mono-methylated and di-methylated myricetin, maintained the MGO trapping ability of myricetin, forming their own mono-MGO adducts. This is in line with findings from other studies on genistein, epigallocatechin gallate, and quercetin [58–60]. The ability to trap MGO is not exclusive to natural compounds. Kinsky et al.'s research [25] showed that an imidazoline derivative adduct, a result of MGO and metformin interaction, was found in the urine samples of diabetic patients who had been prescribed metformin as part of their regular antidiabetic therapy. However, it is essential to understand that while MGO trapping can occur in both in vitro and in vivo settings, the multifaceted in vivo environment, with its numerous interacting physiological systems and factors, might impact the efficiency and effectiveness of the trapping process compared to controlled in vitro conditions.

The current study used a combination of sweet orange extract and pomegranate concentrate, which together provided 700 mg of the supplement. This supplement contained 450 mg of hesperidin, 60 mg of punicalagin, and 190 mg of other non-characterized components. This complex blend makes it challenging to pinpoint the specific active ingredient responsible for reducing reactive α-DCs. This complex blend makes it challenging to pinpoint the specific active ingredient responsible for reducing reactive α-DCs. There has been a long-standing debate in natural product research over the use of whole plant extracts versus individual plant compounds or phytochemicals for therapeutic applications. Both strategies have their strengths and drawbacks, largely due to the inherent biochemical complexity and the bioavailability of the active ingredients. Whole plant extracts consist of a diverse mixture of phytochemicals, such as phenolic acids, flavonoids, tannins, terpenoids, and others. The holistic use of these extracts is often supported by the 'entourage effect' concept, which posits that the combined therapeutic benefits of an entire plant extract exceed that of its isolated components. This is believed to be because of the synergistic

interactions between the various compounds [61,62]. Such synergy might arise from the enhanced bioavailability of certain compounds when present alongside other co-existing components [63,64].

However, the complexity of extracts introduces variability in their composition and, thus, their therapeutic efficacy and safety profile. Achieving standardization and maintaining quality control are often challenging [65,66]. On the other hand, isolated plant compounds allow for precise control over dosage and, consequently, therapeutic action. They can be intensively studied, and their pharmacokinetics, pharmacodynamics, and toxicological properties can be thoroughly characterized [67]. Despite these advantages, isolated compounds might lack the synergy found in whole plant extracts, and their bioavailability can be limited [68,69]. To determine the scavenging activity of MGO for specific citrus and pomegranate polyphenols in humans, additional studies with the use of individual compounds are necessary. When considering the use of plant polyphenols or extracts as supplements and nutraceuticals, their bioavailability should always be taken into account. The oral bioavailability of hesperidin, one of two main constituents from the extract combination used in the current study treatment, has also been a topic of intense scrutiny due to its poor absorption characteristics [70]. The poor bioavailability of hesperidin can be primarily attributed to its highly hydrophilic structure and relatively large molecular size (*M*: 610.56 g/mol), which hinders its passive diffusion across the intestinal epithelium. After oral ingestion, hesperidin remains largely unabsorbed in the small intestine and proceeds to the colon, where it undergoes deglycosylation by the local microbiota, being converted into its more lipophilic aglycone form, hesperetin (*M*: 302.27 g/mol) [71]. The released hesperetin can be absorbed and further metabolized in the liver to glucuronide and sulfate conjugates, which have been identified as the main circulating metabolites in plasma [72]. These conjugates are eliminated in the urine within 24 h, and the total urinary recovery of hesperidin metabolites is generally low, indicating a low overall bioavailability [73]. Nevertheless, it is worth noting that MGO trapping activity has been documented for hesperetin. This suggests that even if hesperidin is not absorbed directly into the bloodstream in its original form, its active metabolite might still exert MGO scavenging activity in the systemic circulation. Also, some of the phase II biotransformation metabolites, such as hesperetin-3′-*O*-glucuronide, hesperetin-7-*O*-glucuronide, and hesperetin-3′-*O*-sulfate [74], can also potentially scavenge MGO as their chemical structure meets the basic requirements of being able to bind reactive α-dicarbonyls [75,76]. It is also worth noting that the bioavailability of hesperidin can be affected by several factors, including the food matrix in which it is consumed, individual variations in gut microbiota, and potential interactions with other dietary compounds [77].

The second main ingredient of the tested supplement—punicalagin—is a large molecule (*M*: 1084.71 g/mol) and is classified as an ellagitannin, which makes it less bioavailable due to limited absorption in the gastrointestinal tract. It is known to undergo hydrolysis to smaller polyphenolic compounds, including ellagic acid (EA), and further biotransformation to urolithins and their isomers by gut microbiota, mainly in the colon [78]. Urolithins and isourolithins are the metabolites that appear in plasma and urine, not the initial punicalagin. Therefore, the bioavailability of punicalagin is primarily determined by the bioavailability of the products formed from its hydrolytic degradation [79]. It is important to note that there is considerable inter-individual variability in the production of urolithins/isourolithins, which has been linked to differences in gut microbiota composition among individuals [80]. Urolithin A and urolithin B are the most frequently observed urolithins in human plasma and urine. A recent study by Peng et al. [81] highlighted that urolithin A mitigates AGE formation by trapping reactive MGO, resulting in the creation of mono-MGO-urolithin A adducts.

Taken together, these findings suggest that the active metabolites of the two main components of sweet orange and pomegranate combination potentially have the ability to scavenge MGO by forming adducts with it, and this could be considered as one of the possible mechanisms that led to a significant decrease in the plasma concentration of

MGO in study subjects. Unfortunately, participants' urine samples were not collected, so identifying any potentially formed adducts was not possible. Further in-depth studies are certainly required to determine the mechanism of action of the active constituents found in sweet orange and pomegranate fruit extracts.

Previous clinical studies using the pure flavonoids quercetin-3-glucoside and epicatechin (160 mg/day and 100 mg/day, respectively) have shown that after 4 weeks of oral administration in apparently healthy (pre)hypertensive adults, only quercetin could statistically significantly reduce plasma MGO concentrations by 10.6%. This reduction slightly exceeds the 9.8% result achieved in our study using CPC. Moreover, the study revealed no statistically significant effect of flavonoids on GO and 3-DG plasma concentrations, suggesting that flavonoids may primarily target MGO [82].

The effect size of the reduction in plasma MGO by CPC with 9.8% was also found with pyridoxamine, with a decrease in plasma MGO of 9% [83]. This result was also mirrored in a well-standardized weight loss intervention study with pyridoxamine, which reported a 9% decrease in fasting MGO [84]. These studies were performed in relatively healthy abdominally obese individuals. In our previous research, we showed that MGO concentrations are associated with incident cardiovascular disease in diabetes, with a difference in plasma MGO concentrations of approximately 5% to 13% between diabetic individuals with and without cardiovascular events [85]. Therefore, the 9.8% reduction in plasma MGO, as we found in this study with CPC, could be of clinical relevance.

The reduction in plasma MGO concentration by polyphenols might be a result of actions other than the direct scavenging of MGO. This could be attributed to their strong antioxidant properties [86,87]. Oxidative stress is considered to participate in reductions in the body's natural detoxification mechanisms such as the expression of Glo1 [88]. The use of substances with strong antioxidant potential such as polyphenols may promote the physiological enhancement of MGO degradation by glo1 [89]. Additionally, the reduction in plasma MGO may also be influenced by the antidiabetic properties of hesperidin or punicalagin, which have shown promise in reducing glucose levels and improving sugar metabolism [90–93].

The current study was a post hoc analysis of a human randomized cross-over clinical trial. One major limitation is that the trial was not originally designed to identify effects on α-dicarbonyl compounds. Nevertheless, we found a significant reduction in MGO, which aligns with previous in vitro findings. It is crucial to emphasize that our study focused on metabolically healthy elderly individuals with no comorbidities, and the supplementation period itself lasted only 4 weeks. Therefore, the long-term impact of the CPCs might differ in high-risk populations, such as those with diabetes and associated vascular complications.

The identification of methods to reduce MGO concentrations could have substantial implications for preventing and managing MGO stress-related chronic diseases. These interventions may impede or slow down the formation of MGO and MGO-derived AGEs, while also ameliorating oxidative stress and suppressing inflammation. This presents a promising approach to disease management. Therefore, exploring novel therapies aimed at lowering α-DCs, including both pharmacological and non-pharmacological strategies (e.g., dietary modifications and physical exercise), carries significant clinical relevance. Additionally, it is crucial to recognize the potential synergy when these therapies are combined with established treatments, possibly enhancing their effectiveness. Adopting this multifaceted approach could lead to a more comprehensive and effective strategy to address chronic conditions associated with elevated MGO and other α-DCs.

3. Materials and Methods

3.1. Study Population and Design

The study was conducted from June 2018 to January 2019 and was approved by the local Medical Ethics Committee of the Maastricht University Medical Centre + and performed in accordance with the Declaration of Helsinki of 1975, as amended in 2013, and with the Dutch Regulations on Medical Research involving Human Subjects from

1998. All participants gave written informed consent before data collection. The study was registered at clinicaltrials.gov as NCT03781999. The detailed design of this research containing CONSORT flow diagram of the study participants was previously described by Ahles et al. [54]. In short, 42 elderly, healthy, non-smoking subjects aged 60–75 were recruited through advertisements in the local media. Exclusion criteria included a BMI (in kg/m^2) lower than 18 and higher than 28, allergy to the investigated product, placebo or citrus fruits, high blood pressure (systolic $\geq$ 140 mmHg, diastolic $\geq$ 90 mmHg), abuse of alcohol and drugs, use of beta-blockers, and other medications that may interfere with the study results. Participants were also excluded in case of recent muscle injury less than one month before the start of the study and medical conditions that might influence outcome measure or participant safety during testing, including but not limited to severe cardiovascular disease, cancer, and Parkinson's disease (concerned measurements of physical activity; not included in this article). This trial was designed as a randomized, placebo-controlled, double-blind, cross-over study. Patients were randomly allocated after enrollment in the study. Randomization was performed using a web service with concealed and random block sizes. Participants ingested a study treatment and placebo capsules for 4 weeks in random order separated by a 4-week period of washout.

3.2. Treatment and Placebo

The treatment was 500 mg *Citrus* × *sinensis* (L.) Osbeck peel extract (containing bioflavonoids) and 200 mg *Punica granatum* L. fruit concentrate (containing ellagitannins and other polyphenols) combination, delivered as a dietary supplement (Citrus & Pomegranate Complex; Actiful®, BioActor BV, Maastricht, The Netherlands). The investigational product was standardized chromatographically (LC) by the manufacturer. The daily dose contained 450 mg of hesperidin and 60 mg of punicalagin; the chemical structures of the main treatment components are shown in Figure 2. Maltodextrin (Gonmisol, Barcelona, Spain) was used as a placebo. The study products were formulated into capsules, each of which contained 350 mg of study treatment or placebo. Subjects were asked to ingest 2 gelatin capsules each morning, prior to breakfast with 200 mL of water for 4 weeks. The treatment and placebo were identical in appearance and taste.

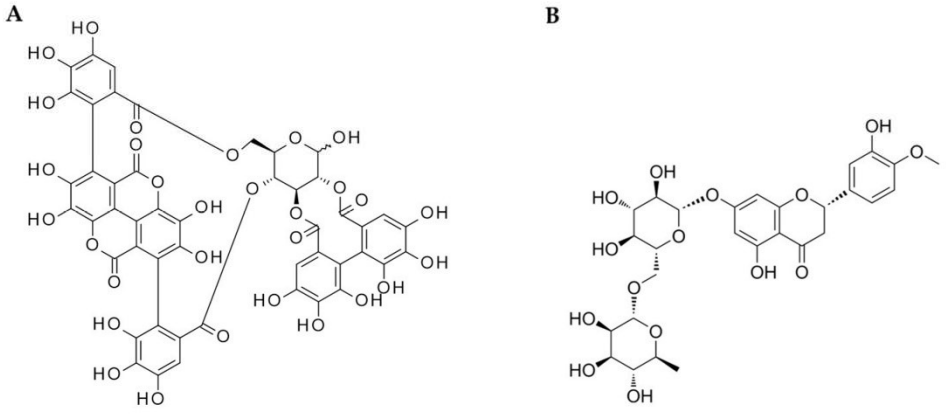

Figure 2. The main components of CPC used as a treatment in the study; (**A**) punicalagin; (**B**) hesperidin.

3.3. Measurement of α-Dicarbonyls in Plasma

Fasting blood samples were collected into Heparin S-Monovette tubes (Sarstedt, Nümbrecht, Germany). Before analysis, all plasma samples stored at −80 °C were thawed and mixed thoroughly. The concentration of α-dicarbonyls in plasma samples was measured with ultra-performance liquid chromatography tandem mass spectrometry (UPLC-MS/MS)

according to the method proposed by Scheijen et al. [94] as previously described. In short, 30 µL EDTA plasma samples were mixed with 90 µL *O*-phenylenediamine (10 mg oPD in 10 mL 1.6 M perchloric acid) in an Eppendorf cup. After an overnight (20 h) incubation at room temperature away from light, 20 µL of the internal standard solution (d4-α-DCs) was added. Samples were mixed and subsequently centrifuged for 10 min at 21,000× *g* at a temperature of 4 °C; then, 2.5 µL was injected for UPLC-MS/MS analysis.

3.4. Instrumentation

A Waters Acquity I-class system combined with a Xevo TQ-XS mass spectrometer (Waters, Milford, MA, USA) equipped with a reversed-phase C18 column (Acquity UPLC HSS T3, 50 × 2.1 mm, 1.8 µm) was employed for the determination of α-dicarbonyl concentrations.

3.5. Statistical Analysis

Statistical analyses were carried out according to a method previously described by Dower et al. [95]. Changes between values of α-dicarbonyls concentration at the start and the end of each 4-week double-blind intervention period were taken as a treatment effect of CPC. All variables were found to be normally distributed. A linear mixed model with compound symmetry as a covariant structure was used to evaluate the treatment effects in this study. The subject was defined as a random effect, while treatment and period were taken as fixed effects. Investigation of treatment–period interaction revealed no carry-over effect of previous treatment and, therefore, it was not included in the final model. Effects of treatment were expressed as mean least squares with 95% Cis, and statistical significance was set at a 2-sided p value of 0.05. SPSS Statistics 23 software was used for all analyses. For data visualization, GraphPad Prism 5 software was used.

4. Conclusions

In conclusion, this is the first human intervention study to investigate the effects of a combination of sweet orange extract and pomegranate fruit concentrate on reactive α-DCs. This study revealed a significant reduction in plasma MGO concentrations. The MGO scavenging effect exhibited by the active compounds in sweet orange and pomegranate holds promise as a potential therapeutic approach for preventing and managing conditions in which MGO plays a pivotal role.

Based on these initial findings, several recommendations and prospective avenues emerge. It is essential to substantiate these preliminary discoveries with broader studies, involving a more diverse group of participants. Investigating the optimal doses of the combined extracts is crucial for refining the MGO scavenging effect. Moreover, determining the specific molecular pathways through which these compounds act will enhance our understanding and may lead to the development of even more effective interventions. If supported by further research, these findings have the potential to influence the creation of specialized dietary supplements or nutraceuticals targeting MGO-related health concerns. Additionally, this study's insights hint at the vast potential of phytochemicals in various fruits and plants that might offer therapeutic properties against MGO. Through these revelations, we are establishing a foundation for future research, aiming for innovative solutions to challenges posed by elevated MGO levels.

Author Contributions: Conceptualization, C.G.S.; data curation, J.L.J.M.S. and K.B.; formal analysis, J.L.J.M.S. and K.B.; methodology, C.G.S. and S.A.; supervision, C.G.S., J.L.J.M.S. and I.F.; visualization, K.B., J.L.J.M.S. and I.F.; writing—original draft, K.B.; writing—review and editing, J.L.J.M.S., C.G.S., P.V., S.A. and I.F. All authors have read and agreed to the published version of the manuscript.

Funding: This research received no external funding. The APC was funded by Wroclaw Medical University. Biological samples were provided by BioActor BV.

Institutional Review Board Statement: The study was conducted in accordance with the Declaration of Helsinki and approved by the Ethics Committee of the Maastricht University Medical Centre+ (protocol code NCT03781999 approved by EC on 14 February 2018).

Informed Consent Statement: Informed consent was obtained from all subjects involved in the study.

Data Availability Statement: The data presented in this study are available on request from the corresponding author.

Conflicts of Interest: S.A. receives a salary from BioActor BV. The other authors declare no conflict of interest.

Abbreviations

3-DG	3-deoxyglucosone
α-DCs	alpha dicarbonyls
AGEs	advanced glycation endproducts
BMI	body mass index
CEL	N^{ϵ}-(1-carboxyethyl)lysine
CPC	citrus and pomegranate extract
Glo1	glyoxalase 1
Glo2	glyoxalase 2
GO	glyoxal
LC	liquid chromatography
MG-H1	N^{δ}-(5-hydro-5-methyl-4-imidazolone-2-yl)ornithine
MGO	methylglyoxal
oPD	d8-*O*-phenylenediamine
RAGE	receptor for advanced glycation endproducts
RCS	reactive carbonyl species
SD	standard deviation
SEM	standard error of the mean
UHPLC-MS/MS	ultra-high-performance liquid chromatography tandem mass spectrometry

References

1. Lehrke, M.; Marx, N. Diabetes Mellitus and Heart Failure. *Am. J. Cardiol.* **2017**, *120*, 37–47. [CrossRef] [PubMed]
2. Bourajjaj, M.; Stehouwer, C.D.A.; Van Hinsbergh, V.W.M.; Schalkwijk, C.G. Role of methylglyoxal adducts in the development of vascular complications in diabetes mellitus. *Biochem. Soc. Trans.* **2003**, *31*, 1400–1402. [CrossRef] [PubMed]
3. Semchyshyn, H.M. Reactive carbonyl species in vivo: Generation and dual biological effects. *Sci. World J.* **2014**, *2014*, 27–31. [CrossRef] [PubMed]
4. Turk, Z. Glycotoxines, carbonyl stress and relevance to diabetes and its complications. *Physiol. Res.* **2010**, *59*, 147–156. [CrossRef]
5. Phillips, S.A.; Thornalley, P.J. The formation of methylglyoxal from triose phosphates: Investigation using a specific assay for methylglyoxal. *Eur. J. Biochem.* **1993**, *212*, 101–105. [CrossRef]
6. Hanssen, N.M.J.; Kraakman, M.J.; Flynn, M.C.; Nagareddy, P.R.; Schalkwijk, C.G.; Murphy, A.J. Postprandial Glucose Spikes, an Important Contributor to Cardiovascular Disease in Diabetes? *Front. Cardiovasc. Med.* **2020**, *7*, 570553. [CrossRef]
7. Tamae, D.; Lim, P.; Wuenschell, G.E.; Termini, J. Mutagenesis and repair induced by the DNA advanced glycation end product N 2-1-(carboxyethyl)-2′-deoxyguanosine in human cells. *Biochemistry* **2011**, *50*, 2321–2329. [CrossRef]
8. Wuenschell, G.E.; Tamae, D.; Cercillieux, A.; Yamanaka, R.; Yu, C.; Termini, J. Mutagenic potential of DNA glycation: Miscoding by (R)- and (S)-N 2-(1-carboxyethyl)2′-deoxyguanosine. *Biochemistry* **2010**, *49*, 1814–1821. [CrossRef]
9. Takahashi, K. The reactions of phenylglyoxal and related reagents with amino acids. *J. Biochem.* **1977**, *81*, 395–402. [CrossRef]
10. Ahmed, N.; Argirov, O.K.; Minhas, H.S.; Cordeiro, C.A.A.; Thornalley, P.J. Assay of advanced glycation endproducts (AGEs): Surveying AGEs by chromatographic assay with derivatization by 6-aminoquinolyl-N-hydroxysuccinimidyl-carbamate and application to Nε-carboxymethyl-lysine- and nε-(1-carboxyethyl)lysine-modified albumin. *Biochem. J.* **2002**, *364*, 1–14. [CrossRef]
11. Ahmed, K.A.; Muniandy, S.; Ismail, I.S. Role of Nε-(carboxymethyl)lysine in the development of ischemic heart disease in type 2 diabetes mellitus. *J. Clin. Biochem. Nutr.* **2007**, *41*, 97–105. [CrossRef] [PubMed]
12. Salahuddin, P.; Rabbani, G.; Khan, R.H. The role of advanced glycation end products in various types of neurodegenerative disease: A therapeutic approach. *Cell. Mol. Biol. Lett.* **2014**, *19*, 407–437. [CrossRef] [PubMed]
13. Kim, Y. Blood and Tissue Advanced Glycation End Products as Determinants of Cardiometabolic Disorders Focusing on Human Studies. *Nutrients* **2023**, *15*, 2002. [CrossRef]
14. Li, J.; Liu, D.; Sun, L.; Lu, Y.; Zhang, Z. Advanced glycation end products and neurodegenerative diseases: Mechanisms and perspective. *J. Neurol. Sci.* **2012**, *317*, 1–5. [CrossRef] [PubMed]

15. Luévano-Contreras, C.; Gómez-Ojeda, A.; Macías-Cervantes, M.H.; Garay-Sevilla, M.E. Dietary Advanced Glycation End Products and Cardiometabolic Risk. *Curr. Diab. Rep.* **2017**, *17*, 1–11. [CrossRef]
16. Sousa Silva, M.; Gomes, R.A.; Ferreira, A.E.N.; Ponces Freire, A.; Cordeiro, C. The glyoxalase pathway: The first hundred years... and beyond. *Biochem. J.* **2013**, *453*, 1–15. [CrossRef]
17. Rabbani, N.; Thornalley, P.J. Dicarbonyl proteome and genome damage in metabolic and vascular disease. *Biochem. Soc. Trans.* **2014**, *42*, 425–432. [CrossRef]
18. Aragonès, G.; Rowan, S.; Francisco, S.G.; Whitcomb, E.A.; Yang, W.; Perini-Villanueva, G.; Schalkwijk, C.G.; Taylor, A.; Bejarano, E. The glyoxalase system in age-related diseases: Nutritional intervention as anti-ageing strategy. *Cells* **2021**, *10*, 1852. [CrossRef]
19. Desai, K.M.; Wu, L. Free radical generation by methylglyoxal in tissues. *Drug Metabol. Drug Interact.* **2008**, *23*, 151–173. [CrossRef]
20. Hollenbach, M. The role of glyoxalase-i (Glo-I), advanced glycation endproducts (AGEs), and their receptor (RAGE) in chronic liver disease and hepatocellular carcinoma (HCC). *Int. J. Mol. Sci.* **2017**, *18*, 2466. [CrossRef]
21. Wetzels, S.; Wouters, K.; Schalkwijk, C.G.; Vanmierlo, T.; Hendriks, J.J.A. Methylglyoxal-derived advanced glycation endproducts in multiple sclerosis. *Int. J. Mol. Sci.* **2017**, *18*, 421. [CrossRef] [PubMed]
22. Subedi, L.; Lee, J.H.; Gaire, B.P.; Kim, S.Y. Sulforaphane inhibits MGO-AGE-mediated neuroinflammation by suppressing NF-κB, MAPK, and AGE–RAGE signaling pathways in microglial cells. *Antioxidants* **2020**, *9*, 792. [CrossRef] [PubMed]
23. Bolton, W.K.; Cattran, D.C.; Williams, M.E.; Adler, S.G.; Appel, G.B.; Cartwright, K.; Foiles, P.G.; Freedman, B.I.; Raskin, P.; Ratner, R.E. Randomized Trial of an Inhibitor of Formation of Advanced Glycation End Products in Diabetic Nephropathy. *Am. J. Nephrol.* **2004**, *24*, 32–40. [CrossRef] [PubMed]
24. Bakris, G.L.; Bank, A.J.; Kass, D.A.; Neutel, J.M.; Preston, R.A.; Oparil, S. Advanced glycation end-product cross-link breakers: A novel approach to cardiovascular pathologies related to the aging process. *Am. J. Hypertens.* **2004**, *17*, S23–S30. [CrossRef]
25. Kinsky, O.R.; Hargraves, T.L.; Anumol, T.; Jacobsen, N.E.; Dai, J.; Snyder, S.A.; Monks, T.J.; Lau, S.S. Metformin Scavenges Methylglyoxal to Form a Novel Imidazolinone Metabolite in Humans. *Chem. Res. Toxicol.* **2016**, *29*, 227–234. [CrossRef]
26. Quinn, C.E.; Hamilton, P.K.; Lockhart, C.J.; McVeigh, G.E. Thiazolidinediones: Effects on insulin resistance and the cardiovascular system. *Br. J. Pharmacol.* **2008**, *153*, 636–645. [CrossRef]
27. Šebeková, K.; Gazdíková, K.; Syrová, D.; Blažíček, P.; Schinzel, R.; Heidland, A.; Spustová, V.; Dzúrik, R. Effects of ramipril in nondiabetic nephropathy: Improved parameters of oxidatives stress and potential modulation of advanced glycation end products. *J. Hum. Hypertens.* **2003**, *17*, 265–270. [CrossRef]
28. Miyata, T.; Van Ypersele De Strihou, C.; Ueda, Y.; Ichimori, K.; Inagi, R.; Onogi, H.; Ishikawa, N.; Nangaku, M.; Kurokawa, K. Angiotensin II receptor antagonists and angiotensin-converting enzyme inhibitors lower in vitro the formation of advanced glycation end products: Biochemical mechanisms. *J. Am. Soc. Nephrol.* **2002**, *13*, 2478–2487. [CrossRef]
29. Miller, A.G.; Tan, G.; Binger, K.J.; Pickering, R.J.; Thomas, M.C.; Nagaraj, R.H.; Cooper, M.E.; Wilkinson-Berka, J.L. Candesartan attenuates diabetic retinal vascular pathology by restoring glyoxalase-I function. *Diabetes* **2010**, *59*, 3208–3215. [CrossRef]
30. Rezaie-Majd, A.; Maca, T.; Bucek, R.A.; Valent, P.; Müller, M.R.; Husslein, P.; Kashanipour, A.; Minar, E.; Baghestanian, M. Simvastatin reduces expression of cytokines interleukin-6, interleukin-8, and monocyte chemoattractant protein-1 in circulating monocytes from hypercholesterolemic patients. *Arterioscler. Thromb. Vasc. Biol.* **2002**, *22*, 1194–1199. [CrossRef]
31. Freund, M.A.; Chen, B.; Decker, E.A. The Inhibition of Advanced Glycation End Products by Carnosine and Other Natural Dipeptides to Reduce Diabetic and Age-Related Complications. *Compr. Rev. Food Sci. Food Saf.* **2018**, *17*, 1367–1378. [CrossRef] [PubMed]
32. Ramis, R.; Ortega-Castro, J.; Caballero, C.; Casasnovas, R.; Cerrillo, A.; Vilanova, B.; Adrover, M.; Frau, J. How does pyridoxamine inhibit the formation of advanced glycation end products? The role of its primary antioxidant activity. *Antioxidants* **2019**, *8*, 344. [CrossRef] [PubMed]
33. He, Y.; Zhou, C.; Huang, M.; Tang, C.; Liu, X.; Yue, Y.; Diao, Q.; Zheng, Z.; Liu, D. Glyoxalase system: A systematic review of its biological activity, related-diseases, screening methods and small molecule regulators. *Biomed. Pharmacother.* **2020**, *131*, 110663. [CrossRef] [PubMed]
34. Piazza, M.; Hanssen, N.M.J.; Persson, F.; Scheijen, J.L.; van de Waarenburg, M.P.H.; van Greevenbroek, M.M.J.; Rossing, P.; Hovind, P.; Stehouwer, C.D.A.; Parving, H.H. Irbesartan treatment does not influence plasma levels of the dicarbonyls methylglyoxal, glyoxal and 3-deoxyglucosone in participants with type 2 diabetes and microalbuminuria: An IRMA2 sub-study. *Diabet. Med.* **2021**, *38*, e14405. [CrossRef]
35. Chopra, A.S.; Lordan, R.; Horbańczuk, O.K.; Atanasov, A.G.; Chopra, I.; Horbańczuk, J.O.; Jóźwik, A.; Huang, L.; Pirgozliev, V.; Banach, M. The current use and evolving landscape of nutraceuticals. *Pharmacol. Res.* **2022**, *175*, 106001. [CrossRef]
36. Carrizzo, A.; Izzo, C.; Forte, M.; Sommella, E.; Di Pietro, P.; Venturini, E.; Ciccarelli, M.; Galasso, G.; Rubattu, S.; Campiglia, P. A novel promising frontier for human health: The beneficial effects of nutraceuticals in cardiovascular diseases. *Int. J. Mol. Sci.* **2020**, *21*, 8706. [CrossRef]
37. Bumrungpert, A.; Pavadhgul, P.; Chongsuwat, R.; Komindr, S. Nutraceutical Improves Glycemic Control, Insulin Sensitivity, and Oxidative Stress in Hyperglycemic Subjects: A Randomized, Double-Blind, Placebo-Controlled Clinical Trial. *Nat. Prod. Commun.* **2020**, *15*, 1–11. [CrossRef]
38. Kanaze, F.I.; Termentzi, A.; Gabrieli, C.; Niopas, I.; Georgarakis, M.; Kokkalou, E. The phytochemical analysis and antioxidant activity assessment of orange peel (*Citrus sinensis*) cultivated in Greece–Crete indicates a new commercial source of hesperidin. *Biomed. Chromatogr.* **2009**, *23*, 239–249. [CrossRef]

39. Calani, L.; Beghe, D.; Mena, P.; Del Rio, D.; Bruni, R.; Fabbri, A.; Dall'Asta, C.; Galaverna, G. Ultra-HPLC−MS^n (Poly)phenolic Profiling and Chemometric Analysis of Juices from Ancient *Punica granatum* L. Cultivars: A Nontargeted Approach. *J. Agric. Food Chem.* **2013**, *61*, 5600–5609. [CrossRef]
40. Bednarska, K.; Fecka, I. Potential of Vasoprotectives to Inhibit Non-Enzymatic Protein Glycation, and Reactive Carbonyl and Oxygen Species Uptake. *Int. J. Mol. Sci.* **2021**, *22*, 10026. [CrossRef]
41. Li, D.; Mitsuhashi, S.; Ubukata, M. Protective effects of hesperidin derivatives and their stereoisomers against advanced glycation end-products formation. *Pharm. Biol.* **2012**, *50*, 1531–1535. [CrossRef]
42. Zhu, H.; Poojary, M.M.; Andersen, M.L.; Lund, M.N. Effect of pH on the reaction between naringenin and methylglyoxal: A kinetic study. *Food Chem.* **2019**, *298*, 125086. [CrossRef] [PubMed]
43. Liu, W.; Ma, H.; Frost, L.; Yuan, T.; Dain, J.A.; Seeram, N.P. Pomegranate phenolics inhibit formation of advanced glycation endproducts by scavenging reactive carbonyl species. *Food Funct.* **2014**, *5*, 2996–3004. [CrossRef]
44. Guo, H.; Liu, C.; Tang, Q.; Li, D.; Wan, Y.; Li, J.H.; Gao, X.H.; Seeram, N.P.; Ma, H.; Chen, H.D. Pomegranate (*Punica granatum*) extract and its polyphenols reduce the formation of methylglyoxal-DNA adducts and protect human keratinocytes against methylglyoxal-induced oxidative stress. *J. Funct. Foods* **2021**, *83*, 104564. [CrossRef]
45. Kumagai, Y.; Nakatani, S.; Onodera, H.; Nagatomo, A.; Nishida, N.; Matsuura, Y.; Kobata, K.; Wada, M. Anti-Glycation Effects of Pomegranate (*Punica granatum* L.) Fruit Extract and Its Components in Vivo and in Vitro. *J. Agric. Food Chem.* **2015**, *63*, 7760–7764. [CrossRef] [PubMed]
46. Xue, M.; Weickert, M.O.; Qureshi, S.; Kandala, N.; Anwar, A.; Waldron, M.; Shafie, A.; Messenger, D.; Fowler, M.; Jenkins, G.; et al. Improved Glycemic Control and Vascular Function in Overweight and Obese Subjects by Glyoxalase 1 Inducer Formulation. *Diabetes* **2016**, *65*, 2282–2294. [CrossRef] [PubMed]
47. Henning, C.; Liehr, K.; Girndt, M.; Ulrich, C.; Glomb, M.A. Extending the spectrum of α-dicarbonyl compounds in vivo. *J. Biol. Chem.* **2014**, *289*, 28676–28688. [CrossRef] [PubMed]
48. Rabbani, N.; Thornalley, P.J. Measurement of methylglyoxal by stable isotopic dilution analysis LC-MS/MS with corroborative prediction in physiological samples. *Nat. Protoc.* **2014**, *9*, 1969–1979. [CrossRef]
49. Odani, H.; Shinzato, T.; Matsumoto, Y.; Usami, J.; Maeda, K. Increase in three α,β-dicarbonyl compound levels in human uremic plasma: Specific in vivo determination of intermediates in advanced Maillard reaction. *Biochem. Biophys. Res. Commun.* **1999**, *256*, 89–93. [CrossRef]
50. Han, Y.; Randell, E.; Vasdev, S.; Gill, V.; Gadag, V.; Newhook, L.A.; Grant, M.; Hagerty, D. Plasma methylglyoxal and glyoxal are elevated and related to early membrane alteration in young, complication-free patients with Type 1 diabetes. *Mol. Cell. Biochem.* **2007**, *305*, 123–131. [CrossRef]
51. Chronakis, I.S. On the molecular characteristics, compositional properties, and structural-functional mechanisms of maltodextrins: A review. *Crit. Rev. Food Sci. Nutr.* **1998**, *38*, 599–637. [CrossRef] [PubMed]
52. Hofman, D.L.; van Buul, V.J.; Brouns, F.J.P.H. Nutrition, Health, and Regulatory Aspects of Digestible Maltodextrins. *Crit. Rev. Food Sci. Nutr.* **2016**, *56*, 2091–2100. [CrossRef] [PubMed]
53. Rytz, A.; Adeline, D.; Lê, K.A.; Tan, D.; Lamothe, L.; Roger, O.; Macé, K. Predicting glycemic index and glycemic load from macronutrients to accelerate development of foods and beverages with lower glucose responses. *Nutrients* **2019**, *11*, 1172. [CrossRef]
54. Ahles, S.; Cuijpers, I.; Hartgens, F.; Troost, F.J. The Effect of a Citrus and Pomegranate Complex on Physical Fitness and Mental Well-Being in Healthy Elderly: A Randomized Placebo-Controlled Trial. *J. Nutr. Health Aging* **2022**, *26*, 839–846. [CrossRef]
55. Zhang, S.; Xiao, L.; Lv, L.; Sang, S. Trapping methylglyoxal by myricetin and its metabolites in mice. *J. Agric. Food Chem.* **2020**, *68*, 9408–9414. [CrossRef] [PubMed]
56. Zhang, Y.; Zhan, L.; Wen, Q.; Feng, Y.; Luo, Y.; Tan, T. Trapping Methylglyoxal by Taxifolin and Its Metabolites in Mice. *J. Agric. Food Chem.* **2022**, *70*, 5026–5038. [CrossRef] [PubMed]
57. Liu, G.; Xia, Q.; Lu, Y.; Zheng, T.; Sang, S.; Lv, L. Influence of Quercetin and Its Methylglyoxal Adducts on the Formation of α-Dicarbonyl Compounds in a Lysine/Glucose Model System. *J. Agric. Food Chem.* **2017**, *65*, 2233–2239. [CrossRef]
58. Wang, P.; Chen, H.; Sang, S. Trapping Methylglyoxal by Genistein and Its Metabolites in Mice. *Chem. Res. Toxicol.* **2016**, *29*, 406–414. [CrossRef]
59. Zhao, Y.; Tang, Y.; Sang, S. Dietary Quercetin Reduces Plasma and Tissue Methylglyoxal and Advanced Glycation End Products in Healthy Mice Treated with Methylglyoxal. *J. Nutr.* **2021**, *151*, 2601–2609. [CrossRef]
60. Zhang, S.; Zhao, Y.; Ohland, C.; Jobin, C.; Sang, S. Microbiota facilitates the formation of the aminated metabolite of green tea polyphenol (−)-epigallocatechin-3-gallate which trap deleterious reactive endogenous metabolites. *Free Radic. Biol. Med.* **2019**, *131*, 332–344. [CrossRef]
61. Mahadevan, S.; Park, Y. Multifaceted therapeutic benefits of *Ginkgo biloba* L.: Chemistry, efficacy, safety, and uses. *J. Food Sci.* **2008**, *73*, R14–R19. [CrossRef] [PubMed]
62. Ben-Shabat, S.; Fride, E.; Sheskin, T.; Tamiri, T.; Rhee, M.H.; Vogel, Z.; Bisogno, T.; De Petrocellis, L.; Di Marzo, V.; Mechoulam, R. An entourage effect: Inactive endogenous fatty acid glycerol esters enhance 2-arachidonoyl-glycerol cannabinoid activity. *Eur. J. Pharmacol.* **1998**, *353*, 23–31. [CrossRef] [PubMed]

63. Nielsen, I.L.F.; Chee, W.S.S.; Poulsen, L.; Offord-Cavin, E.; Rasmussen, S.E.; Frederiksen, H.; Enslen, M.; Barron, D.; Horcajada, M.N.; Williamson, G. Bioavailability is improved by enzymatic modification of the citrus flavonoid hesperidin in humans: A randomized, double-blind, crossover trial. *J. Nutr.* **2006**, *136*, 404–408. [CrossRef] [PubMed]
64. Antony, B.; Merina, B.; Iyer, V.; Judy, N.; Lennertz, K.; Joyal, S. A pilot cross-over study to evaluate human oral bioavailability of BCM-95® CG (Biocurcumax™), a novel bioenhanced preparation of curcumin. *Indian J. Pharm. Sci.* **2008**, *70*, 445–449. [CrossRef]
65. Booker, A.; Jalil, B.; Frommenwiler, D.; Reich, E.; Zhai, L.; Kulic, Z.; Heinrich, M. The authenticity and quality of *Rhodiola rosea* products. *Phytomedicine* **2016**, *23*, 754–762. [CrossRef]
66. Booker, A.; Frommenwiler, D.; Reich, E.; Horsfield, S.; Heinrich, M. Adulteration and poor quality of *Ginkgo biloba* supplements. *J. Herb. Med.* **2016**, *6*, 79–87. [CrossRef]
67. Berman, A.Y.; Motechin, R.A.; Wiesenfeld, M.Y.; Holz, M.K. The therapeutic potential of resveratrol: A review of clinical trials. *npj Precis. Oncol.* **2017**, *1*, 35. [CrossRef]
68. Sitarek, P.; Merecz-Sadowska, A.; Kowalczyk, T.; Wieczfinska, J.; Zajdel, R.; Śliwiński, T. Potential synergistic action of bioactive compounds from plant extracts against skin infecting microorganisms. *Int. J. Mol. Sci.* **2020**, *21*, 5105. [CrossRef]
69. Anand, P.; Kunnumakkara, A.B.; Newman, R.A.; Aggarwal, B.B. Bioavailability of curcumin: Problems and promises. *Mol. Pharm.* **2007**, *4*, 807–818. [CrossRef]
70. Li, Y.M.; Li, X.M.; Li, G.M.; Du, W.C.; Zhang, J.; Li, W.X.; Xu, J.; Hu, M.; Zhu, Z. In vivo pharmacokinetics of hesperidin are affected by treatment with glucosidase-like BglA protein isolated from yeasts. *J. Agric. Food Chem.* **2008**, *56*, 5550–5557. [CrossRef]
71. Brett, G.M.; Hollands, W.; Needs, P.W.; Teucher, B.; Dainty, J.R.; Davis, B.D.; Brodbelt, J.S.; Kroon, P.A. Absorption, metabolism and excretion of flavanones from single portions of orange fruit and juice and effects of anthropometric variables and contraceptive pill use on flavanone excretion. *Br. J. Nutr.* **2009**, *101*, 664–675. [CrossRef] [PubMed]
72. Manach, C.; Morand, C.; Gil-Izquierdo, A.; Bouteloup-Demange, C.; Rémésy, C. Bioavailability in humans of the flavanones hesperidin and narirutin after the ingestion of two dose of orange juice. *Eur. J. Clin. Nutr.* **2003**, *57*, 235–242. [CrossRef] [PubMed]
73. Mullen, W.; Archeveque, M.A.; Edwards, C.A.; Matsumoto, H.; Crozier, A. Bioavailability and metabolism of orange juice flavanones in humans: Impact of a full-fat yogurt. *J. Agric. Food Chem.* **2008**, *56*, 11157–11164. [CrossRef]
74. Nishioka, A.; Tobaruela, E.d.C.; Fraga, L.N.; Tomas-Barberan, F.A.; Lajolo, F.M.; Hassimotto, N.M.A. Stratification of volunteers according to flavanone metabolite excretion and phase ii metabolism profile after single doses of 'pera' orange and 'moro' blood orange juices. *Nutrients* **2021**, *13*, 473. [CrossRef] [PubMed]
75. Shao, X.; Chen, H.; Zhu, Y.; Sedighi, R.; Ho, C.T.; Sang, S. Essential structural requirements and additive effects for flavonoids to scavenge methylglyoxal. *J. Agric. Food Chem.* **2014**, *62*, 3202–3210. [CrossRef]
76. Bednarska, K.; Fecka, I. Aspalathin and Other Rooibos Flavonoids Trapped α-Dicarbonyls and Inhibited Formation of Advanced Glycation End Products In Vitro. *Int. J. Mol. Sci.* **2022**, *23*, 4738. [CrossRef]
77. Erlund, I.; Meririnne, E.; Alfthan, G.; Aro, A. Human nutrition and metabolism: Plasma kinetics and urinary excretion of the flavanones naringenin and hesperetin in humans after ingestion of orange juice and grapefruit juice. *J. Nutr.* **2001**, *131*, 235–241. [CrossRef]
78. Cerdá, B.; Espín, J.C.; Parra, S.; Martínez, P.; Tomás-Barberán, F.A. The potent in vitro antioxidant ellagitannins from pomegranate juice are metabolised into bioavailable but poor antioxidant hydroxy-6H-dibenzopyran-6-one derivatives by the colonic microflora of healthy humans. *Eur. J. Nutr.* **2004**, *43*, 205–220. [CrossRef]
79. Espín, J.C.; Larrosa, M.; García-Conesa, M.T.; Tomás-Barberán, F. Biological significance of urolithins, the gut microbial ellagic acid-derived metabolites: The evidence so far. *Evid.-Based Complement. Altern. Med.* **2013**, *2013*, 270418. [CrossRef]
80. Tomás-Barberán, F.A.; García-Villalba, R.; González-Sarrías, A.; Selma, M.V.; Espín, J.C. Ellagic acid metabolism by human gut microbiota: Consistent observation of three urolithin phenotypes in intervention trials, independent of food source, age, and health status. *J. Agric. Food Chem.* **2014**, *62*, 6535–6538. [CrossRef]
81. Peng, C.Y.; Zhu, H.D.; Zhang, L.; Li, X.F.; Zhou, W.N.; Tu, Z.C. Urolithin A alleviates advanced glycation end-product formation by altering protein structures, trapping methylglyoxal and forming complexes. *Food Funct.* **2021**, *12*, 11849–11861. [CrossRef]
82. Van Den Eynde, M.D.G.; Geleijnse, J.M.; Scheijen, J.L.J.M.; Hanssen, N.M.J.; Dower, J.I.; Afman, L.A.; Stehouwer, C.D.A.; Hollman, P.C.H.; Schalkwijk, C.G. Quercetin, but not epicatechin, decreases plasma concentrations of methylglyoxal in adults in a randomized, double-blind, placebo-controlled, crossover trial with pure flavonoids. *J. Nutr.* **2018**, *148*, 1911–1916. [CrossRef]
83. Van Den Eynde, M.D.G.; Houben, A.J.H.M.; Scheijen, J.L.J.M.; Linkens, A.M.A.; Niessen, P.M.; Simons, N.; Hanssen, N.M.J.; Kusters, Y.H.A.M.; Eussen, S.J.M.P.; Miyata, M.; et al. Pyridoxamine reduces methylglyoxal and markers of glycation and endothelial dysfunction, but does not improve insulin sensitivity or vascular function in abdominally obese individuals: A randomized double-blind placebo-controlled trial. *Diabetes Obes. Metab.* **2023**, *25*, 1280–1291. [CrossRef]
84. Van Den Eynde, M.D.G.; Kusters, Y.H.A.M.; Houben, A.J.H.M.; Scheijen, J.L.J.M.; Duynhoven, J.; Fazelzadeh, P.; Joris, P.J.; Plat, J.; Mensink, R.P.; Hanssen, N.M.J.; et al. Diet-induced weight loss reduces postprandial dicarbonyl stress in abdominally obese men: Secondary analysis of a randomized controlled trial. *Clin. Nutr.* **2021**, *40*, 2654–2662. [CrossRef]
85. Hanssen, N.M.J.; Scheijen, J.L.J.M.; Jorsal, A.; Parving, H.-H.; Tarnow, L.; Rossing, P.; Stehouwer, C.D.A.; Schalkwijk, C.G. Higher Plasma Methylglyoxal Levels Are Associated With Incident Cardiovascular Disease in Individuals With Type 1 Diabetes: A 12-Year Follow-up Study. *Diabetes* **2017**, *66*, 2278–2283. [CrossRef] [PubMed]
86. Azman, N.F.I.N.; Azlan, A.; Khoo, H.E.; Razman, M.R. Antioxidant properties of fresh and frozen peels of citrus species. *Curr. Res. Nutr. Food Sci.* **2019**, *7*, 331–339. [CrossRef]

87. Shiban, M.S.; Al-otaibi, M.M.; Al-Zoreky, N.S. Antioxidant Activity of Pomegranate (*Punica granatum* L.) Fruit Peels. *Food Nutr. Sci.* **2012**, *2012*, 991–996. [CrossRef]
88. Hanssen, N.M.J.; Wouters, K.; Huijberts, M.S.; Gijbels, M.J.; Sluimer, J.C.; Scheijen, J.L.J.M.; Heeneman, S.; Biessen, E.A.L.; Daemen, M.J.A.P.; Brownlee, M. Higher levels of advanced glycation endproducts in human carotid atherosclerotic plaques are associated with a rupture-prone phenotype. *Eur. Heart J.* **2014**, *35*, 1137–1146. [CrossRef]
89. Rabbani, N.; Thornalley, P.J. Emerging Glycation-Based Therapeutics—Glyoxalase 1 Inducers and Glyoxalase 1 Inhibitors. *Int. J. Mol. Sci.* **2022**, *23*, 2453. [CrossRef]
90. Visnagri, A.; Kandhare, A.D.; Chakravarty, S.; Ghosh, P.; Bodhankar, S.L. Hesperidin, a flavanoglycone attenuates experimental diabetic neuropathy via modulation of cellular and biochemical marker to improve nerve functions. *Pharm. Biol.* **2014**, *52*, 814–828. [CrossRef]
91. Rekha, S.S.; Pradeepkiran, J.A.; Bhaskar, M. Bioflavonoid hesperidin possesses the anti-hyperglycemic and hypolipidemic property in STZ induced diabetic myocardial infarction (DMI) in male Wister rats. *J. Nutr. Intermed. Metab.* **2019**, *15*, 58–64. [CrossRef]
92. Dhanya, R.; Jayamurthy, P. In Vitro evaluation of antidiabetic potential of hesperidin and its aglycone hesperetin under oxidative stress in skeletal muscle cell line. *Cell Biochem. Funct.* **2020**, *38*, 419–427. [CrossRef] [PubMed]
93. Pottathil, S.; Nain, P.; Morsy, M.A.; Kaur, J.; Al-Dhubiab, B.E.; Jaiswal, S.; Nair, A.B. Mechanisms of Antidiabetic Activity of Methanolic Extract of *Punica granatum* Leaves in. *Plant* **2020**, *2*, 1609. [CrossRef]
94. Scheijen, J.L.J.M.; Schalkwijk, C.G. Quantification of glyoxal, methylglyoxal and 3-deoxyglucosone in blood and plasma by ultra performance liquid chromatography tandem mass spectrometry: Evaluation of blood specimen. *Clin. Chem. Lab. Med.* **2014**, *52*, 85–91. [CrossRef] [PubMed]
95. Dower, J.I.; Geleijnse, J.M.; Gijsbers, L.; Zock, P.L.; Kromhout, D.; Hollman, P.C.H. Effects of the pure flavonoids epicatechin and quercetin on vascular function and cardiometabolic health: A randomized, double-blind, placebo-controlled, crossover trial. *Am. J. Clin. Nutr.* **2015**, *101*, 914–921. [CrossRef]

P3. Investigation of the Phytochemical Composition, Antioxidant Activity, and Methylglyoxal Trapping Effect of Galega officinalis L. Herb *In Vitro*

molecules

MDPI

Article

Investigation of the Phytochemical Composition, Antioxidant Activity, and Methylglyoxal Trapping Effect of *Galega officinalis* L. Herb In Vitro

Katarzyna Bednarska *, Piotr Kuś and Izabela Fecka

Department of Pharmacognosy and Herbal Medicines, Faculty of Pharmacy, Wroclaw Medical University, ul. Borowska 211, 50-556 Wroclaw, Poland; piotr.kus@umed.wroc.pl (P.K.); izabela.fecka@umed.wroc.pl (I.F.)
* Correspondence: katarzyna.bednarska@student.umed.wroc.pl

Academic Editor: Marcello Iriti
Received: 17 November 2020; Accepted: 7 December 2020; Published: 9 December 2020

check for updates

Abstract: *Galega officinalis* L. has been known for centuries as an herbal medicine used to alleviate the symptoms of diabetes, but its comprehensive chemical composition and pharmacological activity are still insufficiently known. The current study involved the qualitative and quantitative phytochemical analysis and in vitro evaluation of the antioxidative and methylglyoxal (MGO) trapping properties of galega herb. Ultra high-performance liquid chromatography coupled with both the electrospray ionization mass spectrometer and diode-array detector (UHPLC-ESI-MS and UHPLC-DAD) were used to investigate the composition and evaluate the anti-MGO capability of extracts and their components. Hot water and aqueous methanol extracts, as well as individual compounds representing phytochemical groups, were also assessed for antioxidant activity using DPPH (2,2-diphenyl-1-(2,4,6-trinitrophenyl)hydrazyl) and ABTS (2,2′-azino-bis(3-ethylbenz-thiazoline-6-sulfonic acid) assays. Quercetin and metformin were used as a positive control. We confirmed the presence of tricyclic quinazoline alkaloids, guanidines, flavonoids, and hydroxycinnamic acids (HCAs) in galega extracts. The polyphenolic fraction was dominated by mono-, di-, and triglycosylated flavonols, as well as monocaffeoylhexaric acids. The in vitro tests indicated which *G. officinalis* components exhibit beneficial antioxidative and MGO trapping effects. For galega extracts, flavonols, and HCAs, a potent antiradical activity was observed. The ability to trap MGO was noted for guanidines and flavonoids, whereas HCA esters and quinazoline alkaloids were ineffective. The formation of mono-MGO adducts of galegine, hydroxygalegine, and rutin in the examined water infusion was observed.

Keywords: galega; guanidines; flavonoids; phenolic acids; polyphenols; methylglyoxal trapping; antioxidant activity

1. Introduction

Before the development of pharmacological anti-diabetic therapy, traditional medicine was widely used to reduce the symptoms associated with type 2 diabetes (T2D) [1]. Among the over 1000 species of plants used as anti-diabetic agents, *Galega officinalis* L. (*Fabaceae*), also known as galega or goat's rue, deserves some special attention [2]. The flowering aerial parts of galega (*Galegae herba*) were used in the past to alleviate the polyuria associated with long-term hyperglycemia, but also to treat many other conditions from tuberculosis, bubonic plague, and malignant fevers to epilepsy, helminthiasis, and various infectious diseases [3,4]. Moreover, due to its presumed impact on increasing milk yield, galega was used as a galactagogue in humans [5]. At the beginning of the 19th century, it was extensively cultivated as a forage crop in the United States, but in 1986 Keeler et al. [6] reported the clinical symptoms of poisoning in sheep, occurring at doses of about 0.8 g of dried *G. officinalis*

herb per kilogram of body weight per day; thus, its continued use in agriculture has been limited [7]. Despite such toxic potential in high doses, *G. officinalis* is still used to manage the early stages of T2D or as part of its complementary treatment in several countries, including Bulgaria and the United Kingdom, where it is recommended for use in diabetes mellitus by the British Medicine Herbal Association [8,9]. The therapeutic dose of galega herb in humans recommended by Youngken in *A Textbook of Pharmacognosy* [10] is 4 g per day; therefore, it is many times lower than the dose causing toxic effects on animals. Early pharmacological studies showed that *Galegae herba* demonstrates hypoglycemic activity and the glucose-lowering effect has been attributed to the presence of guanidine derivatives, especially galegine and hydroxygalegine, in the raw material [11,12]. Galegine became the basis for the synthesis of metformin (1,1-dimethylbiguanide), commonly used as a first-line drug for monotherapy and combination therapy to manage hyperglycemia in T2D [13]. Research on galegine and its derivatives (guanidines and biguanides) was considered a milestone in the development of oral antidiabetic pharmacotherapy. Other than the ability to reduce hepatic gluconeogenesis, increase insulin sensitivity, and inhibit the absorption of glucose, metformin has also been found to be potentially useful in reducing the risk of diabetic vascular complications [14,15]—in particular, those associated with the accompanying increase in reactive carbonyl species (RCS) plasma levels and both their direct tissue toxicity and indirect toxicity by leading to the formation of harmful advanced glycation and oxidation end products (AGEs and AOPPs, respectively) [15]. Currently, among RCS, methylglyoxal (MGO) is considered as the main precursor of the non-enzymatic glycation and oxidation of proteins, which results in the formation of AGEs and AOPPs [16]. One of the possible mechanisms of action responsible for this preventive effect is lowering the RCS concentration by trapping reactions with specific compounds. Several in vitro and in vivo studies have demonstrated that a reduction in the MGO plasma concentration could be an effective strategy for the direct alleviation of diabetic vascular complications [16–18]. So far, the established biological properties of *G. officinalis* are anti-hyperglycemic [17], antimicrobial [18], and anti-aggregate [19,20]. However, the literature provides little information on the antioxidant properties, and no research has referred to the methylglyoxal trapping capacity of goat's rue extracts. Both of these biological activities may contribute to limiting the damage caused by hyperglycemia in complications of diabetes. According to recent research, *Galegae herba* extracts could be beneficial for the prevention of kidney tissue damage in diabetes [21]. Due to the structural similarity to metformin, the galegine present in *G. officinalis* may demonstrate analogy RCS trapping activity. Moreover, many recent studies have reported that other groups of phytochemicals commonly occurring in plants—e.g., flavonoids and phenolic acids—also scavenge RCS and free radicals such as reactive oxygen species (ROS), which both demonstrate a prominent role in the pathogenesis of endothelial dysfunction related to diabetes mellitus [22,23]

However, although the therapeutic properties of goat's rue have long been recognized and appreciated in traditional medicine, the study of the phytochemical profile of the *G. officinalis* herb has been barely addressed. Previous studies on the composition of this species were focused on seed phytochemistry, mainly concerning amino compounds [24]. The chemical constitution of its polyphenolic fraction has received much less attention.

Therefore, the aim of the study was to determine the comprehensive phytochemical composition of the *G. officinalis* herb and the quantitative analysis of individual polyphenolic and guanidine compounds. Moreover, based on the obtained phytochemical profile of *Galegae herba*, rutin, chlorogenic acid, and galegine were selected to represent various groups of natural compounds in galega (flavonoids, hydroxycinnamic acids, and guanidines, respectively). Since the *G. officinalis* herb has been used in the treatment of diabetes for centuries, we decided to test this plant material and selected representative compounds for MGO trapping capacity and non-enzymatic antioxidative activity to assess whether they have properties potentially useful in the prevention of diabetes vascular complications.

2. Results and Discussion

2.1. Chemical Composition of G. officinalis Extracts

The efficacy of the plant extracts is deemed to rely on the characteristics and activity of their complex chemical components; therefore, a comprehensive analysis of the phytochemical composition of *G. officinalis* herb is crucial in order to understand its potentially beneficial biological mechanisms of action. In the current study, the preliminary UHPLC-ESI-MS analysis indicated a higher content of guanidine and polyphenolic compounds in the hot water extract (infusion) of galega than its aq. methanol extracts. Moreover, the separation of the individual compounds (peaks) was distinctly better in the water extract. The water infusion is also the simplest and most popular pharmaceutical form of medicinal plant preparation and administration. For these reasons, the hot water extract from galega herb was used for further quantitative analysis.

The UHPLC-ESI-MS analysis of *G. officinalis* hot water and aq. methanol extracts led to the detection of 39 compounds. Guanidine derivatives and tricyclic quinazoline alkaloids were identified as nitrogen compounds using positive electrospray ionization. In the negative mode, we revealed—to our best knowledge, for the first time—the presence of hydroxycinnamic acid esters (HCAs) with hexaric acid. Other phenolic acids, as well as their sugar derivatives, were also detected. Moreover, various glycosides of flavonols and flavanonols were recognized in the analyzed *G. officinalis* extracts. Identified or tentatively identified constituents along with their *m/z* (in negative and/or positive ESI-QqTOF-MS), MS/MS fragments, and maxima of UV-Vis adsorption are presented in Table 1. The chemical structures of the selected identified phytoconstituents are shown in Figure 1. Nevertheless, for most detected flavonoids and HCAs, further spectroscopic analyses should be carried out to clarify their chemical structure.

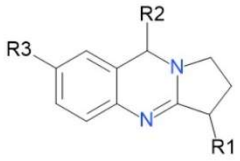

QUINAZOLINE ALKALOIDS	R1	R2	R3
Vasicine	OH	H	H
Vasicinol	OH	H	OH
Vasicine-*O*-hexoside	*O*-hexose	H	H
Vasicinone	OH	=O	H

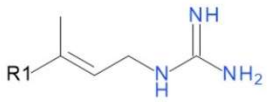

GUANIDINES	R1
Galegine	CH_3
Hydroxygalegine	CH_2-OH

Figure 1. Structures of quinazoline alkaloids and guanidines identified in the *G. officinalis* herb.

Table 1. UHPLC-ESI-MS data of *G. officinalis* herb components in negative and/or positive ion mode.

Peak No.	t_R [min]	λ_{max} [nm]	$[M-H]^-$ (*m/z*) / $[M+H]^+$ (*m/z*)	Error [ppm]	MS/MS (*m/z*)	Identification Proposal
1	0.89	200	209.0309	−1.6	165 $[M-44/CO_2-H]^-$	Hexaric acid
2	1.28	250	191.0203	−1.8	111 $[M-44/CO_2-36/2xH_2O-H]^-$	Hexaric acid monolactone
3	1.49	–	144.1132	−1.2	-	Hydroxygalegine
4	4.32	325	371.0618	0.4	209 $[M-162/caffeoyl-H]^-$, 191 $[209-18/H_2O-H]^-$, 147 $[209-18/H_2O-44/CO_2-H]^-$, 179 $[CA-H]^-$, 135 $[CA-44/CO_2-H]^-$, 129 $[209-44/CO_2-36/2xH_2O-H]^-$, 111 $[209-44/CO_2-54/3xH_2O-H]^-$	Monocaffeoylhexaric acid 1
5	5.48	–	205.0977	−2.9	187 $[M-18/H_2O+H]^+$	Vasicinol
6	7.5	–	128.1185	−2.2	-	Galegine
7	8.34	325	371.0613	1.8	209 $[M-162/caffeoyl-H]^-$, 191 $[209-18/H_2O-H]^-$, 147 $[209-18/H_2O-44/CO_2-H]^-$, 179 $[CA-H]^-$, 135 $[CA-44/CO_2-1I]^-$, 129$[209-44/CO_2-36/2xI_2O-1I]^-$, 111 $[209-44/CO_2-54/3xH_2O-H]^-$	Monocaffeoylhexaric acid 2
8	8.74	206, 285	189.1029	−3.5	171 $[M-18/H_2O+H]^+$, 144 $[M-18/H_2O-27/CHN+H]^+$, 118 $[M-18/H_2O-27/CHN-26/C_2H_2+H]^+$	Vasicine
9	9.49	325	371.0621	−0.1	209 $[M-162/caffeoyl-H]^-$, 191 $[209-18/H_2O-H]^-$, 147 $[209-18/H_2O-44/CO_2-H]^-$, 179 $[CA-H]^-$, 135 $[CA-44/CO_2-H]^-$, 129$[209-44/CO_2-36/2xH_2O-H]^-$, 111 $[209-44/CO_2-54/3xH_2O-H]^-$	Monocaffeoylhexaric acid 3
10	11.84	313	355.0671	0.9	209 $[M-146/coumaroyl-H]^-$, 191 $[209-18/H_2O-H]^-$, 147 $[209-18/H_2O-44/CO_2-H]^-$, 163 $[CuA-H]^-$, 129 $[209-44/CO_2-36/2xH_2O-H]^-$, 119 $[CuA-4/CO_2-H]^-$, 111 $[209-44/CO_2-54/3xH_2O-H]^-$	Monocoumaroylhexaricacid 1
11	11.92	285	285.0617	0.6	152/153 [a] $[M-132/pentose-H]^-$, 108/109 [a] $[PA-44/CO_2-H]^-$	Protocatechuic acid *O*-pentoside
12	12.31	208	351.1565	−0.2	189 $[M-162/hexose+H]^+$, 171 $[M-162/hexose-18/H_2O+H]^+$	Vasicine-*O*-hexoside

Table 1. *Cont.*

Peak No.	t_R [min]	λ_{max} [nm]	[M − H]⁻ (*m*/*z*) / [M + H]⁺ (*m*/*z*)	Error [ppm]	MS/MS (*m*/*z*)	Identification Proposal
13	12.43	325	371.0614	1.6	209 [M − 162/caffeoyl − H]⁻, 191 [209 − 18/H_2O − H]⁻, 147 [209 − 18/H_2O − 44/CO_2 − H]⁻, 179 [CA − H]⁻, 135 [CA − 44/CO_2 − H]⁻, 129[209 − 44/CO_2 − 36/2xH_2O − H]⁻, 111 [209 − 44/CO_2 − 54/3xH_2O − H]⁻	Monocaffeoylhexaric acid 4
14	12.71	314	355.0671	0.4	209 [M − 146/coumaroyl − H]⁻, 191 [209 − 18/H_2O − H]⁻, 147 [209 − 18/H_2O − 44/CO_2 − H]⁻, 163 [CuA–H]⁻, 129 [209 − 44/CO_2 − 36/2xH_2O − H]⁻, 119 [CuA − 44/CO_2 − H]⁻, 111 [209 − 44/CO_2 − 54/3xH_2O − H]⁻	Monocoumaroylhexaricacid 2
15	13.24	325	385.0765	0.9	209 [M − 176/feruloyl − H]⁻, 193 [FeA − 191 − H]⁻, 191 [M − 193 − H or 209 − 18/H_2O − H]⁻, 147 [209 − 18/H_2O − 44/CO_2 − H]⁻, 111 [209 − 44/CO_2 − 54/3xH_2O − H]⁻	Monoferuloylhexaric acid 1
16	14.3	325	385.0775	1.0	209 [M − 176/feruloyl − H]⁻, 193 [FeA − H]⁻, 191 [M − 193 − H or 209 − 18/H_2O − H]⁻, 147 [209 − 18/H_2O − 44/CO_2 − H]⁻, 111 [209 − 44/CO_2 − 54/3xH_2O − H]⁻	Monoferuloylhexaric acid 2
17	14.82	325	385. 0773	0.7	209 [M − 176/feruloyl − H]⁻, 193 [FeA − H]⁻, 191 [M − 193 − H or 209 − 18/H_2O − H]⁻, 149 [194v − 44/CO_2 − H]⁻, 147 [209 − 18/H_2O − 44/CO_2 − H]⁻, 111 [209 − 44/CO_2 − 54/3xH_2O − H]⁻	Monoferuloylhexaric acid 3
18	15.1	315	325.0922	1.5	163 [M − 162/hexose − H]⁻, 119 [CuA − 44/CO_2 − H]⁻	Coumaric acid *O*-hexoside
19	15.12	285	417.1050	−1.6	152/153 [a] [M − 264/2 pentose − H]⁻, 108/109 [a] [PA − 44/CO_2 − H]⁻	Protocatechuic acid *O*-di-pentoside
20	15.21	312	355.0665	1.2	209 [M − 146/coumaroyl − H]⁻, 191 [209 − 146–18/H_2O − H]⁻, 147 [209 − 18 − 44/CO_2 − H]⁻, 163 [CuA − H]⁻, 129 [209 − 44/CO_2 − 36/2xH_2O − H]⁻, 119 [CuA − 44/CO_2 − H]⁻, 111 [209 − 44/CO_2 − 54/3xH_2O − H]⁻	Monocoumaroylhexaricacid 3
21	15.58	211	203.0825	−4.2	185 [M–18/H_2O+H]⁺	Vasicinone
22	16.54	325	385.0753	1.3	209 [M − 176/feruloyl − H]⁻, 193 [385 − 191 − H]⁻, 191 [M − 193 − H]⁻, 147 [191 − 44/CO_2 − H]⁻, 111 [209 − 44/CO_2 − 54/3xH_2O − H]⁻	Monoferuloylhexaric acid 4
23	17.59	325	353.0512	1.8	191 [M − 162/caffeoyl − H]⁻, 179 [CA − H]⁻, 111 [QA − 44/CO_2 − 36/2xH_2O − H]⁻	Chlorogenicacid [S]

Table 1. *Cont.*

Peak No.	t_R [min]	λ_{max} [nm]	$[M-H]^-$ (*m/z*) / $[M+H]^+$ (*m/z*)	Error [ppm]	MS/MS (*m/z*)	Identification Proposal
24	18.39	312	163.0401	−0.1	119 $[M-44/CO_2-H]^-$	*p*-Coumaricacid [S]
25	19.98	290	465.1030	1.8	303 $[M-162/\text{hexose}-H]^-$, 285 $[M-162/\text{hexose}-18/H_2O-H]^-$	Taxifolin-3-*O*-hexoside
26	20.94	254, 354	755.2036	1.2	609 $[M-146/\text{deoxyhexose}-H]^-$, 300/301 [a] $[M-2\times146/\text{dideoxyhexose}-162/\text{hexose}-H]^-$	Quercetin-3-*O*-dideoxyhexosyl–hexoside 1
			757.2224	1.3	611$[M-146/\text{deoxyhexose}+H]^+$, 303 $[M-2\times146/\text{dideoxyhexose}-162/\text{Hexose}+H]^+$	
27	21.06	254, 354	755.2038	0.4	609 $[M-146/\text{deoxyhexose}-H]^-$, 300/301 [a] $[M-2\times146/\text{dideoxyhexose}-162/\text{Hexose}-H]^-$	Quercetin-3-*O*-dideoxyhexosyl-hexoside 2
			757.2215	0.4	465 $[M-2\times146/\text{dideoxyhexose}+H]+$, 303 $[M-2\times146/\text{dideoxyhexose}-162/\text{Hexose}+H]^+$	
28	21.61	265, 344	447.0942	−0.7	285 $[M-162/\text{glucose}-H]^-$	Kaempferol-3-*O*-glucoside (astragalin [S])
29	21.97	265, 344	739.2088	0.5	284/285 [a] $[M-2\times146/\text{dideoxyhexose}-162/\text{hexose}-H]^-$	Kaempferol-3-*O*-dideoxyhexosyl-hexoside 1
30	22.21	265, 344	739.2083	1.0	284/285 [a] $[M-2\times146/\text{dideoxyhexose}-162/\text{hexose}-H]^-$	Kaempferol-3-*O*-dideoxyhexosyl-hexoside 2
31	22.47	255, 353	609.1416	−0.2	300/301 [a] $[M-308/\text{rutinose}-H]^-$	Quercetin-3-*O*-rutinoside (rutin [S])
			611.1634	0,2	303 $[M-308/\text{rutinose}+H]^+$	
32	22.89	255, 353	463.0870	1.8	300/301 [a] $[M-162/\text{galactose}-H]^-$	Quercetin-3-*O*-galactoside (hyperoside [S])
			465.1037	−1.7	303 $[M-162+H/\text{galactose}]^+$	
33	23.32	263, 368	593.1495	3.1	284/285 [a] $[M-308/\text{rutinose}-H]^-$	Kaempferol-3-*O*-deoxyhexosyl-hexoside 1 (nicotiflorin [S])
			595.1681	−3.4	287 $[M-308/\text{rutinose}+H]^+$	
34	24.12	263, 368	593.1505	1.0	284/285 [a] $[M-308/\text{deoxyhexose-hexose}-H]^-$	Kaempferol-3-*O*-deoxyhexosyl-hexoside 2
			595.1683	−3.8	287 $[M-308/\text{deoxyhexose-hexose}+H]^+$	

Table 1. *Cont.*

Peak No.	t_R [min]	λ_{max} [nm]	$[M-H]^-$ (*m*/*z*) / $[M+H]^+$ (*m*/*z*)	Error [ppm]	MS/MS (*m*/*z*)	Identification Proposal
35	24.53	255, 353	623.1608	2.7	315 $[M-308/\text{rutinose}-H]^-$, 300 $[M-308/\text{rutinose}-15/Me^{\bullet}-H]^{-\bullet}$	Isorhamnetin-3-*O*-rutinoside (narcissin [S])
			625.1787	−4.0	317 $[M-308/\text{rutinose}+H]^+$, 300 $[M-308/\text{rutinose}-15/Me^{\bullet}+H]^{+\bullet}$	
36	24.66	254, 348	447.0924	2.9	300/301 [a] $[M-146/\text{rhamnose}-H]^-$	Quercetrin-3-*O*-rhamnoside (quercitrin [S])
37	25.96	255, 353	797.2135	2.5	300/301 [a] $[M-2\times146/\text{dideoxyhexose}-162/\text{hexose}-42/\text{acetyl}-H]^-$	Quercetin-3-*O*-acetyl-dideoxyhexosyl-hexoside
38	26.69	263, 368	431.0973	2.2	284/285 [a] $[M-146/\text{deoxyhexose}-H]^-$	Kaempferol-3-*O*-deoxyhexoside
39	27.13	264, 368	781.2192	−0.1	284/285 [a] $[M-2\times146/\text{dideoxyhexose}-162/\text{hexose}-42/\text{acetyl}-H]^-$	Kaempferol-3-*O*-acetyl-dideoxyhexosyl-hexoside
			783.2373	2.7	287 $[M-2\times146/\text{dideoxyhexose}-162/\text{hexose}-42/\text{acetyl}+H]^+$	

t_R, retention time; λ_{max}, absorbance maximum in UV-Vis spectrum; [a] $[Y0-H]^{-\bullet}/[Y0]^-$; [S] reference standard; CA, caffeic acid; CuA, coumaric acid; FeA, ferulic acid; PA, protocatechuic acid; QA, quinic acid.

2.1.1. Characterization of Quinazoline Alkaloids and Guanidines

UHPLC-ESI-MS analysis in positive electrospray ionization mode allowed us to identify or tentatively identify six nitrogen compounds (Figure 1). Peaks 5, 8, 12, and 21 were classified as tricyclic quinazoline alkaloids, whereas 3 and 6 were assigned as guanidine derivatives. Compound 6 (7.5 min) was identified based on comparison with the authentic reference standard as galegine (*m*/*z* 128). Compound 3 (1.49 min) with a pseudomolecular ion at *m*/*z* 144 corresponded to galegine with a hydroxyl group and was identified as hydroxygalegine. Peaks 8 and 5 with retention times of 8.74 and 5.48 min gave $[M + H]^+$ ions at *m*/*z* 189 and 205. Compound 5 generated a fragment ion at *m*/*z* 187, which indicated the neutral loss of a water molecule $[M - 18 + H]^+$. They were proposed as vasicine (peganine) and hydroxyvasicine (vasicinol), respectively. Their MS/MS fragments were further matched with the literature data [25]. Compound 12 detected at *m*/*z* 351 (12.31 min) was tentatively identified as vasicine-*O*-hexoside. It showed an initial loss of hexose, producing a fragment ion at *m*/*z* 189 $[M - 162 + H]^+$ corresponding to vasicine. Compound 21 showed a base peak $[M + H]^+$ at *m*/*z* 203 and an MS/MS fragment at *m*/*z* 185, which indicated the loss of water. It was tentatively identified as vasicinone based on fragmentation information and data from the literature [26].

2.1.2. Characterization of Phenolic Acids

An analysis of hydroxycinnamic acid (HCAs, t_R at 4.32–18.39 min) and hydroxybenzoic acid (HBAs, 11.92 and 15.12 min) derivatives was carried out in negative electrospray ionization mode. Esters of caffeic, ferulic, and *p*-coumaric acids with hexaric acid (aldaric acid) were recognized as predominant HCAs (Figures 2 and 3). Free hexaric acid and its monolactone were also identified as peaks 1 and 2 with *m*/*z* 209 and 191. Four compounds, 4, 7, 9, and 13, with retention times of 4.32, 8.34, 9.49, and 12.43 min, and *m*/*z* 371, were tentatively identified as monocaffeoylhexaric acid isomers, based on the presence of a fragment ion at *m*/*z* 209 which indicates a neutral loss of a caffeoyl moiety $[M - 162 - H]^-$. All monocaffeoylhexaric acids also represented MS/MS fragments derived from hexaric acid at *m*/*z* 191, 147, 129, and 111 due to the neutral loss of a water molecule $[209 - 18 - H]^-$, CO_2 and a water molecule $[209 - 44 - 18 - H]^-$, CO_2 and two H_2O molecules $[209 - 44 - 36 - H]^-$, and CO_2 and three H_2O molecules $[209 - 44 - 54 - H]^-$, respectively, as well as fragments at *m*/*z* 179 and 135, which suggest the occurrence of a caffeic acid residue $[CA - H]^-$ and its decarboxylated structure $[CA - 44 - H]^-$. Compounds 10, 14, and 20 (t_R at 11.84, 12.71, 15.21 min) with *m*/*z* 355 were tentatively identified as three isomers of monocoumaroylhexaric acid (most likely esters of *p*-coumaric acid, pCuA was confirmed as a free acid). All these esters produced fragment ions at *m*/*z* 209, corresponding to a neutral loss of a coumaroyl moiety $[M - 146 - H]^-$ and *m*/*z* 163 and 119, which indicated the presence of a coumaric acid residue $[CuA - H]^-$ and its decarboxylated form $[CuA - 44 - H]^-$. Peaks 15, 16, 17, and 22 (t_R at 13.24, 14.3, 14.82, 16.54 min) with pseudomolecular ions of 385 Da were assigned as four monoferuloylhexaric acids. They were tentatively identified based on the occurrence of fragments at *m*/*z* 209 resulting from a neutral loss of a feruloyl moiety $[M - 176 - H]^-$. Both monocoumaroylhexaric and monoferuloylhexaric acid isomers have shown further fragmentation patterns similar to the monocaffeoylhexaric acids mentioned above. Compounds 23 and 24 (17.59 and 18.39 min) were identified as chlorogenic and *p*-coumaric acid, respectively, based on comparison with authentic standards. Compounds 11 and 19 (11.92 and 15.12 min) with $[M - H]^-$ ions at *m*/*z* 285 and 417 were tentatively identified as protocatechuic acid *O*-pentoside and *O*-dipentoside. They produced a radical aglycone ion $[Y_0 - H]^{-\bullet}$ at *m*/*z* 152 and 108, as well as an aglycone fragment ion at *m*/*z* 153 and 109 (by the homolytic and heterolytic fission of precursor ions) [27], corresponding to a protocatechuic acid residue after the neutral loss of pentose or dipentose followed by decarboxylation. Similarly, compound 18 (15.1 min) was assigned as coumaric acid *O*-hexoside, exhibiting a deprotonated ion at *m*/*z* 325. It also presented an MS/MS fragment at *m*/*z* 163, which suggests a neutral loss of hexose, and a fragment at *m*/*z* 119, corresponding to coumaric acid after the loss of hexose followed by the loss of CO_2.

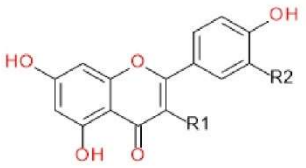

FLAVONOLS	R1	R2
Kaempferol	OH	H
Astragalin	*O*-β-glc	H
Kaempferin	*O*-α-rha	H
Nicotiflorin	*O*-α-rha(1→6)-β-glc	H
Kaempferol-3-*O*-robinoside	*O*-α-rha(1→6)-β-gal	H
Clitorin	*O*-[α-rha(1→2)][α-rha(1→6)]-β-glc	H
Mauritianin	*O*-[α-rha(1→2)][α-rha(1→6)]-β-gal	H
Kaempferol-3-*O*-(4″-acetyl-2″-α-rhamnosyl)-robinoside	*O*-[4-*O*-acetyl-α-rha(1→2)][α-rha(1→6)]-β-gal	H
Quercetin	OH	OH
Hyperoside	*O*-β-gal	OH
Quercitrin	*O*-α-rha	OH
Rutin	*O*-α-rha(1→6)-β-glc	OH
Quercetin-3-*O*-(2″-α-rhamnosyl)-rutinoside	*O*-[α-rha(1→2)][α-rha(1→6)]-β-glc	OH
Quercetin-3-*O*-(2″-α-rhamnosyl)-robinoside	*O*-[α-rha(1→2)][α-rha(1→6)]-β-gal	OH
Quercetin-3-*O*-(4″-acetyl-2″-α-rhamnosyl)-robinoside	*O*-[4-*O*-acetyl-α-rha(1→2)][α-rha(1→6)]-β-gal	OH
Isorhamnetin	OH	OCH_3
Narcissin	*O*-α-rha(1→6)-β-glc	OCH_3

glc, glucose; gal, galactose; rha, rhamnose.

HCA and HEXARIC ACID ESTERS	R1/R2/R3/R4
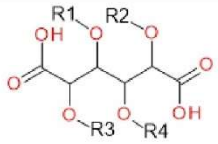	*p*-Coumaroyl
	Caffeoyl
	Feruloyl

Figure 2. Structures of the flavonols and HCAs identified in the *G. officinalis* herb.

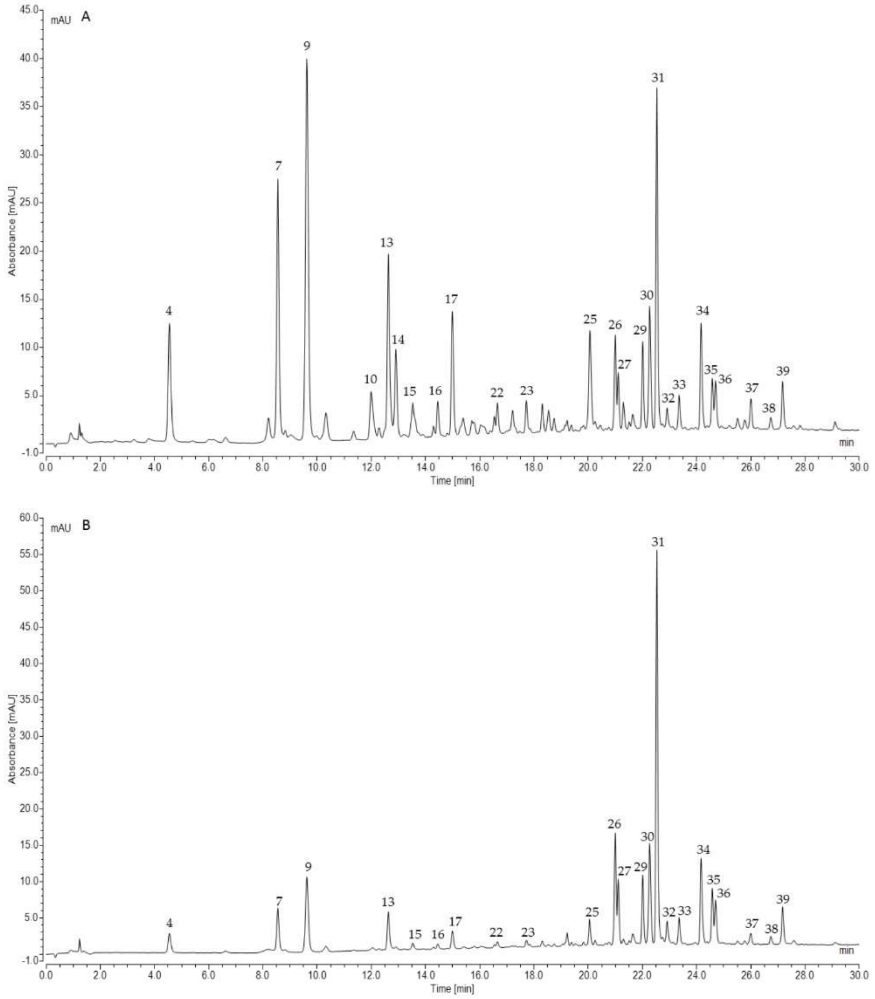

Figure 3. Representative UHPLC chromatograms of *G. officinalis* water infusion at 320 nm (**A**) and 360 nm (**B**).

2.1.3. Characterization of Flavonoids

Mono-, di- and triglycosylated flavonols and flavanonols were characterized based on their UV-Vis (200–600 nm) and MS spectra (in the negative and positive ion mode), and, in some cases, by comparison with authentic standards (t_R). Depending on the structure, the CID of deprotonated flavonoid glycosides produced both radical aglycone and aglycone fragments. In the negative ion mode for flavonols, both homolytic and heterolytic fission was observed under the MS/MS conditions used. In the case of kaempferol glycosides, homolytic fission led to a radical aglycone anion $[Y_0 - H]^{-\bullet}$ at *m*/*z* 284, while heterolytic fission resulted in an anaglycone fragment $[Y_0]^-$ at *m*/*z* 285. Similar fragmentation behavior was found for quercetin derivatives (*m*/*z* 300 and 301) (**1**).

The relative abundance of the radical aglycone to the aglycone product ion was found to be dependent on the collision energy as well as the structure of the aglycone and glycone parts. A relative increase in the radical aglycone product ion formation at a higher collision energy was observed by Hvattum and Ekeberg [28], Cuyckens and Claeys [29], and Davis and Brodbelt [30]. For the reference flavonols, including kaempferol-3-*O*-rutinoside (nicotiflorin), kaempferol-7-*O*-neohesperidoside, quercetin-3-*O*-rutinoside (rutin), quercetin-3-*O*-β-glucoside (isoquercitrin), quercetin-3-*O*-β-galactoside (hyperoside), and quercetin-3-*O*-α-rhamnoside (quercitrin), the collision energy of 20 eV resulted primarily in the formation of aglycone fragment $[Y_0]^-$, whereas a collision energy of 40 eV or higher led to the occurrence of the radical aglycone anion $[Y_0 - H]^{-\bullet}$ [28]. The position of the glycone substitution also affected the fragmentation of the flavonol glycosides. The radical aglycone ions were very abundant for flavonols substituted at C-3. In addition, the ratio $[Y_0 - H]^{-\bullet}$: $[Y_0]^-$ allows the differentiation between flavonol-3-*O*- and -7-*O*-glycosides and can be used in the identification of unknown compounds [29].

The UHPLC-ESI-MS analysis of flavonoids in the negative electrospray ionization mode led us to the identification or tentative identification of fifteen compounds eluted between 19.98 and 27.13 min (Table 1, Figures 2 and 3). Most of the detected flavonoids were *O*-glycosides of flavonols (kaempferol, quercetin, isorhamnetin). We identified seven kaempferol glycosides (28, 29, 30, 33, 34, 38 and 39), six quercetin glycosides (26, 27, 31, 32, 36, and 37), and only one isorhamnetin derivative (35). Moreover, one flavanonol (taxifolin glycoside, 25) was observed. Glucose, galactose, and rhamnose were connected to aglycones as mono-, di-, or trisaccharides.

Peak 25 (19.98 min) with *m/z* 465 was proposed as taxifolin-3-*O*-hexoside, based on the presence of a fragment ion at *m/z* 303 $[M - 162 - H]^-$, indicating a neutral loss of hexose, and 285 $[M - 162 - 18 - H]^-$ after the loss of a water molecule, as well as its characteristic UV-Vis spectrum with λ_{max} at 227 and 289 nm. Compounds 26 and 27 with retention times of 20.49 and 21.06 min and *m/z* 755 were proposed as quercetin-3-*O*-dideoxyhexosyl-hexoside isomers. These compounds produced weak MS/MS fragments at *m/z* 609 $[M - 146 - H]^-$ and base ions at *m/z* 300/301 corresponding to quercetin, which indicated the successive loss of deoxyhexose and disaccharide composed of deoxyhexose and hexose units, from the C-3 position of aglycone. The λ_{max} in their UV-Vis spectrum at 254 and 354 nm confirmed that observation. Champavier et al. [31] previously isolated from *G. officinalis* and elucidated the triglycosidic structure of quercetin-3-*O*-[α-rhamnosyl-(1→2)][α-rhamnosyl-(1→6)]-β-glucoside (quercetin-3-*O*-(2''-α-rhamnosyl)-rutinoside). The same compound and its isomer with β-galactose in place of β-glucose were identified by Hirose et al. [31] in quinoa seeds (*Chenopodium quinoa* Willd.). Therefore, 26 and 27 were carefully characterized as quercetin-3-*O*-[α-rhamnosyl-(1→2)][α-rhamnosyl -(1→6)]-β-glucoside or quercetin-3-*O*-[α-rhamnosyl-(1→2)][α-rhamnosyl-(1→6)]-galactoside (quercetin-3-*O*-(2''-α-rhamnosyl)-robinoside). Other quercetin derivatives, compounds 31, 32, and 36 with $[M - H]^-$ at 609, 463, and 447,were identified as rutin, hyperoside, and quercitrin based on a comparison with authentic standards and base ions at *m/z* 300/301, corresponding to aglycone after the loss of a glycosyl group from C-3.

Compounds 29 and 30 (21.97 and 22.21 min) with *m/z* at 739 produced the MS/MS fragment at 284/285 corresponding to kaempferol and suggested the loss of two deoxyhexoses and one hexose from the glycone part $[M - 146 - 146 - 162 - H]^-$. The λ_{max} in their UV-Vis spectrum at 265 and 344 nm confirmed the aglycone structure. These compounds were proposed as kaempferol-3-*O*-dideoxyhexosyl-hexoside isomers, probably with a branched triglycoside at C-3 exactly as in 26 and 27. Thus, 29 and 30 were tentatively recognized as kaepferol-3-*O*-[α-rhamnosyl-(1→2)][α-rhamnosyl-(1→6)]-β-galactoside (mauritianin) or kaempferol-3-*O*-[α-rhamnosyl-(1→2)][α-rhamnosyl-(1→6)]-β-glucoside (clitorin). Mauritianin was previously isolated from galega herb by Champavier et al. [31]. Both these triglycosides were also separated from the aerial parts of *Acalypha indica* L. [32] and *Salvadora persica* L. [33]. Two next compounds, 33 and 34 at t_R 23.32 and 24.12 min with *m/z* 593, showed the same fragmentation patterns. Their MS/MS spectra revealed ions corresponding to kaempferol released after the neutral loss of disaccharide $[M - 146 - 162 - H]^-$ composed of deoxyhexose

and hexose (probably rhamnose and glucose or galactose). Therefore, they were suggested to be kaempferol-3-*O*-rutinoside (nicotiflorin) after comparison with the authentic standard, and kaempferol-3-*O*-robinoside (kaempferol-3-*O*-robinobioside), respectively. Compounds 28 and 38 (21.61 and 26.69 min) exhibited $[M - H]^-$ ions at *m*/*z* 447 and 431, and the same strong fragment related to the base ion at *m*/*z* 285. The loss of 162 Da from the pseudomolecular ion was related to hexose; therefore, compound 28 was assigned by comparison with the reference standard as astragalin. Compound 38 demonstrated the loss of deoxyhexose $[M - 146 - H]^-$ and was initially elucidated as kaempferol-3-*O*-α-rhamnoside (kaempferin). Peak 35 (24.53 min) showed a pseudomolecular ion at *m*/*z* 623 and MS/MS fragments with 315 and 300 Da (after the cleavage of the methyl radical). The data suggest that 35 would be identified as isorhamnetin-*O*-deoxyhexosyl-hexoside, and comparison with the authentic standard confirmed identification of isorhamnetin-3-*O*-rutinoside (narcissin). Compound 39 with a pseudomolecular ion at *m*/*z* 781 and a retention time of 27.13 min displayed the MS/MS fragment at 284/285, which suggested the presence of kaempferol aglycone substituted in position C-3. Owing to the absence of pure standards, the literature data were diagnostic. Champavier et al. [34] reported the presence of characteristic acetyl triglycoside in *G. officinalis*. After comparison with data from this study, we identified compound 39 as kaempferol-3-*O*-[4-*O*-acetyl-α-rhamnosyl(1→2)][α-rhamnosyl(1→6)]-β-galactoside (kaempferol-3-*O*-(4′′-acetyl-2′′-α-rhamnosyl)-robinoside). Peak 37 exhibited a deprotonated molecule at *m*/*z* 797 and produced a fragment ion at *m*/*z* 300/301, which indicated quercetin being aglycon. Based on the above-mentioned study, analogously to compound 39 we tentatively assigned 37 as quercetin-3-*O*-[4-*O*-acetyl-α-rhamnosyl (1→2)][α-rhamnosyl(1→6)]-β-galactoside (quercetin-3-*O*-(4′′-acetyl-2′′-α-rhamnosyl)-robinoside) or its analog with glucose.

Previous phytochemical research reported that, apart from guanidine derivatives, galega is a rich source of polyphenols, saponins (derivatives of soybean sapogenols, characteristic of the *Fabaceae* family), and alkaloids—mostly quinazoline alkaloids, such as vasicine and vasicinone. Allantoin, medicagol, its methyl ester, and norterpenoid glucoside were isolated from the aerial parts of *G. officinalis* [34]. Terpenes, steroids, tannins, and flavonoids were also found in this plant [35]. The results of the HPLC study by Barchuk et al. [36] revealed the occurrence of 48 phenolic compounds in aq. alcoholic extracts from the galega herb, amongst which only seven polyphenolic compounds were identified: caffeic acid, ferulic acid, cichoric acid, rutin, quercetin, hyperoside, and apigenin. These results are somewhat in agreement with our study. We confirmed the presence of hyperoside and rutin. Quercetin was observed only in the form of glycosides, but caffeic and ferulic acids were observed in the ester forms.

2.2. Quantification of Polyphenols and Guanidines

Before the quantitative analysis, the identification of the compounds present in galega extracts was carried out using the UHPLC-ESI-MS method in the negative and positive electrospray ionization modes. The polyphenolic components detected in *G. officinalis* were classified into two main groups based on structural identification: flavonoids and hydroxycinnamic acids (HCAs). Hence, the individual 24 polyphenolic components in the *Galegae herba* water infusion were quantified by using the authentic standards or corresponding standards for calibration for each group (e.g., rutin as an external reference standard for tentatively identified flavonoids and the respective phenolic acid—caffeic, ferulic, or *p*-coumaric acid for HCAs). Flavonoids and HCAs were quantified by the UHPLC-DAD method, whereas guanidines were quantified by UHPLC-ESI-MS using the same chromatographic conditions and a positive ion mode. The results of chromatographic method validation for authentic and corresponding standards, of which the calibration curves exhibited good linearity at 360, 320, and 280 nm ($R^2 = 0.9999$) are shown in Table 5 (method section). The results from the quantification are summarized in Table 2. Each individual component was expressed as the mg per 1 g of dried herb ± standard deviation (SD).

Table 2. Quantification of polyphenolics and guanidines in water infusions (drug extract ratio, 1:50) from three different batches of *G. officinalis* (Gof1-Gof3), expressed as mg per 1 g of dried plant material.

Compound	t_R [min]	Gof1	Gof2	Gof3	Average
		Content [mg/g] of DW			
Flavonoids					
Taxifolin-3-*O*-hexoside (**25**) [a]	19.98	1.67 ± 0.20	0.26 ± 0.01	0.03 ± 0.00	0.68 ± 0.65
Quercetin-derivative (**26**) [b]	20.94	0.59 ± 0.01	0.91 ± 0.02	0.74 ± 0.03	0.75 ± 0.13
Quercetin-derivative (**27**) [b]	21.06	0.32 ± 0.01	0.47 ± 0.01	0.32 ± 0.01	0.37 ± 0.07
Clitorin (**29**) [b]	21.97	0.32 ± 0.01	0.47 ± 0.01	0.28 ± 0.02	0.35 ± 0.08
Mauritianin (**30**) [b]	22.21	0.67 ± 0.01	0.82 ± 0.02	0.47 ± 0.01	0.65 ± 0.15
Rutin (**31**)	22.47	1.70 ± 0.04	3.31 ± 0.07	2.17 ± 0.08	2.43 ± 0.69
Hyperoside (**32**)	22.89	0.08 ± 0.01	0.20 ± 0.01	0.10 ± 0.01	0.13 ± 0.05
Nicotiflorin (**33**) [b]	23.32	0.14 ±0.01	0.20 ± 0.00	0.13 ± 0.01	0.15 ± 0.03
Kaempferol-3-*O*-robinoside (**34**) [b]	24.12	0.39 ± 0.19	0.65 ± 0.01	0.44 ± 0.04	0,49 ± 0.06
Narissin (**35**) [b]	24.53	0.23 ± 0.01	0.35 ± 0.01	0.13 ± 0.01	0.24 ± 0.09
Quercitrin (**36**) [b]	24.66	0.13 ± 0,01	0.44 ± 0.02	0.02 ± 0.01	0.20 ± 0.19
Kaempferol-derivative (**39**) [b]	27.13	0.20 ±0.01	0.26 ± 0.01	0.14 ± 0.01	0.19 ± 0.05
Sum of flavonoids		6.44 ± 0.52	8.34 ± 0.20	4.97 ± 0.24	6.63 ± 2.24
Hydroxycinnamic acids					
Monocaffeoylhexaric acid isomer 1 (**4**) [c]	4.32	0.39 ± 0.03	0.57 ± 0.02	0.59 ± 0.03	0.52 ± 0.09
Monocaffeoylhexaric acid isomer 2 (**7**) [c]	8.34	0.75 ± 0.02	1.05 ± 0.04	1.02 ± 0.03	0.95 ± 0.14
Monocaffeoylhexaric acid isomer 3 (**9**) [c]	9.49	1.12 ± 0.05	1.58 ± 0.05	1.64 ± 0.22	1.46 ± 0.26
Monocaffeoylhexaric acid isomer 4 (**13**) [c]	12.43	0.38 ±0.03	0.49 ± 0.02	0.48 ± 0.02	0.46 ± 0.05
Monocoumaroylhexaric acid isomer 1 (**10**) [d]	11.84	0.20 ± 0.03	0.20 ± 0.01	0.27 ± 0.01	0.22 ± 0.03
Monocoumaroylhexaric acid isomer 2 (**14**) [d]	12.71	0.35 ± 0.03	0.47 ± 0.04	0.36 ± 0.01	0.39 ± 0.06
Monoferuloylhexaric acid isomer 1 (**15**) [e]	13.24	0.20 ±0.01	0.25 ± 0.01	0.25 ± 0.01	0.23 ± 0.02
Monoferuloylhexaric acid isomer 2 (**16**) [e]	14.30	0.12 ± 0.01	0.14 ± 0.01	0.16 ± 0.01	0.14 ± 0.01
Monoferuloylhexaric acid isomer 3 (**17**) [e]	14.82	0.32 ± 0.02	0.45 ± 0.06	0.47 ± 0.02	0.42 ± 0.07
Monocoumaroylhexaric acid isomer 3 (**20**) [d]	15.21	0.09 ± 0.01	0.07 ± 0.01	0.12 ± 0.03	0.09 ± 0.02
Monoferuloylhexaric acid isomer 4 (**22**) [e]	16.54	0.06 ± 0.01	0.06 ± 0.01	0.06 ± 0.01	0.06 ± 0.01
Chlorogenic acid (**23**)	17.59	0.09 ± 0.01	0.12 ± 0.01	0.10 ± 0.01	0.10 ± 0.01
Sum of hydroxycinnamic acids		4.27 ± 0.26	5.45 ± 0.29	5.53 ± 0.41	5.04 ± 0.77
Sum of polyphenols		10.71 ± 0.78	13.79 ± 0.49	10.5 ± 0.65	11.67 ± 3.01
Guanidines					
Hydroxygalegine (**3**) [f]	1.49	1.98 ± 0.03	1.11 ± 0.06	1.95 ± 0.04	1.68 ± 0.12
Galegine (**6**)	7.50	4.28 ± 0.04	9.38 ± 0.40	6.08 ± 0.17	6.58 ± 0.61
Sum of guanidines		6.26 ± 0.07	10.49 ± 0.46	8.03 ± 0.21	8.26 ± 0.73

[a] quantified as taxifolin; [b] as rutin; [c] as caffeic acid; [d] as *p*-coumaric acid; [e] as ferulic acid; [f] as galegine; DW, dry weight; all reported values (mg/g) are means of three samples in two measurements ($n = 3 \times 2$).

Our study revealed that the predominant flavonoid compound presented in the examined batches was rutin, with the concentration of 1.7–3.3 mg/g DW (on average 2.43 mg/g), followed by quercetin-derivative (26), taxifolin-3-*O*-hexoside (25), and mauritianin or clitorin (peaks 29 or 30) with average concentrations of 0.75, 0.68, and 0.65 mg/g DW, respectively. Taxifolin-3-*O*-hexoside was present at a very varied level between the individual batches of the product, and the highest concentration was assessed in Gof1, up to 1.7 mg/g DW. Among the analyzed HCAs, monocaffeoylhexaric acid isomer 3 (peak 9) was the major component, with a concentration of up to 1.64 mg/g DW (on average 1.46 mg/g). The average content of the other isomers of monocaffeoylhexaric acids 1,2,4 (peaks 4, 7, 13) were 0.52, 0.95, and 0.46 mg/g DW, respectively. Monocoumaroylhexaric and monoferuloylhexaric acid isomers were quantified as minor components below 0.45 mg/g DW. The mean flavonoid sum in the analyzed samples was calculated as 6.63 mg/g DW. The average sums of HCAs and all the quantified polyphenols were 5.04 and 11.67 mg/g DW, respectively. The batch assigned as Gof2 had the highest sums of flavonoids and polyphenols, while the lowest values were observed in Gof3.

Since guanidine derivatives cannot be quantified using DAD, we decided to quantify the content of galegine and hydroxygalegine by UHPLC-ESI-MS using the chromatographic conditions described in paragraph 1.4 (method section). Galegine sulfate was used as an external standard for linear

regression analysis (Table 5). Galegine was present in Galegae herba at the mean concentration of 6.57 mg/g DW. Its highest content was assessed in Gof2 and was 9.37 mg/g DW, while the lowest was in Gof1 and was 4.27 mg/g DW. The average concentration of hydroxygalegine was several times lower, at −1.51 mg/g DW. The highest concentration of hydroxygalegine was observed in Gof1 (1.98 mg/g DW). The mean sum of guanidines in the analyzed samples was calculated as 8.08 mg/g DW. A study of Oldham et al. [24] indicated that the galegine content varied over the plant tissues and growth stages. The highest level of this compound was observed for reproductive tissues (6.32–8.53 mg/g, on average 7.35 mg/g DW), followed by leaves (2.8–6.22 mg/g, on average 4.25 mg/g DW) and the stem (1.27–1.85 mg/g, on average 1.44 mg/g DW). The examined *G. officinalis* herb consists of flowering aerial parts, which explains the relatively high average concentration of galegine.

Therefore, based on the above results, the average daily dose of galega (4 g) recommended for therapeutic purposes contains ~32 mg of guanidines and 47 mg of polyphenols, including about 26 mg of flavonoids and 20 mg of HCAs.

2.3. In Vitro Studies

Many studies suggest that late diabetic complications arise from the reactive carbonyl species' (especially by MGO) induced formation and generation of advanced glycation end products (AGEs) [37,38]. Glycation is usually accompanied by the process of protein oxidation, and when they occur simultaneously, interacting and intensifying each other's adverse effects, they are referred to as glycoxidation processes. In addition to AGEs, analogously advanced oxidation protein products (AOPPs) are created [23,39]. There is no doubt a link between oxidative stress, reactive carbonyl species generation, and the development of diabetic complications. Compounds from various chemical groups may reduce both the in vitro and in vivo non-enzymatic glycation and oxidation of proteins by, among other means, trapping RCS or by acting as scavengers of ROS. Therefore, the MGO trapping capacity and antioxidant activity may contribute to limiting the damage from glycation and oxidation reactions and to complementing existing therapy for the treatment of T2D and its vascular complications.

2.3.1. Non-Enzymatic Antioxidant Activity

The DPPH and ABTS assays are frequently used methods for the evaluation of the antioxidant capacities of natural products; both are spectrophotometric techniques based on the quenching of stable radicals [40–42]. In the current study, hot water and aq. methanol extracts of *Galegae herba*, and individual standard compounds, were assessed for antioxidant activity using the above-mentioned methods. Table 3 shows the values of antioxidant activity expressed as the percent of inhibition and the concentration required for a 50% reduction in the radicals (IC50, μg/mL; μM) obtained for the tested samples. Standard compounds were selected based on the phytochemical study—rutin, chlorogenic acid, and galegine sulfate were used as model compounds from three different chemical groups (flavonoids, HCA esters, and guanidines). Quercetin was chosen due to the well-known antiradical and antioxidative action, and metformin hydrochloride in order to verify whether the compound with a galegine-like structure, used as the drug of choice in the treatment of T2D, possesses similar properties. The antiradical activity of the extracts and selected substances was compared to the effects of gallic acid (DPPH) and Trolox (ABTS). The IC50 values of the galega extracts were calculated from the mean sum of the polyphenols quantified in *G. officinalis*.

Table 3. Antioxidant activity of the *G. officinalis* extracts and selected standard compounds.

Sample	DPPH			ABTS		
	IC50 [μg/mL]	IC50 [μM]	% of Inhibition [a]	IC50 [μg/mL]	IC50 [μM]	% of Inhibition [b]
Aq. methanol (1:1) [c]	11.72 [d]	-	73.00	0.94 [d]	-	85.31
Water infusion [c]	12.97 [d]	-	68.80	1.06 [d]	-	82.34
Chlorogenic acid	27.60	77.90	33.08	2.62	7.41	37.00
Rutin	22.29	36.51	42.91	4.07	6.66	31.02
Quercetin	8.49	28.08	91.76	1.25	4.13	87.14
Galegine sulfate	1656.07	13,020.31	0.90	42.52	334.32	0
Metformin hydrochloride	0	0	0	0	0	0
Gallic acid	2.93	17.25	>100	-	-	-
Trolox	-	-	-	1.48	5.90	61.37

Values are mean triplicate (n = 3); [a] calculated for final concentration 18 μg/mL; [b] calculated for final concentration 2 μg/mL; [c] extracts from galega herb (DER 1:50); [d] calculated from the mean sum of polyphenols.

In the current study, both the *G. officinalis* hot water and aq. methanol (1:1) extracts were effective in scavenging DPPH and ABTS radicals, and even more productive than rutin, chlorogenic acid, and trolox. The percentage inhibition of radicals was concentration-dependent and ranged from 3.14% to 75.48% in the DPPH assay and from 10.92% to 87.76% in the ABTS assay for the water infusion, and from 6.78% to 77.16% in DPPH and from 13.57% to 87.85% in ABTS for the aq. methanol extract (both diluted 1–16×). The obtained results are comparable with the previous report by Shymanska et al. [43] of the antioxidant activity of *G. officinalis* leaves, expressed as values of percentage DPPH radical inhibition in the range of 70.4% to 79.7% for methanolic and 54.6% to 66.8% for aqueous extracts.

The IC50 values of the tested hot water and aq. methanol extracts (calculated for the mean sum of galega polyphenols) were almost identical −12.97 and 11.72 μg/mL in the DPPH method and 1.06 and 0.94 μg/mL in the ABTS assay. The IC50 determined for quercetin in both methods was at a similar level (8.49 and 1.25 μg/mL), which may suggest that the *Galegae herba* antioxidant activity is dependent mainly on the presence of quercetin derivatives. Galegine sulfate showed the lowest inhibitory effect (up 9.49% in ABTS for 9.9 μg/mL), and metformin hydrochloride did not show any antiradical effect under the conditions of the experiment. The IC50 value of the gallic acid standard used as a positive control in the DPPH assay was 2.93 μg/mL (17.25 μM), and trolox, being a positive control in the ABTS test, showed IC50 at 1.48 μg/mL (5.9 μM).

Taking into account the IC50 values expressed in micromolar concentration, the antiradical activity for the individual compounds is arranged in the following order for the DPPH test: gallic acid > quercetin > rutin > chlorogenic acid >>> galegine sulfate. For the ABTS test, the activity is as follows: quercetin > trolox > rutin > chlorogenic acid >>> galegine sulfate.

Though metformin showed no antiradical action related to electron transfer (DPPH, ABTS assays), some studies report their chelating properties, which may inhibit the metal-catalyzed oxidation reactions that form AGEs [44]. The values of % inhibition calculated for both hot water and methanol extracts (at the concentration of 18 mg/mL in DPPH and 2 mg/mL in ABTS) showed a higher inhibitory activity than rutin and chlorogenic acid but lower than quercetin. This may suggest that the antiradical activity of *G. officinalis* is based not only on polyphenolic compounds. The phytochemical analysis of galega extracts indicated the presence of tricyclic quinazoline alkaloids, which, according to recent research, possess a strong antiradical activity [45] and may contribute to the antioxidative potential of *Galegae herba*. Synergism between the identified components of the test extracts can also be assumed.

2.3.2. Methylglyoxal Trapping Capacity

The MGO trapping test was carried out under the simulated physiological conditions for the freshly prepared hot water extract of *Galegae herba* and standards selected to represent different chemical groups of compounds in the analyzed plant material (rutin, chlorogenic acid and galegine sulfate).

As a positive control, quercetin and metformin hydrochloride were used [38,39]. The reaction products were further analyzed with UHPLC-ESI-MS to detect the structure modification of compounds with an MGO trapping potential. Pseudomolecular ions higher by 72 Da in the case of mono-MGO adducts and by 144 Da for di-MGO adducts were searched using the Extract Ion Chromatogram (EIC) function. Phenolic compounds were tested in the negative ion mode, and the guanidine derivatives in the positive mode. Table 4 contains test results for individual compounds and for *G. officinalis* water infusion. Generally, the in vitro study revealed that *G. officinalis* showed MGO trapping activity—some of its components were observed to form adducts with methylglyoxal. Among the tested compounds, rutin, quercetin, galegine sulfate, and metformin hydrochloride exhibited the ability to trap MGO, but trapping activity was not observed for chlorogenic acid. Methylglyoxal reacted with components of *Galegae herba* water infusion—rutin, galegine, and hydroxygalegine. After a 1 h of incubation of the extract with MGO, there were observed two product peaks in positive and one product peak in negative UHPLC-ESI-MS chromatograms. In positive mode, the first peak appeared at 0.98 min with the pseudomolecular ion $[M + H]^+$ at *m/z* 216, and the second at 2.61 min with *m/z* 200, as well as their fragment ions at *m/z* 144 and 128 $[M - 72 + H]^+$, respectively indicating the loss of one MGO molecule (−72 Da) by MS/MS fission. This suggested that the products were mono-MGO conjugates of hydroxygalegine and galegine. In the negative mode, the product peak observed at 8.84 min characterized the pseudomolecular ion at *m/z* 681 $[M - H]^-$ and corresponded to the molecule of the mono-MGO adduct of rutin. The peak was 72 mass units higher than that of rutin (*m/z* 609).

Table 4. Methylglyoxal adducts detected in the reaction mixture of standard compounds and water infusion of *G. officinalis* after 1 h incubation with MGO. Quercetin and metformin hydrochloride were used as a positive control.

Compound	Source	Peak	Mono-MGO Adduct (*m/z*)	di-MGO Adduct (*m/z*)
Chlorogenic acid	S	-	n.d.	n.d.
Rutin	S	a	681.1682 $[M - H]^-$	753.1892 $[M - H]^-$
		b	681.1695 $[M - H]^-$	753.1890 $[M - H]^-$
		c	681.1683 $[M - H]^-$	753.1885 $[M - H]^-$
	Inf	a	681.1684 $[M - H]^-$	n.d.
Quercetin	S	a	373.0569 $[M - H]^-$	445.0779 $[M - H]^-$
		b	373.0564 $[M - H]^-$	n.d.
Galegine sulfate	S	a	200.1367 $[M + H]^+$	n.d.
		b	200.1364 $[M + H]^+$	n.d.
		c	200.1364 $[M + H]^+$	n.d.
Galegine	Inf	a	200.1397 $[M + H]^+$	n.d.
		b	200.1386 $[M + H]^+$	n.d.
		c	200.1388 $[M + H]^+$	n.d.
Hydroxygalegine	Inf	a	216.1334 $[M + H]^+$	n.d.
Metformin hydrochloride	S	a	202.1282 $[M + H]^+$	n.d.

S: standard compound; Inf, water infusion; n.d.: not detected.

Moreover, an additional analysis (using EIC) allowed us to observe several slight signals of deprotonated molecules $[M - H]^-$ at *m/z* 537.1852 and 537.1832 (t_R 8.38 and 8.41 min); 827.1950 and 827.1821 (t_R 7.93 and 8.18 min); and 665.1476, 665.1490, and 665.1513 (t_R 8.97,9.04 and 9.10 min), which corresponded to the adducts of other flavonoids identified in *G. officinalis*, such as taxifolin-3-*O*-hexoside, quercetin-derivatives 26 or 27, and kaempferol-derivatives 33 or 34, respectively

(increased by 72 Da). This suggests the presence of their mono-MGO adducts in the extract. The same method allowed us to identify three galegine mono-MGO adducts (t_R 1.41, 2.28, and 2.61 min). The first adduct was dominating, while the others were several times smaller. For hydroxygalegine, only one mono-adduct was observed. A similar phenomenon was noted for standards used in the analysis of model mixtures. Rutin, when tested individually, was observed to form three methylglyoxal mono-adducts with $[M - H]^-$ at *m*/*z* 681.1682, 681.1695, 681.1683 (t_R 8.54, 8.7, 8.82 min), and three di-adducts at *m*/*z* 753.1892, 753.1890, 753.1885 (t_R 7.97, 8.24, 8.45 min). Similarly, quercetin was able not only to form mono-adducts (t_R 10.93 and 11.06 min), but also the di-adduct with MGO, as shown in Table 4. A study of Bhuiyan et al. [46] suggests that several isomeric forms and diastereoisomers of flavonoid-methylglyoxal adducts may be formed under reaction conditions. In the tested *G. officinalis* hot water extract, the presence of di-MGO adduct of rutin was not detected, perhaps due to the relatively low concentration of rutin or the occurrence of other trapping molecules.

Galegine sulfate and metformin hydrochloride formed only mono-MGO adducts (Table 4). We observed three mono-MGO adducts for galegine sulfate (by analogy to galegine detected in extract), which could be an effect of substitution of different positions in the guanidine group or other structural differences between the formed adducts. MGO adducts of chlorogenic acid after 1 h of incubation were not observed. Some research showed that chlorogenic acid can inhibit AGE formation induced by methylglyoxal, which suggests that chlorogenic acid scavenges MGO by a mechanism other than direct trapping [47].

The scientific literature provides information on the formation of mono- and di-MGO adducts with various flavonoids [48,49]. A study by Van den Eynde et al. [50] showed that quercetin traps methylglyoxal effectively enough to significantly reduce its concentration in human plasma. Trapping activity has also been proven for the guanidine derivatives aminoguanidine [51] and metformin [52]; however, to our best knowledge, the ability to trap methylglyoxal by galegine and hydroxygalegine has been demonstrated for the first time in this study. Based on the results of previous structural studies [46,53], we proposed in Figure 4 the chemical structure of the MGO adducts of rutin, galegine, and hydroxygalegine formed in the experimental conditions.

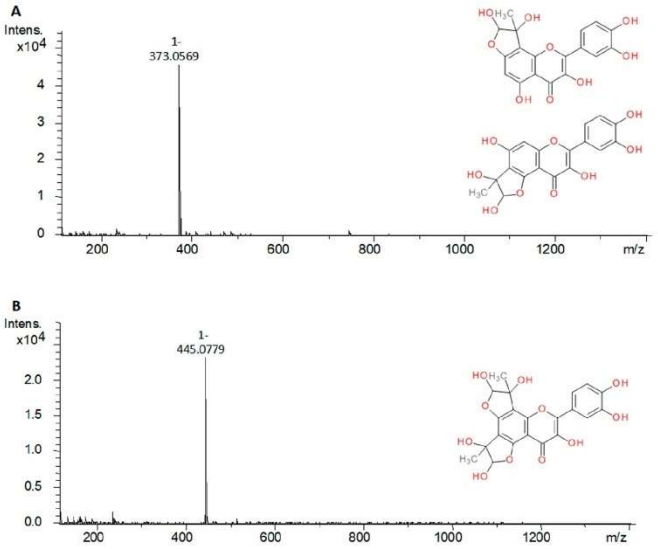

Figure 4. *Cont.*

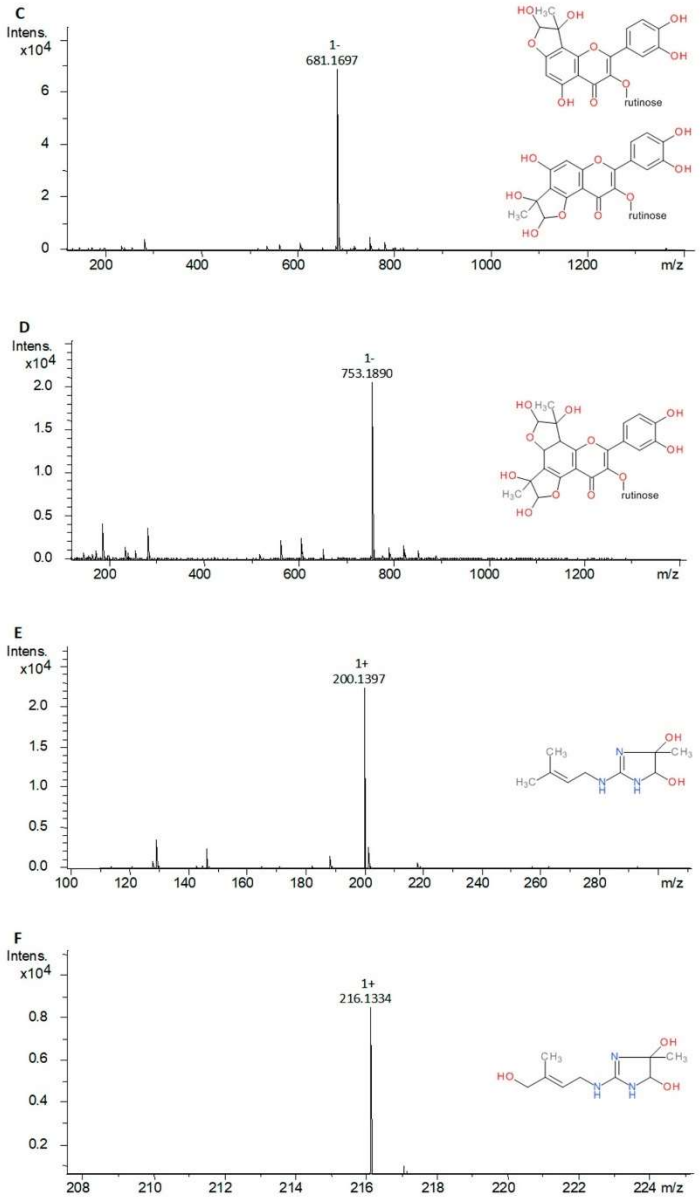

Figure 4. *Cont.*

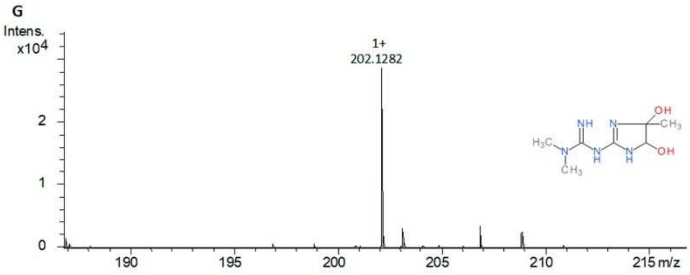

Figure 4. The mass spectra of methylglyoxal adducts and their proposed chemical structure: (**A**), quercetin mono-MGO adduct (373 Da); (**B**), quercetin di-MGO adduct (445 Da); (**C**), rutin mono-MGO adduct (681 Da); (**D**), rutin di-MGO adduct (753 Da); (**E**), galegine mono-MGO adduct (200 Da); (**F**), hydroxygalegine mono-MGO adduct (216 Da); (**G**), metformin mono-MGO adduct (202 Da).

Polyphenols have a beneficial effect on health and can prevent degradative diseases such as T2D, cardiovascular disease, and some cancers through the modulation of several protein functions, as well as antioxidative action and an anti-MGO effect [54]. Flavonols and HCA esters are known as health-promoting and disease-preventing components of many vegetables, fruits, and herbal teas. By contrast, guanidine derivatives are rare plant compounds. Guanidines and quinazoline alkaloids have been identified in several species known for their therapeutic usage but also potential toxicity in livestock [6]. A more recent study by Mooney et al. [55] reported that no toxic effects of galegine were observed in rats at a dose of 600 mg per kilogram body weight for over 28 days. Taking into account the usual daily doses of metformin (up to 3000 mg) in the treatment of T2D patients, the amount of guanidines (32 mg), at the dose of 4 g of *Galegae herba* recommended per day, appears to be safe, and even insufficient to achieve a hypoglycemic effect. Quinazoline alkaloids also possess several interesting pharmacological properties, such as intestinal α-glucosidase and acetylcholine esterase inhibition, as well as anti-inflammatory, antimicrobial, and antioxidative effects [56]. Vasicine and vasicinone were found to be biologically active components of *Adhatoda vasica* (L.) Nees (*Acanthaceae*), a plant used as a herbal medicine for allergen-induced bronchial obstruction and asthma, and as a hepatoprotective and cardioprotective agent [57]. Vasicine was reported to have a protective effect against myocardial infarction [58]. According to the study of Wakhloo et al. [59], vasicine in a dose up to 16 mg (injected intravenous) was well tolerated in humans and showed no undesirable toxic effect in clinical observations. However, the uterus became firm and contracted after long-term vasicine administration, which indicated its oxytocic effect and suggests that it may demonstrate the above-mentioned abortifacient activity [59]. Information available about the safety of quinazoline alkaloids is insufficient, but no adverse effects were reported for *A. vasica* [57].

For these reasons, the use of *G. officinalis* herb in the adjunctive therapy of T2D should be further explored to confirm the underlying mechanism of its action, efficacy, and safety.

3. Materials and Methods

3.1. Plant Material

The dried herb of *Galega officinalis* L. (*Galegae herba*) was obtained from the herbal company FLOS (Zakład Konfekcjonowania Ziół FLOS; Mokrsko, Poland) (batches no. 1099, 1108, 1010, assigned as Gof1, Gof2, and Gof3, respectively) certified GMP and ISO 9002. Voucher specimens were deposited in the Herbarium of the Department of Pharmacognosy and Herbal Medicines (Wroclaw Medical University, Wrocław, Poland). Before extractions herb was finely ground in an IKA A11B (IKA Poland Sp. z o.o.; Warsaw, Poland) analytical mill for 5 min.

3.2. Chemicals and Standards

The following chemicals were used: methylglyoxal (40% in water), 2,2–diphenyl–1–picrylhydrazyl, 2,2-azino-bis-3-ethylbenzothiazoline-6-sulfonic acid, trolox, metformin hydrochloride, 98–100% formic acid, methanol (HPLC grade), acetonitrile (HPLC gradient grade and LC–MS grade), and water (LC–MS grade) were purchased from Merck–Sigma–Aldrich (Sigma–Aldrich Sp. z o.o., Poznań, Poland); NaCl, KCl, Na_2HPO_4 and KH_2PO_4 (reagent grade) were obtained from Chempur (Piekary Śląskie, Poland); quercetin, quercitrin, astragalin, hyperoside, rutin, nicotiflorin, narcissin, taxifolin, gallic acid, *p*-coumaric acid, ferulic acid, caffeic acid, and chlorogenic acid were from Extrasynthese (Genay Cedex, France); galegine sulfate was purchased from SelectLab (Münster, Germany). Water was glass-distilled and deionized.

The stock solutions of standards (1 mg/mL) were prepared by dissolving 5 mg of a reference compound in 5 mL of methanol. Working standard solutions in the range of 10–400 µg/mL were made by mixing with 50% aq. (aqueous) methanol (*v*/*v*), filtered through hydrophilic Millex Syringe Filters (Durapore 0.22 µm; Millipore, Burlington, MA, USA) and stored at −20 °C.

3.3. Preparation of Extracts

A total of 0.2 g of dried and finely powdered plant material was extracted with 10 mL of boiling water for 15 min (infusion) as well with 10 mL of methanol or water-methanol mixture (1:1, 3:7; *v*/*v*) using an ultrasonic bath (Bandelein Sonorex Digital 10P; Bandelin, Berlin, Germany) at 40 °C for 15 min. After 15 min the extracts were passed through a Durapore 0.22 µm filter (Millipore; Burlington, MA, USA) into vials, and the filtrate was analyzed using UHPLC-ESI-MS (Bruker Daltonics; Bremen, Germany) and UHPLC–DAD (Thermo Fisher Scientific; Waltham, MA, USA). The drug extract ratio (DER) was 1:50.

3.4. UHPLC-DAD and UHPLC-ESI-MS Analyses

The UHPLC–DAD analyses were conducted on a Thermo Scientific DionexUltiMate 3000 system (Thermo Fisher Scientific; Waltham, MA, USA) equipped with a quaternary pump (LPG-3400D, Thermo Fisher Scientific; Waltham, MA, USA), rapid separation photodiode array detector (DAD–3000) and UltiMate 3000RS autosampler (WPS-3000). The separation of compounds was carried out on a Kinetex C18 column (150 mm × 2.1 mm × 2.6 µm) (Phenomenex; Torrance, CA, USA) and its temperature was maintained at 35 °C using a temperature-controlled column compartment (TCC-3000). The injection volume was 1 µL. The mobile phases used to create the gradient were 0.1% (*v*/*v*) formic acid in water and 0.1% (*v*/*v*) formic acid in acetonitrile as eluents A and B, respectively. The following gradient elution program, at a flow rate of 0.4 mL/min, based on the solvents A and B, was applied: 0–5 min, 100% A; 5–30 min, 100–70% A; 30–32 min, 70–10% A; 32–36 min 10% A. Then, the system returned to the initial setting and was washed with 100% A until the system was stabilized before the next analysis. Spectral measurements were recorded in the wavelength range 200–600 nm, in steps of 2 nm as well as at 220, 254, 280, 320, and 360 nm. Data acquisition was performed with the Chromeleon Chromatography Data System (Thermo Fisher Scientific; Waltham, MA, USA). Amounts of different quantified compounds were calculated as mean values from duplicate UHPLC analyses based on the calibration curves of the corresponding standard compounds or expressed as equivalents of appropriate, related compound (taking into consideration the molar mass differences).

For the UHPLC-ESI-MS analyses, an UHPLC system, set as above, was coupled with Compact ESI-QqTOF-MS (Bruker Daltonics; Bremen, Germany). Nitrogen at 2.0 bar pressure, temperature 210 °C, and flow 0.8 L/min was used as drying and nebulizing gas in the electrospray ionization interface (ESI). Data were acquired in both positive and negative mode. The ion source temperature was set at 100 °C and the capillary voltage was 4500 V (ESI+) or 2200 V (ESI−). The collision energy was 8.0 eV and for MS/MS it was 35 and 40 eV. Sodium formate clusters in concentrations of 10 mM were used for internal calibration. Analyses were run in the same chromatographic conditions as described

above. System control and data acquisition were carried out with the Compass Data Analysis software (Bruker Daltonics; Bremen, Germany). The amount of galegine was calculated as the mean value from duplicate analyses based on the calibration curve of galegine sulfate used as an external standard.

The determination of the methylglyoxal adducts formation was performed using the same UHPLC and QqTOF-MS hardware configuration and mobile phases. The column was thermostatted at 4 ± 1 °C and the injection volume was 1 μL. The following gradient elution program, at a flow rate of 0.3 mL/min, based on the solvents A and B was applied: 0–12 min, 97–65% A; 12–14 min, 65% A; 14–17 min, 65–20% A; 17–19 min 20% A. Then, the system returned to the initial setting and was washed with 97% A until the system was stabilized before the next analysis. The negative and positive-ion polarity mode was applied and other settings were as previously described except capillary voltage, which was set at 5000 V.

3.5. Validation of Chromatographic Methods and Quantification

The applied UHPLC methods were validated by the determination of linearity, LOD, and LOQ. The calibration equations for quantified polyphenols and galegine sulfate were assessed at 5 concentration levels, and duplicate injections were performed for each concentration. The values of LOD were established at a signal-to-noise ratio (S/N) of 3 and LOQ were calculated at S/N of 10. The results of the method validation for authentic and corresponding standards, of which the calibration curves exhibited a good linearity (R^2, 0.9985–0.9999), are shown in Table 5. The average values (mg per 1 g of dried galega herb) and standard deviations (SD) for all the quantified compounds were determined from three independent plant extracts, each in two repetitions.

3.6. In Vitro Studies

3.6.1. DPPH Radical Scavenging Assay

The radical scavenging ability against the DPPH radical was measured according to the Blois method with slight modification [60]. In a 96-well microplate, 20 μL of each sample at different concentrations was mixed with 200 μL of 0.3 mM methanolic solution of DPPH. The plate was incubated for 30 min in the dark at ambient temperature and the absorbance was recorded at 517 nm using a Multiskan GO microplate spectrophotometer (Thermo Fisher Scientific; Waltham, MA, USA). Gallic acid was used as a positive control. All the measurements were performed in triplicate. The percentage of DPPH free radical scavenging activity was calculated as follows:

$$\% \text{ DPPH scavenge rate} = (A0 - A1)/A0 \times 100\%, \quad (1)$$

where A0 is the mean absorbance of the control and A1 is the mean absorbance of the extract/standard with DPPH. The IC50 values were calculated using linear regression analysis and used to express the antioxidant capacity.

Table 5. Validation parameters of the standard compounds for UHPLC-DAD and UHPLC-ESI-MS analysis.

Compound	Method	Λ [nm]	Linear Equation	R^2	Range [μg/mL]	LOD [μg/mL]	LOQ [μg/mL]
Chlorogenic acid	UHPLC-DAD	320	y = 0.0051x − 0.0009	0.9999	10–250	0.16	0.50
Caffeic acid	UHPLC-DAD	320	y = 0.00301x + 0.00047	0.9999	10–250	0.56	1.87
p–Coumaric acid	UHPLC-DAD	320	y = 0.00250x − 0.00003	0.9999	10–250	0.57	1.90
Ferulic acid	UHPLC-DAD	320	y = 0.00321x + 0.00018	0.9999	10–250	0.48	1.61
Hyperoside	UHPLC-DAD	360	y = 0.00612x + 0.00007	0.9999	10–400	0.11	0.36
Rutin	UHPLC-DAD	360	Y = 0.0097x − 0.000007	0.9999	10–400	0.16	0.50
Taxifolin	UHPLC-DAD	280	y = 0.02357x + 0.00163	0.9999	10–400	0.08	0.28
Galegine sulfate	UHPLC-ESI-MS	$[M + H]^+$	y = 1.00029x − 0.00008	0.9985	10–400	0.01	0.03

λ, wavelength; y = ax + b, y − peak area; R^2, coefficient of determination; LOD, limit of detection; LOQ, limit of quantitation; $n = 2 \times 5$.

3.6.2. ABTS Radical Scavenging Assay

The ABTS radical scavenging activity was measured according to the slightly modified method of Chen and Kang [61]. ABTS and potassium persulfate were dissolved in deionized water to final concentrations of 7 and 2.45 mM, respectively. These two solutions were mixed and incubated in the dark at 25 °C for 12 h and subsequently diluted with methanol to reach an absorbance maximum at 734 nm. Next, 200 µL of the obtained reagent was mixed with 2 µL of the tested sample. After incubating at room temperature for 15 min, the absorbance was read at 734 nm using a Multiskan GO microplate spectrophotometer (Thermo Fisher Scientific; Waltham, MA, USA), and Trolox was used as a positive control. All the measurements were performed in triplicate. The ABTS radical scavenging activity was calculated as follows:

$$\% \text{ ABTS scavenge rate} = (A0 - A1)/A0 \times 100\%, \quad (2)$$

where A0 is the mean absorbance of the control and A1 is the mean absorbance of the extract/standard with ABTS. The IC50 values were calculated using linear regression analysis and used to express the antioxidant capacity.

3.6.3. Methylglyoxal Trapping Assay

Methylglyoxal trapping capacity of selected compounds and *G. officinalis* extracts was measured according to the Sang et al. [62] method with slight modification. Briefly, 3 mM methylglyoxal (MGO) was incubated for 1 h with quercetin, rutin, chlorogenic acid, galegine sulfate, metformin hydrochloride (1 mM), and *G. officinalis* hot water extract (1 mL, DER 1:50; equivalent of 20 mg of dried herb) in 100 mM of phosphate buffered saline (PBS; pH 7.4) at 37 °C to equal physiological temperature and shaken at 40 revolutions per minute. The samples were further analyzed using UHPLC-ESI-MS to investigate their ability to form adducts with MGO.

4. Conclusions

Previous research proves the hypoglycemic properties of *Galegae herba* extracts but does not draw attention to its potential positive effect on the prevention of vascular complications related to hyperglycemia. Our study proved that *G. officinalis* contains compounds that exhibit both antioxidant activity and the ability to trap methylglyoxal. Both of these properties play an important role in preventing and delaying diabetes complications.

An in-depth analysis of galega herb revealed the presence not only of guanidines and tricyclic quinazoline alkaloids but also of flavonoid glycosides and HCA esters. The main components in the polyphenolic fraction were flavonols and monocaffeoylhexaric acids. The in vitro tests allowed us to determine which individual *G. officinalis* components show beneficial antioxidative and anti-MGO effects. Flavonols such as rutin and HCAs such as chlorogenic acid exhibited a potent antiradical activity. On the other hand, the ability to trap MGO was noted for guanidines (galegine and hydroxygalegine) and flavonoids (mainly flavonols), whereas the HCA esters and quinazoline alkaloids were ineffective. The UHPLC-ESI-MS method confirmed the presence of mono-MGO adducts of galegine, hydroxygalegine, and metformin, as well as mono-MGO and di-MGO adducts of rutin and quercetin in the reaction mixtures from model tests.

In the light of the results from the phytochemical and in vitro studies, it can be assumed that the polyphenols and guanidines contained in the extracts of *G. officinalis* herb indicate antioxidant and MGO trapping potential, which can be used in the future in the prevention of vascular complications of diabetes. Nevertheless, further research on an in vivo model is necessary.

Author Contributions: Conceptualization, I.F.; methodology, I.F., P.K., and K.B.; validation, K.B. and P.K.; formal analysis, K.B., I.F., and P.K.; investigation, K.B. and P.K.; data curation, K.B. and I.F.; writing—original draft preparation, K.B.; writing—review and editing, I.F. and P.K.; visualization, K.B. and I.F.; supervision, I.F.; project administration, I.F. and K.B.; funding acquisition, I.F. and K.B. All authors have read and agreed to the published version of the manuscript.

Funding: This research was financially supported by the Wroclaw Medical University (grant number STM.D110.20.131).

Conflicts of Interest: The authors declare no conflict of interest. The funders had no role in the design of the study; in the collection, analysis, or interpretation of data; in the writing of the manuscript; or in the decision to publish the results.

Abbreviations

T2D	type 2 diabetes mellitus
MGO	methylglyoxal
G. officinalis	*Galega officinalis*
t_R	retention time
λ_{max}	absorbance maximum in UV-Vis spectrum
ROS	reactive oxygen species
RCS	reactive carbonyl species
AGEs	advanced glycation end products
AOPPs	advanced oxidation end products
UHPLC	ultra high-performance liquid chromatography
DAD	diode array detector
ESI-MS	electrospray ionization mass spectrometry
ABTS	2,2′-azino-bis(3-ethylbenzthiazoline-6-sulfonic acid)
DPPH	2,2-diphenyl-1-(2,4,6-trinitrophenyl)hydrazyl
HCAs	hydroxycinnamic acids
IC50	the half maximal inhibitory concentration
EIC	extracted ion chromatogram
DER	drug extract ratio

References

1. Farzaei, F.; Morovati, M.R.; Farjadmand, F.; Farzaei, M.H. A Mechanistic review on medicinal plants used for diabetes mellitus in traditional Persian medicine. *J. Evid. Based Complement. Altern. Med.* **2017**, *22*, 944–955. [CrossRef] [PubMed]
2. Delaviz, H.; Mohammadi, J.; Ghalamfarsa, G.; Mohammadi, B.; Farhadi, N. A review study on phytochemistry and pharmacology applications of Juglans regia plant. *Pharmacogn. Rev.* **2017**, *11*, 145. [PubMed]
3. Witters, L.A. The blooming of the French lilac. *J. Clin. Investig.* **2001**, *108*, 1105–1107. [CrossRef] [PubMed]
4. Tabares, F.P.; Jaramillo, J.V.B.; Ruiz-Cortés, Z.T. Pharmacological Overview of Galactogogues. *Vet. Med. Int.* **2014**, *2014*, 1–20. [CrossRef]
5. Nagalievska, M.; Sabadashka, M.; Hachkova, H.; Sybirna, N. *Galega officinalis* extract regulate the diabetes mellitus related violations of proliferation, functions and apoptosis of leukocytes. *BMC Complement. Altern. Med.* **2018**, *18*, 1–13. [CrossRef]
6. Keeler, R.F.; Johnson, A.E.; Stuart, L.D. Toxicosis from and possible adaptation to Galega officinalis in sheep and the relationship to verbesina encelioides toxicosis. *Vet. Hum. Toxicol.* **1986**, *28*, 309–315.
7. Anadón, A.; Martínez-Larrañaga, M.R.; Ares, I.; Martínez, M.A. Poisonous Plants of the Europe. In *Veterinary Toxicology: Basic and Clinical Principles*, 3rd ed.; Elsevier: Amsterdam, The Netherlands, 2018; Chapter 62; pp. 891–909. [CrossRef]
8. Vronsk, L.V.; Timoftevich, N.; Ezhned, M.A.; Barchuk, O. The otherview of of medicinal plants that express hypoglycemic activity. *Pharm. Rev.* **2014**, *2*, 142–148. [CrossRef]
9. British Herbal Medicine Association. *British Herbal Pharmacopoeia*; The Association: London, UK, 1976; p. 93.
10. Youngken, H. *Textbook of Pharmacognosy*, 6th ed.; The Blakiston Company: Philadelphia, PA, USA, 1958; p. 56.
11. Pulito, C.; Sanli, T.; Rana, P.; Muti, P.; Blandino, G.; Strano, S. Metformin: On ongoing journey across diabetes, cancer therapy and prevention. *Metabolites* **2013**, *3*, 1051–1075. [CrossRef]
12. Watanabe, C. Studies in metabolic changes induced by the administration of guanidine bases. *J. Biol. Chem.* **1918**, *33*, 253–265. [CrossRef]
13. Bretzel, R.G.; Voigt, K.; Schatz, H. The United Kingdom Prospective Diabetes Study (UKPDS). Implications for the pharmacotherapy of type 2 diabetes mellitus. *Exp. Clin. Endocrinol. Diabetes* **1998**, *106*, 369–372. [CrossRef]

14. Kender, Z.; Fleming, T.; Kopf, S.; Torzsa, P.; Grolmusz, V.; Herzig, S.; Schleicher, E.; Rácz, K.; Reismann, P.; Nawroth, P.P. Effect of metformin on methylglyoxal metabolism in patients with type 2 diabetes. *Exp. Clin. Endocrinol. Diabetes* **2014**, *122*, 316–319. [CrossRef] [PubMed]
15. Han, Y.; Randell, E.; Vasdev, S.; Gill, V.; Gadag, V.; Newhook, L.A.; Grant, M.; Hagerty, D. Plasma methylglyoxal and glyoxal are elevated and related to early membrane alteration in young, complication-free patients with Type 1 diabetes. *Mol. Cell. Biochem.* **2007**, *305*, 123–131. [CrossRef] [PubMed]
16. Rodrigues, T.; Matafome, P.; Santos-Silva, D.; Sena, C.; Seiça, R. Reduction of methylglyoxal-induced glycation by pyridoxamine improves adipose tissue microvascular lesions. *J. Diabetes Res.* **2013**, *2013*, 1–9. [CrossRef] [PubMed]
17. Shojaee, S.S.; Vahdati, A.; Assaei, R.; Sepehrimanesh, M. Effect of *Galega officinalis* leaf powder and *Trigonella foenum-graecum* seed powder on blood glucose levels and weight gain in a diabetes mellitus rat model. *Comp. Clin. Path.* **2013**, *24*, 145–148. [CrossRef]
18. Pundarikakshudu, K.; Patel, J.K.; Bodar, M.S.; Deans, S.G. Anti-bacterial activity of *Galega officinalis* L. (Goat's Rue). *J. Ethnopharmacol.* **2001**, *77*, 111–112. [CrossRef]
19. Atanasov, A.T.; Spasov, V. Inhibiting effect of desalted extract from *Galega officinalis* L. on platelet aggregation. *Folia Med.* **1999**, *41*, 46–50.
20. Atanasov, A.T.; Chorbanov, B.P.; Dimitrov, B.D. Anti-aggregation activity of crude water extract of *Galega officinalis* L. fractionated on Sephadex G-25 and Sepharose 4B. *Folia Med.* **2002**, *44*, 45–49.
21. Seyd-Hosein, A.-E.; Majid Shokoohi, A.A.; Asghar, R.; Hamed Shoorei, H.K. Protective effect of *Galega officinalis* extract on streptozotocin-induced kidney damage and biochemical factor in diabetic rats. *Crescent J. Med. Biol. Sci.* **2017**, *4*, 108–114.
22. Kim, J.H.; Kim, M., II; Syed, A.S.; Jung, K.; Kim, C.Y. Rapid identification of methylglyoxal trapping constituents from onion peels by pre-column incubation method. *Nat. Prod. Sci.* **2017**, *23*, 247–252. [CrossRef]
23. Li, X.; Zheng, T.; Sang, S.; Lv, L. Quercetin inhibits advanced glycation end product formation by trapping methylglyoxal and glyoxal. *J. Agric. Food Chem.* **2014**, *62*, 12152–12158. [CrossRef]
24. Oldham, M.; Ransom, C.V.; Ralphs, M.H.; Gardner, D.R. Galegine content in goatsrue (*Galega officinalis*) varies by plant part and phenological growth stage. *Weed Sci.* **2011**, *59*, 349–352. [CrossRef]
25. Singh, A.; Kumar, S.; Reddy, T.J.; Rameshkumar, K.B.; Kumar, B. Screening of tricyclic quinazoline alkaloids in the alkaloidal fraction of *Adhatoda beddomei* and *Adhatoda vasica* leaves by high-performance liquid chromatography/electrospray ionization quadrupole time-of-flight tandem mass spectrometry. *Rapid Commun. Mass Spectrom.* **2015**, *29*, 485–496. [CrossRef] [PubMed]
26. Liu, W.; Shi, X.; Yang, Y.; Cheng, X.; Liu, Q.; Han, H.; Yang, B.; He, C.; Wang, Y.; Jiang, B.; et al. In vitro and in vivo metabolism and inhibitory activities of vasicine, a potent acetylcholinesterase and butyrylcholinesterase inhibitor. *PLoS ONE* **2015**, *10*, e0129759. [CrossRef] [PubMed]
27. Yamagaki, T.; Watanabe, T. Hydrogen radical removal causes complex overlapping Isotope patterns of aromatic carboxylic acids in negative-ion matrix-assisted laser desorption/ionization mass spectrometry. *Mass Spectrom.* **2012**, *1*, A0005. [CrossRef]
28. Hvattum, E.; Ekeberg, D. Study of the collision-induced radical cleavage of flavonoid glycosides using negative electrospray ionization tandem quadrupole mass spectrometry. *J. Mass Spectrom.* **2003**, *38*, 43–49. [CrossRef]
29. Cuyckens, F.; Claeys, M. Determination of the glycosylation site in flavonoid mono-O-glycosides by collision-induced dissociation of electrospray-generated deprotonated and sodiated molecules. *J. Mass Spectrom.* **2005**, *40*, 364–372. [CrossRef]
30. Davis, B.D.; Brodbelt, J.S. An investigation of the hemolytic saccharide cleavage of deprotonated flavonol 3-*O*-glycosides in a quadrupole ion trap mass spectrometer. *J. Mass Spectrom.* **2008**, *43*, 1045–1052. [CrossRef]
31. Hirose, Y.; Fujita, T.; Ishii, T.; Ueno, N. Antioxidative properties and flavonoid composition of *Chenopodium quinoa* seeds cultivated in Japan. *Food Chem.* **2010**, *119*, 1300–1306. [CrossRef]
32. Nahrstedt, A.; Hungeling, M.; Petereit, F. Flavonoids from *Acalypha indica*. *Fitoterapia* **2006**, *77*, 484–486. [CrossRef]
33. Owis, A.I.; El-Hawary, M.S.; El Amir, D.; Aly, O.M.; Abdelmohsen, U.R.; Kamel, M.S. Molecular docking reveals the potential of *Salvadora persica* flavonoids to inhibit COVID-19 virus main protease. *RSC Adv.* **2020**, *10*, 19570. [CrossRef]

34. Champavier, Y.; Allais, D.P.; Chulia, A.J.; Kaouadji, M. Acetylated and non-acetylated flavonol triglycosides from *Galega officinalis*. *Chem. Pharm. Bull.* **2000**, *48*, 281–282. [CrossRef] [PubMed]
35. Peiretti, P.G.; Gai, F. Fatty acid and nutritive quality of chia (*Salvia hispanica* L.) seeds and plant during growth. *Anim. Feed Sci. Technol.* **2009**, *148*, 267–275. [CrossRef]
36. Barchuk, O.Z.; Lysiuk, R.M.; Denys, A.I.; Zaliska, O.M.; Smalyuh, O.G. Experimental study of goat's rue (*Galega Officinalis* L.) herb and its liquid extracts. *Pharma Innov. J.* **2017**, *6*, 393–397.
37. Vlassara, H.; Palace, M.R. Diabetes and advanced glycation endproducts. *J. Intern. Med.* **2002**, *251*, 87–101. [CrossRef] [PubMed]
38. Maessen, D.E.M.; Stehouwer, C.D.A.; Schalkwijk, C.G. The role of methylglyoxal and the glyoxalase system in diabetes and other age-related diseases. *Clin. Sci.* **2015**, *128*, 839–861. [CrossRef] [PubMed]
39. Piwowar, A.; Rorbach-Dolata, A.; Fecka, I. The antiglycoxidative ability of selected phenolic compounds—An in vitro study. *Molecules* **2019**, *24*, 2689. [CrossRef] [PubMed]
40. Tiveron, A.P.; Melo, P.S.; Bergamaschi, K.B.; Vieira, T.M.F.S.; Regitano-d'Arce, M.A.B.; Alencar, S.M. Antioxidant activity of brazilian vegetables and its relation with phenolic composition. *Int. J. Mol. Sci.* **2012**, *13*, 8943–8957. [CrossRef]
41. Giuffrè, A.M. Bergamot (*Citrus bergamia*, Risso): The Effects of cultivar and harvest date on functional properties of juice and cloudy juice. *Antioxidants* **2019**, *8*, 221. [CrossRef]
42. Zapata, M.; Chaparro, D.; Rojano, B.; Alzate, A.; Restrepo, L.; Maldonado, M. Effect of storage time on physicochemical, sensorial, and antioxidant characteristics, and composition of mango (cv. Azúcar) juice. *Emir. J. Food Agric.* **2017**, *29*, 367–377. [CrossRef]
43. Vergun, O.; Shymanska, O.; Rakhmetov, D.; Grygorieva, O.; Ivanišová, E.; Brindza, J. Parameters of antioxidant activity of *Galega officinalis* L. and *Galega orientalis* Lam. (*Fabaceae* Lindl.) plant raw material. *Potravin. Slovak J. Food Sci.* **2020**, *14*, 125–134. [CrossRef]
44. Calderon Moreno, R.; Navas-Acien, A.; Escolar, E.; Nathan, D.M.; Newman, J.; Schmedtje, J.F.; Diaz, D.; Lamas, G.A.; Fonseca, V. Potential role of metal chelation to prevent the cardiovascular complications of diabetes. *J. Clin. Endocrinol. Metab.* **2019**, *104*, 2931–2941. [CrossRef] [PubMed]
45. Duraipandiyan, V.; Balachandran, C.; Ignacimuthu, S.; Sankar, C.; Balakrishna, K. Properties of vasicine acetate synthesized from vasicine isolated from *Adhatoda vasica* L. *BioMed Res. Int.* **2015**, *2015*, 7–14. [CrossRef] [PubMed]
46. Bhuiyan, M.N.I.; Mitsuhashi, S.; Sigetomi, K.; Ubukata, M. Quercetin inhibits advanced glycation end product formation via chelating metal ions, trapping methylglyoxal, and trapping reactive oxygen species. *Biosci. Biotechnol. Biochem.* **2017**, *81*, 882–890. [CrossRef] [PubMed]
47. Gugliucci, A.; Bastos, D.H.M.; Schulze, J.; Souza, M.F.F. Caffeic and chlorogenic acids in Ilex paraguariensis extracts are the main inhibitors of AGE generation by methylglyoxal in model proteins. *Fitoterapia* **2009**, *80*, 339–344. [CrossRef] [PubMed]
48. Hwang, S.H.; Kim, H.Y.; Zuo, G.; Wang, Z.; Lee, J.Y.; Lim, S.S. Anti-glycation, carbonyl trapping and anti-inflammatory activities of chrysin derivatives. *Molecules* **2018**, *23*, 1752. [CrossRef]
49. Shao, X. Scavenging Effects of Dietary Flavonoids on Reactive Dicaronyl Species and Their Possible Implications on the Inhibition of the Formation of Advanced Glycation-End Products. Ph.D. Thesis, The State University of New Jersey, New Brunswick, NJ, USA, 2010.
50. Van Den Eynde, M.D.G.; Geleijnse, J.M.; Scheijen, J.L.J.M.; Hanssen, N.M.J.; Dower, J.I.; Afman, L.A.; Stehouwer, C.D.A.; Hollman, P.C.H.; Schalkwijk, C.G. Quercetin, but not epicatechin, decreases plasma concentrations of methylglyoxal in adults in a randomized, double-blind, placebo-controlled, crossover trial with pure flavonoids. *J. Nutr.* **2018**, *148*, 1911–1916. [CrossRef]
51. Thornalley, P.J. Use of aminoguanidine (pimagedine) to prevent the formation of advanced glycation endproducts. *Arch. Biochem. Biophys.* **2003**, *149*, 31–40. [CrossRef]
52. Kinsky, O.R.; Hargraves, T.L.; Anumol, T.; Jacobsen, N.E.; Dai, J.; Snyder, S.A.; Monks, T.J.; Lau, S.S. Metformin scavenges methylglyoxal to form a novel imidazolinone metabolite in humans. *Chem. Res. Toxicol.* **2016**, *29*, 227–234. [CrossRef]
53. Lo, T.W.C.; Westwood, M.E.; McLellan, A.C.; Selwood, T.; Thornalley, P.J. Binding and Modification of Proteins by Methylglyoxal under Physiological Conditions. *J. Biol. Chem.* **1994**, *269*, 32299–32305.
54. Yeh, W.J.; Hsia, S.M.; Lee, W.H.; Wu, C.H. Polyphenols with antiglycation activity and mechanisms of action: A review of recent findings. *J. Food Drug Anal.* **2017**, *25*, 84–92. [CrossRef]

55. Mooney, M.H.; Fogarty, S.; Stevenson, C.; Gallagher, A.M.; Palit, P.; Hawley, S.A.; Hardie, D.G.; Coxon, G.D.; Waigh, R.D.; Tate, R.J.; et al. Mechanisms underlying the metabolic actions of galegine that contribute to weight loss in mice. *Br. J. Pharmacol.* **2008**, *153*, 1669–1677. [CrossRef] [PubMed]
56. Rachana, R.; Basu, S.; Pant, M.; Priyanka, K.M.; Sonam, S. Review & Future Perspectives of Using Vasicine, and Related Compounds. *Indo Glob. J. Pharm. Sci.* **2011**, *1*, 85–98.
57. Rachana, R.; Pant, M.; Basu, S. Cytoprotective activity of *Adhatoda vasica* extract and vasicine against tobacco smoke induced cytotoxicity. *J. Pharm. Technol. Res. Manag.* **2013**, *1*, 109–117. [CrossRef]
58. Jiang, T.; Zhang, L.; Ding, M.; Li, M. Protective effect of vasicine against myocardial infarction in rats via modulation of oxidative stress, inflammation, and the PI3K/AKT pathway. *Drug Des. Devel. Ther.* **2019**, *13*, 3773–3784. [CrossRef]
59. Wakhloo, R.L.; Kaul, G.; Gupta, O.P.; Atal, C.K. Safety of vasicine hydrochloride in human volunteers. *Indian J. Pharmacol.* **1980**, *12*, 129–131.
60. Blois, M.S. Antioxidant determinations by the use of a stable free radical. *Nature* **1958**, *181*, 1199–1200. [CrossRef]
61. Chen, L.; Kang, Y.H. Antioxidant and enzyme inhibitory activities of plebeian herba (*Salvia plebeia* R. Br.) under different cultivation conditions. *J. Agric. Food Chem.* **2014**, *62*, 2190–2197. [CrossRef]
62. Sang, S.; Shao, X.; Bai, N.; Lo, C.Y.; Yang, C.S.; Ho, C.T. Tea polyphenol (-)-epigallocatechin-3-gallate: A new trapping agent of reactive dicarbonyl species. *Chem. Res. Toxicol.* **2007**, *20*, 1862–1870. [CrossRef]

Sample Availability: Samples of the plants and compounds are available from authors.

P4. Aspalathin and Other Rooibos Flavonoids Trapped α-Dicarbonyls and Inhibited Formation of Advanced Glycation End Products *In Vitro*

International Journal of
Molecular Sciences

MDPI

Article

Aspalathin and Other Rooibos Flavonoids Trapped α-Dicarbonyls and Inhibited Formation of Advanced Glycation End Products In Vitro

Katarzyna Bednarska [1] and Izabela Fecka [1,2,*]

[1] Department of Pharmacognosy and Herbal Medicines, Faculty of Pharmacy, Wroclaw Medical University, ul. Borowska 211, 50-556 Wroclaw, Poland
[2] The Committee on Therapeutics and Pharmaceutical Sciences, The Polish Academy of Sciences, pl. Defilad 1, 00-901 Warszawa, Poland
* Correspondence: izabela.fecka@umw.edu.pl

Abstract: The excessive dietary intake of simple sugars and abnormal metabolism in certain diseases contribute to the increased production of α-dicarbonyls (α-DCs), such as methylglyoxal (MGO) and glyoxal (GO), the main precursors of the formation of advanced glycation end products (AGEs). AGEs play a vital role, for example, in the development of cardiovascular diseases and diabetes. *Aspalathus linearis* (Burman f.) R. Dahlgren (known as rooibos tea) exhibits a wide range of activities beneficial for cardio-metabolic health. Thus, the present study aims to investigate unfermented and fermented rooibos extracts and their constituents for the ability to trap MGO and GO. The individual compounds identified in extracts were tested for the capability to inhibit AGEs (with MGO or GO as a glycation agent). Ultra-high-performance liquid chromatography coupled with an electrospray ionization mass spectrometer (UHPLC–ESI–MS) was used to investigate α-DCs' trapping capacities. To evaluate the antiglycation activity, fluorescence measurement was used. The extract from the unfermented rooibos showed a higher ability to capture MGO/GO and inhibit AGE formation than did the extract from fermented rooibos, and this effect was attributed to a higher content of dihydrochalcones. The compounds detected in the extracts, such as aspalathin, nothofagin, vitexin, isovitexin, and eriodictyol, as well as structurally related phloretin and phloroglucinol (formed by the biotransformation of certain flavonoids), trapped MGO, and some also trapped GO. AGE formation was inhibited the most by isovitexin. However, it was the high content of aspalathin and its higher efficiency than that of metformin that determined the antiglycation and trapping properties of green rooibos. Therefore, *A. linearis*, in addition to other health benefits, could potentially be used as an α-DC trapping agent and AGE inhibitor.

Keywords: methylglyoxal; glyoxal; advanced glycation end products; trapping of dicarbonyls; *Aspalathus linearis*; rooibos; dihydrochalcones; flavonoids; MGO; AGEs

Citation: Bednarska, K.; Fecka, I. Aspalathin and Other Rooibos Flavonoids Trapped α-Dicarbonyls and Inhibited Formation of Advanced Glycation End Products In Vitro. *Int. J. Mol. Sci.* **2022**, *23*, 14738. https://doi.org/10.3390/ijms232314738

Academic Editor: Dong-Sung Lee

Received: 30 October 2022
Accepted: 23 November 2022
Published: 25 November 2022

Publisher's Note: MDPI stays neutral with regard to jurisdictional claims in published maps and institutional affiliations.

1. Introduction

Nowadays, it is well established that diet can significantly affect the metabolic health of the human body. In recent years, dietary habits have evolved all over the world, and the consumption of simple carbohydrates in the diet of the average person in developed countries has increased dramatically [1]. The increase in the prevalence of cardio-metabolic diseases, including obesity, type 2 diabetes, and the vascular complications of diabetes, is thought to be associated with a significant spike in the consumption of simple sugars, especially glucose and fructose. One of the mechanisms linking the increased intake of monosaccharides with the development of metabolic disorders is the overproduction of α-dicarbonyl compounds (α-DCs), such as methylglyoxal (MGO) and glyoxal (GO) [2,3]. Both MGO and GO are formed by the non-enzymatic and enzymatic degradation of monosaccharides; therefore, they may be produced in excess during the sustained consumption of large

amounts of carbohydrates [4]. An elevated glucose metabolism may result in increased MGO formation mainly through the polyol pathway [5]. Moreover, lipid peroxidation with the increased production of highly reactive aldehydes, including glyoxal, may occur as a result of oxidative stress and lipid disorders induced by hyperglycemia [6]. However, glucose is not the only contributor to α-DC formation. The hepatic metabolism of fructose skips the regulated steps of glycolysis, which additionally impairs normal lipid and carbohydrate metabolism and results in the increased production and generation of MGO [7]. The concentration of methylglyoxal is therefore significantly higher in people with diabetes and on average is up to 2–4 times higher [8]. α-DCs are characterized by extremely high reactivity and the ability to interact with primary amine and guanidine groups of biomacromolecules by nucleophilic addition to form Schiff bases [9]. Subsequently, Schiff bases can undergo cyclization to produce glycosylamines, which are further rearranged to produce stable ketoamines (Amadori products) [10]. Both Schiff bases and Amadori products are products of reversible reactions. However, they can also be further transformed by oxidation, dehydration, polymerization, and oxidative degradation reactions, giving origin to advanced glycation end products (AGEs) [11]. The non-enzymatic protein glycation reaction described above can be triggered not only by α-DCs but also by reducing sugars (e.g., glucose and fructose), which contain electrophilic carbonyl groups [12].

However, it is assumed that α-DC activity exceeds that of the reduction of sugars by up to several hundred times. The process of non-enzymatic glycation occurs under physiological conditions in the body [13]. Nevertheless, since α-DCs are essentially derived through the metabolism of carbohydrates, the higher the glycemia, the more the non-enzymatic glycation process is enhanced [14]. This is particularly important in patients with poorly controlled, long-term hyperglycemia, as increased concentrations of both α-DCs and AGEs contribute significantly to the development and progression of the vascular complications of diabetes and other metabolic disorders [14]. Albumins are especially vulnerable to glycation modifications induced by high concentrations of simple sugars and α-DCs [15]. In a population of healthy individuals, the percentage of glycated albumin is estimated to range from 1 to 10%, whereas in a population of individuals with the vascular complications of diabetes, it may be as high as 30% [16]. Among the many mechanisms of interference in the glycation pathway proposed as being able to reduce the concentration of α-DCs and thus, in the long run, AGEs, one of the most promising besides lowering carbohydrate intake seems to be trapping α-DC compounds [17]. In the past, there were great hopes for the clinical utility of aminoguanidine, the first known methylglyoxal scavenger and AGE inhibitor. The ability of aminoguanidine to delay the progression of the vascular complications of diabetes, including retinopathy and nephropathy, has been demonstrated, as has its ability to inhibit protein glycation modifications in vivo. Nevertheless, further clinical trials were discontinued due to some serious side effects occurring after long-term treatment, including gastrointestinal disorders and anemia [18].

In continuing the search for anti-α-DC treatments, plants and isolated natural compounds have received increasing attention in recent years [19–21]. *Aspalathus linearis* (Burman f.) R. Dahlgren, also known as rooibos or redbush tea, is a popular plant raw material widely used around the world, and its beneficial health properties, especially in the context of cardiometabolic health, are fairly well recognized [22]. This plant is cultivated for its herbal tea, which occurs in two varieties, unfermented (green rooibos, GR) and fermented (red rooibos, RR) [23]. The hypoglycemic properties of *A. linearis* have been previously demonstrated; therefore, it is particularly recommended for patients with pre-diabetic and diabetic conditions as a complementary treatment [24]. However, the positive effects of *A. linearis* on the cardiovascular system are not limited to potential glucose-lowering activity. A study by Marnewick et al. [25] revealed that the regular consumption of traditional rooibos tea significantly improved lipid profile as well as redox status, which are both important for vascular health. In fact, the benefits associated with the use of rooibos tea appear to be far more extensive and according to new studies may also include the reduction of oxidative stress [26], inflammation [27], insulin resistance [28], protein glyca-

tion [29], and the alleviation of pancreatic β-cell dysfunction [30]. Nevertheless, despite such intensive research on the cardio-metabolic benefits of *A. linearis* extracts, to date, it has not been evaluated whether their mechanism of action also includes methylglyoxal and glyoxal trapping. Of particular interest in this context seems to be aspalathin, the main and predominant component in green rooibos, for which α-DC-trapping activity has not yet been demonstrated. However, the ability to uptake MGO has been reported in structurally similar compounds, including phloretin and phlorizin (apple constituents), which may suggest that aspalathin and *A. linearis* may possess analogous activity [31].

With this in mind, the aim of the present study is to investigate the MGO- and GO-trapping capacity of aspalathin and other phytochemicals present in the infusions and hydroethanolic extracts of *A. linearis* as well as to compare the trapping capacity of green and red rooibos tea. In addition, the antiglycation properties of fermented and unfermented rooibos hydroethanolic extracts were investigated. Selected individual compounds present in *A. linearis* and their potential intestinal metabolite phloroglucinol were also investigated in in vitro models with MGO and GO as the glycation agents.

2. Results and Discussion

The accumulation of AGEs is believed to be a factor contributing to the development of chronic metabolic diseases, such as metabolic syndrome, diabetes, and the vascular complications of diabetes [32]. Since in developed countries the prevalence of diseases associated with AGEs is increasing, research on the inhibitors of advanced glycation end-product formation has received much interest in recent years [33–35]. Natural products in particular have received a lot of attention due to their high level of safety and affordability.

Antiglycation activity has so far been reported for many plant raw materials, such as green tea [36,37], ginger [38], marjoram [39], Japanese star anise [40], buckwheat [41], and mung bean [42]. It has been shown that for some plant extracts, such as extracts of *Scutellaria alpina* L. and *Solidago altissima* L., antiglycation activity correlates with the content of flavonoids, and it is flavonoids that are largely responsible, through various mechanisms, for the ability to inhibit the formation of AGEs [43]. Individual compounds for which antiglycation and *α-dicarbonyl* trapping activity has been demonstrated include quercetin [44], kaempferol [45], rutin [46], hyperoside [47], myricetin [11], phlorizin [31], and many others.

Considering the already known beneficial effects of rooibos tea on the cardiovascular system, its safety of use, and ubiquity, as well as its richness in flavonoids—compounds that may exhibit anti-α-dicarbonyls and anti-AGE activity—we chose this plant material to examine whether it could potentially be effective as an agent in preventing the formation of advanced glycation end products. For this purpose, in the first place, the qualitative composition of *A. linearis* extracts was determined and the flavonoid content of hydroethanolic extracts in green and red rooibos was quantified (GRE and RRE, respectively). Based on the results, compounds with different chemical structures—the C-glycosides of the dihydrochalcones, flavones, and flavanones—were selected and investigated in the antiglycation test (MGO and GO models) and the α-dicarbonyl trapping assay. This study also covered an investigation of the antiglycation and trapping activity of hydroethanolic extracts and infusions of green and red rooibos. The final step was to identify the adducts formed as a result of trapping and propose the potential structures formed, as well as to demonstrate how structural differences in flavonoid compounds affect trapping ability. Our previous research included the study of flavonoid *O*-glycosides (e.g., rutin, isoquercitrin, and hyperoside) in this regard, while in this work we focused on *C*-glycosidic compounds [47–49].

2.1. Phytochemical Profile of Rooibos Extracts

In an effort to understand potential differences in the biological activity of green (GR) and red rooibos (RR), both GR and RR were subjected to phytochemical composition analysis. For this purpose, their infusions and hydroethanolic extracts were prepared as described in Section 3.3 and analyzed using UHPLC–ESI–MS. Identified constituents along

with their *m/z* in negative ion mode and MS/MS fragments are presented in Table 1. The flavonoid profile was identical in both types of extracts. Therefore, further studies were conducted only with hydroethanolic extracts—GRE and RRE.

Table 1. UHPLC–ESI–MS data of red (RR) and green rooibos (GR) components in negative ion mode.

No.	Rt [min]	$[M-H]^-$	MS/MS	Error [ppm]	Compound	Rooibos Type	Source
1.	8.47	255.0504	193, 165	−0.31	Pisidic acid	RR	[50]
2.	13.76	341.0879	179, 135	1.87	1-*O*-caffeoylglucose	RR	[50]
3.	14.75	325.0929	119	1.64	(*E*)-PPAG	RR	[51]
4.	15.08	289.0713	203, 109	0.29	Epicatechin	RR	[50]
5.	17.98	609.1450	-	−0.93	Luteolin-6,8-di-*C*-glucoside or galactoside	RR, GR	[52]
6.	18.12	449.1089	329, 193, 135	1.13	Eriodictyol-*C*-glucoside 1	RR, GR	[52]
7.	18.82	449.1092	329, 193, 135	1.80	Eriodictyol-*C*-glucoside 2	RR, GR	[52]
8.	18.89	449.1085	329, 193, 135	0.24	Eriodictyol-*C*-glucoside 3	RR, GR	[52]
9.	19.15	449.1074	329, 193, 135	−1.98	Eriodictyol-*C*-glucoside 4	RR, GR	[52]
10.	19.40	579.1329	399, 369	−3.62	Luteolin-*C*-glucoside-*C*-arabinoside (carlinoside)	GR	[53]
11.	20.44	447.0937	357, 327	2.14	Luteolin-*C*-glucoside 1 (isoorientin or orientin)	RR, GR	[52]
12.	20.62	447.0937	357, 327	2.14	Luteolin-*C*-glucoside 2 (isoorientin or orientin)	RR, GR	[52]
13.	20.96	451.1254	331, 209	3.01	Aspalathin	RR, GR	S
14.	21.80	431.0994	341, 311	3.65	Apigenin-*C*-glucoside 1 (vitexin)	RR, GR	S
15.	21.97	609.1461	300/301	0.87	Queretin-3-*O*-robinobioside (bioquercetin, bioquercitrin)	RR	[50]
16.	22.19	431.0988	341, 311	2.26	Apigenin-*C*-glucoside 2 (isovitexin)	RR, GR	S
17.	22.29	609.1461	300/301	0.87	Queretin-3-*O*-rutinoside (rutin)	RR	S
18.	22.41	463.0883	300/301, 271	1.39	Quercetin-3-*O*-β-galactoside (hyperoside)	RR	S
19.	22.70	463.0878	300/301, 271, 255	0.31	Quercetin-3-*O*-β-glucoside (isoquercitrin)	RR	S
20.	23.30	435.1293	345, 315	0.42	Nothofagin	RR, GR	[53]
21.	24.87	451.1254	331, 209	3.01	Aspalathin isomer	RR, GR	[52]
22.	25.34	461.1077	446, 298/299 283/284	−1.49	Methyl-luteolin-*O*-glucoside or galactoside (e.g., chrysoeriol-*O*-glucoside/ galactoside)	RR	[54]
23.	25.65	493.1343	361, 331, 209	−0.6	Acetylaspalathin	RR	[50]
24.	27.55	287.0565	151, 135	3.25	Eriodictyol	GR	S
25.	29.13	285.0405	285	2.05	Luteolin	GR	S
26.	32.82	299.0560	284	1.45	Chrysoeriol	GR	S

Rt, retention time; S reference standard; RR, red rooibos; GR, green rooibos.

The infusions and hydroethanolic extracts from the fermented (RR) and unfermented (GR) raw material were rich in the dihydrochalcone C-glycosides aspalathin and nothofagin (peaks 21 and 20). Acetylaspalathin (peak 23) was observed only in RR. They also contained two pairs each of diastereoisomers of eriodictyol glucosides 1–4: (S)-6-C-, (R)-6-C, (S)-8-C-, and (R)-6-C-glucoside of eriodictyol (peaks 6–9). These compounds are formed by

the natural process of aspalathin oxidation during fermentation and storage, and they have a dark brown color [50]. They are responsible for the color change of rooibos leaves from green to red brown during rooibos tea production [55]. The most abundant group of flavonoids found in fermented A. linearis was flavones. In analyzed rooibos extracts, positional isomers of apigenin and luteolin C-glycosides were identified: vitexin/isovitexin (peaks 14, 16) and orientin/isoorientin (peaks 11, 12), as well as di-C-glycosides such as carlinoside (peak 10). Orientin and isoorientin are formed from aspalathin by the intermediate flavanones 8-C- and 6-C-glucosides of eriodictyol [56]. Similarly, vitexin and isovitexin are formed from nothofagin by the respective C-glucosides of naringenin. The aglycones of flavones, such as luteolin and chrysoeriol, and flavanones, mainly eriodictyol, were also identified in the unfermented plant material (peaks 24–26), whereas flavonol O-glycosides, such as bioquercetin (quercetin-3-O-robinobioside, peak 15), rutin, hyperoside, and isoquercitrin (peaks 17–19) were detected in higher amounts in fermented A. linearis. The main difference in the composition of both types of rooibos is the amount of aspalathin, which is significantly higher in the non-fermented plant material. In the fermented raw material, it undergoes oxidation processes and is converted to eriodictyol-C-glucosides. However, both types of rooibos tea are rich sources of flavonoids, whose beneficial effect on health is undeniable.

Only the presence of aspalathin, vitexin, isovitexin, rutin, isoquercitrin, hyperoside, eriodictyol, luteolin and chrysoeriol was confirmed by standards; the other compounds were tentatively identified based on the literature.

2.2. Quantification of Flavonoids

In the next step, we determined the content of the main identified flavonoids in GRE and RRE. The concentration of dihydrochalcones, flavanones, flavones, and flavonols and the sum of flavonoids (expressed as mg/100 mL of hydroethanolic extract or 1 g of raw plant material) were quantified by the HPLC–DAD method using the external standards. We also converted the obtained results into micromolar concentrations. Table 2 shows the results of the quantitative analysis of flavonoid content.

The hydroethanolic extract of green rooibos (GRE) contained mainly dihydrochalcones at 46 mg/100 mL (1019.4 μM/L), predominantly aspalathin at 41.2 mg/100 mL (911.3 μM/L), and nothofagin at 4.7 mg/100 mL (108.2 μM/L), as well as flavone derivatives at 13.3 mg/100 mL (301.9 μM/L), especially C-glucosides of luteolin. The hydroethanolic extract of red rooibos (RRE) was especially rich in flavone derivatives: isoorientin, orientin, vitexin, isovitexin, and aglycones at a total of 7.3 mg/100 mL (184 μM/L), and a similar concentration of dihydrochalcones at 2.9 mg/100 mL (65.2 μM/L) and flavanones at 2.5 mg/100 mL (55.3 μM/L). Flavonols (3-O-robinobioside, 3-O-β-galactoside, and 3-O-β-glucoside of quercetin) were minor components of GRE and RRE. The sums of the flavonoids found in the two raw materials were extremely different. While unfermented rooibos contained as much as 65.5 mg/100 mL (1443.1 μM/L) of flavonoids, fermented rooibos contained only 13.6 mg/100 mL (320.2 μM/L). Thus, GRE was approximately 4.5 times richer in flavonoids and 15.6 times richer in dihydrochalcones than RRE.

Since we only had standards for aspalathin, vitexin, isovitexin, hyperoside, isoquercitrin, apigenin, luteolin, and chrysoeriol, the remaining compounds were calculated semi-quantitatively using available standards as described in Table 2.

Table 2. Flavonoid content in hydroethanolic extracts from green and red rooibos (GRE and RRE; 1:100, *m/v*) expressed in mg per 100 mL of hydroethanolic extract and 1 g of dry plant material and μM/L. The main components are highlighted.

Compound	GRE				RRE			
	mg/100 mL or 1 g		μM		mg/100 mL or 1 g		μM	
	Mean	SD	Mean	SD	Mean	SD	Mean	SD
DIHYDROCHALCONES:	45.95	1.28	1019.42	28.34	2.93	0.12	65.16	2.69
Aspalathin	41.23	1.28	911.26	28.25	2.36	0.13	52.25	2.78
Nothofagin [1]	4.72	0.02	108.16	0.51	0.56	0.01	12.91	0.21
FLAVANONES:	1.86	0.22	41.39	4.93	2.49	0.10	55.27	2.29
Eriodictyol-6-*C*-glucoside [2]	1.07	0.14	23.85	3.04	1.55	0.10	34.36	2.31
Eriodictyol-8-*C*-glucoside [2]	0.79	0.17	17.54	3.85	0.94	0.03	20.91	0.57
FLAVONES:	13.26	0.14	301.87	3.31	7.30	0.35	184.04	4.53
Luteolin-6-*C*-glucoside (isoorientin) [3]	4.93	0.03	109.96	0.63	3.14	0.13	70.04	2.89
Luteolin-8-*C*-glucoside (orientin) [4]	4.09	0.07	91.30	1.64	2.35	0.08	52.52	1.72
Apigenin-8-*C*-glucoside (vitexin)	1.39	0.16	32.35	3.78	0.40	0.04	9.47	0.86
Apigenin-6-*C*-glucoside (isovitexin)	2.66	0.05	61.78	1.20	0.13	0.01	2.92	0.15
Luteolin	0.08	0.01	2.74	0.32	1.05	0.02	36.84	0.76
Apigenin + chrysoeriol [5]	0.10	0.01	3.74	0.24	0.33	0.05	12.25	1.96
FLAVONOLS:	4.44	0.19	80.44	3.16	0.91	0.04	15.73	0.59
Queretin-3-*O*-robinobioside (bioquercetin, bioquercitrin) [6]	2.98	0.20	48.95	3.23	0.82	0.03	13.44	0.50
Quercetin-3-*O*-β-galactoside (hyperoside)	0.72	0.04	15.23	0.76	0.06	0.01	1.36	0.23
Quercetin-3-*O*-β-glucoside (isoquercitrin)	0.75	0.02	16.25	0.43	0.04	0.00	0.94	0.04
SUM OF FLAVONOIDS	65.51	1.52	1443.13	33.64	13.63	0.53	320.20	7.92

[1] calculated as aspalathin; [2] calculated as eriodictyol-7-*O*-β-glucoside; [3] calculated as isovitexin; [4] calculated as vitexin; [5] calculated as apigenin; [6] calculated as rutin; $n = 5$; green color, green rooibos; red color, red rooibos; the darker the color, the higher the content.

2.3. Inhibition of Glycation by Rooibos Flavonoids and Related Compounds

In the present study, in vitro models using bovine albumin as the target protein and methylglyoxal or glyoxal as the glycation agent were used to evaluate the anti-AGE activity of the rooibos hydroethanolic extracts (GRE and RRE), aspalathin (ASP), vitexin (VT), isovitexin (IVT), eriodictyol (ER), and compounds with a similar structure, such as dihydrochalcone phloretin (PLT, phloretin is an aglycone of nothofagin) and phloroglucinol (PLG), which reflects the arrangement of the flavonoid A ring. Aminoguanidine (AG) and metformin (MET) were used as positive controls. AG is the most potent known inhibitor of non-enzymatic protein glycation [57], and MET is the first-choice drug in diabetic patients with a biguanide core; its anti-AGE activity has also been demonstrated in previous studies [58,59].

As shown in Figure 1, the results obtained in the two glycation models differed markedly from each other. In the model using methylglyoxal, all the tested compounds showed rather high inhibitory activity against AGE formation. The greatest antiglycation activity was observed for apigenin-C-glucosides, i.e., isovitexin (84.92 ± 0.36%) and vitexin (81.77 ± 4.67%), and these values exceeded the activity of the aminoguanidine (74.81 ± 2.16%) used as a reference. Moreover, phloretin (78.76 ± 1.23%), being a dihydrochalcone structurally similar to aspalathin, exhibited potent anti-AGE activity at the aminoguanidine level. The main component of green rooibos, aspalathin, demonstrated slightly lower activity in inhibiting AGEs at 60.62 ± 2.86%, but this result was still above the activity of metformin (52.28 ± 13.82%). Phloroglucinol, whose structure forms the core of rooibos dihydrochalcones, exhibited antiglycation activity similar to aspalathin (60.03 ± 4.84%). This compound is used as an antispasmodic drug in some countries and showed the ability to capture reactive carbonyl species in earlier studies [60]. Eriodictyol was the least effective in inhibiting MGO-mediated AGEs (42.98 ± 2.65%).

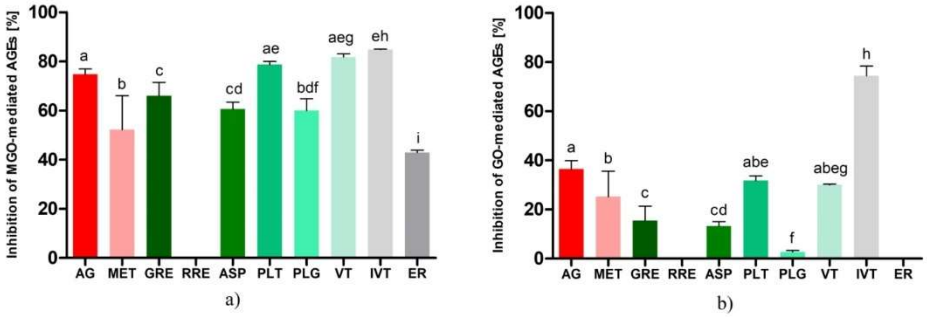

Figure 1. Antiglycation activity after seven days of incubation of bovine serum albumin with glycation agents (0.5 mM) and tested compound (1.5 mM) or hydroethanolic extracts (500 µL, DER 1:100) expressed as % inhibition of: (**a**) MGO mediated-AGE formation, (**b**) GO-mediated AGE formation. Results are representative of three experiments performed in triplicate ± SD. Values not sharing a common letter are significantly different at $p < 0.05$ according to Tukey's multiple comparisons test. Abbreviations: AG, aminoguanidine; MET, metformin; GRE, green rooibos extract; RRE, red rooibos extract; ASP, aspalathin; PLT, phloretin; PLG, phloroglucinol; VT, vitexin; IVT, isovitexin; ER, eriodictyol.

Among the rooibos products, using identical sample volumes and drug–extract ratios (500 µL, DRE 1:400), only the hydroethanolic extract from unfermented A. linearis (GRE) demonstrated inhibitory activity against bovine albumin glycation in a model with MGO. The inhibitory activity of GRE was 66.06 ± 5.26%, which was comparable to that of aspalathin (difference not statistically significant).

In the glyoxal-induced glycation model, isovitexin was also the most potent antiglycation agent (81.94 ± 0.63%), and its inhibitory potential against AGE formation was more than two-fold higher than that of aminoguanidine (36.49 ± 3.42%) and three-fold higher than that of metformin (25.24 ± 10.37%). The differences were statistically significant. The glycation-inhibitory activity of phloretin and vitexin was similarly lower at 31.75 ± 1.94% and 30.06 ± 1.17%, respectively. Aspalathin revealed a glycation inhibitory effect of 13.32 ± 1.7%. The activity of phloroglucinol was marginal (2.72 ± 0.54%), and no inhibitory effect on glyoxal-triggered AGE formation was observed for eriodictyol.

In the model with GO as the glycation agent, as in the previous model with MGO, only GRE among the extracts tested exhibited an inhibitory effect on protein glycation. The inhibitory effect of the hydroethanolic extract of unfermented rooibos was observed at 15.58 ± 5.53%.

The beneficial effect of A. linearis in reducing glycation damage was reported by Kamakura et al. [61], who found that green rooibos extract effectively reduced AGE-induced reactive oxygen species levels. According to the work of Pringle et al. [62] an extract of unfermented A. linearis demonstrated the same glycation inhibition potential (about 50%) as aminoguanidine, the positive control in a glycation model with BSA as the target protein and glucose as the trigger for the glycation process. In our experiment, GRE activity was slightly but statistically significantly lower than that of aminoguanidine. Moreover, the fermented rooibos extract failed to display any antiglycation activity, whereas the same study by Pringle et al. [62] reported that fermented rooibos extract was superior to green rooibos extract in glycation inhibitory activity. Furthermore, in a study conducted by Kinae et al. [63], fermented red rooibos extract effectively inhibited the formation of glycated albumin by nearly 30%. In examining the antidiabetic potential of fermented A. linearis, these authors found a significant reduction in AGEs in the plasma of rats with streptozotocin-induced diabetes in response to alkaline and aqueous extract. Differences in the biological activity of fermented and unfermented rooibos, as well as their extracts, can be

attributed to different extraction techniques and the content of individual active ingredients in the raw plant material depending on the place of harvest and the storage conditions.

According to our qualitative analysis of extracts, unfermented rooibos contained about 4.5 times more flavonoids than fermented rooibos. The most significant difference in composition was the high concentration of dihydrochalcones in the unfermented raw material (about 15.6 times higher than in the fermented one). This leads to the conclusion that the antiglycation activity of rooibos tea may be mainly attributed to the presence of dihydrochalcones, more precisely to the predominant component aspalathin. This conclusion seems to be supported by the fact that in both glycation models with MGO and GO used in the experiment, the activity of the green rooibos extract corresponded to the antiglycation activity of aspalathin (for MGO it was 66% vs. 60% and for GO it was 15% vs. 13%).

The individual compound that showed the strongest ability to inhibit AGEs in both models we tested was isovitexin. Kim et al. [64] reported the relatively high activity of isovitexin toward the inhibition of non-enzymatic protein glycation (IC50 = 85.2 μM, while IC50 for aminoguanidine used as a reference compound was 961 μM), additionally revealing the strong inhibitory activity of this compound against aldose reductase, which may be advantageous in the context of the prevention of diseases associated with high concentrations of AGEs. In our experiment, vitexin, particularly in the model with MGO as a glycation agent, exhibited high activity. These results are comparable to data from glycation models using MGO and glucose as inducers of protein glycation modifications. Peng et al. [42] reported more than 85% efficacy of vitexin in inhibiting AGEs in both in vitro models mentioned above. Drygalski et al. [65] reported recently on the antiglycation properties of phloroglucinol and found that it inhibited MGO- and GO-induced protein glycation by approximately 54% in both systems. Our results partially confirm these data in the methylglyoxal model, but such high activity was not observed in the used glyoxal model. These differences may be due to variations in the used concentrations and incubation conditions. The results for eriodictyol were consistent with those published by Liu et al. [66], who observed 40% inhibitory activity against methylglyoxal-induced AGEs. Under the conditions of our experiment, eriodictyol did not show inhibition against GO-mediated AGEs; data in the literature do not provide information on the activity of eriodictyol in this particular model. The percentage differences in the activity of each compound between the MGO-BSA and GO-BSA models were notable. This could be associated with the fact that during the process of the non-enzymatic glycation of proteins different types of AGEs are synthesized; some of them have fluorescence (e.g., PEN—pentosidine) while others do not show fluorescence properties (e.g., CML—carboxymethyl-lysine) [67]. The amounts and proportions in which they are produced depend on the glycation agent and the time of reaction. In a study by Nevin et al. [68], it was demonstrated that a model using human sperm as the matrix for glycation and GO as the inducer resulted in a statistically significantly higher amount of CML without fluorescent properties than when MGO was used as the trigger of glycation. In our experiment, we measured fluorescence. Therefore, it is likely that the activity results were lower in the model with glyoxal because some of the AGEs formed could not be included in the measurement. This should be considered a limiting factor of our study.

2.4. α-Dicarbonyl Compound Trapping and Adduct Analysis

The green and red rooibos hydroethanolic extracts (GRE and RRE), as well as selected individual flavonoids identified in the extracts and related compounds, were evaluated for α-dicarbonyl uptake capacity. After 1 h of incubation, the formation of adducts was investigated using the UHPLC–ESI–MS method. The Extract Ion Chromatogram (EIC) mode was used to search for pseudomolecular ions enlarged by the mass of one or two molecules of methylglyoxal (72 or 144 Da) and, similarly, glyoxal (58 and 116 Da). In this study, phloretin and phloroglucinol were used as reference compounds with recognized activity for the direct trapping of reactive α-dicarbonyls [31,69] A summary of the results

including retention times, *m/z*, and the identification of adducts is shown in Table 3 for the reaction with methylglyoxal, and in Table 4 for the reaction with glyoxal. The source indicates whether adducts were observed in the reaction with extract or standard.

Table 3. Adducts of methylglyoxal and investigated compounds formed after 1 h of incubation in pH 7.4 phosphate buffer solution at 37 °C.

Compound	Source	R_t [min]	$[M-H]^-$	Error [ppm]	MGO-Adduct/Precursor
Aspalathin	S	20.99	451.1254	3.01	Aspalathin
		19.85	523.1475	4.45	mono-MGO-aspalathin a
		21.45	523.1473	4.07	mono-MGO-aspalathin b
	GRE	20.99	451.1254	3.01	Aspalathin
		19.85	523.1475	4.45	mono-MGO-aspalathin a
		21.45	523.1473	4.07	mono-MGO-aspalathin b
		25.65	523.1469	3.31	mono-MGO-aspalathin c
		26.93	523.1449	−0.51	mono-MGO-aspalathin d
Nothofagin	GRE	23.33	435.1293	0.42	Nothofagin
		21.95	507.1519	3.24	mono-MGO-nothofagin a
		23.43	507.1512	1.86	mono-MGO-nothofagin b
		28.05	507.1521	3.63	mono-MGO-nothofagin c
Vitexin	S	21.81	431.0994	3.65	Vitexin
		20.55	503.1205	3.07	mono-MGO-vitexin a
		20.86	503.1208	3.66	mono-MGO-vitexin b
Isovitexin	S	22.19	431.0988	2.26	Isovitexin
		20.82	503.1191	0.29	mono-MGO-isovitexin a
		21.50	503.1185	−0.90	mono-MGO-isovitexin b
Eriodictyol	S	27.51	287.0565	3.25	Eriodictyol
		21.50	359.0772	1.40	mono-MGO-eriodictyol a
		21.57	359.0771	1.28	mono-MGO-eriodictyol b
		22.46	359.0777	2.80	mono-MGO-eriodictyol c
		24.67	359.0775	2.24	mono-MGO-eriodictyol d
Phloretin	S	31.59	273.0780	2.56	Phloretin
		27.05	417.1197	2.73	di-MGO-phloretin a
		27.46	417.1198	2.97	di-MGO-phloretin b
		28.82	345.0993	1.07	mono-MGO-phloretin
Phloroglucinol	S	2.02	125.0245	4.79	Phloroglucinol
		4.28	197.0549	2.02	mono-MGO-phloroglucinol a
		8.43	269.0813	−2.97	di-MGO-phloroglucinol a
		14.56	341.1067	−1.64	tri-MGO-phloroglucinol a
		14.82	269.0814	−2.60	di-MGO-phloroglucinol b
		15.01	341.1069	−1.05	tri-MGO-phloroglucinol b
		16.71	269.0812	−3.34	di-MGO-phloroglucinol c
		17.32	197.0540	−2.53	mono-MGO-phloroglucinol b

S, standard; GRE, green rooibos hydroethanolic extract; letters of the alphabet (a–d) represent different isomers of the same compound.

First, the ability to trap methylglyoxal and glyoxal was tested on reference compounds (phloretin, phloroglucinol) and individual flavonoids identified in the rooibos extracts (aspalathin, vitexin, isovitexin, and eriodictyol). The same tests were performed with GRE and RRE.

In the 1 h reaction of phloroglucinol with methylglyoxal, the formation of as many as seven new peaks on the chromatogram was observed. Two of these peaks with *m/z* 197 were identified as mono-MGO-phloroglucinol. This was confirmed by the presence of daughter ions with *m/z* 125 corresponding to phloroglucinol $[M–72–H]^-$. Another three chromatographic peaks at *m/z* 269 were recognized as isomers of di-MGO-phloroglucinol. Their daughter ions with *m/z* 179 suggested the loss of one molecule of methylglyoxal

and one molecule of water [M–72–18–H]$^-$, while the ions with *m/z* 125 corresponded to the precursor ion, indicating the dissociation of two MGO molecules [M–144–H]$^-$. The remaining two chromatographic peaks were annotated as tri-MGO-phloroglucinol isomers because the *m/z* of ions matched that of phloroglucinol increased by three methylglyoxal molecules and was 341. A similar decomposition pattern to that of di-MGO-phloroglucinol was observed herein, as ions at *m/z* 251 corresponded to tri-MGO-phloroglucinol with a loss of methylglyoxal and water [M–72–18–H]$^-$. In addition, a characteristic ion at *m/z* 125 was also evident, representing the deprotonated phloroglucinol ion and implying the detachment of three methylglyoxal molecules [M–216–H]$^-$. In the reaction of phloroglucinol with glyoxal, only two additional peaks appeared on the chromatogram after one hour. The first one was assigned as di-GO-phloroglucinol since its pseudo-molecular ion was at *m/z* 241, which is equivalent to the phloroglucinol precursor increased by 116 Da, meaning two GO molecules. Meanwhile, the second peak was designated as mono-GO-phloroglucinol since its *m/z* of 183 analogously corresponded to the attachment by phloroglucinol of one glyoxal molecule (58 Da). Mass spectra of the adducts formed by phloroglucinol and MGO/GO are shown in Figure 2 and the proposed chemical structures are shown in Figure 3.

Table 4. Adducts of glyoxal and investigated compounds formed after 1 h of incubation in pH 7.4 phosphate buffer solution at 37 °C.

Compound	Source	R_t [min]	[M − H]$^-$	Error [ppm]	GO-Adduct/Precursor
Aspalathin	S	20.99	451.1254	3.01	Aspalathin
		18.68	509.1311	3.10	mono-GO-aspalathin a
		19.81	509.1310	2.90	mono-GO-aspalathin b
		24.86	509.1316	4.08	mono-GO-aspalathin c
	GRE	20.99	451.1254	3.01	Aspalathin
		18.68	509.1314	3.69	mono-GO-aspalathin a
		19.81	509.1320	4.07	mono-GO-aspalathin b
		24.86	509.1318	4.47	mono-GO-aspalathin c
Nothofagin	GRE	23.33	435.1293	0.40	Nothofagin
Vitexin	S	21.81	431.0994	3.65	Vitexin
		19.03	489.1033	−0.01	mono-GO-vitexin a
		19.19	489.1044	2.23	mono-GO-vitexin b
Isovitexin	S	22.19	431.0988	2.26	Isovitexin
Eriodictyol	S	27.51	287.0565	3.25	Eriodictyol
		21.56	345.0813	0.73	mono-GO-eriodictyol a
		22.13	345.0810	−0.13	mono-GO-eriodictyol b
Phloretin	S	31.59	273.0780	2.56	Phloretin
		26.88	331.0833	4.59	mono-GO-phloretin
Phloroglucinol	S	2.02	125.0245	4.79	Phloroglucinol
		8.15	241.0482	2.9	di-GO-phloroglucinol a
		13.79	183.0366	1.36	mono-GO-phloroglucinol a

S, standard; GRE, green rooibos extract; letters of the alphabet (a–c)represent different isomers of the same compound.

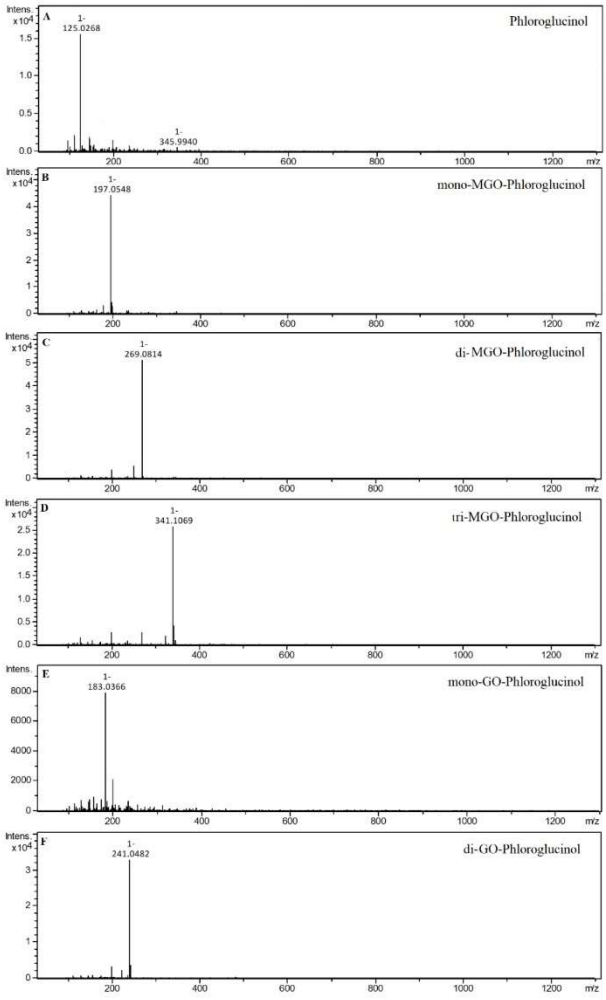

Figure 2. Mass spectra of phloroglucinol and its methylglyoxal/glyoxal adducts after 1 h of incubation in pH 7.4 phosphate buffer solution at 37 °C; (**A**), phloroglucinol; (**B**), mono-MGO-phloroglucinol; (**C**), di-MGO-phloroglucinol; (**D**), tri-MGO-phloroglucinol; (**E**), mono-GO-phloroglucinol; (**F**), di-GO-phloroglucinol. Other isomers are also possible.

The phloroglucinol structure determines the trapping reaction of α-dicarbonyls—the arrangement of -OH groups in the benzene ring in the meta position relative to each other provides the conditions for MGO/GO addition. The arrangement of phloroglucinol present in the structure of dihydrochalcones and other flavonoids—the A-ring with unsubstituted -OH groups (2 or 3) and unsubstituted carbons between them—is essential for the trapping activity of compounds. This conclusion is in line with the findings of a work by Liu and Gu [70]. They described the trapping ability of phloroglucinol derivatives as a metabolite of algae from the species *Fucus vesiculosus* L., obtaining results coinciding with our results. The authors of another publication describing the structural requirements for flavonoids to trap methylglyoxal stated that the A-ring is essential for MGO uptake, and the hydroxyl group

at C-5 of the A-ring is strongly supportive of the methylglyoxal trapping capacity [71]. In their earlier work, the same authors indicated that the two unsubstituted carbons in ring A at positions 2′ and 4′ were the primary active sites for chalcones to trap MGO [31].

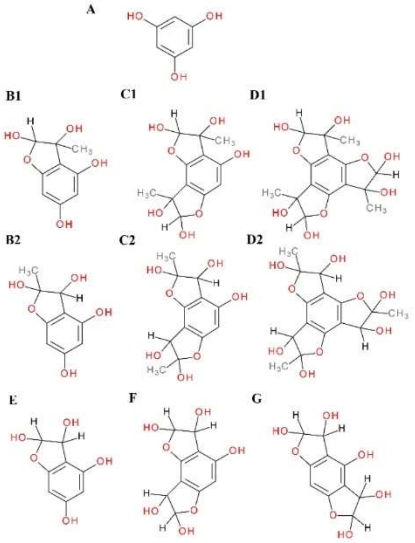

Figure 3. Proposals for chemical structures of adducts formed in the reaction of phloroglucinol with methylglyoxal/glyoxal after 1 h of incubation in pH 7.4 phosphate buffer solution at 37 °C; (**A**), phloroglucinol; (**B1**), hemiacetal form of mono-MGO-phloroglucinol; (**B2**), hemiketal form of mono-MGO-phloroglucinol; (**C1**), hemiacetal form of di-MGO-phloroglucinol; (**C2**), hemiketal form of di-MGO-phloroglucinol; (**D1**), hemiacetal form of tri-MGO-phloroglucinol; (**D2**), hemiketal form of tri-MGO-phloroglucinol; (**E**), mono-GO-phloroglucinol; (**F**), di-GO-phloroglucinol isomer a; (**G**), di-GO-phloroglucinol isomer b. Other isomers are also possible.

The trapping activity of MGO and GO by phloroglucinol differed. Phloroglucinol inhibited MGO-triggered glycation at the level of aspalathin and GRE and was more effective in this regard than was metformin. However, the compound's ability to inhibit the formation of glycation end products with GO was negligible—only a few percent. The literature reports that phloroglucinol also exhibits antioxidant properties in the DPPH assay favorable for antiglycation activity [70], although there are also reports that phloroglucinol did not reduce H_2O_2-induced intracellular protein oxidation or carbonylation [72].

Dihydrochalcone with known trapping properties served as a reference compound in the experiment; phloretin produced three new chromatographic peaks after 1 h of incubation with methylglyoxal. Two of these peaks, whose pseudo-molecular masses were equal to *m/z* 417, were identified as di-MGO-phloretin, as their $[M–H]^-$ corresponded to the phloretin deprotonated ion (*m/z* 273) increased by 144 Da (two MGO). The remaining formed adduct had an ion *m/z* of 345 and was designated as mono-MGO-phloretin since its mass corresponded to that of phloretin after the attachment of one MGO molecule. In the one-hour reaction of phloretin with glyoxal, the formation of a single monoadduct was observed with *m/z* equal to 331. The ion of the phloretin *m/z* 273 corresponded to the mass of the mono-GO-phloretin adduct minus the mass of one molecule of glyoxal $[M–58–H]^-$. This is consistent with previous reports of phloretin's ability to trap MGO and GO and confirms that the experimental conditions provided the potential for adduct formation. Mass spectra of the adducts formed by phloretin and MGO/GO are shown in Figure 4.

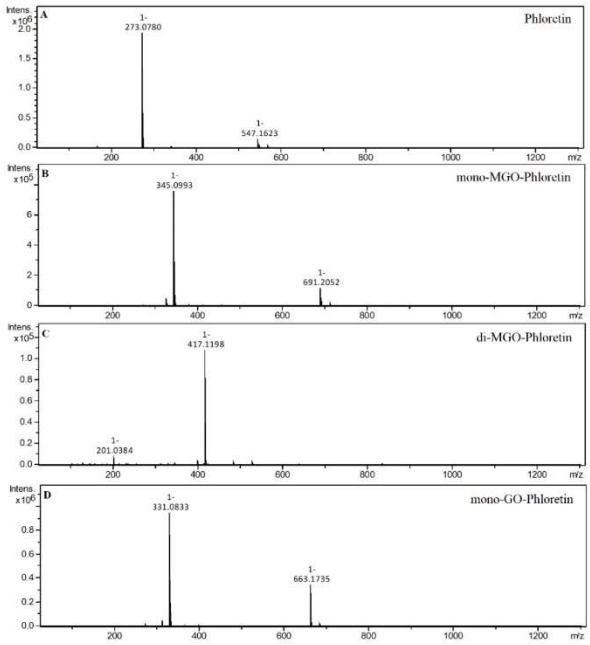

Figure 4. Mass spectra of phloretin and its methylglyoxal/glyoxal adducts after 1 h of incubation in pH 7.4 phosphate buffer solution at 37 °C; (**A**), phloretin; (**B**), mono-MGO-phloretin; (**C**), di-MGO-phloretin; (**D**), mono-GO-phloretin. Other isomers are also possible.

In the reaction of aspalathin with methylglyoxal, the formation of two new peaks on the chromatogram was observed after 1 h of reaction. Both were identified as mono-MGO-aspalathin due to an *m/z* ion mass of 523 corresponding to that of the aspalathin ion plus one molecule of methylglyoxal. In addition, the degradation profile corresponded to that observed for aspalathin in the extract, with the presence of daughter ions at *m/z* 505 $[M–18–H]^-$ and 415 $[M–36–72–H]^-$ reflecting the loss of one water molecule or two water molecules and one methylglyoxal molecule, respectively (described above). The presence of as many as four mono-MGO-aspalathin adducts was identified in GRE; two of them were identical to the aspalathin standard and the other two appeared on the chromatogram at around 26 and 27 min. These were probably isomeric forms, which were formed by different ways of attaching MGO to the phloroglucinol ring of aspalathin at the C-5′ position and the -OH group at the 4′ or 6′ position or the presence of an aspalathin isomer in the extract (see Table 1). In addition, the heterocyclic rings formed may have had a hemiketal or hemiacetal structure. In the reaction of aspalathin with glyoxal, after incubation, similarly to the reaction of GRE and glyoxal the formation of three chromatographic peaks with a pseudo-molecular ion at *m/z* 509 was observed, which corresponded to the attachment of one molecule of glyoxal and the formation of mono-GO-adducts $[451 + 58–H]^-$. To the best of our knowledge, this is the first time that the trapping ability of methylglyoxal and glyoxal has been described for aspalathin. The example LC chromatograms of aspalathin and its MGO/GO adducts are shown in Figure 5. Mass spectra of the adducts formed by aspalathin and MGO/GO are shown in Figure 6 and the proposed chemical structures are shown in Figure 8.

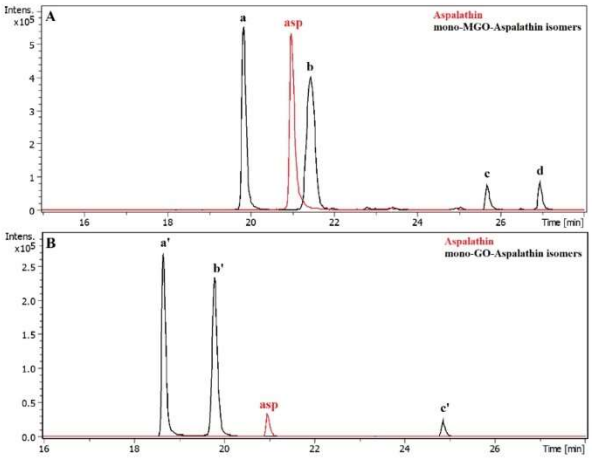

Figure 5. Representative LC chromatograms of aspalathin and its methylglyoxal (**A**)/glyoxal (**B**) adducts after 1 h of incubation in pH 7.4 phosphate buffer solution at 37 °C; (**A**), mono-MGO-aspalathin; (**B**) mono-GO-aspalathin; a, mono-MGO-aspalathin a; b, mono-MGO-aspalathin b; c, mono-MGO-aspalathin c; d, mono-MGO-aspalathin d; a′, mono-GO-aspalathin a; b′, mono-GO-aspalathin b; c′, mono-GO-aspalathin c; asp, aspalathin.

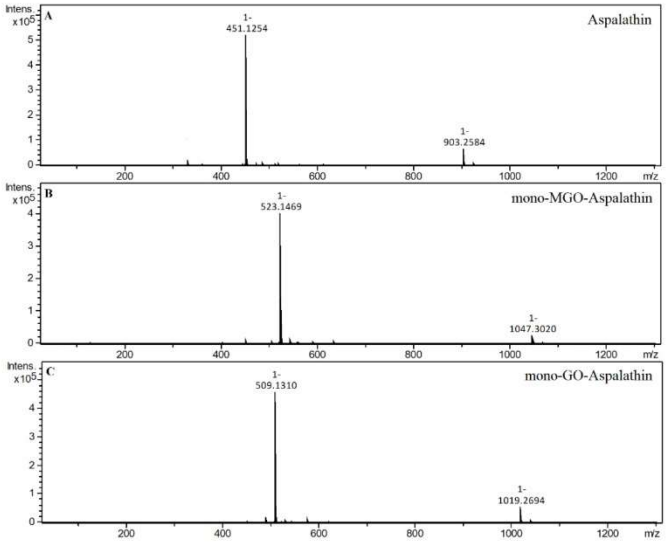

Figure 6. Mass spectra of aspalathin and its methylglyoxal/glyoxal adducts after 1 h of incubation in pH 7.4 phosphate buffer solution at 37 °C; (**A**), aspalathin; (**B**), mono-MGO-aspalathin; (**C**), mono-GO-aspalathin.

The hydroethanolic extracts of green and red rooibos were also tested for their ability to trap MGO and GO. Only in the unfermented rooibos extracts was the ability of individual compounds to form adducts with methylglyoxal and glyoxal observed, and the fermented rooibos extracts did not demonstrate trapping properties.

After one hour of incubation of the GRE and methylglyoxal, the appearance of new peaks on the chromatogram was observed. Under the experimental conditions, monoadducts with MGO were formed by aspalathin and nothofagin. The reaction of methylglyoxal and aspalathin proceeded in the same way as for the standard described above, although after 1 h of incubation as many as four monoadducts of aspalathin and MGO were formed (see Table 3). The formation of adducts in the reaction with glyoxal, on the other hand, proceeded for aspalathin in exactly the same manner with both the extract and the single compound samples (Table 4).

Since we did not use a nothofagin standard, observations were made only for the nothofagin contained in the green rooibos extract. In the reaction with methylglyoxal, four new chromatographic peaks were formed, labeled as mono-MGO isomers of nothofagin. Their *m/z* was 507, which corresponded to the mass of the precursor ion *m/z* 436 increased by the mass of one molecule of methylglyoxal (72 Da). To the best of our knowledge, this is the first time that the trapping ability of methylglyoxal has been described for nothofagin. Mass spectra of the adducts formed by nothofagin and MGO are shown in Figure 7 and the proposed chemical structures are shown in Figure 8. In this experiment, nothofagin contained in the green rooibos extract was not observed to form adducts after 1 h of incubation with glyoxal.

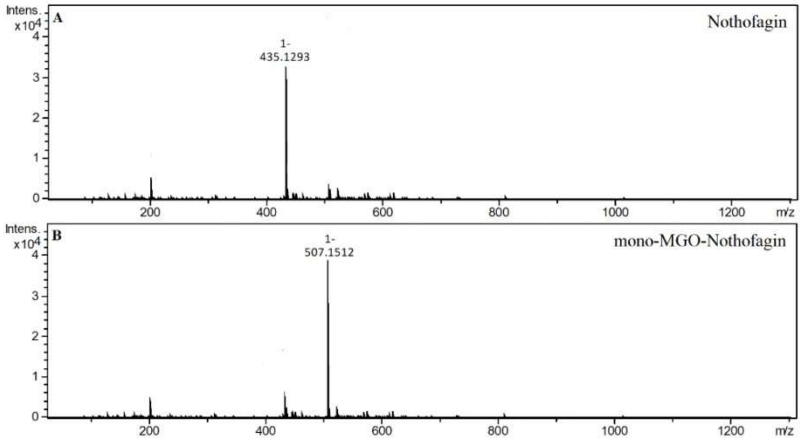

Figure 7. Mass spectra of nothofagin and its methylglyoxal adduct after 1 h of incubation in pH 7.4 phosphate buffer solution at 37 °C; (**A**), nothofagin; (**B**), mono-MGO-nothofagin.

The *C*-glycosylated flavones vitexin and isovitexin in a 1 h reaction with methylglyoxal produced two new chromatographic peaks, each with $[M - H]^-$ at 503, suggesting that under the experimental conditions two mono-adducts each were formed for vitexin and isovitexin. These deprotonated ions corresponded to a vitexin and isovitexin precursor ion mass of 431 plus one molecule of methylglyoxal (72 Da). The decay spectrum revealed the presence of ions 413 and 311 formed by the loss of fragments with 90 Da and 120 Da, respectively, from the cross-ring cleavages of the hexose unit. This indicates that in the cleavage, the glucose moiety is degraded first rather than the heterocyclic structure of the methylglyoxal adduct. Mass spectra of the adducts formed by vitexin and isovitexin and MGO/GO are shown in Figures 9 and 10, respectively. The proposed chemical structures of the adduct are shown in Figure 11 for vitexin and Figure 12 for isovitexin.

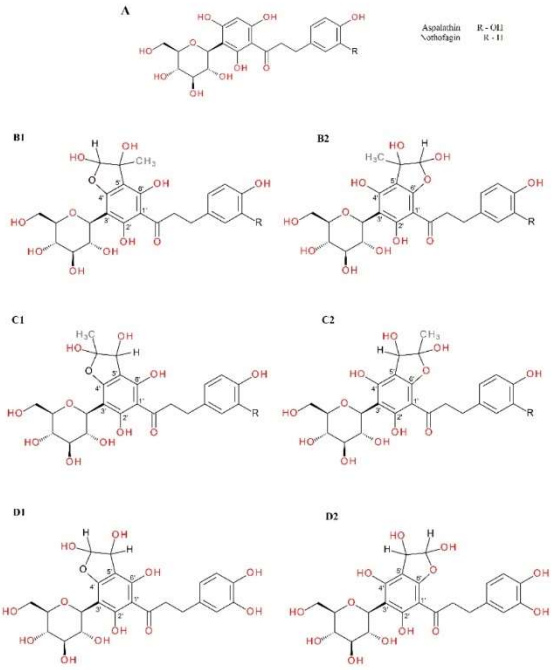

Figure 8. Proposals for chemical structures of adducts formed in the reaction of aspalathin/nothofagin with methylglyoxal/glyoxal after 1 h of incubation in pH 7.4 phosphate buffer solution at 37 °C; (**A**), aspalathin/nothofagin; (**B1**,**B2**), hemiacetal forms of mono-MGO-aspalathin/nothofagin; (**C1**,**C2**), hemiketal forms of mono-MGO-aspalathin/nothofagin; (**D1**,**D2**), mono-GO-aspalathin isomers. Other isomers are also possible.

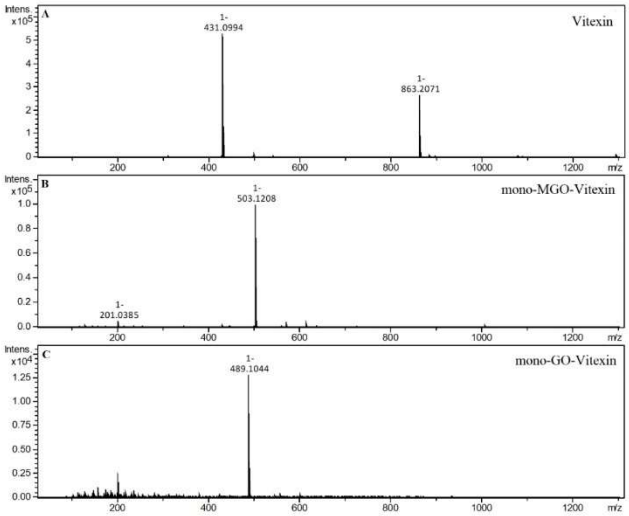

Figure 9. Mass spectra of vitexin and its methylglyoxal/glyoxal adducts after 1 h of incubation in pH 7.4 phosphate buffer solution at 37 °C; (**A**), vitexin; (**B**), mono-MGO-vitexin; (**C**), mono-GO-vitexin.

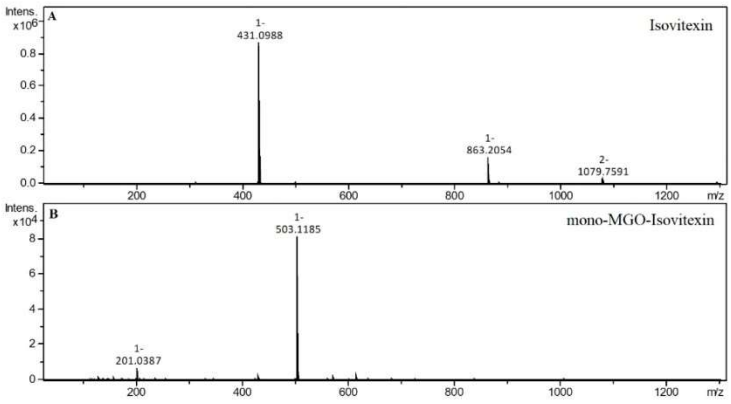

Figure 10. Mass spectra of isovitexin and its methylglyoxal adduct after 1 h of incubation in pH 7.4 phosphate buffer solution at 37 °C; (**A**), isovitexin; (**B**), mono-MGO-isovitexin.

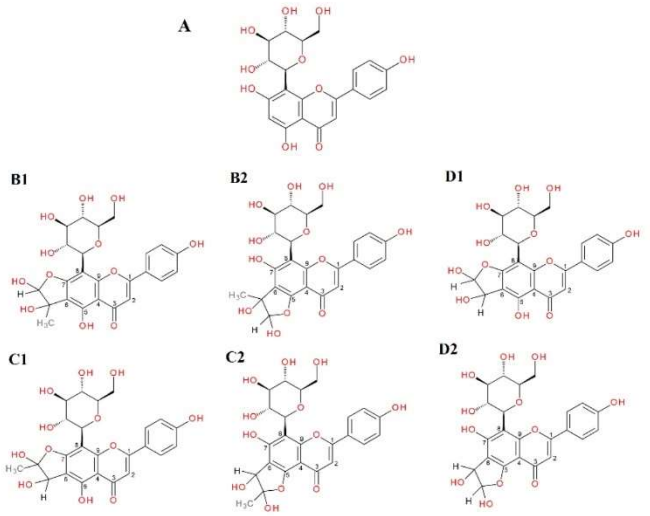

Figure 11. Proposals for chemical structures of adducts formed in the reaction of vitexin with methylglyoxal/glyoxal after 1 h of incubation in pH 7.4 phosphate buffer solution at 37 °C; (**A**), vitexin; (**B1**,**B2**), hemiacetal forms of mono-MGO-vitexin; (**C1**,**C2**), hemiketal forms of mono-MGO-vitexin; (**D1**,**D2**), mono-GO-vitexin isomers. Other isomers are also possible.

Previous studies on vitexin and isovitexin in MGO trapping reported inconsistent results. A study by Peng et al. [42] showed that vitexin and isovitexin lack the ability to direct methylglyoxal capture. However, another more recent study by Ni et al. [73] found that vitexin binds methylglyoxal to form adducts.

In the reaction of vitexin with glyoxal, two new peaks appeared on the chromatogram after one hour. Both were assigned as mono-GO-vitexin since their deprotonated ion at *m/z* 489 was equivalent to the mass of the vitexin precursor ion (*m/z* 431) increased by 58 Da, meaning one molecule of glyoxal.

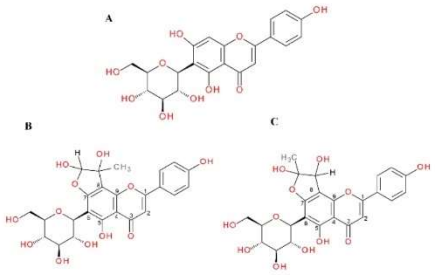

Figure 12. Proposals for chemical structures of adducts formed in the reaction of isovitexin with methylglyoxal after 1 h of incubation in pH 7.4 phosphate buffer solution at 37 °C; (**A**), isovitexin; (**B**), hemiacetal form of mono-MGO-isovitexin; (**C**) hemiketal form of mono-MGO-isovitexin. Other isomers are also possible.

In this experiment, isovitexin was not observed to form adducts after incubation with glyoxal. Both vitexin and isovitexin have one position each in the A-ring where the dicarbonyl MGO/GO can be attached; these are the C-6 or C-8 sites, respectively. If, as in the case of vitexin, there is a C-6 carbon, then two adducts can be formed with an -OH group at C-5 or C-7 with two forms of hemiketal or hemiacetal for each version. For isovitexin with an unsubstituted C-8 position, adducts are formed only with an -OH group at C-7 and again with two forms of hemiketal and hemiacetal. Therefore, isovitexin can have only two mono-adducts, while vitexin hypothetically can produce as many as four. Although it is most likely that only two are preferentially predominant, we do not actually know which. Isovitexin did not produce adducts with GO, so the C-8 position appears to be less favored, most likely due to differences in the C-8 surroundings and substituents at adjacent positions (-OH group free or in the C-ring heterocyclic system). As indicated, these reactions lead to the formation of at least several different stereoisomers of adducts of specific compounds with α-DCs, and some of them are preferentially formed due to their favorable electron configuration. At this stage of research, however, we are not able to determine their chemical structures specifically. For this purpose, further structural studies are necessary.

After the incubation of MGO with the only representative flavanones, i.e., eriodictyol, four additional chromatographic peaks were noted on the chromatogram labeled as mono-MGO-eriodictyol. Their pseudo-molecular ions were at *m/z* 359, which corresponds to the ion of the precursor *m/z* 287 enlarged by 72 Da (one molecule of MGO). For the reaction of eriodictyol with glyoxal, two additional peaks appeared on the chromatogram after 1 h of incubation. Both of these peaks were identified as mono-GO-eriodictyol (*m/z* 345, which corresponds to the mass of the eriodictyol ion increased by the mass of one glyoxal molecule). In *A. linearis*, C-glycosides of eriodictyol have been identified; according to the literature, glucose is substituted into the eriodictyol in a manner similar to that observed in the C-glycosides of apigenin and luteolin (at the C-6 or C-8 position of the A-ring). We did not have standards for specific eriodictyol-C-glycosides, so we used aglycone; however, based on the results for vitexin and isovitexin, it can be assumed that the eriodictyol-C-glycosides found in rooibos may also at least partially possess MGO- and GO-trapping properties. Further studies are needed for confirmation. Mass spectra of the adducts formed by eriodictyol and MGO/GO are shown in Figure 13.

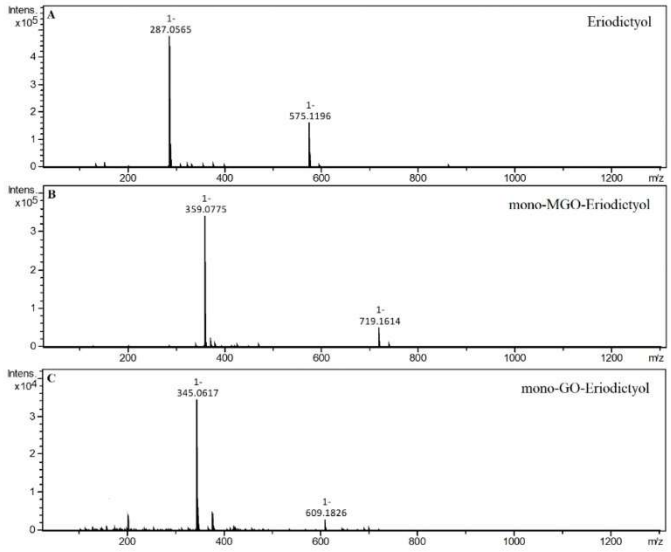

Figure 13. Mass spectra of eriodictyol and its methylglyoxal/glyoxal adducts after 1 h of incubation in pH 7.4 phosphate buffer solution at 37 °C; (**A**), eriodictyol; (**B**), mono-MGO-eriodictyol; (**C**), mono-GO-eriodictyol.

Although three different subgroups of flavonoids—dihydrochalcones (aspalathin, nothofagin, and phloretin), flavones (vitexin and isovitexin) and flavanones (eriodictyol)—show different C-ring structures, all can effectively capture methylglyoxal, indicating that the C-ring of flavonoids may not play an important role in trapping MGO. By contrast, for nothofagin and isovitexin, we did not observe the ability to form adducts with glyoxal, although the two compounds have a different C-ring structure: Nothofagin as a dihydrochalcone has an open C-ring, while isovitexin as a flavone has a C-ring in closed form.

The structure of the B-ring does not seem to play a key role in the ability to trap α-dicarbonyls. In our test, both aspalathin with two -OH groups and phloretin and nothofagin possessing only one -OH group in the B-ring exhibited the ability to trap methylglyoxal. However, only phloretin was able to form diadducts with MGO, undoubtedly influenced by the fact that it does not have a substituted C-glucose in the A-ring. The importance of the A-ring structure of flavonoids was described above.

In summary, A. linearis extracts were rich in dihydrochalcones, flavanones, flavones, and flavonols. However, green rooibos extract had several times more flavonoids—especially aspalathin and nothofagin—than red rooibos extract. In the antiglycation assay, isovitexin demonstrated the highest activity in both glycation models with MGO and GO, and its activity was statistically significantly higher than that of aminoguanidine, a compound considered one of the most potent inhibitors of non-enzymatic glycation. Only green rooibos extract inhibited the glycation process at a level comparable to isolated aspalathin (no statistically significant difference), which suggests that it is aspalathin as the main component found in GR and GRE in the greatest amounts that determines the antiglycation activity. Indeed, red rooibos did not display the ability to inhibit protein glycation in any of the models. Some compounds tested, despite their ability to trap GO, showed no activity against glyoxal-induced glycation inhibition (e.g., eriodictyol). This was likely influenced by factors such as pH, reaction time, process temperature, and the fact that glyoxal is present in hydrated forms in solution (described in detail below). Others, despite their lack of GO-trapping ability, were able to inhibit the glyoxal-triggered glycation process, perhaps due to the strong antioxidant properties that are a component of the

antiglycation effect. This study revealed that under the experimental conditions, all tested compounds demonstrated activity towards the direct trapping of methylglyoxal, while only aspalathin, vitexin, and eriodictyol exhibited the ability to trap glyoxal. Phloretin and phloroglucinol used as reference compounds showed trapping activity against both α-dicarbonyls. No MGO or GO adducts were observed for RRE, which is probably due to low concentrations of flavonoids in the extract, compared to GRE (320.2 μM/L vs. 1443.1 μM/L). In GRE, only dihydrochalcones were a source of MGO (aspalathin and nothofagin) and GO (aspalathin) adducts.

It is known that non-enzymatic antiglycation activity usually results from a number of different mechanisms of reaction. The literature reports that components of the inhibitory effect on the glycation process include antioxidant activity, the ability to chelate transition metals, and the capacity of compounds to trap α-DCs [39]. Frequently, these activities occur synergistically, especially in the group of natural compounds known as flavonoids. An example of a compound acting through all of these mechanisms is quercetin—well known in the context of inhibiting the glycation process, which is characterized by very strong antiradical activity, chelating properties, and the ability to trap methylglyoxal and glyoxal [44,74]. Given the above, it is important to keep in mind that often compounds exhibiting only some of these mechanisms may ultimately fail to exert a strong antiglycation effect, and sometimes compounds characterized by only one of these mechanisms may act as a potent antiglycation agent. This seems to be the case with isovitexin, which has proven most potent as an inhibitor of GO-induced glycation while lacking the ability to trap it. However, isovitexin has both the ability to chelate transition metals and strong antioxidant properties, which taken together can result in a strong antiglycation effect. Therefore, the scavenging of reactive dicarbonyls appeared to not be a major mechanism for isovitexin to inhibit protein glycation. However, given these considerations, another issue must be taken into account. Individual compounds reacted (or failed to react) differently with methylglyoxal and glyoxal. The discrepancy in the number of adducts formed in the reaction with MGO and GO is likely attributable to the fact that, as structural studies suggest, in aqueous solutions the main forms of GO are the hydrated monomer, dimer, and trimer. Consequently, the reactions of the investigated compounds with glyoxal were significantly slowed down by the transformation of the above-mentioned forms of GO to free GO [31]. Thus, there is a possibility that both isovitexin and nothofagin, which in our experiment did not demonstrate GO-trapping ability, may bind it under different experimental conditions. However, some other compounds from the group of flavones (vitexin) or dihydrochalcones (aspalathin and phloretin) have shown the potential to attach glyoxal molecules under given experimental conditions; therefore, it can be assumed that for isovitexin and nothofagin, this process takes place slightly less readily, perhaps due to the molecular spatial conditions. Further structural studies are needed to explain these discrepancies.

An important aspect that should be considered is the fact that aspalathin, despite its high antiglycation as well as trapping properties, has an extremely low level of bioavailability—at less than 1% [75]. However, aspalathin as a C-glycoside is metabolized with the involvement of bacterial enzymes in the large intestine, where low-molecular metabolites, such as phloroglucinol, have the chance to be absorbed into the circulation and can have a systemic antiglycation and trapping effect [76]. At this point, it should be mentioned that phloroglucinol is not an aspalathin-specific metabolite, but is a structural core of most flavonoids, which can exert their biological effects even with poor bioavailability of precursor flavonoids [77,78]. There is also evidence that the C-glycosides of flavonoids such as aspalathin and nothofagin present in *A. linearis*, which are metabolized in the large intestine, may exert local beneficial anti-AGE and anti-α-dicarbonyl effects in conditions such as irritable bowel syndrome. Bacterial metabolites that act deleteriously in excess on the digestive system and cause unpleasant symptoms in the form of irritation play a major role in these conditions [79]. One such bacterial metabolite is methylglyoxal. Thus, the use of dihydrochalcones and other flavonoids broken down in the intestine with the

production of phloroglucinol can also exert a local effect by reducing the concentration of methylglyoxal as an irritant [80].

3. Materials and Methods

3.1. Plant Material

Dried, crushed leaves and apical parts of shoots of Aspalathus linearis (Burm. f.) R. Dahlgren plantations in South Africa were used to prepare infusions and hydroethanolic extracts. Two types of raw materials were used: unfermented (green rooibos, GR) and fermented (red rooibos, RR) purchased from the Polish tea manufacturer Oxalis ("OXALIS POLSKA SP. Z O.O.; Radzionków, Poland").

3.2. Preparation of Extracts

Before the preparation of the extracts, both types of raw material were finely ground, each for 5 min, using an IKA A11B analytical mill (IKA Polska Sp. z o.o.; Warsaw, Poland). Then, 0.25 g of the powdered plant material was weighed on an analytical balance, placed in appropriately labeled volumetric flasks, and extracted with 25 mL of boiling water (infusions) or a mixture of water and ethanol (50%, *v/v*) for 15 min. The DER was 1:100. An ultrasonic bath (Bandelin Sonorex Digital 10P; Bandelin, Berlin, Germany) at 40 °C was used for hydroethanolic extraction. After 15 min, the extracts were centrifuged and then filtered using 0.22 µm diameter Durapore filters into vials. The filtrates were used for phytochemical analysis and in vitro tests. Hydroethanolic extracts from GR and RR were designated GRE and RRE, while infusions were designated GRI and RRI, respectively.

3.3. Chemicals

Methylglyoxal (MGO, 40% in water), glyoxal (GO, 40% in water), methanol (HPLC grade), acetonitrile (HPLC gradient grade and LC-MS grade), water (LC-MS grade), bovine serum albumin, DMSO, 98–100% formic acid, phloroglucinol (CAS No. 108-73-6), phloretin (CAS No. 60-82-2), eriodictyol (CAS No. 552-58-9), aspalathin (CAS No. 6027-43-6), aminoguanidine hydrochloride (CAS No. 16139-18-7), and metformin hydrochloride (CAS No. 1115-70-4) were purchased from Merck-Sigma-Aldrich (Sigma-Aldrich Sp. z o.o., Poznań, Poland). Vitexin (CAS No. 3681-93-4), isovitexin (CAS No. 38953-85-4), hyperoside (CAS No. 482-36-0), isoquercitrin (CAS No. 482-35-9), rutin (CAS No. 153-18-4), eriodictyol-7-O-β-glucoside (CAS No. 38965-51-4), apigenin (CAS No. 520-36-5), luteolin (CAS No. 491-70-3), and chrysoeriol (CAS No. 491-71-4) were purchased from Extrasynthese (Genay Cedex, France). NaCl, KCl, Na_2HPO_4, and KH_2PO_4 (reagent grade) were obtained from Chempur (Piekary Śląskie, Poland). Water used in the study was deionized. The stock solutions of standards for in vitro assays were prepared by dissolving the reference compound in 5 mL of a suitable solvent, filtered through hydrophilic Millex Syringe Filters Durapore 0.22 µm (Sigma-Aldrich, Poznań, Poland) and stored at −20 °C.

Stock solutions (1 mg/mL) for quantitative and semiquantitative analysis were made by dissolving 5 mg of flavonoid in 5 mL of methanol. Working standard solutions in the range of 10–250 g/mL (6 measurement points for each pattern) were prepared by mixing with 50% aq. methanol (*v/v*), filtered through hydrophilic Millex Syringe Filters, Durapore 0.22 µm (Sigma-Aldrich, Poznań, Poland) and stored at −20 °C.

3.4. Phytochemical Profile of Extracts

Phytochemical analysis of extracts was conducted using the Thermo Scientific Dionex UltiMate 3000 UHPLC system (Thermo Fisher Scientific; Waltham, MA, USA) incorporated with Compact ESI-QTOF-MS (Bruker Daltonics; Bremen, Germany), quaternary pump (LPG-3400D), and UltiMate 3000 RS autosampler (WPS-3000). Compounds were separated on a Kinetex C18 column (150 × 2.1 mm, particle size 2.6 µm) (Phenomenex; Torrance, CA, USA) and a temperature-controlled column compartment (TCC-3000) was used to maintain its temperature at 40 °C. Mobile phases consisted of 0.1% (*v/v*) formic acid in water (solvent A) and 0.1% (*v/v*) formic acid in acetonitrile (solvent B). The following gradient mobile

phase program at a flow rate of 0.3 mL/min was used: 0–12 min, 97–65% A in B; 12–14 min, 65% A in B; 14–17 min, 65–20% A in B; 17–19 min, 20% A in B. Then, the system was returned to the initial settings and washed with 97% A in B until the system was stabilized before the next analysis. Negative ion mode (ESI−) was used for data acquisition. Nitrogen was used as a nebulizing gas at 210 °C temperature, 2.0 bar pressure, and 0.8 L/min flow rate. For internal calibration, sodium formate clusters (10 mM) were used. The injection volume was 2.5 µL. Additional operating conditions of the mass spectrometer were as follows: the capillary voltage was set at 5 kV, the collisional energy was 8.0 eV, and for the MS2 mode, it was 40 eV. The data processing was carried out using Compass Data Analysis software (Bruker Daltonics; Bremen, Germany). The same method was used to analyze the formation of MGO and GO adducts.

The content of aspalathin and other flavonoids in extracts was quantified using the HPLC–DAD method described in Section 3.4.

3.5. Quantification of Flavonoids

HPLC–DAD analysis was performed on a Smartline system (Knauer, Germany) with a pump (Managare 5000), dynamic mixing chamber (V7119-1), DAD 2800 detector, manual 6-port 2-channel injection valve (A1366), and column thermostat (Jetstream Plus). Data were processed using EuroChrom for Windows Basic Edition V3.05 (V7568-5). The separation was carried out on a Hypersil GOLD C18 column (250 × 4.6 mm, particle size 5 µm) with a C18 precolumn (10 × 4.6 mm, size 5 µm) (Thermo scientific, USA). The following eluents were used: C, 1.5% formic acid in water (*v/v*) and D, 1.5% formic acid in acetonitrile (*v/v*). HPLC gradient was as follows: 10%, 25%, 65%, 80% (D in C) at time points of 0-30-33-50 min. The flow rate was 0.9 mL/min, and the injection volume was 20 µL. The column was operated at 20 °C. The spectral measurements were made in the wavelength range 200–600 nm in steps of 2 nm. Dihydrochalcones and flavanones were analyzed at 280 nm, while flavones and flavonols were analyzed at 360 nm.

The HPLC–DAD method was validated according to ICH guidelines for linearity, detection and quantification limits, and intra- and inter-day precision. Calibration curves for the quantified flavonoids were determined from 6 measurement points, and double injections were performed for each concentration. The range of correlation coefficients of the calibration curves (r) used in the calculations was 0.999 to 0.9999.

Flavonoid content (mg/100 mL of hydroethanolic extract or 1 g of dry plant material) was determined using the external standard method from the areas of the corresponding peaks. Dihydrochalcones, flavanones, flavones, flavonols, and total flavonoids were calculated by summing the content of compounds from these (sub)groups. Nothofagin was calculated as an aspalathin equivalent. Similarly, orientin and isoorientin were expressed as vitexin and isovitexin, and eriodictyol-C-glucosides were expressed as eriodictyol-7-O-β-glucoside. The concentrations of other flavonoids were quantified using their corresponding standards. Mean content and standard deviations were calculated from five independent measurements. We also converted the obtained results into micromolar concentrations.

3.6. Glycation Process and Fluorescence Measurement of AGEs

3.6.1. In Vitro Glycation Model

The glycation model was created based on a slightly modified published method [46]. In the proposed model, BSA serves as the protein and α-DCs serve as glycation agents. In short, 21.2 µM BSA was incubated with MGO or GO at 0.5 mM in 100 mM sodium phosphate buffer (pH 7.4) with 0.02% (*m/v*) sodium azide, which prevented microorganism growth in a test tube. Compounds investigated for antiglycation activity were added at a final concentration of 1.5 mM. Hydroethanolic extracts (DER 1:400) were added at a volume of 500 µL. Then, the reaction solution was incubated in simulated physiological conditions at 37 °C, shaken at 50 revolutions per minute for 7 days in closed vials secured with parafilm tape, and kept away from sunlight.

3.6.2. Antiglycation Assay

The fluorescent intensity of α-DC-mediated AGEs formed during incubation was analyzed using a Synergy HTX Multi-Mode Microplate Reader (BioTek Instruments Inc., Winooski, VT, USA) at a wavelength of 360 nm for excitation (λ_{ex}) and 460 nm for emission (λ_{em}). Data processing was carried out using Gen5 Software (BioTek Instruments Inc., Winooski, VT, USA). The measurements from three experiments were all performed in triplicate, and the percent inhibition of AGE formation was calculated using the following equation:

$$\text{Inhibition of } \alpha\text{-DC-mediated AGEs [\%]} = -\{1 - [(FI_1)/(FI_0)]\} \times 100$$

where FI_0 is the mean fluorescence intensity of the blank sample and FI_1 is the mean fluorescence intensity of the tested sample.

3.7. α-Dicarbonyl Trapping and Adduct Analysis

The direct MGO- and GO-trapping capacity of individual compounds and extracts was investigated according to the published method of Shao et al. [71] with slight modifications. Briefly, 0.6 mM of freshly prepared MGO or GO solution was incubated with 0.2 mM of an individual compound or 500 µL of *A. linearis* hydroethanolic extract (DER 1:400) and 0.1 M PBS (pH 7.4 was determined immediately before use) at 37 °C and shaken at 50 rpm for 1 h. The reaction was stopped by adding 2.5 µL of glacial acetic acid and transferring Eppendorf tubes with the collected samples to an ice water bath. Next, the samples were carefully filtered through hydrophilic Millex Syringe Filters (Durapore 0.22 µm; Millipore, Burlington, MA, USA) and analyzed using UHPLC–ESI–MS (described in Section 3.4) to test their capacity to form adducts with MGO and GO.

3.8. Statistical Analysis

All data are presented as mean ± standard deviation (SD). Data were analyzed using the Shapiro–Wilk test to assess the normality of distribution, followed by one-way analysis of variance (ANOVA) with Tukey's multiple comparison test using the GraphPad Prism 9 software, and p values equal to or less than 0.05 were considered significant.

4. Conclusions

Dicarbonyls are ubiquitous in our bodies since they are metabolic intermediates and can be generated from glycolysis and lipid peroxidation. Reducing their concentration in the human body can be achieved through diet—primarily by eliminating excess simple sugars from the diet. However, since in some pathological conditions their overproduction is not only related to diet, attempts are also being made to reduce their concentration in the body through the use of MGO- and GO-trapping compounds, among others.

This study demonstrated that in addition to the many health properties attributed to green and red rooibos, this plant material may also be considered as a potential adjunctive anti-α-dicarbonyl agent preventing the onset and development of glycation-related conditions. Since there are currently no pharmacological strategies to decrease α-DC levels as an early preventive measure against AGE-induced diseases, it is important to search for adjunctive therapies. Our study indicates that green rooibos, probably due to its high concentration of aspalathin and nothofagin, exhibits MGO- and GO-trapping activity and antiglycation potential, unlike red rooibos. However, compounds present in both unfermented and fermented *A. linearis* can trap MGO and GO and inhibit the glycation process induced by α-DCs. Further studies using in vivo models are needed to confirm and expand our results.

Author Contributions: Conceptualization, I.F.; methodology, validation, formal analysis, investigation, and data curation, K.B. and I.F.; writing—original draft preparation, K.B.; writing—review and editing, I.F.; visualization, K.B. and I.F.; supervision, I.F.; project administration and funding acquisition, I.F. and K.B. All authors have read and agreed to the published version of the manuscript.

Funding: This research was financially supported by Wroclaw Medical University (grant number SUBK.D110.22.045).

Institutional Review Board Statement: Not applicable.

Informed Consent Statement: Not applicable.

Data Availability Statement: Data supporting reported results are available from the corresponding author.

Conflicts of Interest: The authors declare no conflict of interest.

References

1. Ye, S.; Matthan, N.R.; Lamon-Fava, S.; Aguilar, G.S.; Turner, J.R.; Walker, M.E.; Chai, Z.; Lakshman, S.; Urban, J.F.; Lichtenstein, A.H. Western and heart healthy dietary patterns differentially affect the expression of genes associated with lipid metabolism, interferon signaling and inflammation in the jejunum of Ossabaw pigs. *J. Nutr. Biochem.* **2021**, *90*, 108577. [CrossRef] [PubMed]
2. Rippe, J.M.; Angelopoulos, T.J. Relationship between added sugars consumption and chronic disease risk factors: Current understanding. *Nutrients* **2016**, *8*, 697. [CrossRef] [PubMed]
3. Aragno, M.; Mastrocola, R. Dietary sugars and endogenous formation of advanced glycation endproducts: Emerging mechanisms of disease. *Nutrients* **2017**, *9*, 385. [CrossRef] [PubMed]
4. Masterjohn, C.; Park, Y.; Lee, J.; Noh, S.K.; Koo, S.I.; Bruno, R.S. Dietary fructose feeding increases adipose methylglyoxal accumulation in rats in association with low expression and activity of glyoxalase-2. *Nutrients* **2013**, *5*, 3311–3328. [CrossRef]
5. Mizukami, H.; Osonoi, S. Pathogenesis and molecular treatment strategies of diabetic neuropathy collateral glucose-utilizing pathways in diabetic polyneuropathy. *Int. J. Mol. Sci.* **2021**, *22*, 94. [CrossRef] [PubMed]
6. Goudarzi, M.; Kalantari, H.; Rezaei, M. Glyoxal toxicity in isolated rat liver mitochondria. *Hum. Exp. Toxicol.* **2018**, *37*, 532–539. [CrossRef]
7. Wei, Y.; Wang, D.; Moran, G.; Estrada, A.; Pagliassotti, M.J. Fructose-induced stress signaling in the liver involves methylglyoxal. *Nutr. Metab.* **2013**, *10*, 32. [CrossRef]
8. Subramanian, U.; Nagarajan, D. All-Trans Retinoic Acid supplementation prevents cardiac fibrosis and cytokines induced by Methylglyoxal. *Glycoconj. J.* **2017**, *34*, 255–265. [CrossRef]
9. de Oliveira, M.G.; de Medeiros, M.L.; Tavares, E.B.G.; Mónica, F.Z.; Antunes, E. Methylglyoxal, a Reactive Glucose Metabolite, Induces Bladder Overactivity in Addition to Inflammation in Mice. *Front. Physiol.* **2020**, *11*, 290. [CrossRef]
10. Younis, N.; Sharma, R.; Soran, H.; Charlton-Menys, V.; Elseweidy, M.; Durrington, P.N. Glycation as an atherogenic modification of LDL. *Curr. Opin. Lipidol.* **2008**, *19*, 378–384. [CrossRef]
11. Kim, Y.S.; Kim, J.; Kim, K.M.; Jung, D.H.; Choi, S.; Kim, C.S.; Kim, J.S. Myricetin inhibits advanced glycation end product (AGE)-induced migration of retinal pericytes through phosphorylation of ERK1/2, FAK-1, and paxillin in vitro and in vivo. *Biochem. Pharmacol.* **2015**, *93*, 496–505. [CrossRef] [PubMed]
12. Rezaeinezhad, A.; Eslami, P.; Mirmiranpour, H.; Ghomi, H. The effect of cold atmospheric plasma on diabetes-induced enzyme glycation, oxidative stress, and inflammation; in vitro and in vivo. *Sci. Rep.* **2019**, *9*, 19958. [CrossRef] [PubMed]
13. Yusufoğlu, B.; Yaman, M.; Karakuş, E. Determination of the most potent precursors of advanced glycation end products in some high-sugar containing traditional foods using high-performance liquid chromatography. *J. Food Process. Preserv.* **2020**, *44*, e14708. [CrossRef]
14. Bellia, C.; Zaninotto, M.; Cosma, C.; Agnello, L.; Bivona, G.; Marinova, M.; Lo Sasso, B.; Plebani, M.; Ciaccio, M. Clinical usefulness of Glycated Albumin in the diagnosis of diabetes: Results from an Italian study. *Clin. Biochem.* **2018**, *54*, 68–72. [CrossRef]
15. Giglio, R.V.; Lo Sasso, B.; Agnello, L.; Bivona, G.; Maniscalco, R.; Ligi, D.; Mannello, F.; Ciaccio, M. Recent updates and advances in the use of glycated albumin for the diagnosis and monitoring of diabetes and renal, cerebro-and cardio-metabolic diseases. *J. Clin. Med.* **2020**, *9*, 3634. [CrossRef]
16. Raghav, A.; Ahmad, J.; Alam, K.; Khan, A.U. New insights into non-enzymatic glycation of human serum albumin biopolymer: A study to unveil its impaired structure and function. *Int. J. Biol. Macromol.* **2017**, *101*, 84–99. [CrossRef]
17. Borg, D.J.; Forbes, J.M. Targeting advanced glycation with pharmaceutical agents: Where are we now? *Glycoconj. J.* **2016**, *33*, 653–670. [CrossRef]
18. Thornalley, P.J. Use of aminoguanidine (Pimagedine) to prevent the formation of advanced glycation endproducts. *Arch. Biochem. Biophys.* **2003**, *149*, 31–40. [CrossRef]
19. Chen, X.Y.; Huang, I.M.; Hwang, L.S.; Ho, C.T.; Li, S.; Lo, C.Y. Anthocyanins in blackcurrant effectively prevent the formation of advanced glycation end products by trapping methylglyoxal. *J. Funct. Foods* **2014**, *8*, 259–268. [CrossRef]

20. Kim, J.H.; Zhang, K.; Lee, J.; Gao, E.M.; Lee, Y.J.; Son, R.H.; Syed, A.S.; Kim, C.Y. Trapping of Methylglyoxal by Sieboldin from *Malus baccata* L. and Identification of Sieboldin-Methylglyoxal Adducts Forms. *Nat. Prod. Sci.* **2021**, *27*, 245–250. [CrossRef]
21. Gao, X.; Ho, C.T.; Li, X.; Lin, X.; Zhang, Y.; Chen, Z.; Li, B. Phytochemicals, Anti-Inflammatory, Antiproliferative, and Methylglyoxal Trapping Properties of Zijuan Tea. *J. Food Sci.* **2018**, *83*, 517–524. [CrossRef] [PubMed]
22. Smith, C.; Swart, A. Aspalathus linearis (Rooibos)-a functional food targeting cardiovascular disease. *Food Funct.* **2018**, *9*, 5041–5058. [CrossRef] [PubMed]
23. Chen, W.; Sudji, I.R.; Wang, E.; Joubert, E.; Van Wyk, B.E.; Wink, M. Ameliorative effect of aspalathin from rooibos (*Aspalathus linearis*) on acute oxidative stress in Caenorhabditis elegans. *Phytomedicine* **2013**, *20*, 380–386. [CrossRef]
24. Son, M.J.; Minakawa, M.; Miura, Y.; Yagasaki, K. Aspalathin improves hyperglycemia and glucose intolerance in obese diabetic ob/ob mice. *Eur. J. Nutr.* **2013**, *52*, 1607–1619. [CrossRef] [PubMed]
25. Marnewick, J.L.; Rautenbach, F.; Venter, I.; Neethling, H.; Blackhurst, D.M.; Wolmarans, P.; MacHaria, M. Effects of rooibos (*Aspalathus linearis*) on oxidative stress and biochemical parameters in adults at risk for cardiovascular disease. *J. Ethnopharmacol.* **2011**, *133*, 46–52. [CrossRef]
26. Dludla, P.V.; Muller, C.J.F.; Joubert, E.; Louw, J.; Essop, M.F.; Gabuza, K.B.; Ghoor, S.; Huisamen, B.; Johnson, R. Aspalathin protects the heart against hyperglycemia-induced oxidative damage by up-regulating Nrf2 expression. *Molecules* **2017**, *22*, 129. [CrossRef]
27. Suchal, K.; Malik, S.; Khan, S.I.; Malhotra, R.K.; Goyal, S.N.; Bhatia, J.; Kumari, S.; Ojha, S.; Arya, D.S. Protective effect of mangiferin on myocardial ischemia-reperfusion injury in streptozotocin-induced diabetic rats: Role of AGE-RAGE/MAPK pathways. *Sci. Rep.* **2017**, *7*, 42027. [CrossRef]
28. Mazibuko-Mbeje, S.E.; Dludla, P.V.; Roux, C.; Johnson, R.; Ghoor, S.; Joubert, E.; Louw, J.; Opoku, A.R.; Muller, C.J.F. Aspalathin-enriched green rooibos extract reduces hepatic insulin resistance by modulating PI3K/AKT and AMPK pathways. *Int. J. Mol. Sci.* **2019**, *20*, 633. [CrossRef]
29. Uličná, O.; Vančová, O.; Božek, P.; Čársky, J.; Šebeková, K.; Boor, P.; Nakano, M.; Greksák, M. Rooibos tea (*Aspalathus linearis*) partially prevents oxidative stress in streptozotocin-induced diabetic rats. *Physiol. Res.* **2006**, *55*, 157–164. [CrossRef]
30. Moens, C.; Muller, C.J.F.; Bouwens, L. In vitro comparison of various antioxidants and flavonoids from Rooibos as beta cell protectants against lipotoxicity and oxidative stress-induced cell death. *PLoS ONE* **2022**, *17*, e0268551. [CrossRef]
31. Shao, X.; Bai, N.; He, K.; Ho, C.T.; Yang, C.S.; Sang, S. Apple polyphenols, phloretin and phloridzin: New trapping agents of reactive dicarbonyl species. *Chem. Res. Toxicol.* **2008**, *21*, 2042–2050. [CrossRef] [PubMed]
32. Ruiz, H.H.; Ramasamy, R.; Schmidt, A.M. Advanced glycation end products: Building on the concept of the "common soil" in metabolic disease. *Endocrinology* **2020**, *161*, bqz006. [CrossRef] [PubMed]
33. Takeuchi, M.; Yamagishi, S. Possible Involvement of Advanced Glycation End-Products (AGEs) in the Pathogenesis of Alzheimers Disease. *Curr. Pharm. Des.* **2008**, *14*, 973–978. [CrossRef] [PubMed]
34. Song, Q.; Liu, J.; Dong, L.; Wang, X.; Zhang, X. Novel advances in inhibiting advanced glycation end product formation using natural compounds. *Biomed. Pharmacother.* **2021**, *140*, 111750. [CrossRef]
35. Cordell, G.A. Sixty challenges—A 2030 perspective on natural products and medicines security. *Nat. Prod. Commun.* **2017**, *12*, 1371–1379. [CrossRef]
36. Ramlagan, P.; Rondeau, P.; Planesse, C.; Neergheen-Bhujun, V.S.; Bourdon, E.; Bahorun, T. Comparative suppressing effects of black and green teas on the formation of advanced glycation end products (AGEs) and AGE-induced oxidative stress. *Food Funct.* **2017**, *8*, 4194–4209. [CrossRef]
37. Babu, P.V.A.; Sabitha, K.E.; Shyamaladevi, C.S. Therapeutic effect of green tea extract on oxidative stress in aorta and heart of streptozotocin diabetic rats. *Chem. Biol. Interact.* **2006**, *162*, 114–120. [CrossRef]
38. Nakagawa, T.; Yokozawa, T.; Kim, Y.A.; Kang, K.S.; Tanaka, T. Activity of Wen-Pi-Tang, and purified constituents of Rhei Rhizoma and glycyrrhizae radix against glucose-mediated protein damage. *Am. J. Chin. Med.* **2005**, *33*, 817–829. [CrossRef]
39. Perez Gutierrez, R.M. Inhibition of advanced glycation end-product formation by *Origanum majorana* L. in vitro and in streptozotocin-induced diabetic rats. *Evid.-Based Complement. Altern. Med.* **2012**, *2012*, 598638. [CrossRef]
40. Kim, H.Y.; Kim, K. Protein glycation inhibitory and antioxidative activities of some plant extracts in vitro. *J. Agric. Food Chem.* **2003**, *51*, 1586–1591. [CrossRef]
41. Lee, C.C.; Lee, B.H.; Lai, Y.J. Antioxidation and antiglycation of Fagopyrum tataricum ethanol extract. *J. Food Sci. Technol.* **2015**, *52*, 1110–1116. [CrossRef]
42. Peng, X.; Zheng, Z.; Cheng, K.W.; Shan, F.; Ren, G.X.; Chen, F.; Wang, M. Inhibitory effect of mung bean extract and its constituents vitexin and isovitexin on the formation of advanced glycation endproducts. *Food Chem.* **2008**, *106*, 475–481. [CrossRef]
43. Grzegorczyk-Karolak, I.; Gołab, K.; Gburek, J.; Wysokińska, H.; Matkowski, A. Inhibition of advanced glycation end-product formation and antioxidant activity by extracts and polyphenols from *Scutellaria alpina* L. and *S. altissima* L. *Molecules* **2016**, *21*, 739. [CrossRef] [PubMed]
44. Li, X.; Zheng, T.; Sang, S.; Lv, L. Quercetin inhibits advanced glycation end product formation by trapping methylglyoxal and glyoxal. *J. Agric. Food Chem.* **2014**, *62*, 12152–12158. [CrossRef] [PubMed]
45. Yang, B.-n.; Choi, E.-h.; Shim, S.M. Inhibitory activities of kaempferol against methylglyoxal formation, intermediate of advanced glycation end products. *Appl. Biol. Chem.* **2017**, *60*, 57–62. [CrossRef]

46. Bhuiyan, M.N.I.; Mitsuhashi, S.; Sigetomi, K.; Ubukata, M. Quercetin inhibits advanced glycation end product formation via chelating metal ions, trapping methylglyoxal, and trapping reactive oxygen species. *Biosci. Biotechnol. Biochem.* **2017**, *81*, 882–890. [CrossRef]
47. Bernacka, K.; Bednarska, K.; Starzec, A.; Mazurek, S.; Fecka, I. Antioxidant and Antiglycation Effects of Cistus × incanus Water Infusion, Its Phenolic Components, and Respective Metabolites. *Molecules* **2022**, *27*, 2432. [CrossRef]
48. Bednarska, K. Potential of Vasoprotectives to Inhibit Non-Enzymatic Protein Glycation, and Reactive Carbonyl and Oxygen Species Uptake. *Int. J. Mol. Sci.* **2021**, *22*, 10026. [CrossRef]
49. Bednarska, K.; Kuś, P.; Fecka, I. Investigation of the phytochemical composition, antioxidant activity, and methylglyoxal trapping effect of *Galega officinalis* L. Herb in vitro. *Molecules* **2020**, *25*, 5810. [CrossRef]
50. Stander, M.A.; Van Wyk, B.E.; Taylor, M.J.C.; Long, H.S. Analysis of Phenolic Compounds in Rooibos Tea (*Aspalathus linearis*) with a Comparison of Flavonoid-Based Compounds in Natural Populations of Plants from Different Regions. *J. Agric. Food Chem.* **2017**, *65*, 10270–10281. [CrossRef]
51. Joubert, E.; Jolley, B.; Koch, I.S.; Muller, M.; Van der Rijst, M.; de Beer, D. Major production areas of rooibos (*Aspalathus linearis*) deliver herbal tea of similar phenolic and phenylpropenoic acid glucoside content. *S. Afr. J. Bot.* **2016**, *103*, 162–169. [CrossRef]
52. Walters, N.A.; de Villiers, A.; Joubert, E.; de Beer, D. Improved HPLC method for rooibos phenolics targeting changes due to fermentation. *J. Food Compos. Anal.* **2017**, *55*, 20–29. [CrossRef]
53. Iswaldi, I.; Arráez-Román, D.; Rodríguez-Medina, I.; Beltrán-Debón, R.; Joven, J.; Segura-Carretero, A.; Fernández-Gutiérrez, A. Identification of phenolic compounds in aqueous and ethanolic rooibos extracts (*Aspalathus linearis*) by HPLC-ESI-MS (TOF/IT). *Anal. Bioanal. Chem.* **2011**, *400*, 3643–3654. [CrossRef] [PubMed]
54. Gattuso, G.; Caristi, C.; Gargiulli, C.; Bellocco, E.; Toscano, G.; Leuzzi, U. Flavonoid glycosides in bergamot juice (*Citrus bergamia* Risso). *J. Agric. Food Chem.* **2006**, *54*, 3929–3935. [CrossRef]
55. Stalmach, A.; Mullen, W.; Pecorari, M.; Serafini, M.; Crozier, A. Bioavailability of C-linked dihydrochalcone and flavanone glucosides in humans following ingestion of unfermented and fermented rooibos teas. *J. Agric. Food Chem.* **2009**, *57*, 7104–7111. [CrossRef]
56. Krafczyk, N.; Heinrich, T.; Porzel, A.; Glomb, M.A. Oxidation of the dihydrochalcone aspalathin leads to dimerization. *J. Agric. Food Chem.* **2009**, *57*, 6838–6843. [CrossRef]
57. Bolton, W.K.; Cattran, D.C.; Williams, M.E.; Adler, S.G.; Appel, G.B.; Cartwright, K.; Foiles, P.G.; Freedman, B.I.; Raskin, P.; Ratner, R.E.; et al. Randomized Trial of an Inhibitor of Formation of Advanced Glycation End Products in Diabetic Nephropathy. *Am. J. Nephrol.* **2004**, *24*, 32–40. [CrossRef]
58. Kiho, T.; Kato, M.; Usui, S.; Hirano, K. Effect of buformin and metformin on formation of advanced glycation end products by methylglyoxal. *Clin. Chim. Acta* **2005**, *358*, 139–145. [CrossRef]
59. Beisswenger, P.J.; Ruggiero-Lopez, D. Metformin inhibition of glycation processes. *Diabetes Metab.* **2003**, *29*, S95–S96. [CrossRef] [PubMed]
60. Sugiura, S.; Minami, Y.; Taniguchi, R.; Tanaka, R.; Miyake, H.; Mori, T.; Ueda, M.; Shibata, T. Evaluation of anti-glycation activities of phlorotannins in human and bovine serum albumin-methylglyoxal models. *Nat. Prod. Commun.* **2017**, *12*, 1793–1796. [CrossRef]
61. Kamakura, R.; Son, M.J.; de Beer, D.; Joubert, E.; Miura, Y.; Yagasaki, K. Antidiabetic effect of green rooibos (*Aspalathus linearis*) extract in cultured cells and type 2 diabetic model KK-Ay mice. *Cytotechnology* **2015**, *67*, 699–710. [CrossRef] [PubMed]
62. Pringle, N.A.; Koekemoer, T.C.; Holzer, A.; Young, C.; Venables, L.; Van De Venter, M. Potential Therapeutic Benefits of Green and Fermented Rooibos (*Aspalathus linearis*) in Dermal Wound Healing. *Planta Med.* **2018**, *84*, 645–652. [CrossRef] [PubMed]
63. Kinae, N.; Shimoi, K.; Masumori, S.; Harusawa, M.; Furugori, M. Suppression of the Formation of Advanced Glycosylation Products by Tea Extracts. *ACS Publ.* **1994**, *547*, 68–75. [CrossRef]
64. Kim, J.M.; Jang, D.S.; Lee, Y.M.; Yoo, J.L.; Kim, Y.S.; Kim, J.H.; Kim, J.S. Aldose-reductase- and protein-glycation-inhibitory principles from the whole plant of Duchesnea chrysantha. *Chem. Biodivers.* **2008**, *5*, 352–356. [CrossRef]
65. Drygalski, K.; Siewko, K.; Chomentowski, A.; Odrzygóźdź, C.; Zalewska, A.; Krętowski, A.; MacIejczyk, M. Phloroglucinol Strengthens the Antioxidant Barrier and Reduces Oxidative/Nitrosative Stress in Nonalcoholic Fatty Liver Disease (NAFLD). *Oxid. Med. Cell. Longev.* **2021**, *2021*, 8872702. [CrossRef]
66. Liu, J.; Yang, Z.; Cheng, Y.; Wu, Q.; He, Y.; Li, Q.; Cao, X. Eriodictyol and naringenin inhibit the formation of AGEs: An in vitro and molecular interaction study. *J. Mol. Recognit.* **2020**, *33*, e2814. [CrossRef]
67. Perrone, A.; Giovino, A.; Benny, J.; Martinelli, F. Advanced Glycation End Products (AGEs): Biochemistry, Signaling, Analytical Methods, and Epigenetic Effects. *Oxid. Med. Cell. Longev.* **2020**, *2020*, 3818196. [CrossRef]
68. Nevin, C.; McNeil, L.; Ahmed, N.; Murgatroyd, C.; Brison, D.; Carroll, M. Investigating the Glycating Effects of Glucose, Glyoxal and Methylglyoxal on Human Sperm. *Sci. Rep.* **2018**, *8*, 9002. [CrossRef]
69. Lee, S.M.; Na, M.K.; Na, R.B.; Min, B.S.; Lee, H.K. Antioxidant activity of two phloroglucinol derivatives from Dryopteris crassirhizoma. *Biol. Pharm. Bull.* **2003**, *26*, 1354–1356. [CrossRef]
70. Liu, H.; Gu, L. Phlorotannins from brown algae (*Fucus vesiculosus*) inhibited the formation of advanced glycation endproducts by scavenging reactive carbonyls. *J. Agric. Food Chem.* **2012**, *60*, 1326–1334. [CrossRef]
71. Shao, X.; Chen, H.; Zhu, Y.; Sedighi, R.; Ho, C.T.; Sang, S. Essential structural requirements and additive effects for flavonoids to scavenge methylglyoxal. *J. Agric. Food Chem.* **2014**, *62*, 3202–3210. [CrossRef] [PubMed]

72. Mendes, V.; Vilaça, R.; De Freitas, V.; Ferreira, P.M.; Mateus, N.; Costa, V. Effect of myricetin, pyrogallol, and phloroglucinol on yeast resistance to oxidative stress. *Oxid. Med. Cell. Longev.* **2015**, *2015*, 782504. [CrossRef] [PubMed]
73. Ni, M.; Song, X.; Pan, J.; Gong, D.; Zhang, G. Vitexin Inhibits Protein Glycation through Structural Protection, Methylglyoxal Trapping, and Alteration of Glycation Site. *J. Agric. Food Chem.* **2021**, *69*, 2462–2476. [CrossRef] [PubMed]
74. Erlund, I. Review of the flavonoids quercetin, hesperetin, and naringenin. Dietary sources, bioactivities, bioavailability, and epidemiology. *Nutr. Res.* **2004**, *24*, 851–874. [CrossRef]
75. Muller, C.J.F.; Joubert, E.; Chellan, N.; Miura, Y.; Yagasaki, K. New insights into the efficacy of aspalathin and other related phytochemicals in type 2 diabetes—A review. *Int. J. Mol. Sci.* **2022**, *23*, 356. [CrossRef]
76. Kreuz, S.; Joubert, E.; Waldmann, K.H.; Ternes, W. Aspalathin, a flavonoid in Aspalathus linearis (rooibos), is absorbed by pig intestine as a C-glycoside. *Nutr. Res.* **2008**, *28*, 690–701. [CrossRef] [PubMed]
77. Blaut, M.; Schoefer, L.; Braune, A. Transformation of flavonoids by intestinal microorganisms. *Int. J. Vitam. Nutr. Res.* **2003**, *73*, 79–87. [CrossRef]
78. Labib, S.; Erb, A.; Kraus, M.; Wickert, T.; Richling, E. The pig caecum model: A suitable tool to study the intestinal metabolism of flavonoids. *Mol. Nutr. Food Res.* **2004**, *48*, 326–332. [CrossRef]
79. Zhang, S.; Jiao, T.; Chen, Y.; Gao, N.; Zhang, L.; Jiang, M. Methylglyoxal induces systemic symptoms of irritable bowel syndrome. *PLoS ONE* **2014**, *9*, e105307. [CrossRef]
80. van der Lugt, T.; Opperhuizen, A.; Bast, A.; Vrolijk, M.F. Dietary advanced glycation endproducts and the gastrointestinal tract. *Nutrients* **2020**, *12*, 2814. [CrossRef]

Oświadczenia współautorów

WROCŁAW, 18.09.2023

miejscowość, data

Katarzyna Bednarska
tytuł, imię i nazwisko

Szkoła Doktorska Uniwersytetu Medycznego we Wrocławiu
miejsce zatrudnienia

OŚWIADCZENIE WSPÓŁAUTORA

Oświadczam, że w pracach:

- Bednarska K., Fecka I. 2021; Potential of Vasoprotectives to Inhibit Non-Enzymatic Protein Glycation, and Reactive Carbonyl and Oxygen Species Uptake. *Int. J. Mol. Sci.* 22(18), 10026.

(autorzy, rok wydania, tytuł, czasopismo lub wydawca, tom, strony)

Mój udział polegał na: współuczestnictwie w opracowaniu metodologii, wykonaniu walidacji metody, poszczególnych analiz, obróbce pozyskanych danych, wizualizacji wyników, przygotowaniu pierwszego oryginalnego tekstu manuskryptu, pozyskaniu funduszy (współudział w przygotowaniu projektu finansującego badania), korespondencji z redakcją.

- Bednarska K., Fecka I., Scheijen J.L.J.M., Sanne A., Vangrieken P., Schalkwijk C.G. 2023; A citrus and pomegranate complex reduces methylglyoxal in healthy elderly subjects: secondary analysis of a double-blind randomized cross-over clinical trial. *Int. J. Mol. Sci.* 2023, *24*(17), 13168.

(autorzy, rok wydania, tytuł, czasopismo lub wydawca, tom, strony)

Mój udział polegał na: wykonaniu analiz, nadzorowaniu uzyskiwanych danych, przygotowaniu pierwszego oryginalnego tekstu manuskryptu, wizualizacji wyników, przetwarzaniu pozyskanych danych, pozyskaniu funduszy (związanych z opublikowaniem manuskryptu) i korespondencji z redakcją.

- Bednarska K., Kuś P., Fecka I. 2020; Investigation of the Phytochemical Composition, Antioxidant Activity, and Methylglyoxal Trapping Effect of Galega officinalis L. Herb In Vitro. Molecules, 25(24), 5810.

(autorzy, rok wydania, tytuł, czasopismo lub wydawca, tom, strony)

Mój udział polegał na: współuczestnictwie w opracowaniu metodologii, wykonaniu walidacji metody, analiz, obróbce pozyskanych danych, wizualizacji wyników, przygotowaniu pierwszego oryginalnego tekstu manuskryptu, pozyskaniu funduszy (współudział w przygotowaniu projektu finansującego badania), korespondencji z redakcją.

- Bednarska K., Fecka I. 2022; Aspalathin and Other Rooibos Flavonoids Trapped α-Dicarbonyls and Inhibited Formation of Advanced Glycation End Products In Vitro. *Int. J. Mol. Sci.* 2022, *23*(23), 14738.
  (autorzy, rok wydania, tytuł, czasopismo lub wydawca, tom, strony)

Mój udział polegał na: współuczestnictwie w opracowaniu koncepcji, metodologii, wykonaniu walidacji metody, analiz, obróbce pozyskanych danych, wizualizacji wyników, przygotowaniu pierwszego oryginalnego tekstu manuskryptu, pozyskaniu funduszy (kierownik projektu finansującego badania), korespondencji z redakcją.

podpis współautora

Uniwersytet Medyczny we Wrocławiu
KATEDRA I ZAKŁAD FARMAKOGNOZJI
I LEKU ROŚLINNEGO
profesor
prof. dr hab. Izabela Fecka

podpis promotora

Wrocław, 18.09.2023

miejscowość, data

dr. hab. Izabela Fecka, prof. UMW
tytuł, imię i nazwisko

Uniwersytet Medyczny we Wrocławiu, Wydział Farmaceutyczny, KiZ Farmakognozji i leku Roslinnego
miejsce zatrudnienia

OŚWIADCZENIE WSPÓŁAUTORA

Oświadczam, że w pracach:

- Bednarska K., Fecka I. 2021; Potential of Vasoprotectives to Inhibit Non-Enzymatic Protein Glycation, and Reactive Carbonyl and Oxygen Species Uptake. *Int. J. Mol. Sci.* 22(18), 10026.

(autorzy, rok wydania, tytuł, czasopismo lub wydawca, tom, strony)

Mój udział polegał na: opracowaniu koncepcji, nadzorowaniu projektu, współudziale w opracowaniu metodologii, obróbce pozyskanych danych, wizualizacji wyników, recenzji i edycji oryginalnego tekstu manuskryptu, a także na współudziale w pozyskaniu funduszy (opiekun naukowy w projekcie dla Młodych Naukowców) i zarządzaniu projektem.

- Bednarska K., Fecka I., Scheijen J.L.J.M., Sanne A., Vangrieken P., Schalkwijk C.G. 2023; A citrus and pomegranate complex reduces methylglyoxal in healthy elderly subjects: secondary analysis of a double-blind randomized cross-over clinical trial. *Int. J. Mol. Sci.* 2023, *24*(17), 13168.

(autorzy, rok wydania, tytuł, czasopismo lub wydawca, tom, strony)

Mój udział polegał na: recenzji i edycji oryginalnego tekstu manuskryptu, przetwarzaniu pozyskanych danych, wizualizacji wyników.

- Bednarska K., Kuś P., Fecka I. 2020; Investigation of the Phytochemical Composition, Antioxidant Activity, and Methylglyoxal Trapping Effect of Galega officinalis L. Herb In Vitro. Molecules, 25(24), 5810.

(autorzy, rok wydania, tytuł, czasopismo lub wydawca, tom, strony)

Mój udział polegał na: opracowaniu koncepcji, nadzorowaniu projektu, współudziale w opracowaniu metodologii, obróbce pozyskanych danych, wizualizacji wyników, recenzji i edycji oryginalnego tekstu manuskryptu, a także współudziale w pozyskaniu funduszy (opiekun naukowy w projekcie dla Młodych Naukowców) i zarządzaniu projektem.

- Bednarska K., Fecka I. 2022; Aspalathin and Other Rooibos Flavonoids Trapped α-Dicarbonyls and Inhibited Formation of Advanced Glycation End Products In Vitro. *Int. J. Mol. Sci.* 2022, *23*(23), 14738.
  (autorzy, rok wydania, tytuł, czasopismo lub wydawca, tom, strony)

Mój udział polegał na: współuczestnictwie w opracowaniu koncepcji, metodologii, obróbce pozyskanych danych, wizualizacji wyników, recenzji i edycji oryginalnego tekstu manuskryptu, a także współudziale w nadzorowaniu projektu, pozyskaniu funduszy, zarządzaniu projektem.

---

podpis współautora

Uniwersytet Medyczny we Wrocławiu
KATEDRA I ZAKŁAD FARMAKOGNOZJI
I LEKU ROŚLINNEGO
profesor
prof. dr hab. Izabela Fecka

---

podpis promotora

Wrocław, 7.08.2023
miejscowość, data

dr. hab. Piotr Kuś
tytuł, imię i nazwisko

Uniwersytet Medyczny we Wrocławiu
miejsce zatrudnienia

OŚWIADCZENIE WSPÓŁAUTORA

Oświadczam, że w pracy:

Bednarska K., Kuś P., Fecka I. 2020; Investigation of the Phytochemical Composition, Antioxidant Activity, and Methylglyoxal Trapping Effect of Galega officinalis L. Herb In Vitro. Molecules, 25(24), 5810.

(autorzy, rok wydania, tytuł, czasopismo lub wydawca, tom, strony)

mój udział polegał na pomocy w opracowaniu metodologii i walidacji metod chromatograficznych i spektrometrycznych, uczestnictwie w wykonaniu analiz, ocenie i interpretacji uzyskanych wyników oraz recenzji i edycji oryginalnego tekstu manuskryptu.

podpis współautora

Uniwersytet Medyczny we Wrocławiu
KATEDRA I ZAKŁAD FARMAKOGNOZJI
I LEKU ROŚLINNEGO
profesor
prof. dr hab. Izabela Fecka

podpis promotora

Maastricht 25-8-2023

place, date

Philippe Vangrieken, PhD
title, first and last name

Maastricht University
place of employment

CO-AUTHOR STATEMENT

I hereby declare that in the article:

- Bednarska K., Fecka I., Scheijen J.L.J.M., Sanne A., Vangrieken P., Schalkwijk C.G. 2023; A citrus and pomegranate complex reduces methylglyoxal in healthy elderly subjects: secondary analysis of a double-blind randomized cross-over clinical trial. *Int. J. Mol. Sci.* 2023, *24*(17), 13168.

(authors, year of publication, title, journal or publisher, volume, pages)

My contribution to the above work included: reviewing and editing the original manuscript text.

.....
Co-author signature

Uniwersytet Medyczny we Wrocławiu
KATEDRA I ZAKŁAD FARMAKOGNOZJI
I LEKU ROŚLINNEGO
profesor
prof. dr hab. Izabela Fecka

.....
Supervisor signature

28/0/2023

place, date

Jean L.J.M. Scheijen, PhD
title, first and last name

Maastricht University
place of employment

CO-AUTHOR STATEMENT

I hereby declare that in the article:

- Bednarska K., Fecka I., Scheijen J.L.J.M., Sanne A., Vangrieken P., Schalkwijk C.G. 2023; A citrus and pomegranate complex reduces methylglyoxal in healthy elderly subjects: secondary analysis of a double-blind randomized cross-over clinical trial. *Int. J. Mol. Sci.* 2023, *24*(17), 13168.

(authors, year of publication, title, journal or publisher, volume, pages)

My contribution to the above work included: project supervision, formal analysis (performing samples preparation and spectrometric analyses), processing of the acquired data, review and editing of the original manuscript text, processing of the data acquired, and visualization of the results.

Co-author signature

Uniwersytet Medyczny we Wrocławiu
KATEDRA I ZAKŁAD FARMAKOGNOZJI
I LEKU ROŚLINNEGO
profesor
prof. dr hab. Izabela Fecka

Supervisor signature

Maastricht, 29-08-2023

place, date

Casper G. Schalkwijk, Prof.
title, first and last name

Maastricht University
place of employment

CO-AUTHOR STATEMENT

I hereby declare that in the article:

- Bednarska K., Fecka I., Scheijen J.L.J.M., Sanne A., Vangrieken P., Schalkwijk C.G. 2023; A citrus and pomegranate complex reduces methylglyoxal in healthy elderly subjects: secondary analysis of a double-blind randomized cross-over clinical trial. *Int. J. Mol. Sci.* 2023, *24*(17), 13168.

(authors, year of publication, title, journal or publisher, volume, pages)

My contribution to the above work included: study conceptualization, methodology development (laboratory part), project supervision, and reviewing and editing the original manuscript text.

.....
Co-author signature

Uniwersytet Medyczny we Wrocławiu
KATEDRA I ZAKŁAD FARMAKOGNOZJI
I LEKU ROŚLINNEGO
profesor
prof. dr hab. Izabela Fecka

Supervisor signature

Maastricht, August 25, 2023

place, date

Sanne Ahles, M. S.
title, first and last name

BioActor BV
place of employment

CO-AUTHOR STATEMENT

I hereby declare that in the article:

- Bednarska K., Fecka I., Scheijen J.L.J.M., Sanne A., Vangrieken P., Schalkwijk C.G. 2023; A citrus and pomegranate complex reduces methylglyoxal in healthy elderly subjects: secondary analysis of a double-blind randomized cross-over clinical trial. *Int. J. Mol. Sci.* 2023, *24*(17), 13168.

(authors, year of publication, title, journal or publisher, volume, pages)

My contribution to the above work included: methodology development (clinical part), and review and editing of the original manuscript text.

.....
Co-author signature

Uniwersytet Medyczny we Wrocławiu
KATEDRA I ZAKŁAD FARMAKOGNOZJI
I LEKU ROŚLINNEGO
profesor

.....
prof. dr hab. Izabela Fecka
Supervisor signature

Całkowity dorobek naukowy

Katarzyna Bednarska Wrocław, 04.09.2023 r.

Wykaz publikacji

1. Publikacje w czasopismach naukowych

1.1 Publikacje w czasopiśmie z IF

Lp.	Opis bibliograficzny	IF	Punkty
1	**Bednarska Katarzyna**, Kuś Piotr, Fecka Izabela: Investigation of the phytochemical composition, antioxidant activity, and methylglyoxal trapping effect of Galega officinalis L. herb in vitro, Molecules, 2020, vol. 25, nr 24, art.5810 [27 s.], DOI:10.3390/molecules25245810	4,412	140
2	**Bednarska Katarzyna**, Fecka Izabela: Potential of vasoprotectives to inhibit non-enzymatic protein glycation, and reactive carbonyl and oxygen species uptake, International Journal of Molecular Sciences, 2021, vol. 22, nr 18, art.10026 [22 s.], DOI:10.3390/ijms221810026	6,208	140
3	**Bednarska Katarzyna**, Fecka Izabela: Aspalathin and other rooibos flavonoids trapped α-dicarbonyls and inhibited formation of advanced glycation end products in vitro, International Journal of Molecular Sciences, 2022, vol. 23, nr 23, art.14738 [27 s.], DOI:10.3390/ijms232314738	5,6	140
4	Bernacka Karolina, **Bednarska Katarzyna**, Starzec Aneta, Mazurek Sylwester, Fecka Izabela: Antioxidant and antiglycation effects of Cistus × incanus water infusion, its phenolic components, and respective metabolites, Molecules, 2022, vol. 27, nr 8, art.2432 [22 s.], DOI:10.3390/molecules27082432	4,6	140
5	Fecka Izabela, **Bednarska Katarzyna**, Włodarczyk Maciej: Fragaria x ananassa cv. Senga Sengana leaf: an agricultural waste with antiglycation potential and high content of ellagitannins, flavonols, and 2-pyrone-4,6-dicarboxylic acid, Molecules, 2022, vol. 27, nr 16, art.5293 [30 s.], DOI:10.3390/molecules27165293	4,6	140
6	**Bednarska Katarzyna**, Fecka Izabela, Scheijen Jean L. J. M., Ahles Sanne, Vangrieken Philippe, Schalkwijk Casper G.: A citrus and pomegranate complex reduces methylglyoxal in healthy elderly subjects: secondary analysis of a double-blind randomized cross-over clinical trial, International Journal of Molecular Sciences, 2023, vol. 24, nr 17, art.13168 [14 s.], DOI:10.3390/ijms241713168	5,6*	140
7	Fecka Izabela, **Bednarska Katarzyna**, Kowalczyk Adam: In vitro antiglycation and methylglyoxal trapping effect of peppermint leaf (Mentha × piperita L.) and its polyphenols, Molecules, 2023, vol. 28, nr 6, art.2865 [21 s.], DOI:10.3390/molecules28062865	4,6*	140

** IF 2022*

1.2 Publikacje w czasopiśmie bez IF

Lp.	Opis bibliograficzny	Punkty
1	Bernacka Karolina, **Bednarska Katarzyna**, Urbanowicz Iwona, Fecka Izabela: Rooibos - dobry wybór!, Farmacja Polska, 2021, vol. 77, nr 7, s. 403-424, DOI:10.32383/farmpol/142109	70

2. Abstrakty

Lp.	Opis bibliograficzny
1	**Bednarska Katarzyna**, Fecka Izabela: Badania składu fitochemicznego Geranii robertiani herba w zakresie związków wielofenolowych, W: III Ogólnopolska Konferencja Naukowa "Współczesne zastosowanie metod analitycznych w farmacji i medycynie". Wrocław, 9 kwietnia 2018 r. Książka abstraktów 2018, 19 poz.P2, [[Dostęp 12.04.2018]. Dostępny w: http://www.farmacja.wroclaw.pl/images/ksi%C4%85%C5%BCka%20abstrakt%C3%B3w%20kwiecie%C5%84%202018.pdf]
2	**Bednarska Katarzyna**, Czwojdzińska Marta, Sikorska Karolina, Baranowski Jakub, Sawicka Ewa: Oko jako narzędzie wczesnej diagnostyki choroby Alzheimera, W: IV Ogólnopolska Konferencja Naukowa "Współczesne zastosowanie metod analitycznych w farmacji i medycynie". Wrocław, 12 kwietnia 2019 r. Książka abstraktów 2019, [13], [[Dostęp 18.04.2019]. Dostępny w: http://www.farmacja.wroclaw.pl/images/ksia%CC%A8z%CC%87ka-abstrakto%CC%81w-kwiecien%CC%81-2019.pdf]
3	**Bednarska Katarzyna**, Matwiej Marta, Fecka Izabela: Izolacja geraniny z ziela iglicy pospolitej, W: IV Ogólnopolska Konferencja Naukowa "Współczesne zastosowanie metod analitycznych w farmacji i medycynie". Wrocław, 12 kwietnia 2019 r. Książka abstraktów 2019, [14], [[Dostęp 18.04.2019]. Dostępny w: http://www.farmacja.wroclaw.pl/images/ksia%CC%A8z%CC%87ka-abstrakto%CC%81w-kwiecien%CC%81-2019.pdf]
4	Czwojdzińska Marta, **Bednarska Katarzyna**, Sawicka Ewa: Nowoczesne metody wykrywania i identyfikacji koronawirusów u zwierząt, W: IV Ogólnopolska Konferencja Naukowa "Współczesne zastosowanie metod analitycznych w farmacji i medycynie". Wrocław, 12 kwietnia 2019 r. Książka abstraktów 2019, [18], [[Dostęp 18.04.2019]. Dostępny w: http://www.farmacja.wroclaw.pl/images/ksia%CC%A8z%CC%87ka-abstrakto%CC%81w-kwiecien%CC%81-2019.pdf]
5	Fecka Izabela, **Bednarska Katarzyna**, Kuś Piotr: Rutwica lekarska - nowe właściwości i perspektywy zastosowania, W: V Ogólnopolska Konferencja Naukowa "Współczesne zastosowanie metod analitycznych w farmacji i medycynie". [Online], 27 listopada 2020 r. Książka abstraktów 2020, s. 11
6	**Bednarska Katarzyna**, Fecka Izabela: Badanie zdolności rutyny i trokserutyny do pułapkowania metyloglioksalu, W: V Ogólnopolska Konferencja Naukowa "Współczesne zastosowanie metod analitycznych w farmacji i medycynie". [Online], 27 listopada 2020 r. Książka abstraktów 2020, s. 19-20
7	Bernacka Karolina, Starzec Aneta, **Bednarska Katarzyna**, Fecka Izabela: Ziele czystka szarego - czy właściwości popularnego suplementu znajdują potwierdzenie w badaniach naukowych?, W: VI Ogólnopolska Konferencja Naukowa "Współczesne zastosowanie metod analitycznych w farmacji i medycynie". Wrocław, 03 grudnia 2021 r. Książka abstraktów, Wrocław 2021, s. 15

Lp.	Opis bibliograficzny
8	Boczek Zuzanna, Magiera Sabina, Podgórska Pola, **Bednarska Katarzyna**, Fecka Izabela: Antyglikacyjne właściwości mięty pieprzowej i jej głównych składników, W: VI Ogólnopolska Konferencja Naukowa "Współczesne zastosowanie metod analitycznych w farmacji i medycynie". Wrocław, 03 grudnia 2021 r. Książka abstraktów, Wrocław 2021, s. 24

Impact Factor : 35,620 *(liczba prac : 7)*

Punkty ministerialne : 1050,0